PHOSPHORUS REACTIONS IN THREE CONTRASTING SOILS AMENDED WITH BIOCHAR

BY

JOSEPH OSAFO EDUAH

(10200549)

THIS THESIS IS SUBMITTED TO THE UNIVERSITY OF GHANA, LEGON IN PARTIAL FULFILLMENT OF THE REQUIREMENT FOR THE AWARD OF PHD SOIL SCIENCE DEGREE

Department of Soil Science

School of Agriculture

University of Ghana

Legon, Accra, Ghana

MARCH, 2018

DECLARATION

I hereby declare that this thesis does not incorporate without acknowledgement, any material previously submitted for a degree in any University. To the best of my knowledge and belief, the thesis contains no material published or written by another person except where due reference is made in the thesis behalf.

…….. ……..

Joseph Osafo Eduah Date

(Student)

…… …….

Prof. M. K. Abekoe Date

(Principal Supervisor)

……. ……

Dr. E. K. Nartey Date

(Co-supervisor)

…….. ……..

Prof. H. Breuning-Madsen Date

(Co-supervisor)

DEDICATION

I dedicate this PhD thesis to the loving memory of Professor Henrik Breuning-Madsen under whose supervision I carried out most of the research at University of Copenhagen, Denmark. He passed away two days after my VIVA.

ACKNOWLEDGEMENT

Glory be to God for His divine grace and mercies for all these years. “Indeed, He who began a good work with me has surely crowned it with much triumph”.

I am deeply indebted to my principal supervisor, Prof. Mark. K. Abekoe, for his constructive criticisms, guidance and enormous contributions towards the successful completion of this research. I am very grateful for the extent you went to make sure my work was done and completed on time. God richly bless you.

I would like to express my sincere gratitude to my co-supervisors, Dr. Eric. K. Nartey and Prof. H. Breuning-Madsen their critique and massive contributions towards my research work. Not forgetting the lecturers at the Department of Soil Science who in one way or the other made substantial inputs in my work. May God bless you.

Much appreciation goes to Danida Fellowship Centre for financing my PhD studies under Green Cohesive Agricultural Resource Management (WEBSOC) project. To Prof. Mathias Neumann Andersen, Dr. Emmanuel Authur and many others on WEBSOC project, I say God bless you abundantly for your mammoth support and assistance

I am very grateful to Prof. Ole O. Borggaard, Dr. Marie L. Bornø and Stephan W. Henriksen for their assistance during my experiments and laboratory work in Denmark. I am also thankful to my PhD colleagues, Akumah A. Mensah, Kossi Koudjega and Komlan A. Ablede at the Department of Soil Science, Ghana, for creating cordial working environment.

I thank my parents and my siblings, most especially, Mr. John O. Eduah for their support and words of encouragement throughout my course of study. Special thanks also goes to my immediate family, Christiana Owusu, Jaden Osabarimah Osafo Eduah and Jesse Osahene Osafo Eduah.

GENERAL ABSTRACT

The reactive nature of phosphate leads to the formation of insoluble Fe, Al and Ca bound P compounds in highly weathered tropical soils. Biochar amendments can change the surface chemical properties of highly weathered tropical soils, and hence affect phosphorus retention and distribution in soils. The overall objective of this study was to investigate P reactions with biochar and biochar amended soils of Ghana for effective P management. To achieve this, three major experiments were conducted: (1) phosphorus adsorptive characteristics of different biochar types namely cocoa pod husk, rice husk, corn cob and palm kernel shell biochar produced at two pyrolysis temperatures (300 ^{o}C and 650 ^{o}C); (2) phosphorus sorption and desorption studies on three constrasting soils amended with corn cob and rice husk biochar produced at 300 ^{o}C, 450 ^{o}C and 650 ^{o}C and (3) phosphorus fractions in corn cob and rice husk biochar produced at three pyrolysis temperatures (300 ^{o}C, 450 ^{o}C and 650 ^{o}C) as well as P fractions in biochar amended soils. In experiment 1, P removal ability of four biochar types namely cocoa pod husk, rice husk, corn cob and palm kernel shell produced at two pyrolysis temperatures (300 ^{o}C and 650 ^{o}C) was investigated by using series of batch experiments. Sorption isotherms and kinetics models were used to assess the removal ability and mechanism of P adorption on the biochar types. The effect of equilibrium pH on P sorption was also examined. Biochar types attained maximum P adsorption within equilibrium time of 6 to 12 h. The maximum adsorption capacity calculated from the Langmuir isotherm was from 4.12 to 13.02 mg g^{-1} in an increasing order of CP300 < CC300 < RH300 < CP650 < PK300 < CC650 < RH650 < PK650 for the studied P concentration ranged of 25- 200 mg P L^{-1}. Generally, biochar types produced at 650 ^{o}C had higher P adosprtion capacity than at 300 ^{o}C. The equilibrium pH for maximum P adsorption varied among biochar types occurring in a range of 2.8 to 4.8. Increasing equilibrium pH decreases P adsorption. Freundlich isotherm coupled with

pseudo second order and Elovich models explained the adsorption data well indicating a chemisorption process on heterogeneous surface of biochar involving ligand exchange (PK300, PK650, CP650), electrostatic attraction (RH300, CC300) and surface precipitation (CP300, CC650, RH650). Palm kernel shell biochar at 650 ^{o}C with the highest P sorption capacity should be the preferred choice for removal of the anion from wastewater. The CP300 having the least P adsorption capacity and with its high total P content, alkaline pH and the presence of carbonate could be exploited for use as a liming material on acid soils. In experiments 2 and 3, incubation studies were conducted for 80 d to investigate the effect of corn cob and rice husk biochar produced at three pyrolysis temperature (300 ^{o}C, 450 ^{o}C and 650 ^{o}C) on P sorption characteristics and fractions in two acid and one neutral soil. The P sorption capacity of the two acid soils i.e. Kokofu Series (384.6 mg kg^{-1}) and Ankasa Series (333.3 mg kg^{-1}) were about three fold more than the neutral soil (Keta Series) (104.2 mg kg^{-1}). Amending the acid soils with biochar increased the equilibrium P concentration in solution at decreasing pyrolysis temperature for the two biochar types. There was, however, an increase in P sorption with increasing pyrolysis temperature in the neutral soil. The amount of P desorbed increased in the acid soils but decreased in the alkaline soil. Biochar produced at 300 ^{o}C had more significant effect on both the decrease in P adsorption and increase in P desorbability in the acid soils. The results of modified Hedley P fractionation showed that the most labile P (Resin-P, $NaHCO_3$-Pi) and organic P pool showed a decreasing trend with increasing pyrolysis temperature in the biochar types. However, the Ca-bound P (HCl-Pi) and residual P increased with increasing pyrolysis temperature. The interaction of biochar with soils resulted in an increase in the most labile P as well as moderately P (NaOH-Pi) fractions in the three soil types making P more available for plant uptake. The increase in the readily available P pool was more significant at relatively lower temperature (300 ^{o}C) than higher pyrolysis temperatures for both biochar types.

However, the increase in calcium-bound P and residual P of the soils was more predominant when both biochar types produced at 650 ^{o}C were applied. The study thus showed that biochar pyrolysed at 300-450 ^{o}C could be used to reduce P sorption and increase P bioavailability in acid soils. The addition of biochar to near neutral soils might increase P retention possibly in the short-term, reducing P bioavailability.

TABLE OF CONTENTS

LIST OF TABLES

PAGE

LIST OF FIGURES

PAGE

CHAPTER ONE

GENERAL INTRODUCTION

The high phosphorus (P) fixing capacity of highly weathered tropical soils including Ghanaian soils has restrained the development of economically sustainable crop production (Brady and Weils, 2001). Phosphorus undergoes several biogeochemical processes such as dissolution, complexation, adsorption and precipitation and these determine the availability of the nutrient in soil solution for plant uptake (Weng et al., 2012; Chintala et al., 2013; Gérard, 2016). These chemical processes are a complex function of several soil properties including, Al and Fe oxide type and content, the amount and type of silicate clays, ionic strength, soil solution pH, calcium carbonate content, concentration of P in solution and the presence of competing anions (Hinsinger, 2001; Eriksson et al., 2015; Gérard, 2016).

The amount of P uptake by plants in acidic and alkaline soils is much restrained due to P sorption. Addition of P to acid soils leads to the formation of insoluble Fe and Al phosphate through ligand exchange and precipitation reactions (Galvao & Salcedo, 2009; Schoumans & Chardon, 2015). A direct relationship between the amount of P adsorbed and crystalline and amorphous Fe and Al oxides have been observed, indicating that in acid soils these oxides are the major P adsorbent (Nartey et al., 1997; Borggaard, 2002). The formation of calcium-P and magnesium-P compounds as well as P adsorption and precipitation by $CaCO_3$ occurs in alkaline and calcareous soils (Amer et al., 1995; Tisdale et al. 1999; Sato et al., 2005, Eriksson et al., 2015). Phosphorus availability has thus become a major factor controlling crop production in tropical weathered soils.

Meeting the world's increasing demand for food in a sustainable way has been an agricultural challenge for the past few decades. The poor fertility status of soils in the tropics as a result of

low P content has aggravated the problem (Gruhn et al., 2000). Considerable P inputs are therefore needed for optimum plant growth (IAEA, 2002).

Organic matter amendment is considered a sustainable approach for remediating P deficiency in tropical soils (Iyamuremye et al., 1996; Haynes and Mokolobate, 2001) through competitive sorption reaction with mineral oxides for P and also direct discharge of P upon decomposition (Siddique and Robinson, 2004). There is fast decomposition rate of organic matter in the tropics with a concomitant high release of carbon dioxide aggravating global warming. Effects of organic matter amendments are often therefore, short-lived thus leading to a short period for improvement in soil fertility (Barthes and Azontode, 2004). The age old tradition of slash and burn as a method of land clearing also further decreases the organic matter contents of soils. There is also the competitive use for plant residue especially in the unimodal rainfall areas of the tropics particularly West Africa where plant residue is stored as animal feed for the long dry season. Consequently, return of plant residue to the soil is minimal.

The use of chemical fertilizers to increase P availability in soil solution has been reported (Nartey et al., 1997). However, application of P fertilizers especially in acidic soils have not had the desired impact on soil productivity and crop yields because of the presence of soluble Al and Fe and high level of sesquioxides and kaolinites tend to adsorb added inorganic P (Nartey et al., 1997; Abekoe and Tieseen, 1998; Chien et al., 2014). The use of inorganic fertilizers may have the desired impact if rates applied are above the sorption maximum of the soils (Abekoe et al., 2000). However, the high cost of the product in the West African subregion coupled with the fact that the producs not readily available makes the use of high application rates impractical. Any approach to solve the P problem in tropical soils must take into consideration cost, availability and persistence of the product in soils.

The use of biochar has been suggested to provide an integrated approach to rectify the challenge of tropical soils infertility (Lehmann and Joseph, 2009). Biochar is a stable carbon rich material, which has gained a lot of attention for the numerous roles it plays in the soil. It is a product of biomass pyrolysis, which is the combustion in oxygen limited environment (Lehmann et al., 2006). It is highly resistant to microbial degradation and can therefore stay in soils for hundreds to thousands of years (Lehman et al., 2006). Biochar has the potential to increase cation exchange capacity, nutrient concentration, soil water retention and alteration of soil pH as well as sequesteration of carbon from the atmosphere (Chen et al., 2011; Lehmann, 2007; Tang et al., 2013). The feedstocks for biochar production abounds in Ghana and are low-cost and mainly obtained from agricultural biomass, industrial and domestic wastes (Duku et al., 2011; Sam et al., 2017).

Ghana as a country generates about 363×10^3 and 1650×10^3 tonnes of rice husk and corn cob biomass, respectively annually (Duku et al., 2011; FAOSTAT, 2008). These wastes are generally disposed of by aerobic burning to pollute the environment. Converting these biomasses into biochar can improve the biomass management and protect the environment (Dong et al., 2013).

Improvement of P availability in soils upon biochar application have been reported in several studies (Lehmann, 2007; Chan et al., 2007; Atkinson et al., 2010). Various mechanisms by which biochar may directly or indirectly control the biotic and abiotic components of the P dynamics have been reported (DeLuca et al., 2009). Biochar contains ample amount of P and therefore can directly release soluble P into soil solution to enhance P availability (Chan et al., 2007; Atkinson et al., 2010). The addition of biochar reduces soil acidity due to its high alkalinity and consequently reduces P precipitation reactions with Fe^{3+} and Al^{3+} (Wang et al.,

2012; Yuan et al., 2011). Joseph et al. (2010) also indicated that application of biochar to soils culminates into the precipitation of Fe-(hydro) oxide on biochar surface. Other studies have on the other hand reported that biochar decreases P availability in most alkaline soils of the tropics due to substantial release of cations including Ca^{2+} and Mg^{2+} (DeLuca et al., 2009).

Even though much work has been conducted on P sorption and availability in soils using P sorption characteristics (Agbenin and Tiessen, 1994; Abekoe and Tiessen, 1998; McDowell and Condron, 2001; Villapando and Graetz, 2001), very limited work has been done on P adsorption characteristics of biochar-soil complex. Studies using different biochar types on soils are required to evaluate the reactivity and sorption characteristices of biochar-soil complex vis-à-vis soil P availability after biochar application.

Feedstock type and pyrolysis temperatures affect the P speciation in biochar, hence its P bioavailability in soils (Cantrell et al., 2012). Biomass contains variable amounts of inorganic P as well as organic P. With increasing pyrolysis temperature, the total P increases (Hossain et al., 2011; Wu et al., 2011; Uchimiya and Hiradate, 2014). However, most of the P are fixed in the ash compounds such as Ca-P, Mg-P, Fe-P at high temperatures and therefore bioavailable P decreases (Cantrell et al., 2012; Iqbal et al., 2015). Studies by Christel et al. (2014), using diffusive gradients in thin films confirmed P unavailability at pyrolysis temperatures above 700 ^{o}C in pig slurry biochar. This is obviously due to the formation of unstable P compounds during thermal breakdown (Cantrell et al., 2012; Thygesen et al., 2011). The need for assessing P forms in biochar at varying carbonization condition which in turn affects its availability in soil solution for plant uptake merits research.

Phosphorus forms in soil and sediments have been investigated by chemical sequential extraction techniques (Chang and Jackson, 1957; Williams et al., 1980; Hedley et al., 1982;

Cross and Schlesinger, 1995; Asomaning et al., 2015). Poultry manure and rice straw biochar increased water extractable P, readily available P (resin-P and $NaHCO_3$ extractable P) and NaOH extractable (Fe and Al- P) P fractions in asandy clay soil (Wang et al., 2014). Wang et al. (2012) also observed large differences in plant P uptake in a pot experiment and established that feedstocks, final pyrolysis temperature and soil type controls P availability. There is limited information on the interactive effect of different biochar types with Ghanaian soils on P sorption and fractions. Availability of such pieces of information will be key to understanding the fate of P in biochar amended highly weathered soils such as those in Ghana and invariably help.in the effective management of P for sustainable crop production. The general objectives of the study were to:

1. determine P adsorptive characteristics of biochar types produced at varying pyrolysis temperatures
2. find out the effect of biochar amendment on P sorption and desorption in soils
3. ascertain the influence of pyrolysis temperature and biomass type on phosphorus fractions in biochar and biochar-amended soils

Thesis format

This PhD thesis has six chapters; the first of which introduces the topic and outline the overall objectives of the study. The second chapter reviews relevant literature on biochar production, physical and chemical properties of biochar as influenced by the feedstock and pyrolysis temperature. It also reviews P dynamics in soils including P kinetics, sorption and fractionation. Chapter three investigates phosphorus removal ability of four biochar types namely cocoa pod husk, rice husk, corn cob and palm kernel produced at two pyrolysis temperatures (300 ^{o}C and

650 ^{o}C) using series of batch experiments. Kinetics models and sorption isotherms were used to assess the removal ability of the biochar types. The effect of equilibrium pH on P sorption and the possible mechanism controlling P adsorption are also examined.

Based on the abundance and easy accessibility of corn cob and rice husk as compared to cocoa pod husk and palm kernel shell residues the former two biochar types were used for subsequent incubation studies (Chapters four and five). An incubation experiment (Chapters four and five) was conducted by amending corn cob biochar and rice husk biochar produced at three different temperatures of 300 ^{o}C, 450 ^{o}C and 650 ^{o}C on two acid soils (Ankasa and Kokofu) and one neutral soil (Keta). Chapter four looked at the effect of the two biochar types at the three pyrolysis temperatures on some chemical properties of the three soil types. It further examined P adsorption and desorption characteristics of the soils and the biochar amended soils. Chapter five focused on assessing the P fractions in the biochar types as influenced by the three pyrolysis temperatures. The P fractions in the three soils upon the application of the biochar types were also examined. Summary, conclusion and recommendation highlight the major results from the studies and are presented in chapter six.

CHAPTER TWO

LITERATURE REVIEW

2.1 Biochar

Biochar is produced by thermochemical breakdown of plant and animal residues (Schmidt et al., 2015; Kammann et al., 2015). In accordance with International Biochar Initiative, biochar is defined as ‘‘a solid material obtained from the carbonization of biomass’’ (http://www.biochar-international.org/biochar). It is also defined by Lehmann and Joseph (2009) as a carbonaceous material obtained from the pyrolysis of organic residues at low temperatures (<700 ^{o}C). Apart from carbon, hydrogen and oxygen as the major elements of biochar, it also contain nitrogen and sulphur (Laird et al., 2010). Biochar can be generated from a various kinds of biomass such as wood waste, cow dung, poultry manure, sewage sludge (Sohi et al. 2010). The chemical and physical properties of biochar is influenced by the biomass type and pyrolysis conditions such as residence time, heating rate and temperature (Spokas et al., 2012). For instance, increasing pyrolysis temperature from 300 to 700 ^{o}C results in high carbon content with a concomitant decrease in N, O and H concentration. The physicochemical properties of biochar differ from the feedstock from which it was produced, characterized by its relatively high surface area, high cation exchange capacity, high C and P contents as compared to the biomass (Lehmann et al., 2011).

A number of research work has been done on the use of biochar on highly weathered tropical soil as well as temperate soils. Most of these research showed much improvement in soil fertility and high crop yield upon the addition of biochar (Lehmann, 2006 and Spokas et al., 2012).

Several research work has suggested the underlying mechanism for the increase in plant available nutrients in tropical soils upon biochar application including direct release of soluble nutrients in biochar into soil solution (Sohi et al., 2010); mineralization of the labile carbon contained in biochar (Lehmann et al., 2009); less nutrient leaching due to the physical and chemical characteristics of biochar (Liang et al., 2006) and minimized N losses via denitrification and volatilization (Cayuela et al., 2013).

The production of biochar is affordable and also environmentally friendly. Apart from the use of biochar in soil fertility and productivity, it has also been deployed in the area of wastewater treatment, climate change mitigation and energy production (Hassan et al., 2012).

2.2 Biomass

Biomass can be categorized as woody- and non-woody feedstock. Duku et al. (2011) reported that globally about 500 million tons of agricultural residues are produced annually. Various biomass are produced in Ghana including crop residues, forest residues, domestic and municipal organic waste (Duku et al., 2011). Most of the agricultural residues are by-products from harvesting and also agroprocessing of crops such as cocoa, rice, maize, oil palm etc. As a results of the abundance and low cost of these residues, it has continually been used as feedstock for the production of biochar. The conversion of these residues into biochar helps in the management as well as reducing the cost associated with the disposal of agricultural and forest waste.

Biomass contains large amounts of cellulose, hemicellulose, lignin, and small amounts of extractives which globally makes it a good feedstock for biochar production. The amount and composition of these components differ with the type of biomass.

McHenry (2009) reported that for a particular biomass to serve as a suitable feedstock for biochar production, it depends on the following properties; moisture content, carbon content, ash content, oxygen, hydrogen, volatiles, cellulose/lignin ratio and calorific value.

2.3 Pyrolysis

Pyrolysis is referred as the thermochemical breakdown of organic residues at high temperatures under limited oxygen condition (Fig. 2.1) (Bridgwater, 1994). Limited oxygen environment helps in the heating of organic residues to a temperature beyond its thermal stability leading to the production of stable solid products. Pyrolysis results in an irreversible altering of chemical and physical content of the biomass. During thermal breakdown of biomass, the reaction pathways of cellulose, hemicellulose and lignin content of biomass differ, leading to the formation of solid, liquid and gaseous products.

The thermal process occurs in three consecutive steps (Demirbas, 2006). The first step involves the loss of water and other volatile compounds (Eqn. 1). During the second step, CO and CO_2 are released as a result of the decomposition of cellulose and hemicellulose. There is also an increase in pyrolysis temperature due to exothermic reaction, however, it is influence by biomass type, reactant temperature and reactor conditions. The release of CH_4, H_2, and C_2H_2 also occurs in this stage (Eqn. 2). The third step basically involves the formation of carbon rich solid material as a result of the slow breakdown of biochar. Biochar becomes less reactive once secondary pyrolysis are formed (Eqn. 3). To futher complete the thermochemical degradation process, an external source of energy is needed.

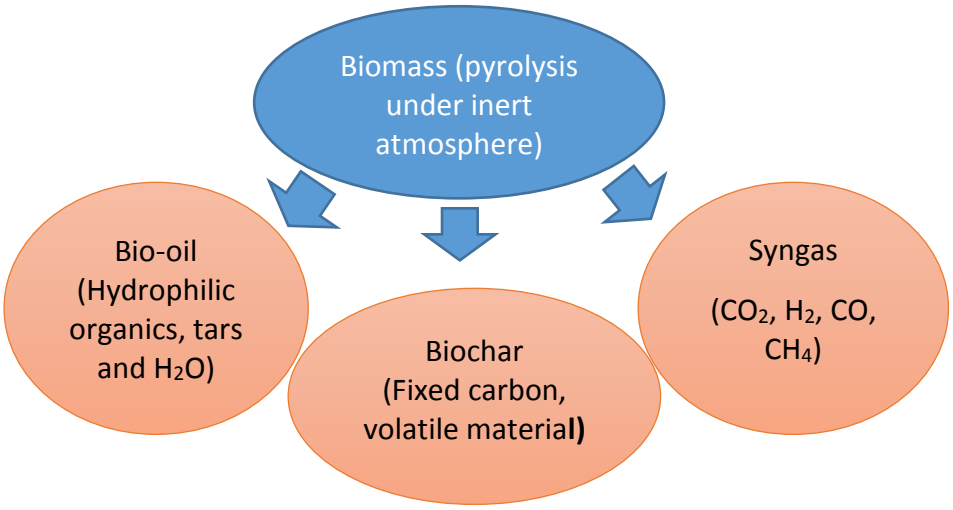

Fig. 2. 1 Simplified diagram showing pyrolysis of biomass (Demirbas, 2006)

$$\text{Biomass} = \text{water} + \text{unreacted soild residues} \qquad \text{Eqn. 1}$$

$$\text{Unreacted solid residue} = (\text{Volatile} + \text{Gases})_1 + (\text{Biochar})_1 \qquad \text{Eqn. 2}$$

$$\text{Biochar}_1 = (\text{Volatile} + \text{Gases})_2 + (\text{Biochar})_2 \qquad \text{Eqn. 3}$$

A number of pyrolysis techniques are presented in Table 2.1. The chemical component of product form (syngas, bio-oil, biochar) during thermodynamic processes is affected by the reactant conditions (Gaunt and Lehmann, 2008; Brewer et al., 2009; Spokas et al., 2012). Pyrolysis conditions including biomass type, temperature level, residence time and oxygen level can be regulated to provide varying types of biochar. Syngas obtained during pyrolysis can be used for energy production as well as improved to specific chemical products such as wood preservative and food flavoring (Lehmann, 2007).

Pyrolysis can be categorized into fast pyrolysis, slow pyrolysis, gasification, hydrothermal pyrolysis and microwaved pyrolysis based on residence time, temperature used and heating rate. Again, the thermal process of pyrolysis can either be exothermic or endothermic depending on the temperature needed for the pyrolysis. Mostly it is endothermic when high temperature is needed and exothermic when the temperature of the reactant reduces (Mok and Antal, 1983). Recently, biochar production is based on modernized pyrolysis conditions (Lima et al., 2010; Lima and Marshall 2010; Spokas et al., 2012). However, the conventional way of producing char is still in existence (Major et al., 2010a; Spokas et al., 2012). The regulation of pyrolysis condition is made possible using the advanced method of pyrolysis, which, when coupled with exact biomass usage, can control the physicochemical characteristics of biochar

.

Table 2. 1 Processes of thermochemical breakdown of organic feedstocks

Pyrolysis process	**Reactor temperature**	**Residency time**	**Heating rate**	**Product yields (% dry feedstock mass)**			**Proximate analysis (% dry weight basis)**				**Pyrolysis product stream**	**Reference**
				Biochar	Bio-oil	Syngas	H_2O	VM	Ash	Fixed C		
Slow pyrolysis	Low temperature pyrolysis (350-500 °C)	Hours	1-100	20-35	15-30	10-35	0-5	5-20	2-10	40-90	Use for commercial biochar production	Laird et al., 2009; Brewer et al., 2009; Yin et al., 2012
Fast pyrolysis	High temperature pyrolysis (450-600 °C)	>2s-< 1 mins	726-9726	10-30	50-70	5-20	0-5	40	30	40-60	Purposely for large production of bio-oil and biochar	Laird et al., 2009; Yin et al., 2012; Bridgewater, 2006
Flash	High temperature pyrolysis (800-1100 °C)	< 2s	700-9000	15-25	60-80	10-20	0-5	5-26	0-40	40-60	To process biomass, degrade waste, generate bio-oil and charcoal	Neves et al., 2011; Amutio et al., 2012; Bridgewater, 2012
Microwave pyrolysis	Moderate temperatures (300-500 °C)	Minutes to hours	n/a	n/a	n/a	n/a	10-25	20-30	20-25	50-60	To generate fuel gases, bio-oil and biochar	Yin et al., 2012;

VM = volatile matter

Table 2.1 Continued

Pyrolysis process	Reactor temperature	Residence time	Heating rate	Product yields (% dry feedstock mass)			Proximate analysis (% dry weight basis)				Pyrolysis product stream	Reference
				Biochar	Bio-oil	Syngas	H_2O	VM	Ash	Fixed C		
Gasification	Very high temperature (> 800 ^oC)	Seconds to minutes	Variable	5-10	0-10	80-95	n/a	n/a	2-10	n/a	Production of synthetic gas (CO, H_2 and CO_2)	Laird et al., 2009; Brewer et al., 2009; Yin et al., 2012
Torrefaction	Mild form of pyrolysis temperature (200-320 ^oC)	Hours	< 1	40-90	0	10-60	0-1	50-85	2-10	13-38	Fuel upgrading of woody biomass and biochar production	Spokas et al., 2012
Hydrothermal carbonization	Wet pyrolysis at temperature (180-200 ^oC)	Minutes to hours	n/a	n/a	n/a	n/a	10-40	50-90	5-15	4-10	To generate biocoal (100% C) powder, can be use to improve soil fertility/ productivity	Funke and Ziegler, 2010

VM = volatile matter

2.4 Stability of biochar in soil

The stability of biochar is due to the formation of aromatic ring structures during the thermal decomposition of the feedstock (Hamer et al., 2004). Glaser et al. (2001) reported that the resistance of biochar to abiotic and biotic breakdown in soils is as a result of the formation of polycyclic aromatic carbon structures. This confirms the high stability of biochar in tropical soils, temperate soils and sediments having residence time over 1500 years (Glaser et al., 2001; Hammond et al., 2009; Krull et al., 2009). The long residence time of biochar in soil allows for effective carbon sequestration (Lehmann et al., 2006).

At high pyrolysis temperature, the carbon content as well as the aromaticity increases leading to biochar stability (Novak et al., 2010), eventually maximizing carbon sequestration ability of the biochar. Plant nutrients are hardly discharged from biochar of high aromaticity and therefore, become less important to the growth of plant (Novak et al., 2010).

The type of biomass have been reported to be the main contributor to biochar stability in soil. Biomass of high lignin content mostly produces biochar of high aromatic carbon content and hence slow decomposition rate (Glaser et al., 2001). Hilscher et al. (2009) using different biochar types pyorlysed under the same temperature in an incubation studies reported that the C mineralization rate of non-woody biochar (2.3-4.5%) was higher than that of wood biochar (0.3-0.5%). The O: C ratio parameter of biochar helps in finding out the stability of biochar based upon its half-life. The O: C ratio is reported to be inversely related to biochar stability and it decreases with increasing pyrolysis temperature (Spokas, 2010). Most often with O: C ratio of 0.2, biochar would have a half-life of 1000 years, whereas it will decrease to 100 years when the O: C ratio is more than 0.6 (Spokas, 2010).

In spite of the aromatic nature of biochar, several studies have reported that biochar can be mineralized through abiotic and biotic processes (Major et al., 2010a). After 12 months of incubation, Masek et al. (2011) reported an increasing oxidation of biochar surface with a concomitant increase in acid functional group generating more negative charges and less positive charges. It has also been established that even though microbes are the driving force behind biochar breakdown, biotic mineralization was less than 3% after 96 days of application. The main cause of biochar loss was due to erosion fluxes (Major et al., 2010a; Masek et al., 2011).

2.5 Effect of pyrolysis temperature and biomass type on biochar properties

Biochar which is heterogeneous in nature has stable and labile components (Sohi et al., 2009). The main components of biochar are carbon, volatile matter, ash content and moisture (Antal and Gronli, 2003). The relative amount of these components determines the physicochemical behaviour and function of biochar as a whole (Brown et al., 2006), which eventually helps to know its suitability for the exact application, as well as mobility and dynamics in an ecosystem (Downie et al., 2009). Microscopic techniques including scanning electron microscopy (SEM), X-ray diffraction (XRD), raman spectroscopy, and energy dispersive X-ray (EDX) spectroscopy are the most commonly used techniques for characterizing different biochar types (Kappler et al., 2014; Yip et al., 2011). These techniques show that biochar is mainly amorphous in nature with some local crystalline structure. With increasing carbonization energy, the biochar crystallites increase in size, leading to an orderly structure of the biochar (Lua et al., 2004). Even though biochar is produced from different biomass under different carbonization conditions, it has high carbon content and strong aromatic structure (Sohi et al.,

2009). The aromatic carbon structure of biochar is usually measured using its elemental hydrogen and/or oxygen to carbon ratios (Krull et al. 2009). Biochar types pyrolysed at temperatures below 500 ^{o}C mostly have H/C ratios more than 0.5, and biochar types charred at temperatures above 500 ^{o}C have H/C ratios less than 0.5. The low H/C ratio implies high level of aromaticity (Laird et al., 2009). These properties (H/C or O/C ratios) explain the chemical stability of biochar in soils (Sohi et al., 2009). Because biochar is recalcitrant, it is able to stay in soils for over 1000 years, which is reported to have about 100 times longer residence times than that of soil organic matter (Verheijen et al., 2010).

The physicochemical properties of biochar is largely controlled by the pyrolysis temperature as well as the feedstock used for the production (Downie et al., 2009; Laird et al. 2009). For instance, the cellulose, hemicellulose and lignin content of woody feedstock is much higher than herbaceous feedstock (Amonette and Joseph, 2009). The high carbon content and hence increase production rate of biochar is because of the high lignin content of the biomass used for the production (Demirbas, 2004). The increase in volatilization and reduction in biochar yield has been reported to be due to high hemicellulose: lignin ratio in feedstock. Biomass with high lignin content generates biochar of high yield (Amonette and Joseph, 2009). Thermochemical break down of high molecular weight hydrocarbon compounds occurs at high pyrolysis temperatures culminating into the increase of syngas and reduction in the yield of biochar. As pyrolysis temperature of hazelnut shell is raised from 400 °C to 700 ^{o}C, it results in 10% reduction in the yield of biochar produced and 17% decrease for sesame stalk (Downie et al., 2009).

The ash content of biochar is reported to increase at the expense of decreasing carbon content (Gaskin et al., 2008). The ash content of biochar consist of inorganic constituents such as calcium, magnesium, sodium, potassium and inorganic carbonates (Joseph et al., 2009). Oftentimes biochar generated from woody biomass has about 1% less ash content whiles about

24% of ash content has been found in biochar produced from non-woody biomass (Joseph et al., 2009).

The pH of biochar varies with pyrolysis temperature and feedstock. Generally, biochar is alkaline although few found acidic depending on feedstock (Ahmad et al., 2014). Several studies have reported that biochar charrd at high temperatures have high pH. The high pH is largely due to the release of alkaline and alkaline earth metals from the feedstock during the pyrolysis process (Ahmad et al., 2014). The pH dynamics of biochar types at varying pyrolysis temperatures is in agreement with studies using Boehm titration, which showed that with increasing pyrolysis temperature total acidity decreases whiles total alkalinity increase (Zhang et al., 2015b). Biochar produced from oak wood at 350 ^{o}C and 600 ^{o}C was acidic (4.84-4.91) (Nguyen et al., 2010). Similar low pH at 4.60 was observed for oak wood biochar produced at 200 ^{o}C, but at 400 ^{o}C and 600 ^{o}C the biochar was neutral to alkaline (6.90-9.50) (Zhang et al., 2015a).

In addition, biochars from corn stover and millet straw at low temperature (200-400 ^{o}C) were also acidic with pH of 4.87-6.11 (Nguyen et al., 2010; Hossain et al., 2011; Zhang et al., 2015b). Positive relationships have been observed between biochar pH and pyrolysis temperature for biochars produced from oak wood (Nguyen et al., 2010; Zhang et al., 2015a), biosolids (Hossain et al., 2011; Chen et al., 2014; Jin et al., 2016), wheat, corn, and maize residues (Nguyen et al., 2010; Wang et al., 2015a; Zhang et al., 2015b), manure (Subedi et al., 2016), and conocarpus wastes (Al-Wabel et al., 2013). Increasing temperature led to higher ash component, which positively correlated with biochar pH, suggesting that ash component is a factor contributing to biochar high pH (Yuan et al., 2011).

Moreover, high pH at high pyrolysis temperature could be due to the disappearance of acidic functional groups such as phenolic and carboxylic groups. With temperature increasing from 200 to 800 ^{o}C, basic functional groups on biochar surface produced from organic wastes increased from 1.15 to 4.55 mmol g^{-1}, whereas acidic functional groups decreased from 5.17 to 1.22 mmol g^{-1}, consistent with the increased biochar pH from 7.5 to 12.8 (Al-Wabel et al., 2013).

Nitrogen content of biochar decrease proportionally with increasing pyrolysis temperature (Gaskin et al. 2008). Woody and non-woody biochar started to lose N at 400 ^{o}C pyrolysis temperature and about 50% N was lost through volatilization at 700 ^{o}C (Knicker, 2007). Because N is mostly bound to organic compounds, at low temperatures of 200^{o}C, N begins to undergo volatilization (DeLuca et al., 2009). Nitrogen is converted to pyridine like structure at high temperatures (>550 °C) (DeLuca et al., 2009). Despite the fact that N can be lost through volatilization, a number of biochar types have been shown to contain high N as a result of heterocyclic N compound formation (Knicker, 2007).

Unlike total N content in biochar, total P and base cations i.e. K, Ca, Mg and Na content increased proportionally with increasing pyrolysis temperature (Zheng et al., 2013). Potassium and phosphorus are lost at temperatures above 700 °C whiles Mg and Ca volatiles at temperatures above 1000 °C (Knicker, 2007). The enrichment of P at high temperatures is attributed to the loss of carbon, and moderately stable P compounds in biomass (Knicker, 2007). It was proven that due to stable P compounds formed at high temperatures (>750 ^{o}C) there was no record of P loss (Bridle and Pritchard, 2004).

Biomass, comprises varying amounts of inorganic and organic P (Uchimiya and Hiradate, 2014). With increasing pyrolysis temperature, the total P content increases (Hossain et al.,

2011; Uchimiya and Hiradate, 2014; Wu et al., 2011). However, most of the P are fixed in the ash compounds such as Ca-P, Mg-P, Fe-P with increasing pyrolysis temperature and therefore bioavailable P decreases (Uchimiya and Hiradate, 2014; Cantrell et al., 2012; Iqbal et al., 2015). Studies by Christel et al. (2014) confirmed no P availability at pyrolysis temperatures above 700 ^{o}C when determining P availability in pig slurry biochar using diffusive gradients in thin films techniques. This is obviously due to the formation of stable P compounds during the carbonization process (Cantrell et al., 2012; Thygesen et al., 2011).

The CEC is the capacity of an adsorbent to adsorb positively charged ions, and raising pyrolysis temperature results in a decrease in CEC of biochar (Gaskin et al. 2008). The functional group mostly the acidic functional groups are the major contributor of the CEC of biochar. Mostly, non-woody and grassy biochar types with relatively high hydroxyl and carboxylic groups have higher CECs than woody biomass (Harvey et al., 2011). A higher CEC values for low pyrolysis biochar types (<350 ^{o}C) may be because of the high amount of acidic functional groups. On the contrary, low CEC values were reported for biochar pyrolysed above 350 ^{o}C (Zhao et al., 2013).The CEC of mallee biochar increased from 18.5 cmol kg^{-1} (pyrolyzed at 200 ^{o}C) to 23.8 cmol kg^{-1} (at 350 ^{o}C) and then decreased to 2.1 cmol kg^{-1} (at 650 ^{o}C).

Electrical conductivity which is much associated with the amount of salt concentration in water, expresses the tendency of a material to conduct electrical current. Biochar types produced from woody biomass have less salt content and therefore low electrical conductivity unlike when produced from non-woody biomass such as manure-derived biochar (Uras et al., 2011). The high electrical conductivity of manure-derived biochar is due to higher concentration of Na^{+}, K^{+}, Mg^{2+}, SO_4^{2-} and PO_4^{3-}, and which can also serve as essential plant nutrient for crop growth. These salt concentration in biochar increases directly with increasing pyrolysis temperature.

However, the level of salt mostly influence by the type of biomass used for the production (Al-Wabel et al., 2013).

Fourier transform infrared spectroscopy (FTIR) spectra have been widely deployed to characterize the functional groups on biochar surfaces. The FTIR spectra on different biochar types at varying temperatures conducted by Yuan et al. (2011) reported that there are substantial quantities of oxygen-containing functional groups (e.g. -COO, -COH, -OH and CO_3^{-2}) on the biochars. Among them, -COO- and -OH contributed extensively to surface charge of the biochars. As pH decreases, the zeta potentials of the biochar samples become less negative, due to the protonation of -COOH and –OH groups. Pyrolysis temperature and biochar feedstock are the two key factors controlling the quantities of functional groups on biochar surface. The abundance of functional groups in biochar decreases with increasing pyrolysis temperature, primarily due to higher degree of carbonization. With increasing temperature, atomic ratios of H/C and O/C decrease, suggesting decrease in abundance of hydroxyl, carboxylic, and amino groups.

The FTIR spectra of functional groups in biochars produced at different temperatures are different. The FTIR spectra of wood and grass biochar changed when pyrolysis temperature increased from 100 to 700 ^{o}C (Keiluweit et al., 2010). During pyrolysis under increasing temperature, most functional groups of lignocellulosic materials are lost. Using FTIR photoacoustic spectroscopy, Yuan et al. (2011) observed decreased intensity of peaks corresponding to carboxylic (-COOH) and hydroxyl(-OH) groups as temperature increased from 300 to 700 ^{o}C for biochars from canola, corn, soybean, and peanut straw. Compared to those at 350 ^{o}C, similar loss of FTIR spectral features were observed for manure biochars produced at 700 ^{o}C (Cantrell et al., 2012). At higher temperature, these functional groups are

ignited, leading to decreased amounts with increasing temperature. In addition to FTIR, nuclear magnetic resonance (NMR) spectra have been used to describe the functional groups of biochar. Li et al. (2013) investigated the formation of functional groups in rice straw and bran biochars produced at 100-800 ^{o}C using two-dimensional ^{13}C NMR correlation spectroscopy. Biochar types from rice straw and bran went through dehydrogenation and aromatization process.

2.6 Effect of biochar on soil properties

Several studies have indicated that biochar has the tendency to change the physical properties of tropical and temperate soils, including surface area, bulk density, aggregate stability, water holding capacity (Sohi et al., 2010). The surface area of soil is key property that controls important soil fertility parameters including water holding capacity, nutrient content, soil aeration and microbial activity (Lehmann, 2006). Increase in agronomic yield of tropical soils amended with biochar has been reported to be as a result of the increased surface area of soil upon biochar application. Although surface area of biochar charred under different temperatures has been reported, not much is known about the surface area of soil-biochar mixture. However, an increase in surface area up to 5.1 times more than that of unamended soil has been reported upon biochar addition (Liang et al., 2006). In incubation studies, the incorporation of biochar at a rate of 1% increased the surface area of clay loam soils from 130 to 150 m^2 g^{-1} (Downie et al., 2009).

Others have observed that addition of waste-derived biochar to weathered tropical soils increased the amount of mesopores at the expense of macropores (Jones et al., 2010). Evidence from other studies have also proven that the increase in the overall net soil surface area of

tropical soils upon biochar amendment is inevitable (Chan et al., 2007) and therefore, may increase water holding capacity and nutrient content of soil (Downie et al., 2009) as well as soil aeration in fine-textured soils (Kolb et al., 2007).

Several research works on Alfisols and Ultisols have reported significant decrease in bulk density of soils when biochar was applied due to the relatively lower bulk density of biochar than mineral soils (Lehmann, 2006; Chen et al., 2011). The addition of rice straw biochar at a rate of 9.4% in annual field work showed a significant reduction in bulk density (Chen et al., 2011). Lehman (2006) also conducted soil column studies using biochar and reported a decrease in bulk density of the control soils from 1.68 to 1.41 Mg m^{-3}. It is therefore obvious in literature that the incorporation of biochar to soils improves the bulk density optimum for plant growth (Brady and Weil, 2002).

Water holding capacity of soil is controlled by other physical soil properties such as surface area, bulk density and aggregate stability (Brodowski et al., 2006). The addition of biochar as low as 0.5% is known to be enough to increase the water holding capacity of soils (Jones et al., 2010; Uzoma et al., 2011). The effect of biochar on the water holding capacity of soils also depends on the soil types. In a study of amending biochar to soils of different textural classes, varying response among the soils were found (Glaser et al., 2002). The moisture content of sandy soil increased by 18% upon the addition of 10% rate of biochar. However, the study recorded a decrease in moisture content in loamy and clay soils. Others have also reported an increase in moisture content in sandy soils (Gaskin et al., 2008). The increase in soil moisture has been attributed to high surface area of biochar by several authors (Gaskin et al., 2008; Glaser et al., 2002). The same biochar type produced at three pyrolysis temperatures were amended to a sandy soil in order to assess soil moisture dynamics. The study reported an

increase in soil moisture content by 18.3, 22.3 and 48.2% when biochar pyrolysed at 300^{o}C, 450 ^{o}C and 550 ^{o}C were applied respectively (Uzoma et al., 2011; Shafie et al., 2012). The researchers established that soil moisture content is much improved with biochar produced at high temperatures (>550 ^{o}C) than low temperatures (300-450 ^{o}C).

The availability of plant nutrients in soil solution have been improved upon biochar application especially in tropical acidic soils. This has been attributed to direct release of soluble plant nutrients, increase in cation exchange capacity and soil pH (Lehmann et al., 2003). Mostly biochars are basic and therefore are used as soil amendment to neutralize acidic soils (Glaser, 2002). The carbonate, bicarbonates, silicates content of biochar make it a liming agent and therefore have the potential of increasing neutral or acidic soil pH (Nguyen et al., 2010). The increase in soil pH is due to the reaction between the acidic functional groups such as carboxylic in biochar and hydrogen ions in soil solution (Lehmann et al., 2003). An increase in soil pH from 4.5 to 6.3 after biochar addition in a short term incubation studies was reported by Uzoma et al. (2011). Similarly, application of varying biochar types at 1% to some soils of the tropics showed 0.59 to 1.05 units increase in pH after 60 days (Yuan et al., 2011). In a 90 day incubation studies, rice husk biochar raised the pH of tea garden soils by 0.52 unit (Wang et al., 2014).

Biochar contains soluble base cations such as Ca^{2+}, Mg^{2+} which when applied to soils, these cations are released, exchanging with Al^{3+} and H^{+} thereby increasing soil CEC. Liang et al. (2006) reported that increase in soil CEC is proportional to an increase in charge density, surface area of soil as well as soil pH (4.8 to 8.5). The CEC of an Alfisol increased from 4.3% to 18% after the application of rice straw biochar in an incubation studies (Yuan et al., 2012). Similarly, Jien and Wang (2013) observed that *Leucaena leucocephala* biochar increased the CEC of a highly weathered tropical soil by 6.4 $cmol_c\ kg^{-1}$. However, other studies have reported

that biochar could not improve the CEC of soils with high initial CEC but rather soils of low initial CEC (Peng et al., 2011).

The direct release of base cations into soil solution after biochar amendment is an indication of soil fertility improvement, which has been reported to be due to the abundance of acidic functional group and also high surface area of biochar (Cheng et al., 2006). The increase in exchangeable plant nutrients including Mg^{2+}, Ca^{2+} and K^{+} in soil solution have severally been observed after biochar incorporation. The amount of these exchangeable cations have been shown to increase more than 60% in biochar amended soils (Wang et al., 2014). For instance, Mg^{2+} and K^{+} concentration in soils amended with corn cob biochar increased from 26 to 235 mg kg^{-1} and 18 to 163 mg kg^{-1} respectively (Wang et al., 2014). The percentage base saturation was raised from 5.4 to 22% (Cheng et al., 2006).

The addition of biochar has proven to decrease N_2O emission from soils of varying physicochemical properties (Stewart et al., 2012). For example, in a study using soybean and soybean biochar, N_2O emission was reduced by 50% and 80% respectively (Wang et al., 2013) On the contrary most studies have indicated that biochar addition did not have any effect on N_2O emission in some tropical soils (Clough et al. 2010). Reduction of N_2O emission is more sensitive to biochar produced at relatively low pyrolysis temperatures (300-400 ^{o}C) than at high temperatures possibly due to the high amount of carboxylic and phenolic groups capable of reducing N_2O emission (Wang et al., 2013).

Steiner et al. (2008) reported that the high CEC of biochar helps in reducing leaching of plant nutrients such as NH_4^{+} making it available for plant uptake. For instance, some researchers observed about 70% reduction of N leaching in a pot experiment (Lehmann et al., 2003; Major et al., 2009). In highly weathered soils, biochar has been affirmed as appropriate soil

amendment for reducing N leaching thereby increasing N use efficiency (Steiner et al., 2008).

2.7 Effect of biochar on phosphorus bioavailability in soil

Results regarding the influence of biochar on P availability in soils have inconsistently been reported in literature. Increased P availability have been observed in soils amended with biochar (Lehmann *et al*., 2006). However, others have reported decreased available P content in a soil column studies involving biochar produced from different feedstock (Novak et al., 2010). The increase in the pH of acid soils upon biochar application due to its high alkalinity (Ca^{2+}, Mg^{2+}) can lead to increase P availability by reducing P precipitation with Al^{3+} and Fe^{3+} (Steiner et al., 2007; Yuan et al., 2011; Chintala et al., 2013). In contrast, application of biochar to neutral and alkaline soils were found to decrease P bioavailability as a result of increased P sorption forming Ca-P and Mg-P compounds (Chintala et al., 2013).

Biochar has high native P content and therefore can directly discharge soluble P and increase its bioavailability in soil solution for plant use (Chan et al., 2007). Biochar can influence P dynamics in soil through its adsorbed chelating organic molecules such as phenolic acids and amino acids (Stevenson and Cole, 1999). The adsorbed organic molecules on biochar surface have the potential to reduce the capacity of Al^{3+}, Fe^{3+} and Ca^{2+} from precipitating P in soil (Xu *et al*., 2014). It is reported that biochar can influence P bioavailability by altering the ion exchange property of soil (Cheng et al., 2008). Newly added biochar to soil mostly has high anion exchange capacity and therefore has the tendency of undergoing competitive reaction with amorphous and crystalline Al and Fe oxides for P sorption (Hunt et al., 2007). Decrease in PZC and increased negative surface charge potential of soil amended with different biochar types have been observed (Hunt et al., 2007). The amount of negative charge on soil surface

at pH 7 is explained by CEC (Jiang et al., 2012). Addition of biochar is able to raise the CEC of soil hence decrease P availability as a result of electrostatic repulsion between the negatively charge soil surface and P ($H_2PO_4^-$ or HPO_4^{2-}) (Jiang et al., 2015). The carboxylic and phenolic functional groups on biochar surface especially on biochar produced at relatively low temperatures form chemical complexes with Fe and Al oxides and as such serves as a competitor with P for adsorption sites on soil surface (Chen et al., 2011; Cui et al., 2011).

The quantity and quality particularly the size and charge of biochar determines the level of competition (Jiang et al., 2015). Biochar is usually fine in size and has highly charged humic acids and thus, can act potentially competent competitor for P and can bring more P to soil solution (Liang et al., 2006). In this way, it reduces P adsorption by highly weathered tropical soils (Chen et al., 2011). Extracted humic acids from maize straw biochar increased P availability twice as much as humic acid from soil (Sohi et al., 2010). Similar observation in Terra Preta (Lehmann et al., 2006) and soil amended with sewage sludge biochar have been reported (Nelson et al., 2011).

The biogeochemical cycle of P in soils occurs by the breakdown of organic P and dissolution of inorganically bound P compounds initiated by microbial activities and hydrolytic enzymes released by plant roots. Soil microbes and enzymes are the major determinants of the breakdown of P (Bohme et al., 2005). The addition of biochar to soil have been reported to increase P mineralization by enhancing microbial activities (Bohme et al., 2005). Approximately 4% increase in microbial biomass was observed after the addition of water hyacinth biochar at a rate of 0.5% in soils from the tropics (Bohme et al., 2005; Jin et al., 2016). The hydrolysis of P is largely influenced by the pH of soil and with high soil pH alkaline phosphatase activities are enhanced (Du et al., 2014; Jin et al., 2016). In an incubation studies

3 to 4 time increase in phosphatase was reported in sandy clay soils amended with corn cob biochar charred at 360 ^{o}C (Du et al., 2014).

2.8 Phosphorus sorption capacity of soils in West Africa

Phosphorus sorption is a major challenge in highly weathered soils (Sanchez and Uehara, 1980; Trolove et al., 2003). In many cases where soils had adequate soil organic matter and nitrogen levels, phosphorus was found to be the most limiting nutrient (Trolove et al., 2003). Soils of tropical Africa are so heavily weathered and extremely variable that it is unwise to generalize. Even though the total amount of phosphorus in tropical soils is variable, highly weathered soils generally have low total phosphorus (Trolove et al., 2003). The myth surrounding soils of the tropics is that they have high P sorption capacity (Mokwunye and Hammond, 1992). Soils that require an addition of at least 100 mg P kg^{-1} of soil to give an equilibrium P concentration of 0.2 mg L^{-1} soil are considered as soils with high phosphorus fixing capacity (Sanchez and Uehara, 1980). Soils with sesquioxide to clay ratio of 0.2 or more are considered to have high P fixing capacity (Buol et al. 1975). The magnitude of phosphorus fixation is generally related to the pH of the soil, the Fe and Al oxides, exchangeable Al, Ca and $CaCO_3$ content.

Based on the crop response to applied P, Sahrawat et al. (1998) reported that most of the soils in the humid and sub-humid areas of West Africa were extremely deficient in available P. This is more severe as the applied P is transformed into stable P forms due to reactions with iron and aluminum oxides in acid soils (Owusu Bennoah et al., 1997; Abekoe and Sahrawat, 2001). Deficiency of phosphate occurs widely in the savannah soils which are high in sesquioxides (Abekoe and Sahrawat, 2001). Fixation of applied P is relatively high in soils derived from volcanic ash. However, the volcanic soils are of rather minor occurrence in the tropics

(Ahenkorah et al., 1993). Due the severity of low P content of some savannah soils of West Africa, plant growth stops as soon as the amount of P stored in the seed is exhausted (Wild and Jones, 1975). Acquaye and Oteng (1972) reported a mean total inorganic P content of 26 savannah soils as 81 mg P kg^{-1}, 93 mg P kg^{-1} for 8 forest/savannah intergrade soils and 124 mg P kg^{-1} for 14 forest soils. Owusu-Bennoah and Acquaye (1989) also reported that the total P values for topsoil of four modal forest soils ranged from 270 to 530 mg P kg^{-1} soil, whereas organic P values ranged from 54 to 243 mg P kg^{-1} soil. Recent report on total P values for some cultivated and uncultivated alkaline soils of the coastal savannah zone of Ghana was in a range of 415-723 mg P kg^{-1} (Asomaning, 2011).

Soils from West Africa have been classified according to their P sorption capacities, as related to soil mineralogy (Juo and Fox, 1977) (Table 2.2).

Since most soils in West Africa have 1:1 silicate clays and Fe and Al oxides, their P sorption capacities, based on Table 2.2, are expected to be low to medium (Owusu-Bennoah and Acquaye, 1989).

However, these P requirement data (Table 2.2) were for six-day period of equilibrating soils with P. Sorption and hence, the standard P requirement, could be more under field conditions where fertilizers undergo a longer period of contact with soils. Secondary, although data available indicate that most West African soils have low to medium P sorption capacities, it has been realized that ferruginous nodules contained in some soils do sorb P and are capable of raising the P sorption levels of whole soils (Tiessen et al., 1993).

Table 2. 2 Classification of standard P requirement (mg P kg^{-1}) as influenced by soil minerals

Standard P requirement at 0.2 mg L^{-1} soil	Scale	Usual mineralogy encountered
< 10	Very low	Quartz, organic materials
10 – 100	Low	2:1 clays, quartz, and 1:1 clays
100 – 500	Medium	1: 1 clays with Fe, Al oxides
500 – 1000	High	Oxides, moderately weathered ash
> 1000	Very high	Desilicated amorphous materials

Source: Juo and Fox, 1977

2.9 Phosphorus sorption in soil

Sorption is vital chemical process in soils because it affects the fate and mobility of plant nutrients and contaminants. Sorption is a general term referring to reactions namely adsorption, precipitation and diffusion into soil crystals, and is used only when the mechanism of retention at the surface is not known (Sparks, 2003). Adsorption refers to the "accumulation of a substance or material at an interface between the solid surface and bathing solution" (Sparks, 2003). It is a two-dimensional chemical process excluding three-dimensional chemical processes such as co-precipitation, surface precipitation and diffusion into the crystal (Scheidegger and Sparks, 1996). Desorption on the other hand is the release of the adsorbate to the soil solution (sorptive solution). Phosphate sorption is a term used to explain chemical and physical reactions that takes P from the soil solution into the soil solid phase (Scheidegger and Sparks, 1996). There are two types of reaction namely P sorption on the surface minerals and formation of P precipitates in soil solution including as Ca-P, Fe-P, Al-P, Mg-P (Trolove et al., 2003).

2.9.1 Acid Soils

Amorphous Al and Fe oxides compounds are the important soil factors that determines its capacity to fix P (Borggaard et al., 1990). This is because the poorly ordered ("amorphous") Fe and Al hydroxides possess very high specific surface area (SSA) which can be as high as 800 $m^2\ g^{-1}$, ten times higher than the SSA of the corresponding crystalline forms. Ferrihydrite and lepidocrocite as amorphous minerals are found to exhibit high P adsorption and adsorption rate (Guzman et al., 1994). Aluminium oxides are found to have high sorption affinity for phosphate than that of iron oxides (Borggaard et al., 1990). On per mole basis Al oxides adsorb almost

50% more of phosphate than oxalate-extractable iron oxides. This could be attributed to relatively high specific surface area (poor crystallinity) of the Al oxides than iron oxides and also a greater charge on the former (Wei et al., 2014). For synthetic oxides the amounts of phosphate adsorbed per m^2 seem to be higher for Al oxides than for iron oxides, although the trend is weak (Wei et al., 2014). This implies that the variation in crystallinity is the major rationale behind the differences in adsorption capacity (Borggaard et al., 1990).

The occurrence of goethite which is mostly promoted by low soil pH and high organic carbon content (Kämpf et al., 2009), mostly has a higher P sorption capacity than hematite (Guzman et al., 1994). Synthetic and natural goethite with varying morphologies have been reported to have of 2.51 µmol P m^{-2} as maximum adsorption capacity for the binuclear complex on the (110) face (Torrent et al., 1992; Strauss et al., 1997, Wang et al., 2013), whereas it is 0.19 to 3.33 µmol P m^{-2} for hematites with different morphologies and crystallinity (Barron et al., 1988; Wang et al., 2013). The P sorption capacity of goethite is relatively higher than kaolinite, due to the spread of ≡Fe-OH groups on entire surface of goethite while ≡Al-OH groups on the surface of kaolinite are found solely at the edges of the crystal structure (Wei et al., 2014).

The smaller particle size of amorphous minerals and hence its larger surface area makes it more soluble than their crystalline minerals. For example, the variscite ($AlPO.2H_2O$) as a crystalline mineral has a surface area of 1.54 m^2/g (Mattlingly, 1975) and its solubility product (K_{SP}) is $10^{-30.5}$ (Wei et al., 2014). On the other hand, its amorphous Al- phosphate counterpart has a surface area of 10.5 m^2/g (Sanchez and Uehara, 1980) and its K_{SP} is $10^{-28.1}$ (Sposito, 2008).

Phosphorus is mostly adsorbed by hydroxyl surface groups of Fe and Al oxides, which below pH of 7-9 develop positive charge through protonation (Sparks, 2003; Sposito, 2008). The reaction of water with Fe or Al ions on a mineral surfaces and also the completion of it

coordination with hydroxyl groups is termed as hydroxylation (Stumm, 1992). Singly, doubly and triple coordination are formed when hydroxyl groups are coordinated by one, two or three Fe atoms respectively (Sparks, 2003; Sposito, 2008). Two different chemical processes are formed due to the protonation of the hydroxyl groups namely; the adsorption of phosphate due to positive electric field created and replacement of protonated hydroxyl groups with phosphate.

Phosphate ions may be adsorbed in monodentate or bidentate form based on the number of hydroxyl groups associated with phosphate that react with Fe atoms, or in binuclear form when two Fe atoms are bonded to two hydroxyl groups in phosphate.

Spectroscopic and microscopic techniques have been employed to observe and investigate the local bonding environment of phosphate with clays and metal oxide surfaces (Parfitt, 1989; Goldsberg and Sposito, 1984). With the use of infrared (IR) absorption, Parfitt, (1989) showed that the adsorption of P by goethite surface led to the loss of hydroxyl group. This affirms that ligand exchange is the mechanism by which phosphate is adsorbed by iron oxides leading to the formation of inner-sphere complex (Weng et al., 2011).

Further studies using spectroscopic techniques have shown that the adsorption of P unto the surface of soil minerals involves; a bidentate, binuclear bridging complex with Fe (III) on iron oxide surfaces and on the edge sites of Al oxides (Luengo et al., 2006; Arai and Sparks, 2007). Wang et al. (2013), studying P adsorption mechanism on ferrihydrite, goethite and hematite also suggested that P adsorption on Fe oxides/hydroxides is principally bidentate binuclear complex. Others have also reported the same P adsorption mechanism on boehmite and goethite (Li et al., 2010; Kim et al., 2011).

Diffusion of the adsorbed phosphate into the solid is termed absorption. Precipitation of Fe and Al oxides on soil mineral surface can result in the trapping of adsorbed P. The trapped P in the nanopores of Fe/Al oxides is then described as occluded thereby becoming unavailable to the plants (Arai and Sparks, 2007).

It is reported that adsorbed P can also be desorbed thermodynamically (Barrow, 1978); however, the rate of P desorption bank on several factors including the type of clay minerals on which the P is adsorbed (Chintala et al., 2014). According to Parfitt (1989), the binding energy between P and soil minerals increases in the order of monodentate > bidentate > binuclear complexes and the chances of P desorption increases in the reverse order. Kirk et al. (1999) proposed that disequilibria-desorbable P and ligand-desorbable P are the two main mechanisms for P desorption.

2.9.2 Alkaline and calcareous soils

The dynamics of P in alkaline and calcareous soils is controlled mainly by adsorption onto the surfaces of calcite, Fe and Al oxides and precipitation as Ca-P (Hedley & McLaughlin, 2005; Olsen et al., 1954; Saavedra & Delgado, 2005; Sato et al., 2005). Several studies have been done on the chemical interactions of soluble P and calcite (Wang & Nancollas, 2008; Boanini, et al., 2010). Surface adsorption following precipitation reaction has been indicated to be the major mechanisms of P removal in alkaline and calcareous soils, decreasing P availability for plant uptake (Boanini, et al., 2010). Phosphate precipitation in soil solutions or on clay surfaces includes metastable intermediate precursor formations namely amorphous calcium phosphate (ACP) and brushite (DCPD) during the precipitation of P in soil solution proceeded by the

formation of least soluble, hydroxyapatite ($Ca_{10}(PO_4)_6(OH)_2$, HAP). Hydroxyapatite is the final stable phase of Ca-P compound formation in neutral to alkaline soils.

Most Ca-Ps can dissolve in acids but insoluble in water (Wang & Nancollas, 2008). The solubility of P is depends largely on both the activities of H^+ and Ca^{2+} in calcareous soils (Olsen et al., 1954). As the activity of H^+ increases, the activities of Al and Fe increase by dissolution of hydroxide precipitates whereas increasing the activity of Ca^{2+} decreases the solubility of P by forming Ca-Ps (Olsen et al., 1954). The Ca to P molar ratio (Ca/P) and their solubility are vital for differentiating among the various phases of Ca-P compounds (Wang & Nancollas, 2008). Among all the Ca-P compounds, hydroxyapatite (HAP), is one of the most stable, the densest and the most insoluble (Boanini, et al., 2010), and is favorably formed under neutral or alkaline environs (Wang & Nancollas, 2008). Hydroxyapatite formation rate is relatively slower than other Ca-Ps (Wang & Nancollas, 2008). When the Ca/P is 1.67, HAP precipitates and when the ratio decreases to 1, brushite precipitates. Transformation of HAP into brushite occurs when the Ca^{2+} ions are consumed in solution (Eqn. 2.4) (Boanini et al., 2010; Oliveira et al., 2007).

$$Ca_{10}(PO_4)_6(OH)_{2(s)} + 4H^+ + 2H_2O \rightleftharpoons 2CaHPO_4.2H_2O_{(s)} + 8Ca^{2+} + 4PO_4^{3-} \quad Eqn.2.4$$

Brushite, which has a chemical formula, $CaHPO_4 \cdot 2H_2O_s$, comprise units of $CaPO_4^-$ arranged in parallel with water molecules as interlayer (Wang & Nancollas, 2008). Brushite is the predominant Ca-P phase below pH 6.5 (Freeman & Rowell, 1981; Wang & Nancollas, 2008), and easily hydrolyzes to the more stable phases of OCP and HAP (Boanini et al., 2010). In soils with pH > 6.3, brushite transforms with time to OCP, which has a chemical formula,

$Ca_8H_2\,PO_4\,6{\cdot}5H_2O_{(s)}$ (Grossl & Inskeep, 1991; Hedley & McLaughlin, 2005; Ippolito et al., 2003). Soils with high amount of calcium carbonate, OCP forms faster without the formation of brushite and therefore serves as an intermediate crystalline phase (Hedley & McLaughlin, 2005). Above pH 6.5, the formation of OCP is more pronounced (Wang & Nancollas, 2008). Octacalcium P is frequently encountered in systems containing Ca-Ps and appears to have a significant role in the chemistry of precipitated Ca-Ps (Brown, 1962). Octacalcium P has a similar structure to HAP as a result of its layered structure consisting of apatitic and hydrated layers (Wang & Nancollas, 2008), although the two minerals are not *iso*structural, and OCP is composed of apatitic layers that are parallel to the *b-c* plane and separated by hydrated layers (Brown, 1962). The amount of water in OCP crystals is about 0.2 times of the brushite, accounting for the lower solubility of OCP (Wang & Nancollas, 2008). Octacalcium P is not stable as compared to HAP and tends to convert to HAP in aaccordance with the chemical equation below (Eqn. 2.5) (Wang & Nancollas, 2008).

$$Ca_8H_2(PO_4)_6.5H_2O_{(s)} + 2Ca^{2+} \leftrightharpoons Ca_{10}(PO_4)_6\,(OH_2)_{(s)} + 4H^+ + 3H_2O \qquad Eqn.\ 2.5$$

It is reported that HAP and OCP were identified by X-ray absorption near-edge structure (XANES) spectroscopy and comprised up to 85% of the total P of slightly alkaline soils at pH of ~7.5 (Beauchemin et al., 2003).

The formation of stable Ca-Ps phases such as HAP can be prevented by the presence of ions in soil solution, culminating into kinetic stabilization of brushite or OCP (Wang & Nancollas, 2008). For example, carbonate ions (CO_3^{2-}) can substitute for PO_4^{3-} ions in HAP (Boanini et al., 2010; Cao et al., 2007), inhibiting HAP crystal growth and its incorporation into the mineral

structure results in a poorly crystalline phase with an increased solubility (Boanini et al., 2010). Because of the similarity of CO_3^{2-} radius and PO_4^{3-} radius, substitution of CO_3^{2-} for PO_4^{3-} readily occurs, thus a long-term inhibitory effect of $CO^2{}_3^-$ on precipitation of HAP is possible (Cao et al., 2007). Carbonate also reacts with Ca to form $CaCO_{3(s)}$ (Eqn. 2.6) at alkaline pH, thus inhibiting formation of not only HAP, but also other Ca-Ps. Therefore, the formation of $CaCO_3$ has to be considered when estimating formation of Ca-Ps, especially in alkaline soil pHs.

$$\boldsymbol{CaCO_{3(s)} \leftrightharpoons Ca^{2+} + CO_3^{2-} \qquad pK_{sp} = 8.48} \qquad \boldsymbol{Eqn.}\ 2.6$$

Magnesium ions, Mg^{2+} are known to significantly inhibit the nucleation and growth of crystalline HAP, thus kinetically stabilizing brushite or OCP during precipitation reactions (Boanini et al., 2010; Cao et al., 2007; Wang & Nancollas, 2008). Boanini et al. (2010) reported that the formation of brushite or OCP is less affected by the presence of CO_3^{2-} and Mg^{2+}, thus they are not as affected as is the formation of HAP. In the presence of Zn^{2+}, there is a significant decrease in the growth of HAP and hence the deformation of the structure (Boanini et al., 2010; Wang & Nancollas, 2008) due to its smaller ionic radius (0.075 nm) with respect to Ca^{2+} ion (0.099 nm) (Boanini et al., 2010). Work done by Xu et al. (2013) indicated that the formation of Ca-P precipitate is hindered in the presence of Mg^{2+} in soil solution pH below 9. However, Mg^{2+} ions promote the formation of Ca-P in alkaline soils of solution of pH between 9.0 and 12.0.

Magnesium ion has the tendency of reducing free Ca activities in slightly acidic soils thereby making soluble complexes of $H_2PO_4^-$ and HPO_4^{2-} available in soil solutions (Xu et al., 2013).

Again, Mg^{2+} ions change phosphate precipitation in soil solution (Millero et al., 2001). This is because the hydrated form of Mg^{2+} ions is of large ionic size and therefore able to decrease the nucleation and crystallization of Ca phosphate precipitates (Yadav et al., 1984). On the contrary, $CaCO_3$ has been found to adsorb P in the presence of Mg^{2+} ions in aquatic environment due to the increase formation of CO_3-Mg-PO_4 bonds on $CaCO_3$ surface (Millero et al., 2001)

Hydrophilic surfaces in organic matter (OM) under biological conditions can also promote the nucleation and growth of OCP crystallites, with functional groups such as phenolic and carboxylic acting as active nucleation sites (Wang & Nancollas, 2008). The adsorption of organic acids onto brushite crystal promote the formation of nuclei for new brushite crystals thereby restricting its transformation of OCP or HAP (Hedley & McLaughlin, 2005; Inskeep & Silvertooth, 1988). For example, humic acid is dominated by carboxyl functional groups, which provide ideal ligands to bind with Ca ions from solutions forming Ca-humate complexes (Alvarez et al., 2004). Grossl and Inskeep (1991) reported that brushite is able to overgrow adsorbed humic and fulvic acids, therefore, the formation of brushite is kinetically favored compared to other Ca-Ps in the presence of organic acids under acidic conditions (Grossl & Inskeep, 1991). A variety of Ca-Ps may coexist in soils, and brushite and OCP may be predominant minerals for calcareous soils rich in OM below and above pH 6.5, respectively. As the stability of Ca-Ps depends on soil pH and ion contents, it is important to know the stability of each Ca-Ps in specific soil conditions for understanding plant available P in calcareous soils.

2.10 Phosphorus adsorption isotherm

Adsorption isotherm shows the distribution of adsobate between the solid phase and the liquid phase when the adsorption reaction approaches an equilibrium state. Phosphorus intensity, capacity and quantity are the three major parameters of P adsorption isotherm controlling P availability in soil solution. The adsorption isotherm is an important technique in assessing the interaction of anions including arsenate with oxides and has been deployed often times in literature to determine soil adsorption capacity (Olsen and Watanabe, 1957; Barrow, 1978). The adsorption capacity of soil serves as a prerequisite for the classification of temperate and tropical soils (Breeuwsma et al., 1986).

Many researchers have reported that P sorption isotherms (Fox and Kampath, 1970) can be used to find out the quantity of added P needed to make P bioavailable in soil solution for optimum plant yield. It is also used to find out the soil components that are involved in the sorption and the nature of the sorption process to know more about the mechanism the sorption process (Barrow, 1979).

A number of adsorption isotherms equations has been used to describe phosphate reaction with Fe and Al minerals including Langmuir equation (Olsen and Watanabe, 1957; Jiao et al., 2008), Freundlich equation (Jiao et al., 2008), Temkin equation (Rudzinski and Panczyk, 2000) and Elovich equation (Dimirkou and Ioannou, 1998). Langmuir, Freundlich and Tempkin isotherm equations are the most widely used to explain the relationship between equilibrium P concentration and P adsorbed by soil minerals (Sanyal et al., 1993).

2.10.1 Langmuir

Langmuir equation was initially developed to describe gas adsorption onto solid surfaces. Olsen and Watanabe (1957) used this equation to explain phosphate adsorption in soils. The underlying assumption of Langmuir equation is that the energy of adsorption is independent of the surface coverage.

The three major principles underlying Langmuir isotherm are;

1. There is a constant energy of adsorption, implying no interaction between adsorbed molecules on the soil surface
2. Adsorption is on localized sites, meaning no translational motion of adsorbed ions in the plane of the surfaces and
3. The maximum adsorption possible corresponds to a complete mono ionic layer.

The nonlinear form of Langmuir equation can be written as:

$$qe = \frac{KQCe}{1 + KCe} \qquad Eqn.2.7$$

Ce (mg L^{-1}) is the equilibrium concentration of adsorbate; Q is a measure of maximum adsorption, the upper limit of adsorbate that can be adsorbed by the adsorbent*;* *K* determines the initial slope of the isotherm and also describes the binding affinity of the adsorbate and the adsorbent. The parameter *b* represents the value of $\boldsymbol{qe}$ that is approached asymptotically as $\boldsymbol{Ce}$ becomes arbitrarily large. By rearrangement, equation 2.7 can be expressed in linear forms such as:

$$\frac{Ce}{qe} = \frac{Ce}{Q} + \frac{1}{QK} \qquad Eqn.2.8$$

The straight line resulting from plotting Ce/qe against *Ce* will have slope equal to 1/Q and an intercept equal to 1/QK.

The efficiency of Langmuir equation can be determined using a dimensionless equilibrium parameter R_L (Malik, 2004). The R_L has been used to know the efficiency of the adsorption process:

$$R_L = \frac{1}{1 + KC_i} \qquad Eqn.2.9$$

where C_i is the initial orthophosphate concentration (mg L^{-1}). The adsorption is considered as irreversible when $R_L = 0$, favorable when $0 < R_L < 1$, linear when $R_L = 0$ and unfavorable when $R_L > 0$.

2.10.2 Freundlich Isotherm

Phosphorus adsorption was initially described using Freundlich equation (Russell and Prescott, 1916). Barrow (1978), suggested that phosphorus retention data from dilute phosphorus solution can be fitted to Freundlich equation in the following form:

$$qe = K_f Ce^n \qquad Eqn.2.10$$

where *Kf* and *n* as empirical parameters represent the binding affinity (mg $^{(1-n)}$ L^{n} kg^{-1}) and the linearity constant respectively.

The equation was formally empirical, without any theoretical physicochemical foundation, and no significance can be attached to the coefficients (Olsen and Watanabe, 1957; Aslam *et al.*, 2000; Arshad et al., 2000; Javid and Rowell, 2003; Chaudhry et al, 2003). It implies an exponential decrease in energy of adsorption, as portions of the occupied surface increases. Freundlich equation can be extrapolated under the assumption that increasing surface coverage leads to a decrease in adsorption energy as a results of the heterogeneous nature of the adsorbent surface. Freundlich equation is normally used in its logarithmic form;

$$\boldsymbol{log\, qe = \frac{1}{n} logCe + log\, Kf} \qquad \boldsymbol{Eqn.2.11}$$

The plot of log *q*e versus log *Ce* has a slope with the value of 1/*n* and an intercept magnitude of log *Kf*. When the Freundlich constant *n is* between 1 and 10, adsorption is considered favorable. The larger the n value, the stronger the interaction between adsorbent and adsorbate. With 1/*n value of* 1, linear adsorption occurs culminating into identical adsorption energies for all sites.

2.11 Factors affecting P adsorption

2.11.1 Organic matter

Phosphorus interaction with organic matter can be directly or indirectly controlling P sorption reactions (Huang and Wang, 1997). Indirectly by inhibiting Fe/Al oxide crystallization and directly by competing for adsorption sites (Borggaard et al., 1990).

Competitive sorption reaction between high molecular weight organic acids such as humic and fulvic acids (Sibanda and Young, 1986) or low molecular weight organic acids and P for soil sorption sites (Hue, 1991) is considered one of the direct effect of organic matter on P availability in soil. Comparatively, organic acids have greater affinity for Al and Fe oxides than P (Huang and Violante, 1986). High molecular weight orgainc acids were also reported to be adsorbed to the structural edges and the exposed hydroxyl of Al and Fe oxides minerals (Huang and Wang, 1997). The chelation of Fe^{3+}, Ca^{2+} and Al^{3+} by organic anions lead to the release of inorganic P bound by these cations (Jones et al., 1996), and organic anions that compete with P adsorption on the surface of soil particles further promote the desorption of adsorbed P (He et al., 1998) resulting in high P concentration in soil solution. Addition of white clover residue lead to the decrease in the point of zero charge (PZC) of the soil (Easterwood and Sartain, 1990). The decrease in PZC would culminate into high cation exchange capacity and increase anion repulsion, leading to increased P availability for plants uptake.

The process by which organic anions alter the chemical structure of an adsorbent through metal complexation and removal is termed as dissolution. Kirk et al. (1999) reported that the oxygen-containing functional groups (-OH, -COOH, -C=O) in soil organic matter can enhance dissolution of soil minerals by complexing and dissolving metals into soil solution and increasing their availability to plants and microorganisms. Two major mechanism leading to P

discharge from the surface of Fe and Al oxides have been proposed. These mechanisms are ligand exchange and ligand enhanced dissolution of oxides of Al and Fe. Ligand exchange (Eqn. 2.12) is a chemical reaction which involves the exchange of P from soil surface with organic ligands, consequently discharging P into soil solution (Nagarajah et al., 1968; Hue, 1991; Geelhoed et al., 1999). Ligand enhanced dissolution involves the adsorption of organic ligand at adsorbent surface (i.e. surface of Fe and Al oxides), leading to the dissociation of the adsorbent and discharge of adsorbed P into the soil solution (Earl et al., 1979; Jones et al., 1996; Kirk et al., 1999).

On the other hand, organic matter interaction with aluminium and iron oxides also increase P adsorption capacity by inhibiting their crystallization and polymerization (Schwertmann, 1991). Crystallization of ferrihydrite was normally inhibited or delayed by organic acids by the effect of phosphate adsorbed on the ferrihydrite surface hindering aggregation prior to hematite formation (Bigham et al., 2002). The retardation of crystal growth of amorphous and poorly crystalline aluminium and iron oxides by organic acids, results in high specific surface areas thereby increasing P adsorption capacity of soil (Huang and Wang, 1997).

2.11.2 Effect of concentration of adsorbate

Adsorption process can be affected by the concentration of organic and inorganic compounds. Anbia and Hariri (2010) pointed out that the initial concentration serves as a key factor for controlling all mass transfer resistance of the adsorbate between the liquid and solid phases. Concentration determines the capacity factor of the adsorption (Rumhayati et al., 2012). According to Rumhayati et al. (2012) phosphate adsorption on acrylamide-ferrihydrite gel is

higher at relatively low concentration because at higher concentrations there is interaction amongst the ions thereby decreasing affinity of the ions to be sorbed.

Quantity of adsorbent also influences P adsorption process since it tells the amount of P that can be adsorbed by the adsorbent for any given initial P concentration (Mostafapour et al., 2013). At the early stage of adsorption process, there is high P removal efficiency due to high vacancy of the exchangeable sites of the adsorbent (Pandey et al., 2009; Kaczala et al., 2009). The high adsorption efficiency of P can also be ascribed to the increase in the amount of adsorbent as well as availability of adsorption sites for solute adsorption (Li et al., 2010; Mostafapour et al., 2013). The adsorption rate is dependent on the availability of the exchangeable surface sites. At the early stage of the adsorption process, most of the adsorptive sites are uncovered and therefore the rate of adsorption increases whereas as the covered surface increases, the adsorption rate declines. Eventually, at certain stage of the adsorption process, even upon further addition of adsorbent, there will be no more adsorption, and at that time, the adsorption process is said to be at equilibrium (Mostafapour et al., 2013).

2.11.3 Temperature

Temperature influences the rate of physical and chemical reactions. There are three main effect of temperature on phosphorus reaction in soil (Barrow, 1979).

1. The position of the equilibrium between phosphate in solution and adsorbed phosphate,
2. The rate of movement from adsorbed to firmly-held, and
3. Rate of movement from firmly-held to adsorbed phosphate.

Mostly, the rate of phosphorus reaction with soil increase with increasing temperature (Barrow, 1979). Theoretically, a rise in temperature increases the kinetic energy of molecules leading to

the formation of new reaction state. The molar solubility of Al, Fe and Ca compounds such as variscite, strengite and apatite increases at high temperatures. High temperature also increase soil microbial activities which intend helps in the discharge of phosphate from organic materials. White (1981) reported that raising temperature from 298 K to 308 K leads to an increase in P adsorption in soils.

The rate of P dissolution increases as temperature increases and further reaction with soil minerals forming insoluble P compounds. For every 288 K increase in temperature results in 33% reduction of available P (Tisdale et al., 1985).

Phosphorus adsorption in tropical soils are relatively higher than in temperate soils. Due to high temperatures, tropical soils are dominated with high amount of sesquioxides. A number of studies have indicated that at high temperatures, phosphorus adsorption increases (Muljadi et al., 1966; Kuo and Lotse, 1974).

2.11.4 Effect of time on P sorption

Phosphorus adsorption by soils and many soil components follow two distinct patterns: an initial fast reaction proceeded by a slower reaction. The adsorption reaction involving exchange of phosphate for anions and ligands on the surface of Fe and Al oxides are extremely rapid (White, 1981; Tisdale et al., 1985). The slower continuing adsorption reactions may involve such changes as:

a. Diffusive penetration or chemisorption of surface-adsorbed phosphorus into soil constituents, e.g. the incorporation of phosphorus into hydroxy aluminum or iron polymers and occlusion of phosphorus in the surface of calcite.

b. The precipitation of a phosphorus compound for which the solubility product has been exceeded.

These slow reactions involve a change in the bonding strength between phosphorus and mineral surface from more lightly bound to more tightly bound types which are less accessible to plants.

An important practical aspect of time is the period after application of fertilizer. On some soils with high adsorption capacity, the period of reaction is short, whereas on others the period may last for months or even years. For instance the slow reaction of phosphate with oxides has been attributed to formation of iron phosphate, forming a surface coating on the oxides (Jonasson et al., 1988). The porous structure often observed in goethite may similarly account for slow phosphate adsorption but also for slow desorption and thus irreversibility (Cornell and Giovanoli, 1986). Accordingly, adsorption of phosphate by well crystallized goethite having few pores was complete after 3 days and remained constant up to 260 days (Cornell and Giovanoli, 1986; Schwertmann, 1991). According to Schwertmann (1991) aluminium substituted goethite crystals are generally smaller and less porous than non-substituted goethite crystals therefore the former should adsorb phosphate faster than the latter.

2.12 Phosphorus desorption

2.12.1 Soluble salts (phosphorus-free solution)

Phosphorus desorption has been studied using water and P-free solutions such as potassium chloride (KCl) and calcium chloride ($CaCl_2$) to induce desorption. The amount of P released (P desorbed) after equilibrating soil with deionized water at a ratio (soil/deionized water) ranging from 1:10 to 1: 100 have been reported in many literature (Dimirkou et al., 1993). The use of 0.01 M $CaCl_2$ has been used to examine P desorption in kinetic studies. Studies have

shown that 0.01 M $CaCl_2$ is similar to the ionic strength of natural soil solution (Robbins et al., 1999).

A study conducted by McDowell and Sharpley (2003) on the extraction of soil phosphorus with different soil to $CaCl_2$ solution for predicting plant availability in sandy soils under varying extraction times observed a significant increase in $CaCl_2$ extractable P per kg soil by soil: extractant ratio of 1:10 compared with 1:2. They further elucidated that the significant increase of P with the high extraction ratio (i.e. 1:10) was attributed to an ion exchange reaction. It was further elucidated that P in extraction solution and that of the exchange sites of the soil surface may reach equilibrium with 2 hours of shaking. Further increase in the extraction solution ratio from 1:2 to 1:10 will lead to more P released from the exchange sites until another equilibrium is reached (Sposito, 2008). Others have argued that the release of P from colloidal exchange sites could be due to chemical dissolution of P bound to organic and inorganic compounds since Cl^- ions can poorly be exchanged with P (Jaszbereni and Loch, 1996).

Phosphorus desorption studies conducted on some temperate soils using varying extraction solution ratios (soil: 0.01 M $CaCl_2$ salt) have shown that the amount of P desorbed increased as the extraction solution ratio widened (Hesketh and Brookes, 2000). The use of 0.01M $CaCl_2$ has been recommended as a worldwide soil extractant for P desorption (Houba et al., 1986). In earlier studies, significant relationship has been obtained between the 0.01M $CaCl_2$ desorbed P and P fertilizer dose and between $CaCl_2$-P and the estimated P balance (Jaszbereni and Loch, 1996). They also reported the importance of 0.01M $CaCl_2$ in predicting the P supply potential using the soils under 40 years of cultivation. Recent investigations on the use of 0.01 $CaCl_2$ have also revealed that this extractant can be used to characterize the potentially available P and the P in solution (McDowell and Sharpley, 2003). The disadvantage of these methods

however is, they release small concentrations of P since new equilibrium is established as the P concentration in soil solution increased. More P is released as the extraction process is repeated (Freese et al., 1995).

2.12.2 Phosphorus binding materials

The release of P from soil surface can also be studied by using material that can strongly bind P, by making sure that P activity in soil solution is low to enable the continuous released of P from soil colloids. Anion exchange resins (AER), hydrous ferric oxide (HFO) and Fe or Fe-Al oxide impregnated filter paper have been used as P binding materials (Abrams and Jarrel, 1992).

Anion exchange resins have been considered as competitive exchangers with those soil colloids that are in dynamic equilibrium with the soil solution. At low pH (i.e. 4.3 to 5.1), $H_2PO_4^-$ is removed from the soil colloidal surface and is anchored onto the anion exchange resin. Anion exchange is the main mechanism controlling P removal from soil solution and as such there is a likelihood of P competition with other anions at the resin sorption sites, principally if the activities of other anions are high. On the contrary, surface precipitation and adsorption through ligand exchange are the two main mechanism controlling P reaction with resin coated with metal oxides (Menon et al., 1990). Traina et al. (1986) reported that this reaction is usually irreversible despite the fact that other anions including selenate and organic acids have been shown to compete with P sorbed to crystalline and amorphous Fe and Al oxides. The resin extraction method is considered the best chemical based soil P tests for assessment of P availability for plant uptake (Ibrikci et al., 1992).

The ability of resin to adsorbed P from solution depends largely on the chemical of the resin such as resin-OH, resin-Cl, and resin-HCO_3 (Freese et al., 1995). Freese et al. (1995) stated that the HCO_3^- form is better than the Cl^- form because the HCO_3^- form of the resin adsorb high amount of exchangeable P from acid and alkaline tropical soils. In a study, the P adsorbed by resin-HCO_3 was significantly and directly related to plant growth, seemingly because it is similar to the chemistry of the rhizosphere soil due to HCO_3^- accumulation in the medium (Sibbesen, 1978).

The use of Fe or Fe-Al oxide coated filter paper has been considered as better alternative for inorganic P sink than the resin (Sharpley, 1991). The two major drawbacks of this method however made it inappropriate to study P desorption in soils under long term cultivation. First and foremost, the Fe-Al oxide coated filter paper strips are usually not stable when used for longer desorption times, resulting in substantial losses of the P sink in to the soil sample. Fine size soil particles are trapped by the filter during extraction and since any P in association with these particles are accounted for as P extracted, there is always an overestimation of the amount of P extracted (Freese et al., 1995).

The use of cation anion exchange resin membranes (CAERM) has also been reported in literature (McKean and Warren, 1996; Delgado and Torrent, 2000) for extraction of soil P. The reports revealed that this method is in general effective in extracting more amounts of P than the other methods. The relative effectiveness of CAERM method is probably due to promoted dissolution of metal phosphates. It decreases cation activity in soil solution with concomitant decrease in the ionic activity product and promoting metal phosphate dissolution (Delgado and Torrent, 2000).

2.13 Adsorption Kinetics

Studies on P adsorption using sorption isotherms is relevant for the determination of the effectiveness of adsorption. However, it is also important to find out the mechanism controlling P adsorption. Kinetics models have been used to assess the mechanism underlying P adsorption and its potential rate limiting steps including mass transport and chemical reaction processes (Huang *et al*., 2008). Adsorption kinetics is defined as the rate of removal of adsorbate that influences the time the adsorbate stays in the solid-liquid interface (Huang et al., 2008).

Over the years, different mathematical models have been used to describe adsorption data. These mathematical models have been categorized into two, namely adsorption reaction models and adsorption diffusion reaction models. Adsorption diffusion model emphases on the movement of adsorbate from aqueous solution into the pores of adsorbent whiles adsorption reaction model also explains the rate of chemical interaction between adsorbate and adsorbent (Qiu et al., 2009).

Examples of adsorption kinetic models that have been proposed to comprehend the adsorption reactions and potential rate-controlling step are pseudo-first order model, pseudo second-order model, intraparticle diffusion model (Weber and Morris, 1963) and Elovich's model. The above-mentioned models are the most widely used models in several kinetics studies (Cheng et al., 2008; Huang et al., 2008; Rosa et al., 2008).

2.13.1 Adsorption reaction model

Pseudo first-order model

The sorption of low molecular weight organic acids onto char in a liquid-solid phase systems was first described using Lagergren's first-order rate equation in 1898. Lagergren's first-order

rate equation is also considered as pseudo first order model. This model has also been used to remove chemical pollutants from wastewater during the last four decades (Ho, 2004).

In the Lagergren's equation, the sorption rate is directly related to the number of available sorption sites:

$$\frac{dq_t}{dt} = k_1(q_e - q_t) \qquad Eqn.2.12$$

where q_t (µg g^{-1}) is the amount of PO_4-P adsorbed onto the solid fraction at a time t (h), q_e (µg g^{-1}) is the PO_4-P sorption capacity at equilibrium, and k_1 is the Lagergren's first-order rate constant of sorption (h^{-1}).

Eqn. 2.12 was integrated with the boundary conditions of t=0 to t = t and q_t=0 to q_t = q_t to yield:

$$\ln \frac{q_e}{q_e - q_t} = k_1 t \qquad Eqn.2.13$$

and thus:

$$qt = q_t\left(1 - e^{-k_1 t}\right) \qquad Eqn.2.14$$

Eqn. 2.14 may be rearranged to a linear form:

$$\log(q_e - q_t) = \log q_e - \frac{k_1}{2.303} t \qquad Eqn.2.15$$

Plotting $\log(q_e - q_t)$ versus *t* it is possible to find out the kinetic constant k_1.

Pseudo-second-order model

A second order kinetic model was first used to explain the removal of NH_4^+ ions from zeolite by divalent cation in solution (Blanchard et al., 1984).

Contrary to the Lagergren's first-order equation, for the application of the pseudo-second-order rate equation it is not necessary to know the equilibrium sorption capacity in advance. The differential equation corresponding to the pseudo-second order equation is the following (Ho and McKay, 1998):

$$\frac{dq_t}{dt} = k_2(q_e - q_t)^2 \qquad \textbf{Eqn. 2.16}$$

where k_2 (μg^{-1} g h^{-1}) is the pseudo-second order kinetic constant.

In this expression, as it was in the Lagergren's equation, the number of available sorption sites (to which q_e-q_t is proportional) is the driving force for sorption.

Separating the variables in Eqn. 2.16:

$$\frac{dq_t}{(q_e - q_t)^2} = k_2 dt \qquad \textbf{Eqn. 2.17}$$

Integrating equation (2.17) for the boundary conditions t = 0 to t = t and q_t = 0 to q_t = q_t:

$$q_t = \frac{q_e^2\, k_t t}{1 + q_e k_2 t} \qquad \textbf{Eqn. 2.18}$$

which is the integrated rate law for a second-order reaction and can be rearranged to give:

$$q_t = \frac{t}{\frac{1}{k_2 q_e^2} + \frac{t}{q_e}} \qquad \textbf{Eqn. 2.19}$$

The linear form of Eqn. 2.19 is:

$$\frac{t}{q_t} = \frac{1}{k_2 q_e^2} + \frac{1}{q_e} t \qquad \textbf{Eqn. 2.20}$$

The pseudo second-order equation constants can be determined experimentally by plotting t/q_t versus t.

Elovich model

Elovich's model is a rate equation based on the sorption capacity which was first used in 1934 by Zeldowitsch (Zeldowitsch, 1934) to explain how manganese dioxide adsorbed carbon monoxide, which exponential decrease with an increase in the quantity of gas adsorbed. The Elovich model was formally developed to explain chemisorption kinetics (Wu et al., 2009), and has been used for modeling adsorption processes of adsorbents with heterogeneous surfaces (Cheung et al., 2001).

The expression is usually called the Elovich's equation:

$$\frac{dq_t}{dt} = a \exp^{-\alpha q_t} \qquad \textbf{Eqn. 2.21}$$

where, a (μg g^{-1} h^{-1}) is the initial sorption rate, α (g μg^{-1}) is a constant for the specific system.

The integrated form of Eqn. 2.21 is:

$$q_t = \frac{2.303}{\alpha}\log(t+\beta) - \frac{2.303}{\alpha}\log\beta \qquad \textbf{Eqn. 2.22}$$

$\boldsymbol{\beta}$ (g µg^{-1}) is the desorption constant ($\beta = \frac{1}{\alpha a}$)

This Elovich's equation has been commonly used for the kinetics description of chemisorption of gases onto heterogeneous solids and has also been used for phosphorus sorption by sediments (Detenbeck and Brezonik, 1991). Chien and Clayton (1980) simplified Elovich's equation to describe phosphorus (PO_4) release and sorption in soils. Elovich model has also been used to describe the removal of chemical pollutants from wastewater by wood char (Cheung et al., 2001). Other studies have reported the used of Elovich model to describe the exchange of ^{32}P between the goethite surface and the solution phase (Heimberg et al., 2001).

Assuming that $a\alpha >> 1$ and by applying the boundary conditions of $q_t = 0$ at $t = 0$ and $q_t = q_t$ at $t = t$, then Eqn. 2.22 becomes the simplified Elovich's equation:

$$q_t = \frac{1}{\alpha}\ln(a\alpha) + \frac{1}{\alpha}\ln(t) \qquad \textbf{Eqn. 2.23}$$

Thus, *a* and α can be deduced from the slope and the intercept of a straight line plot of q_t versus ln(t).

2.13.2 Adsorption diffusion model

Adsorption diffusion models are developed based on four sequential steps (Lazaridis and Asouhidou, 2003);

1. Transport in the bulk solution

2. Film diffusion entailing the transport of adsorbate across the liquid film around the adsorbent.
3. Intra-particle diffusion entailing the transport of adsorbate in the pores and also along the walls of the ores of the adsorbent
4. Mass action which entails the chemical reaction (adsorption and desorption) between the adsorbate and the adsorbent.

All the above-mentioned processes are involved in a typical liquid-solid adsorption. However, the mass action and transport in bulk solution are often a rapid processes and therefore not considered in kinetic study. Consequently, liquid film diffusion or intraparticle diffusion controls the kinetic adsorption processes and one or both of them can be the potential rate limiting steps (Meng, 2005).

Weber-Morris model also known as intraparticle diffusion model is widely used as adsorption diffusion model (Weber and Morris, 1963);

$$q_t = K_i t^{1/2} + C \qquad Eqn.2.24$$

where *Ki* the intraparticle diffusion rate constant (g μg^{-1}) and C (g μg^{-1}) is a constant associated to the boundary layer thickness: the larger is the value of C, the greater is the effect of the boundary layer. The intraparticle diffusion model tells whether film diffusion or intraparticle diffusion is the potential rate limiting step. The model shows that when the plot of q_t against $t^{1/2}$ is linear, then intraparticle diffusion is the sole rate-limiting step. However, both film

diffusion and intraparticle diffusion becomes the rate limiting steps when the plot is multi-linear implying that two steps occurred simultaneously

2.14 Phosphorus fractionation

Phosphorus fractionation is a valid method to find out the P fractions in soils and also to assess the chemistry and weathering processes of soils (Chang and Jackson, 1957; Cross and Schlesinger, 1995). Information on P speciation is a criterion to developing a comprehensive remediation techniques to minimize the impact of agricultural development on the ecosystem. Foreknowledge on P forms helps to comprehend how soil chemical properties affect soil fertility and environmental quality. The chemical rationale underlying P fractionation method is to displace P from soil adsorption sites by other anions in soil solution, to change the adsorption properties of the soil surface, or to dissolve compounds bound to P.

Soil P occurs in different chemical forms and as such vary distinctly in their chemical behaviour, mobility and availability in soils. Identification of the different P pools will therefore give detailed information on P forms and its bioavailability in soil. One of the ways for identifying P pools in soils has been the use of various chemical reagents to purposely dissolve the different P forms based on the bonding strength between P moieties and other organic and mineral compounds.

Several P fractionation procedures have been used to assess P dynamics in soil and other natural environment. These involves specific methods for finding out inorganic P forms (Chang and Jackson 1957; Hieltjes and Lijklema 1980), organic P forms including microbial P (Sommers et al. 1972; Bowman and Cole 1978; and Ivanoff et al. 1998), both inorganic and

organic P forms (van Eck, 1982; Psenner et al. 1988; Ruttenberg, 1992; Tiessen and Moir, 2008), and also organic, inorganic and microbial P forms (Hedley et al. 1982a).

Hedley P fractionation procedure has been one of the commonly used method (Hedley et al. 1982a). This procedure has been further modified (Tiessen and Moir; 1993; Asomaning et al., 2015). Some of the description of P compounds and extractant used in Hedley P fractionation (Hedley et al., 1982b) is shown in Table 2.3.

The Hedley fractionation consists of chemical sequential extraction of inorganic and organic P pools using chemicals of varying extraction strength, culminating into different soil P with varying levels of lability namely, most labile P, moderately labile P and stable P fractions (Hedley et al. 1982b).

The most labile P consist of anion extractable inorganic P (resin Pi) and sodium bicarbonate-extractable inorganic P ($NaHCO_3$-Pi). The most labile P is considered to be available in soil solution for plant uptake (Hedley et al., 1982b; Tiessen and Moir; 1993; Cross and Schlesinger, 1995; Asomaning et al., 2015). Several work done have reported that estimated P (Pi) of resin and $NaHCO_3$ was directly related to plant P uptake (Bowman et al., 1978; van der Zee et al., 1987; Menon et al., 1989; Sharpley, 1991).

In tropical soils including Oxisols, the most labile P are usually very low (Cross and Schlesinger 1995; Tiessen and Moir 1993). In a study by Francisco Alisson et al. (2010) on tropical soils of Southeastern Brazil, to determine the soil P pools in a chemical sequentially extracted faction in a tropical coffee-agroecosystem concluded that the labile P (Resin-P and $NaHCO_3$-Pi) accounts for less than 5% of the total P pools. They further observed a rapid decrease of the labile P fractions.

Table 2. 3 Description of phosphorus compounds and chemical extractants in the Hedley et al (1982b)

		Inorganic P Pools (Pi)		
Resin	$NaHCO_3$-Pi	NaOH-Pi	HCl-Pi	Reference
Forms of soil Pi as a reservoir of plants nutrients	Extracts additional Pi that is available to plants	Dissolves Fe and Al-P partially and desorbs Pi from the surfaces of Fe and Al oxides	Dissolves acid-soluble P in the forms of calcium phosphates and Pi which is occluded within sesquioxides	[1]
Non-occluded Pi	Non-occluded Pi	Non-occluded Pi	Occluded Pi	[2]
Soluble and labile Pi: Anion resin- or water-extractable	Labile Pi in equilibrium with the soil solution: isotopically extractable	Secondary mineral Pi: chemisorbed to surfaces of Al and Fe oxides and carbonates	Primary P minerals that are acid extractable	[3]
Most plant available Pi that is adsorbed on surfaces of crystalline P compounds	Readily plant available Pi	Of lesser plant availability and is chemisorbed to amorphous and crystalline Al and Fe	Stable Ca-bound phosphate	[4]

Source: Hedley et al (1982b); References: [1] Hedley et al. (1982a,b); Tiessen and Moir, 1993; [2] Walker and Syers (1976); [3] Smeck (1985); [4] Wager et al. (1984)

Table 2.3 Contd.

		Inorganic P Pools (Pi)		
Resin	$NaHCO_3$-Pi	NaOH-Pi	HCl-Pi	Reference
Labile Pi adsorbed on surfaces of crystalline compounds	Labile Pi adsorbed on surfaces of crystalline compounds	Less labile Pi associated with exteriors of amorphous Al and Fe phosphates	Largely calcium-bound	[5]
Directly exchangeable with the soil solution and is biologically available	Labile Pi that's is adsorbed onto colloids	More resistant Pi that is associa-ted with humic compounds and adsorbed to Al and Fe	More stable Pi of minerals of low solubility such as apatite	[6]
Rapid turnover Pi	Rapid turnover Pi	Slow turnover Pi	Slow turnover	[7]

Source: Hedley et al (1982b); References: [5] Tiessen et al. (1984); [6] Schoenau et al. (1989); [7] Trasar-Capeda et al. (1986).

Table 2.3 Contd.

Organic P Pools (Po)		Residual P Pool	
$NaHCO_3$-Po	NaOH-Po	Residual P	Reference
Labile form of soil Po and Po held at the internal surfaces of the soil aggregates	Pi and Po compounds held more strongly by chemisorption to Al and Fe compounds of the soil surfaces	Occluded phosphates and the most stable organic phosphates	[1]
Non-occluded Po	Non-occluded Po	Occluded Pi	[2]
Labile Po in equilibrium with the soil Solution: isotopically extractable	Secondary minerals Po: chemisorbed to surfaces of Al and Fe oxides and carbonates	Occluded Pi: physically encapsulated in the minerals that have no structural phosphorus	[3]
Labile Po is easily mineralized and Contributes to plant available P	Stable Po that is involved with long term transformation of P in soils	Probably included stable humic acid and humus and relatively insoluble Pi and Po	[4]

References: [1] Hedley et al. (1982a,b); Tiessen and Moir, 1993; [2] Walker and Syers (1976); [3] Smeck (1985); [4] Wager et al. (1986)

Table 2.3 Contd.

Organic P Pools (Po)		Residual P Pool	
NaHCO3-Po	NaOH-Po	Residual P	Reference
Labile Po is easily mineralized and Contributes to plant available P	Stable Po that is involved with long term transformation of P in soils	occluded Pi covered with ses-quioxides and other Po	[5]
Labile Po is easily mineralized and Contributes to plant available P	More resistant Po that is associated with humic compounds and adsorbed to Al and Fe	Highly resistant Pi and Po of low bioavailability	[6]
Rapid turnover Po	Rapid and slow turnover Po	No information	[7]

Source: Hedley et al (1982b); References: [5] Tiessen et al. (1984); [6] Schoenau et al. (1989); [7] Trasar-Capeda et al. (1986).

This was attributed to P immobilization by microbes to acquire the needed energy to degrade other organic residues in the soil. Similarly, a five year successive cropping with rice on unfertilized Ultisol in La Cote D'Iviore decreased the amount of the labile P_i from 10.8 mg P kg^{-1} to 7.6 mg P kg^{-1} (Abekoe and Sahrawat, 2003). In a short term study, the application of liquid swine manure to Orthic Black Chernozem did not raise the most labile P pools but rather the P from the manure was transformed into moderately and recalcitrant P pools.

Qian and Schoenau (2000) examined the short-term effect of a single addition of liquid swine manure on P fractions in some temperate soils. Other studies reported increase in Resin-P and $NaHCO_3$-P concentration during cultivation under a slash and burn but eventually decreased later after cultivation (Armando, 1998). On the contrary, the addition of liquid swine manure during cultivation under slash and burn elevated the amount of resin extractable inorganic P (Simard et al., 1995). Phosphorus pools in soil after 20 years addition of feedlot manure was studied (Dormaar and Chang, 1995). They reported that the resin-extractable Pi and the $NaHCO_3$-extractable Pi and Po increased with feedlot manure additions. The soil labile P fraction ranged from 15 to 46% of total P representing considerable potential pollutant.

The sodium hydroxide-extractable P (NaOH-Pi) is considered as the moderately labile P pool and is the most abundant Pi fraction in most tropical soils (Cross and Schlesinger, 1995; Francisco Alisson da et al., 2010). This fraction is held by chemisorption to Fe and Al complexes (Hedley et al. 1982a). Indeed, $NaHCO_3$-Pi and NaOH-Pi are not completely separate pools, but represent a continuum of Fe- and Al-associated P extractable pool in acid soils (Tiessen and Moir, 1993).

The soil organic P pool made up of $NaHCO_3$-organic P ($NaHCO_3$-Po) and NaOH-organic P (NaOH-Po) are considered more labile and moderately labile P pools respectively. The $NaHCO_3$-Po is the organic P adsorbed on soil colloidal surfaces which is easily mineralizable (Andrew et

al., 2004) whiles the NaOH-Po is the organic P that is bound strongly by chemical sorption to the Fe and Al oxides of the soil surfaces. The NaOH-Po pool is chemically and physically protected and therefore more stable than the $NaHCO_3$-Po. Studies conducted with ^{33}P labeling confirmed that the application of mineral fertilizer on highly weathered low-P soils (Buehler et al., 2002) and moderately weathered high-P soils (Daroub et al., 2000) did affect neither the Po nor the stable P fractions (HCl-P and residual-P). Lack of increment in Po concentration in tropical soils is attributed to the rapid mineralization of Po in the tropics, regardless of P fertilization. Moreover, a decline in P was also reported by Agbenin and Goladi (1998) for a tropical Alfisol with continuous application of cow dung. However, as the incubation was prolonged particularly in highly weathered tropical soils, up to 90% of the applied P was transformed into moderately labile Po within 60 days (Abekoe and Tiessen, 1998).

The labile P fractions exist in equilibrium with moderately labile P fractions, and these two P pools are also sensitive to change because of fertilizer application or nutrient depletion (Schmidt et al., 1996). Path analyses showed that transformations between P fractions depended on the stage of soil development, type of P sources, and soil properties (Tiessen et al., 1984; Zheng et al., 2002). For instance, in moderately weathered soils, approximately 86% of resin-P originated from $NaHCO_3$-Pi and NaOH-Pi, and in highly weathered soil, 80% of resin-P derived from labile and moderately labile Po (Tiessen et al., 1984). In a dairy manure system, approximately 86% of resin-P originated from applied fertilizer Pi but added manure Po was transformed into labile and moderately labile Po (Zheng et al., 2002). As a number of factors contribute to transformations of P fractions, it is difficult to exactly determine the kinetics of exchange reactions. A conceptualized model based on P cycles categorized soil P transformation into three components such as slow Pi, rapid Pi and Po and slow Po (Tiessen et al., 1984). Moreover, the role of soil microbial activities,

P uptake by plants, root exudation, and other rhizosphere processes (Hinsinger, 2001) have paramount importance on soil-P transformations.

The hydrochloric acid- extractable P pool (HCl-Pi) is defined as being Ca-associated P and are commonly low in high weathered soils (Cross and Schlesinger 1995). The residual P pool comprises occluded inorganic P and stable organic P acting as a reservoir for phosphorus. The proportion of the residual P has been suggested to be an indicator of degree of weathering (Maria et al., 2004). The residual P pool is very high in strongly weathered tropical soils, which leads to the inclusion of extraction with strong mineral acids including 18M $H_2SO_4^-$ and 12M HCl at high temperatures to improve P recovery and distinction between inorganic and organic forms of P (Tiessen and Moir, 2008). Despite the recalcitrance of the residual pool, Chen et al. (2000) observed significant decreases in residual P in soils under forests compared with adjacent grasslands, suggesting the residual pool was being utilized to support plant growth. Similarly, Hedley et al. (1982b) found that half of the substantial depletion in total soil P that occurred as a result of 65 years of cropping with no P inputs was from the residual pool. These findings suggest that residual P is far from recalcitrant with respect to bioavailability over a long term. Studies conducted in root study containers also revealed that most of the P depletion that occurred in the rhizosphere (0-1 mm) of rape (*Brassica napus*) over only 14 days was from the residual pool, while there was minimal depletion of $NaHCO_3$ organic P (Magid et al.1996). However, Guo et al. (2000) suggested that in highly weathered soil, the residual P continued to accumulate with plant growth but decreased over time with plant growth in slightly weathered soils

2.15 Scientific errors in phosphorus determination during fractionation

2.15.1 Precipitation of Humic acid

Most alkali soil extracts including $NaHCO_3$ and NaOH contain significant quantities of dissolved organic macromolecules. The dissolved organic matter does not interfere directly with the colorimetric determination of inorganic P in diluted soil extracts, the precipitation of humic acid components as a consequence of the decrease in pH following the addition of the acid-molybdate reagent can cause significant interference. This problem can be easily overcome by pretreatment of the alkali soil extract with mineral acid to a pH of 1.5 which results in the precipitation of humic acid which is then removed by centrifugation prior to addition of the molybdate reagent to the neutralized extract (Tiessen and Moir 2008). However, it should also be noted that in a highly organic material, the acidic precipitation of humic acids following alkali extraction may co-precipitate inorganic P. In a recent study of organic wetland soils, approximately 50% of inorganic phosphate was co-precipitated following acidification, which in turn influenced the estimate of organic phosphorus content (Turner et al., 2006). High variability of repeated measuring of $NaHCO_3$-Po and NaOH-Po were also reported by Magid et al. (1996). Problems in the determination of Pi are mentioned in Tiessen and Moir (1993), especially the possibility that Pi is precipitated along with the organic matter upon acidification and erroneously determined as Po (Pt-Pi).

2.15.2 Hydrolysis of Organic matter

The addition of strong mineral acid to an alkaline extract during the determination of inorganic P has the potential to cause significant hydrolysis of a fraction of the dissolved organic P, which in

turn can result in underestimation of the organic P and overestimation of inorganic P content. Using 1M HCl extractant to extract soil inorganic P culminated into 3% of D-glucose-6-phosphate, glycerophosphate or phytic acid and 40% hydrolysis of p-nitrophenyl phosphate (Ivanoff et al., 1998). However, studies have shown little or no hydrolysis of inositol hexaphosphate and glycerophosphate following sequential extraction soil P with concentrated (18 M) H_2SO_4 (Bowman, 1989).

This acid hydrolysis could occur as a consequence of adding the colour-forming acid-molybdate reagent during determination of inorganic P in a diluted extract. Thus, the most commonly used reagent based on the method originally developed by Murphy and Riley (1962) contains 1.25 M sulfuric acid (H_2SO) and has the potential to hydrolyse some dissolved organic P. However, Dick and Tabatabai (1977) developed a modified acid-molybdate colorimetric technique which involved adding citrate-arsenite to complex excess molybdate, which effectively means that any inorganic P released from acid hydrolysis of organic P was not determined by colorimetry. It is also possible that some hydrolysis of organic P could occur during pretreatment of alkali extracts to precipitate humic acid which involves the addition of significant quantities of strong mineral acid (e.g. 0.9 M H_2SO_4) to lower the pH to 1.5 (Tiessen and Moir, 2008).

2.16 Summary of literature review

It is clear from the review that tropical soils are highly weathered and generally typified by dominance of sesquioxides, high acidity, low organic carbon and low fertility. Phosphorus applied to acidic soils from organic and inorganic sources gradually reacts with Fe and Al compounds and is transformed into relatively insoluble P compounds. Phosphprus therefore exists in several forms based on its reactivity in the soil environment. The forms of P in soil can be assessed using Hedley fractionation method. The use of sorption isotherm to evaluate P requirement is considered a better

option to conventional soil test. Amendment of biochar to soils has been suggested to provide an integrated approach to rectify P deficiency in tropical soils. However, its effect is highly dependent on the feedstock and pyrolysis temperature. Much work has been carried out on P sorption and fractions of tropical soils. Notwithdtanding, little or no work has been done on P sorption characteristics, P reactions including P fractions in biochar amended Ghanaian soils.

CHAPTER THREE

PHOSPHORUS ADSORPTIVE CHARACTERISTICS OF DIFFERENT BIOCHAR TYPES

3.1 Introduction

The rapid increase in urbanization and the expansion of industrial and agricultural production have culminated in the generation and discharge of large amounts of phosphorus-rich urban sewage, industrial and agricultural wastewater into natural water bodies. In 2005 the urban areas of Ghana generated about 763,698 m^3 of wastewater daily, resulting in approximately 280 million m^3 over the entire year. This volume of wastewater is expected to increase to 530 million m^3 in 2020 (Agodzo, 2008). Although phosphorus is an essential nutrient for the growth of plants and other living organisms, it can also serve as an environmental pollutant (Dodds et al., 2008; Almeelbi et al., 2012). About 0.02 $mg \cdot L^{-1}$of dissolved phosphate in water bodies is considered to have potential risk to the proliferation of algal growth (USEPA, 1995). The increased phosphate in water bodies as a result of inappropriate and frequent discharge of waste water stimulates excessive growth of phytoplankton and algae which in turn decrease the quality of drinking water (Dodds et al., 2008). Thus, in order to reduce the negative effects of overloading water bodies with phosphorus, it is necessary to assess various strategies and evaluate the P removal effectiveness of adsorbents that could be exploited for use as waste water cleansing agents of orthophosphate ions prior to waste water discharge into natural water bodies (Biswas et al., 2008).

A number of technologies including biological, chemical, and physical treatment methods have been developed for the removal of phosphate from domestic and industrial waste water (Karaca et al., 2014). Alum, lime and iron salts have been used to precipitate orthophosphate ions as a conventional chemical process of wastewater treatment. However, the large quantities of

chemicals required in the process and the generation of secondary products leads to economic burden (Clark et al., 1997; Pratt et al., 2012). The high cost of deploying electrodialysis and reverse osmosis for physical water treatment has also been reported (Kumar et al., 2010).

Biochar has gained a lot of attention in recent times not only for its role in soil fertility improvement and carbon sequestration but also as a low-cost adsorbent for wastewater treatment. Recent reports have indicated that biochar has a strong ability to remove chemical contaminants in water including orthophosphate, organic contaminants and heavy metals (Kasozi et al., 2010; Eduah, 2012; Yao et al., 2012; Zhang et al., 2016).

Adsorption kinetics studies of P have shown that mallee charred at 750 ^{o}C with particle size less than 1 mm requires only 1 h to be saturated with the nutrient (Zhang et al., 2016). Phosphorus removal efficiency of *Posidonia oceanica* biochar produced at 650 ^{o}C showed two-fold increase in P adsorption from 3 to 15 h, attaining maximum adsorption in 15 h (Wahab et al, 2011). Maize straw biochar charred at 300 ^{o}C showed rapid P adsorption attaining equilibrium in less than 1 hour (Zang et al., 2011). The varying rate and amount of P adsorption show that the adsorptive properties including pH, surface area, functional groups of biochar for phosphorus highly depends on the feedstock and pyrolysis temperature (Zhao et al., 2013). It is therefore, necessary to determine the optimum pyrolysis temperature for biochar types produced from their respective feedstocks for P adsorption.

Rice husk, corn cob, cocoa pod husk and palm kernel shell are agricultural wastes and potential biochar feedstocks which abound in Ghana (Duku et al., 2011). It is estimated that respectively, about 363×10^3, 1650×10^3 and 305×10^3 tonnes of rice husk, corn cob and cocoa pod biomass are generated annually in Ghana (Duku et al., 2011). Biochar from these feedstocks has hardly been exploited for use as P adsorbents in Ghana.

For biochar to be used as a P adsorbent for treating wastewater, it is incumbent first to understand the P sorption characteristics of the various biochar types. The adsorption characteristics would provide the basic information to inform scientists as to the right choice of adsorbent to select and an insight into the adsorption mechanisms. It is in the light of these that this study seeks to:

1. determine the equilibration time for P adsorption on different biochar types prepared from rice husk, corn cob, cocoa pod husk and palm kernel shell
2. ascertain the pH for maximum adsorption of P by the biochar types
3. elucidate the possible mechanism controlling P adsorption onto biochar.

3.2 Materials and methods

3.2.1 Preparation of Biochar

Four feedstocks viz. corn cob, rice husk, cocoa pod husk and palm kernel shell feedstocks were charred at three different temperatures (300, 450 and 650 ^{o}C) using Nabertherm furnace at CSIR-Kwadaso, Kumasi. The samples were washed with de-ionised water and air dried. Each biochar sample was ground in a stainless steel mill and passed through a 2 mm sieve to obtain a less than 2 mm sized fraction. Each biochar type was further dried in an oven at 70 ^{o}C. Biochar samples were saved for characterization, and subsequent P adsorption (Chapter three) and incubation studies (Chapters four and five).

3.2.2 Characterization of biochar

3.2.2.1 pH

Two grammess (2 g) of biochar were weighed in triplicate into 50 mL beakers and 20 mL of deionized water added to give a biochar to water ratio of 1:10. The suspension was shaken for 1 h

in a reciprocating shaker, left to stand for 1 h to equilibrate in a room housing a pH meter. The glass electrode pH meter (pH-mV-Temp PL-700PV) was standardized using three buffer solutions of pH 4, 7 and 10. The glass electrode was then rinsed with deionized water and then used to measure the pH of the biochar samples by gently immersing the glass electrodes into the supernatants. The values obtained were recorded as the pH of the biochar in water. All measurements were done in triplicates.

3.2.2.2 Total Carbon and Total Nitrogen

Total carbon and total nitrogen were measured using dry combustion in a 1350℃ (ELTRA CS-500 analyzer). The device was initially calibrated with known standards to yield ± 2% accuracy. About 200 mg of ground biochar (< 0.5 mm) was weighed into a crucible, inserted into the furnace, and the total nitrogen and total carbon measured.

3.2.2.3 Cation exchange capacity

The cation exchange capacity of the biochar was determined using $BaCl_2$ / Triethanolamine (TEA) solution buffered at pH 8.2. About 2 g of biochar sample were weighed into 100 mL plastic bottles and 40 mL of 0.2 M $BaCl_2$ -TEA solution added. The suspension was shaken for 1 h in a reciprocating shaker and then filtered through a 0.45 µm filter paper. The filtrate was collected into an empty plastic bottle. The biochar residue was leached with four portions of 10 mL 0.1 M $MgSO_4.7H_2O$ solution. The leachate was collected into a separate clean plastic bottle. The concentration of Ba^{2+} in the leachate was determined using Atomic absorption spectrometer. The CEC of biochar was calculated as:

$$\mathbf{cmol_c kg^{-}} = \frac{\mathbf{AAS\ reading\ (mg/L)} \times \mathbf{40\ mL} \times \mathbf{10^3\ (g)} \times \mathbf{10^2 (cmol)} \times \mathbf{2^*}}{\mathbf{Weight\ of\ soil} \times \mathbf{10^6\ (\mu g)} \times \mathbf{137.3}} \qquad (3.1)$$

3.2.2.4 Determination of other elements using Inductively Couple Plasma analysis (ICP-OES)

Total phosphorus, total base cations (Ca, Mg, Na, K), Si and heavy metals (Al, Fe, Cu, Mn, Sr, B, Zn) were determined by wet oxidation and subsequent measurement of the respective concentrations using inductively coupled plasma optical emission spectrometry (ICP-OES). Briefly, 0.5 g ground biochar samples in triplicates were digested in HNO_3 and HCl.

The biochar samples were digested in triplicate and ICP-OES elemental quantification was done using a Perkin Elmer Optima 5300DV instrument (Waltham, USA). Blank digests from the reagents were also prepared and the concentrations of the various elemens read. The elements were analysed in axial mode, except for P, Ca, K, Mg and Na, which were present in sufficient concentrations to necessitate the use of radial mode. Standards were run with each analysis session for calibration and to check the accuracy of measurements over the time of the sample run.

3.2.2.5 Fourier Transform Infrared (FTIR)

The functional groups on the biochar types were examined using photoacoustic spectroscopy (PAS)-FTIR. The biochar samples were not pre-treated before the spectroscopic analysis apart from grinding and sieving to < 1 mm and oven drying at 40 ^{o}C. The FTIR-PAS spectra were obtained from a Nicolet 6700 (ThermoScientific, USA) spectrometer equipped with a PA-301 photoacoustic detector (Gasera Ltd., Finland). A helium gas purging flow was used to reduce the noise produced by the evaporation of moisture from the samples. Activated charcoal was used as

background with 200 scans. The samples were packed in small ring cups 10 mm in diameter. For each sample, 128 scans in the mid-infrared region between 4000 and 500 cm^{-1} at a resolution of 4 cm^{-1} were recorded and averaged. Prior to spectroscopic analysis, the spectra were smoothened by the Savitzky-Golay algorithm (Savitzky and Golay, 1964) and normalised by mean using the Unscrambler X v.10.3 software (CAMO software, Oslo, Norway).

3.2.2.6 X-ray analysis

The X-ray powder analysis was done on the ground (< 1mm) and oven dried (40 ^{o}C) biochar samples to identify crystalline minerals present. The fine powder was packed into a rectangular glass sample holder with an area of (25 mm × 16 mm) 4 cm and a depth of 1 mm. The surface of the packed powder was pressed and smoothed with a piece of flat glass. The weight of loaded sample was kept between 0.40 and 0.45 g. All slides were scanned from 10^{o} to 60^{o} 2θ on a Siemens D-500 X-ray diffractometer using a Cu-K_{α} radiation source with a generating voltage of 40 kV and a current of 40 mA.

3.2.3 Phosphorus Adsorption Kinetics Experiment

The orthophosphate stock solution containing 300 mg P L^{-1} was prepared from KH_2PO_4 salt of analar grade. A 0.5 g of biochar was weighed into 50 mL centrifuge tube and appropriate volume of the stock solution added and 0.01 M KCl added and topped up to 30 mL to attain a final P concentration of 100 mg/L and ionic strength of 10 mM KCl. The tubes were then shaken on an end-to-end shaker at 120 rpm for 24 h at room temperature. Enough samples were in the centrifuge tubes were prepared to allow for sub sampling after 1, 3, 5, 9, 15 and 24 h of shaking. The suspension after removal from the shaker was centrifuged at 3500 rpm for 15 min and the resulting

supernatant filtered through a 0.45 µm filter paper. The concentration of P in filtrate i.e. equilibrium P concentration Ce (mg/L) was determined by the colorimetric molybdenum-blue method (John, 1970). The concentration of P adsorbed (qt) (mg/g) was computed from the mass balance equation as follows:

$$\mathbf{qt} = \frac{\mathbf{(Ci - Ce)V}}{\mathbf{M}} \qquad (\mathbf{3.2})$$

Where *V* is the volume of the aqueous solution (L) and *M* is the dry weight in grams of biochar (adsorbent). The kinetics experiments were repeated three times and the average data and standard deviations reported. Four kinetics models (chemical and diffusion models) were applied to the time generated data to predict and understand the potential rate limiting steps and in part, the P adsorption mechanism(s) on each biochar type.

$$\frac{\mathbf{dq_t}}{\mathbf{dt}} = \mathbf{K_1(q_e - q_t)} \qquad \textbf{Pseudo first order} \qquad (\mathbf{3.3})$$

$$\frac{\mathbf{dq_t}}{\mathbf{dt}} = \mathbf{K_2(q_e - q_t)^2} \qquad \textbf{Pseudo second order} \qquad (\mathbf{3.4})$$

$$\frac{\mathbf{dq_t}}{\mathbf{dt}} = \boldsymbol{\alpha}\,\mathbf{exp(-\beta q_t)} \qquad \textbf{Elovich} \qquad (\mathbf{3.5})$$

$$\mathbf{q_t = K_i t^{1/2} + C} \qquad \textbf{Intraparticle diffusion} \qquad (\mathbf{3.6})$$

3.2.4 Adsorption Isotherm

Various volumes of the 300 mg/L P stock solution were pipetted into 50 mL centrifuge bottles into which had been weighed 0.5 g biochar. Volumes of the 0.01 M KCl was added and topped up to 30 mL to attain ionic strengths of 10 mM KCl and various P concentrations of 0 (blank), 25, 50, 75, 100, 125, 150 and 200 mg P/L. The suspensions in centrifuge bottles were shaken on an end-to-end shaker at 120 rpm for 24 h at room temperature. The suspension was then centrifuged (3500 rpm, 15 min) and the resulting supernatant filtered through a 0.45 µm filter paper. The filtrate was analyzed for phosphorus by the colorimetric molybdenum-blue method (John, 1970). The same procedures for the kinetics studies were then used to determine equilibrium and adsorbed phosphate concentrations. The P adsorption data were then fitted to the Langmuir and Freundlich equations.

$$\mathbf{q_t = \frac{KQCe}{1 + KCe}} \qquad \textbf{Langmuir} \quad (3.7)$$

$$\mathbf{q_t = K_f Ce^n} \qquad \textbf{Freundlich} \quad (3.8)$$

3.2.5 Effect of pH on P adsorption

Various volumes of the 300 mg/L P stock solution and the 0.01 M KCl were pipetted into 50 mL centrifuge bottles into which had been weighed 0.5 g biochar. These were adjusted to pHs of 2.5, 3.5, 4.5, 5.5, 6.5, 7.5 and 8.5 using HCl and NaOH and topped up to the 30 mL volume with pre adjusted de-ionised water at the aforementioned initial pHs to final P concentration of 200 mg/L and ionic strengths of 10 mM KCl. The suspensions in centrifuge bottles were shaken on an end-to-end shaker at 120 rpm for 24 h at room temperature. The suspensions were then centrifuged

(3500 rpm, 15 min) and the resulting supernatant filtered through a 0.45 µm filter paper. The equilibrium pH of the filtrates were determined and their respective equilibrium P concentrations also determined by the colorimetric molybdenum-blue method (John, 1970).

The effect of pH on P adsorption experiments were repeated three times. The average data and standard deviations are reported.

3.2.6 Statistical analysis

The amount of P adsorbed at the different shaking times and at the different pHs were subjected to analysis of variance (ANOVA) using GenStat 12 to establish whether there were differences in the biochar type at various pyrolysis temperatures with regards to P sorption from aqueous solution. The fitting of data to adsorption and kinetics models were done using RStudio, Origin Lab 12 and Microsoft excel sheet.

3.3 Results

3.3.1 Characterization of Biochar

Some chemical properties of the various biochar types used for the study are shown in Table 3.1. The biochar types herein after would be designated CP300, CP650 for cocoa pod husk biochar tpyes at 300 and 650 ^{o}C respectively RH300, RH650 for rice husk biochar tpyes at 300 and 650 ^{o}C respectively, CC300, CC600 for corn cob biochar tpyes at 300 and 650 ^{o}C respectively and PK300 and PK600 for palm kernel shell biochar tpyes at 300 and 650 ^{o}C respectively. Generally the higher temperature produced biochar with higher pH, irrespective of feedstock type and pH of biochars were in the increasing order of PK < RH < CP ≈ CC. Strikingly, it is only the PK biochar types which did not have alkaline pH with the pH being 5.5 and 6.7 respectively for PK300 and

PK650. The pH of RH300 and RH650 were 7.1 and 9.6, respectively. The CC and CP biochar types had pHs between 8.5 and 10.3.

The carbon contents of the biochar types also increased witth increasing pyrolysis temperature and was in the order of PK > CC > CP > RH. The total C content of the biochar types was in a range of 57.94 to 61.96% for cocoa pod husk biochar, 41.58 to 42.55% rice husk biochar, 72.98 to 78.07% corn cob biochar and 81.99 to 89.58% palm kernel shell biochar.

The CEC of the biochar ypes were in the general order of CP > CC > RH > PK with the higher temperature giving lower CECs.

The total P content of the biochar types increased as the pyrolysis temperature was raised from 300 ^{o}C to 650 ^{o}C varied from 2.45 to 3.16 mg g^{-1} for cocoa pod husk biochar (CP300 and CP650), 1.19 to 1.52 mg g^{-1} rice husk biochar (RH300 to RH650), 1.54 to 1.94 mg g^{-1} corn cob biochar (CC300 and CC650) and 0.17 to 0.25 mg g^{-1} palm kernel shell biochar (PK300 and PK650).

Similar to the trend in the CEC values, cocoa pod husk biochar had the highest total P concentration and the least was palm kernel shell biochar.

The total Ca, Mg, K and Na concentration of all the biochar types ranged from 1.95 to 11.71 mg g^{-1}, 0.27 to 8.86 mg g^{-1}, 0.45 to 58.94 mg g^{-1} and 0.17 to 1.94 mg g^{-1} respectively. Generally, the amount of base cation concentration increased in the order of palm kernel biochar < rice husk biochar < corn cob biochar < cocoa pod husk biochar.The total C content of the biochar types was in a range of 57.94 to 61.96% for cocoa pod husk biochar, 41.58 to 42.55% rice husk biochar, 72.98 to 78.07% corn cob biochar and 81.99 to 89.58% palm kernel biochar. Increasing the pyrolysis temperature of all the biochar types resulted in an increase in the total C content.

Table 3. 1 Chemical composition of the four biochar types at two different pyrolysis temperatures

Biochar	Cocoa pod husk		Rice husk		Corn cob		Palm kernel shell	
Temperature	300 °C	650 °C	300 °C	650 °C	300 °C	650 °C	300 °C	650 °C
Abbreviation	CP300	CP650	RH300	RH650	CC300	CC650	PK300	PK650
pH (H_2O)	8.50	10.21	7.11	9.50	8.90	10.30	5.51	6.70
C (%)	57.94	61.96	41.58	42.55	72.98	78.07	81.99	89.58
Total N (g kg^{-1})	3.91	2.73	1.77	1.21	2.93	1.91	3.82	2.12
Total P (g kg^{-1})	2.45	3.16	1.19	1.52	1.54	1.94	0.17	0.25
CEC ($cmol_c$ kg^{-1})	63.50	53.00	49.40	38.00	38.02	30.10	27.90	22.10
Ca (g kg^{-1})	9.60	11.71	2.07	3.29	3.32	4.19	1.95	2.94
Mg (g kg^{-1})	7.23	8.86	0.91	1.27	2.43	3.43	0.27	0.33
K (g kg^{-1})	0.17	0.22	0.19	1.52	1.54	1.94	0.17	0.25
Na (g kg^{-1})	41.33	58.94	5.34	8.19	24.71	30.80	0.45	0.58
Si (g kg^{-1})	8.91	28.36	138.53	194.49	13.94	14.44	9.74	14.41
Al (mg kg^{-1})	457.92	986.67	1260.00	1875.00	574.56	1103.33	1043.59	2108.96
Fe (mg kg^{-1})	385.61	653.33	1250.97	1659.88	616.99	946.11	684.38	1492.80
Mn (mg kg^{-1})	374.91	373.91	403.90	509.14	95.59	128.92	25.07	43.96
Cu (mg kg^{-1})	27.10	31.83	1.10	1.25	nd	14.50	32.83	21.83
Zn (mg kg^{-1})	106.22	146.33	31.73	90.95	138.17	164.20	23.49	42.58
B (mg kg^{-1})	35.56	47.10	7.15	9.65	10.06	13.14	2.02	3.14
Sr (mg kg^{-1})	48.01	61.32	7.26	9.04	12.44	19.23	8.32	10.89

nd = not detected

The total N content of the four biochar types decreased from 300 ºC to 650 ºC. These values ranged from 1.21 to 3.91 for the biochar types. Averagely, cocoa pod husk biochar had the highest concentration of total N as compared to the other biochar types.

The Si concentration varied among the studied biochar types from 8.91 to 28.36 mg g^{-1}, 138.53 to 194.49 mg g^{-1}, 13.94 to 14.44 mg g^{-1} and 9.74 to 14.41 mg g^{-1} for cocoa pod husk, rice husk, corn cob and palm kernel shell biochar respectively. The study showed a substantial concentration of heavy metals (Fe, Al, Mn, Cu, Zn, B, Sr and V) in all the biochar types. The concentration of these heavy metals increased at increasing pyrolysis temperature. The heavy metal concentration was relatively high in cocoa pod husk biochar with the exception of Fe and Al which were high in rice husk biochar and palm kernel shell biochar.

The FTIR-PAS spectra of all the biochar types at two pyrolysis temperatures are shown in Fig. 3.1 a-d. The peak at about 3400 cm^{-1} indicates the presence of O-H stretching and strong hydrogen bonding (Yuan et al., 2011).

The carboxylic C stretch was around 1720 cm^{-1} and 1396 cm^{-1} (Bourke et al., 2007; Brewer et al., 2009). Adsorption at 2925cm^{-1} suggested the presence of aliphatic -CH_2 groups which disappeared at 650 ºC (Chun et al., 2004). The peak at 3050 cm^{-1} of palm kernel biochar and rice husk biochar was assigned to the aromatic C-H out of plane bend, indicating the presence of adjacent aromatic hydrogen. This peak was not found at the low temperature (300 ºC). The stretching vibration of silicates was at peaks 800 cm^{-1}, 780 cm^{-1}, 820 cm^{-1} and 1100 cm^{-1} (Bourke et al., 2007). The peaks at 875 cm^{-1} and 1000 cm^{-1} correspond to the content of carbonate and phosphate in the biochar types (Brewer et al., 2009).

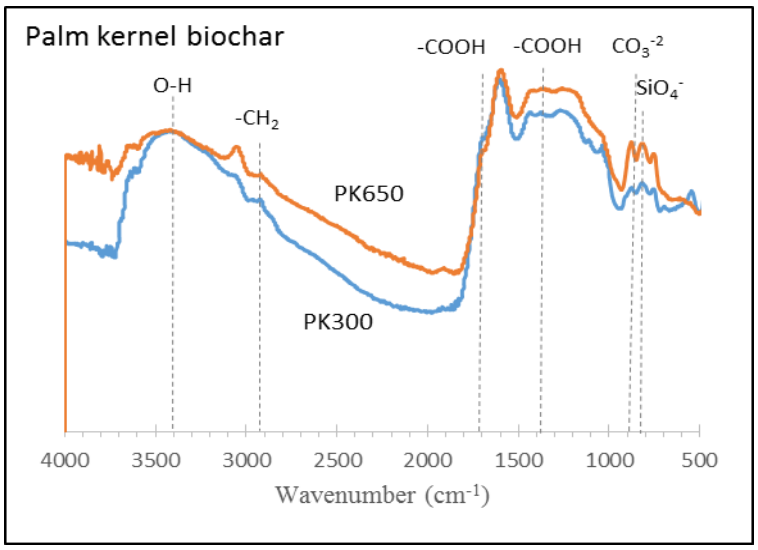

Fig. 3.1a Photoacoustic spectroscopy-FTIR analysis of palm kernel biochar (PK300 & PK650)

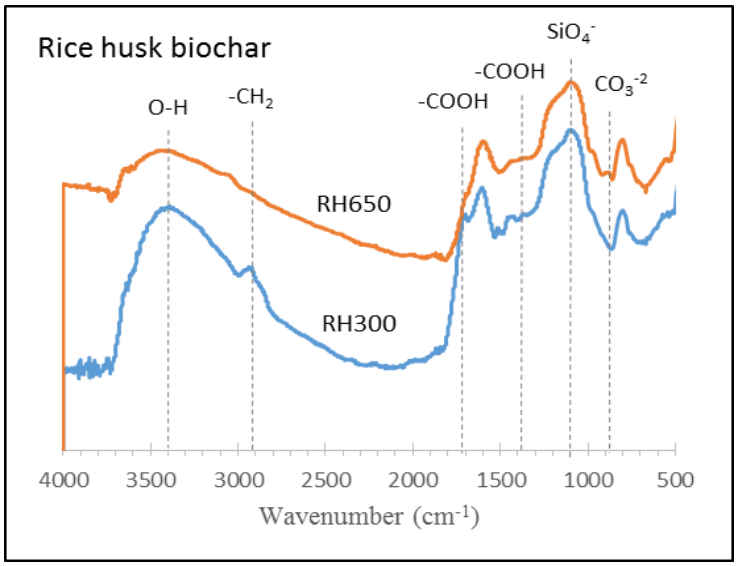

Fig. 3.1b Photoacoustic spectroscopy-FTIR analysis of rice husk biochar (RH300 & RH650)

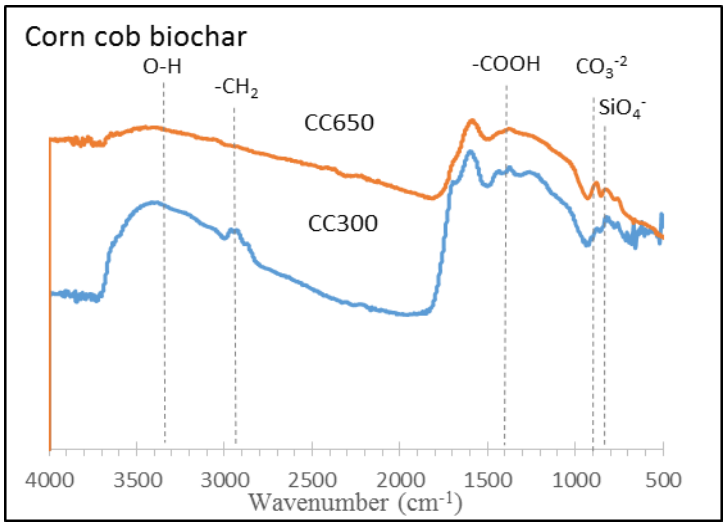

Fig. 3.1c Photoacoustic spectroscopy-FTIR analysis of corn cob biochar (CC300 & CC650)

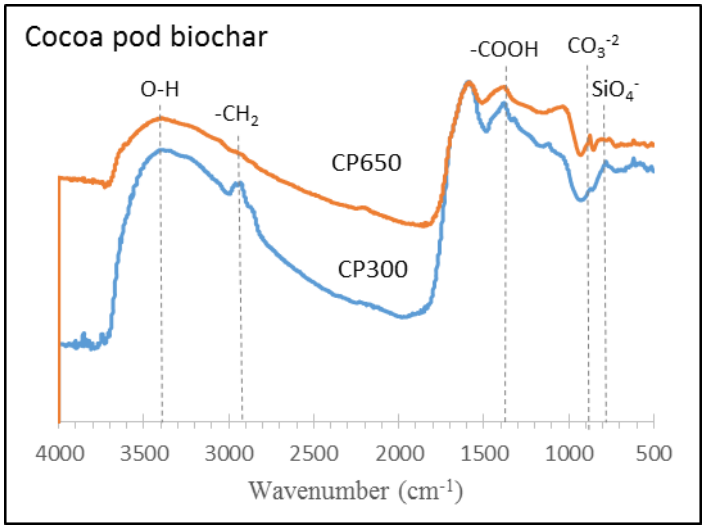

Fig. 3.1d Photoacoustic spectroscopy-FTIR analysis of cocoa pod husk biochar (CP300 & CP650)

The mineral composition of the biochar types at the two pyrolysis temperatures are shown in Table 3.2. The analysis indicated the presence of quartz (SiO_2) in all the biochar types. Calcite ($CaCO_3$) was also found but with the exception of palm kernel shell biochar. Ankerite ($Ca(Fe,Mg,Mn)(CO_3)_2$) and sylvite (KCl) were present in cocoa pod husk and rice husk respectively. All the identified crystalline minerals peak intensity increased with increasing pyrolysis temperature (Appendix 3A).

3.3.2 Effect of shaking time on P adsorption

The effect of shaking time on phosphorus sorption on all the biochar types at the two pyrolysis temperatures, 300 ^{o}C and 650 ^{o}C was investigated to determine the time it takes to attain equilibrium (Fig. 3.2). The results showed that the adsorption of P from solution onto all the biochar types at the two pyrolysis temperatures significantly ($p < 0.05$) increased rapidly in the first few hours and progressively decreased until approaching an apparent equilibrium varying from 6 to 12 h. The CP300 had the least equilibrium time (6 h) having maximum P adsorption of 2.47 mg g^{-1}.

Rice husk biochar at 300 ^{o}C (RH300), RH650 and PK300 reached P equilibrium adsorption at 9 hours with a concomitant P maximum adsorption of 3.69 mg g^{-1}, 7.53 mg g^{-1} and 5.54 mg g^{-1} respectively. At 12 h of shaking time, CP650, CC300, CC600 and PK650 attained P adsorption equilibrium with respective P adsorption of 5.80 mg g^{-1}, 3.75 mg g^{-1}, 6.51 mg g^{-1} and 9.09 mg g^{-1}.

Table 3. 2 Minerals detected in biochar types using X-ray powder diffraction

Biochar	Minerals
CCP300	SiO_2, $CaCO_3$, $Ca(Fe,Mg,Mn)(CO_3)_2$
CP650	SiO_2, $CaCO_3$, $Ca(Fe,Mg,Mn)(CO_3)_2$
CC300	SiO_2, $CaCO_3$,
CC650	SiO_2, $CaCO_3$
RH300	SiO_2, $CaCO_3$, KCl
RH650	SiO_2, $CaCO_3$, KCl
PK300	SiO_2
PK650	SiO_2

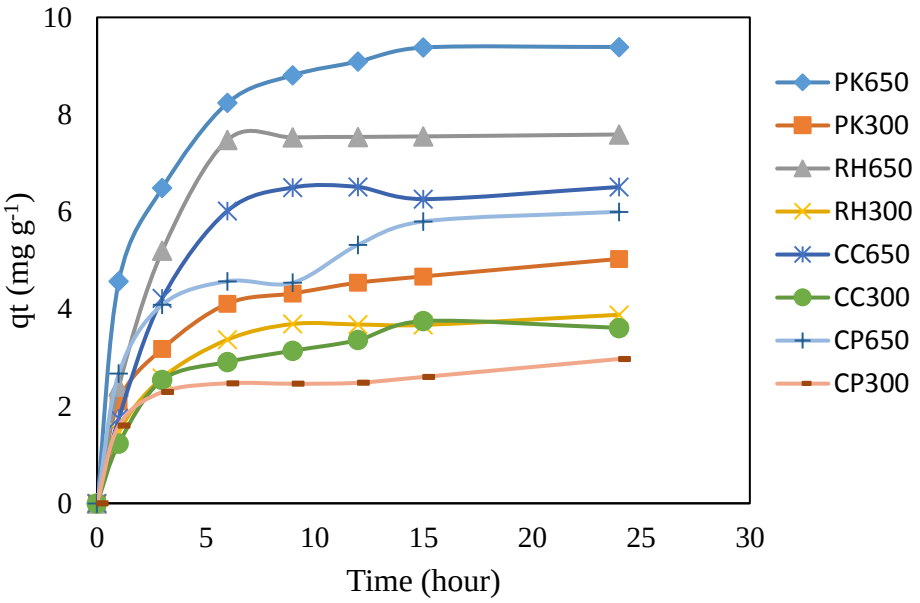

Fig. 3.2 Effect of contact time on P adsorption capacity of plam kernel biochar, rice husk biochar, corn cob biochar and cocoa pod husk biochar at two pyrolysis temperatures (300 ºC and 650 ºC)

3.3.3 Phosphorus Adsorption modeling

To predict and understand the P adsorption mechanism and the potential rate limiting steps, four mathematical models namely pseudo first order model, pseudo second-order model, Elovich model and Weber Morris Intraparticle diffusion model were applied to the data generated from the effect of time on P adsorption experiment.

Table 3.3 shows the parameters derived from the application of the pseudo first order, pseudo second order and Elovich kinetics models with their respective experimental P adsorbed (Qe) and coefficient of determination (R^2). The calculated P adsorbed at equilibrium, qe of the Pseudo first order model was in a range of 2.6 to 10.2 mg g^{-1}. The qe values of each of the four biochar types at various pyrolysis temperatures were relatively not closer to their respective experimental P adsorbed values (Qe) (Fig. 3.3a & b). The adsorption rate constant, K_1 varied from 0.17 to 0.47 h^{-1}. Biochar types, PK300, RH300 and CC300 had relatively low adsorption rate (K_1) as compared to when produced at 650 ^oC (RH650, PK650 and CC650). However, K_1 of CP300 was higher than CP650.

Pseudo second order model had a calculated qe values varying from 3.0 to 10.3 mg g^{-1} which was relatively closer to the experimental values (Qe).

Table 3.3 Kinetics rate parameters for phosphorus adsorption onto palm kernel biochar (PK), rice husk biochar (RH), corn cob biochar (CC) and cocoa pod husk biochar (CP) at two different pyrolysis temperatures (300 ^{o}C and 650 ^{o}C)

Biochar		Pseudo First Order			Pseudo Second Order			Elovich		
	Qe $(mg\ g^{-1})^{a}$	$qe\ (mg\ g^{-1})^{b}$	$K_1\ (h^{-1})^{c}$	R^2	$qe\ (mg\ g^{-1})^{d}$	$K_2\ (mg\ g^{-1}\ h^{-1})^{e}$	R^2	$ß\ (g\ mg^{-1})^{f}$	$a\ (mg\ g^{-1}\ h^{-1})^{g}$	R^2
CP300	3.0	2.6	0.47	0.85	3.0	0.22	0.99	2.70	39.25	0.95
CP650	6.0	5.4	0.37	0.79	6.2	0.09	0.99	0.96	14.27	0.95
RH300	3.9	3.1	0.26	0.93	4.1	0.15	0.99	1.16	5.51	0.97
RH650	7.6	6.3	0.46	0.90	8.8	0.06	0.99	0.50	8.41	0.95
CC300	3.6	3.1	0.27	0.94	4.2	0.11	0.99	1.17	4.14	0.95
CC650	6.5	7.2	0.44	0.94	7.7	0.05	0.98	0.55	3.25	0.95
PK300	5.0	3.5	0.17	0.94	5.1	0.12	0.99	1.03	8.85	0.99
PK650	9.4	10.2	0.38	0.90	10.3	0.06	0.99	0.54	22.94	0.99

[a]Experimental P adsorbed
[b]Calculated P adsorbed of the Pseudo First Order kinetic
[c]Pseudo First Order adsorption rate constant
[d]Calculated P adsorbed of the Pseudo Second Order kinetic
[e]Pseudo Second Order adsorption rate constant
[f]Desorption constant related to the extent of surface coverage and activation energy for chemisorption
[g]Initial adsorption rate of the Elovich model

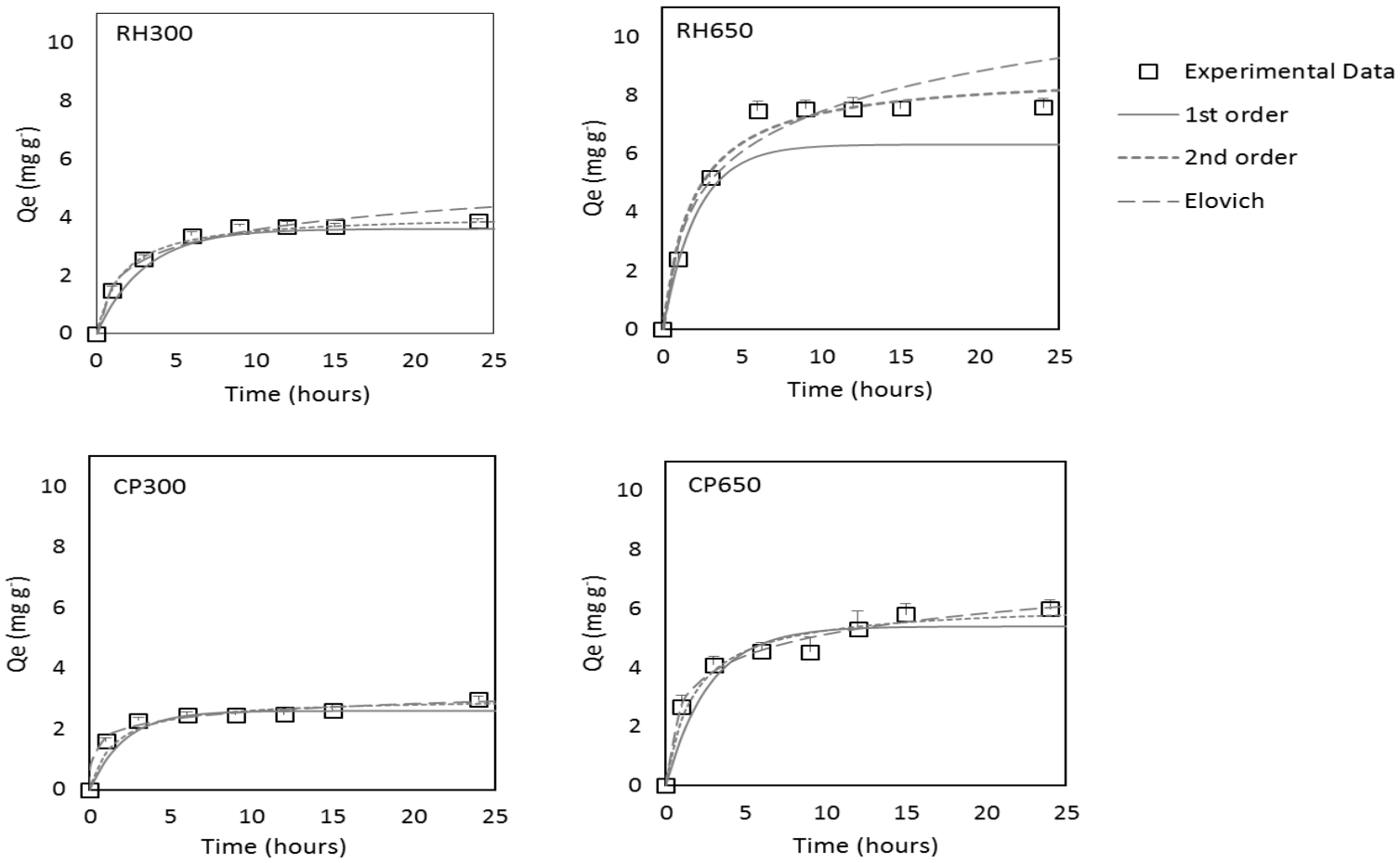

Fig. 3.3a Kinetics models (Pseudo first order, Pseudo second order & Elovich) of P onto cocoa pod husk and rice husk biochar at 300 ^{o}C and 650 ^{o}C

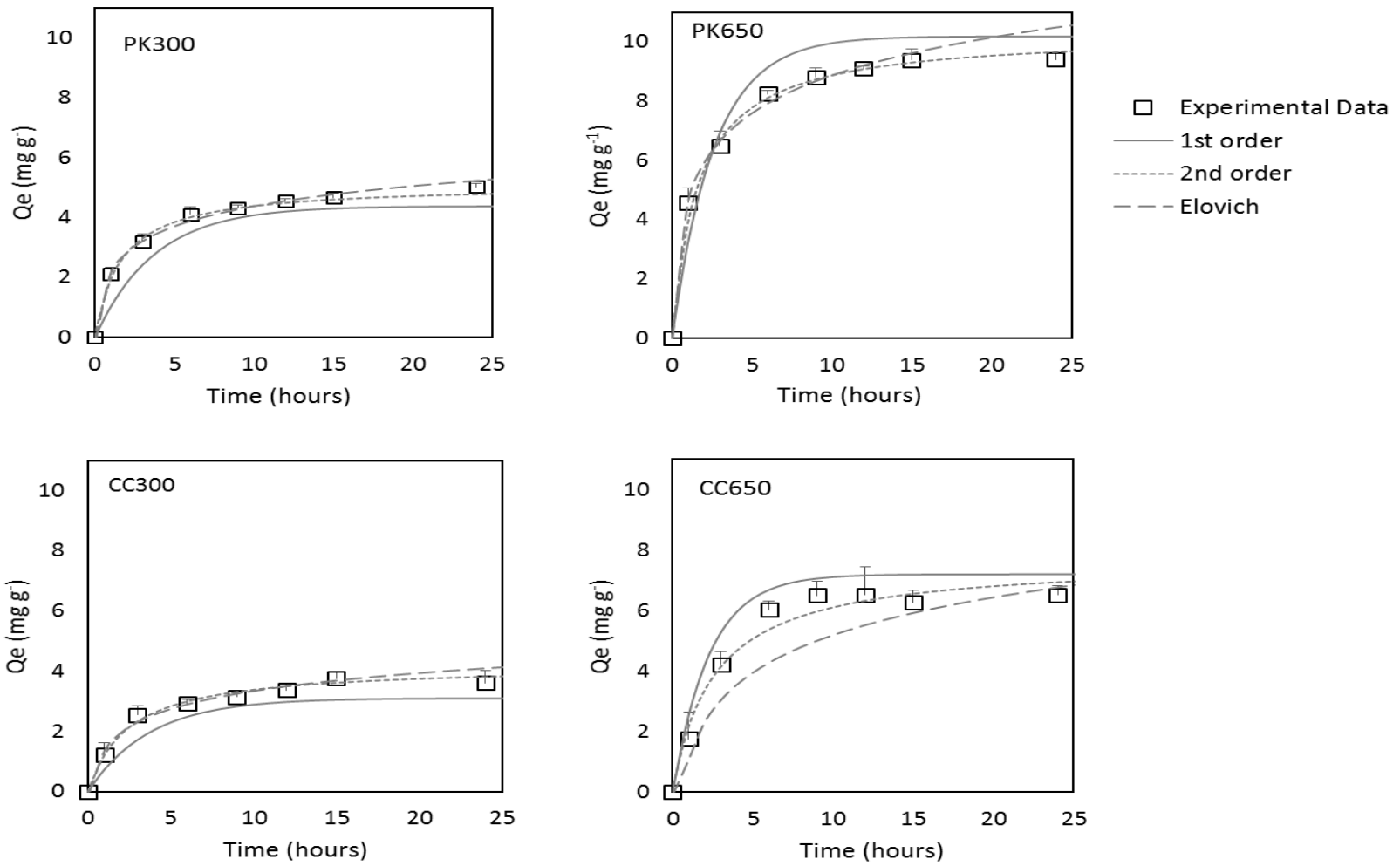

Fig. 3.3b Kinetics models (Pseudo first order, Pseudo second order & Elovich) of P onto palm kernel shell and corn cob biochar at 300 ^{o}C and 650 ^{o}C.

The adsorption rate constant, K_2 (mg g^{-1} h^{-1}) ranged from 0.06 to 0.22 mg g^{-1} h^{-1}. Contrary to the adsorption rate constant of Pseudo first order, the K_2 values were relatively higher for 300 ^oC- produced biochar types than the 650 ^oC- produced biochar types.

The initial adsorption rate, α of the Elovich model varied among all the adsorbents from 3.25 to 39.25 mg g^{-1} h^{-1} increasing in the order of CC650 < CC300 < RH300 < RH650 < PK300 < CP650 < PK650 < CP300. The desorption constant, ß was relatively higher for the 300^OC-biochar types than the 650 ^oC-biochar types. It increased in the order of RH650 < PK650 < CC650 < CP650 < PK300 < RH300 < CC300 < CP300.

The Weber-Morris (1963) intraparticle diffusion model parameters were calculated (Table 3.4) to determine whether film diffusion or intraparticle diffusion is the rate limiting step. Per the model, should the sorption mechanism be intraparticle diffusion then a plot of q_t versus $t^{1/2}$ will be linear. Intraparticle diffusion is considered the sole rate-limiting step when the graph passes through the origin. When the sorption process is controlled by more than one mechanism, then the plot will be multi-linear.

The plot of q_t versus $t^{1/2}$ for P sorption on all the biochar types are multi-linear in nature (Fig. 3.4) implying that two step film diffusion and intraparticle diffusion occurred simultaneously (Weber-Morris, 1963). The values of the intraparticle diffusion model constants are shown in Table 3.4. The intraparticle diffusion rate constant, K_i was higher for the 650 ^oC-biochartypes than the 300 ^oC-biochar types. The C (mg g^{-1}) values which indicate the thickness of the boundary layer was observed to be relatively small for the low temperature (300 ^oC) biochar types.

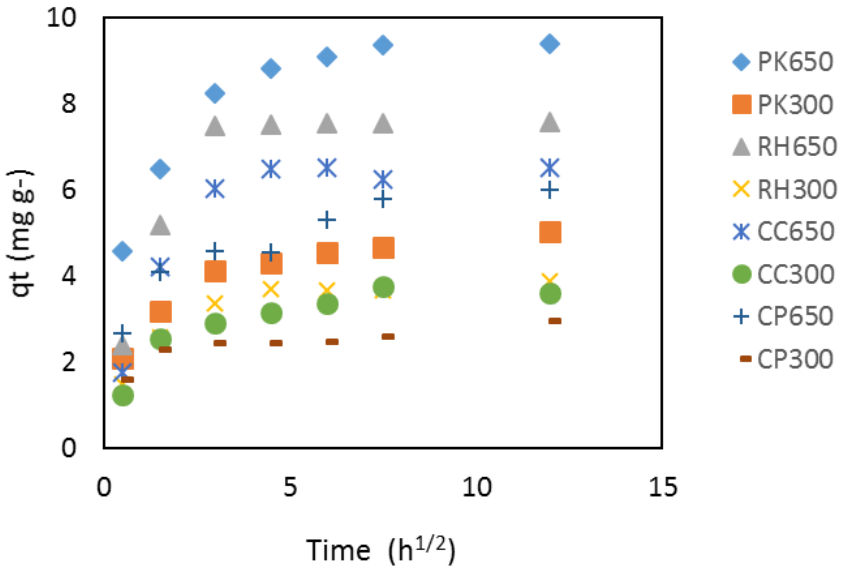

Fig. 3.4 Intraparticle diffusion modeling for kinetics of phosphorus adsorption onto the four biochar types at two different pyrolysis temperatures (300 ºC and 650 ºC)

Table 3. 4 Intraparticle diffusion parameters related to phosphorus diffusion onto the four biochar types at two different pyrolysis temperatures ((300 ºC and 650 ºC)

Biochar	K_i $(mg\ g^{-1}\ hr^{0.5})^a$	$C\ (mg\ g^{-1})^b$	R^2
CP300	0.11	1.91	0.65
CP650	0.38	3.05	0.85
RH300	0.30	1.68	0.84
RH650	0.58	3.00	0.66
CC300	0.28	2.00	0.72
CC650	0.63	3.90	0.65
PK300	0.33	2.50	0.81
PK650	0.63	5.30	0.82

[a]Intraparticle diffusion rate

[b]Boundary layer

3.3.4 Phosphorus adsorption isotherm

To further elucidate the adsorption properties of the different biochar types two isotherm equations namely Langmuir and Freundlich isotherms were tested. The goodness of fit of the models was ascertained by the respective R^2 values. Table 3.5 shows the calculated parameters of Langmuir and Freundlich isotherms together with the dimensionless factor R_L for all the biochar types. The two sorption isotherm models fitted the data well with $R^2 > 0.95$. However, the Freundlich model fitted the data better considering the relatively higher R^2 for most of the biochar types as compared with the Langmuir model. The calculated dimensionless factor R_L for all the biochar types were between 0 and 1 indicating that all the adsorbent (biochar types) used in the study were ideal for P adsorption (Appendix 3B).

The maximum monolayer sorption capacity (Q) of all biochar types was between 4.12-13.02 mg g^{-1} increasing in the order of CP300 < CC300 < RH300 < CP650 < PK300 < CC650 < RH650 < PK650. It was clear from the study that P sorption capacity of all the biochar types was relatively higher at 650 ^oC than 300 ^oC. The K value which is the bonding energy did not vary much among the biochar types ranging between 0.01 and 0.02 L mg^{-1}. It is obvious from the study that RH650 and PK650 had relatively the highest K_f values among the biochar types. The interactive energy between P and biochar surface (n) varied from 1.60 to 2.41.

3.3.5 Effect of equilibrium pH on phosphorus adsorption

The effect of equilibrium pH of P adsorption on the eight biochar types at initial solution pH between 2.5 and 8.5 are presented in Figures 3.6a & b).

Table 3. 5 Adsorption isotherm parameters for phosphorus adsorption onto palm kernel biochar (PK), rice husk biochar (RH), corn cob biochar (CC) and cocoa pod husk biochar (CP) at two different pyrolysis temperatures (300 ºC and 650 ºC)

Biochar	Langmuir			Freundlich		
	$Q\ (mg\ g^{-1})$*	$K\ (L\ mg^{-1})$	R^2	$K_f\ (mg\ g^{-1})(mg\ L)^n$	n	R^2
CP300	4.12	0.02	0.96	0.36	2.41	0.99
CP650	7.13	0.01	0.99	0.29	1.77	0.98
RH300	6.48	0.02	0.98	0.46	2.12	0.99
RH650	9.96	0.02	0.98	0.76	2.21	0.99
CC300	4.71	0.01	0.97	0.23	1.92	0.98
CC650	8.66	0.01	0.96	0.23	1.60	0.98
PK300	7.71	0.01	0.98	0.28	1.73	0.97
PK650	13.02	0.02	0.98	1.07	2.27	0.99

*Langmuir P sorption capacity

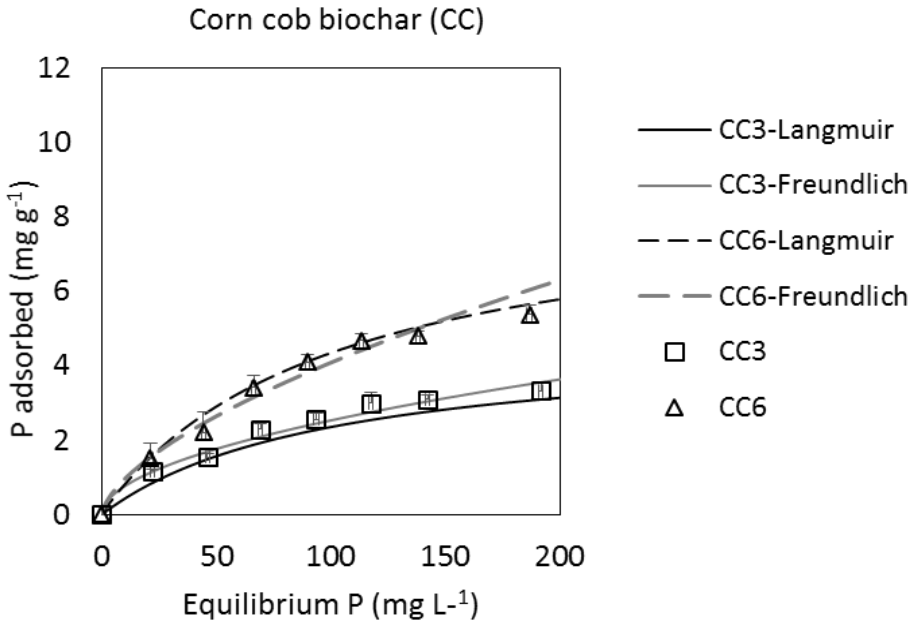

Fig. 3.5a Langmuir and Freundlich isotherms of P onto corn cob biochar (CC300 & CC650)

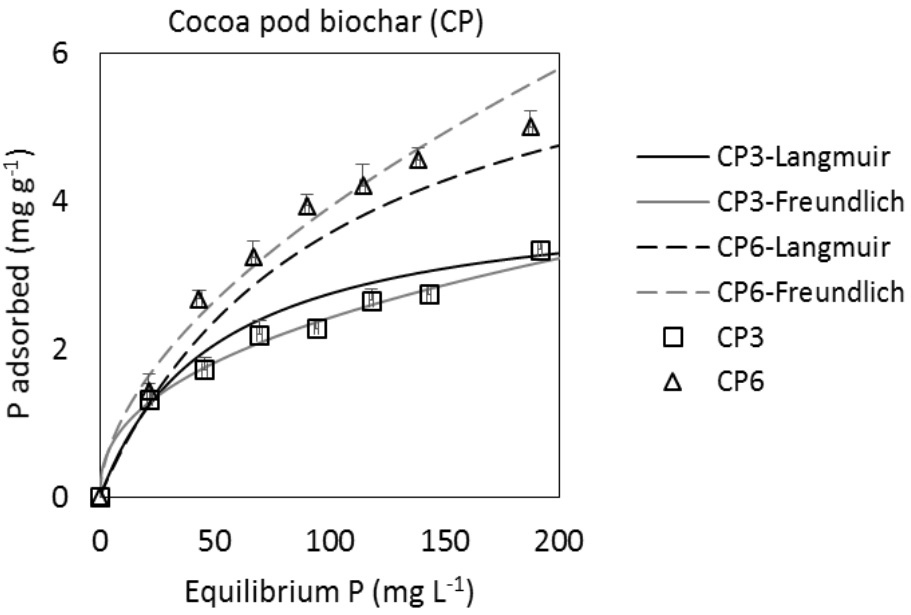

Fig.3.5b Langmuir and Freundlich isotherms of P onto cocoa pod husk biochar (CP300 & CP650)

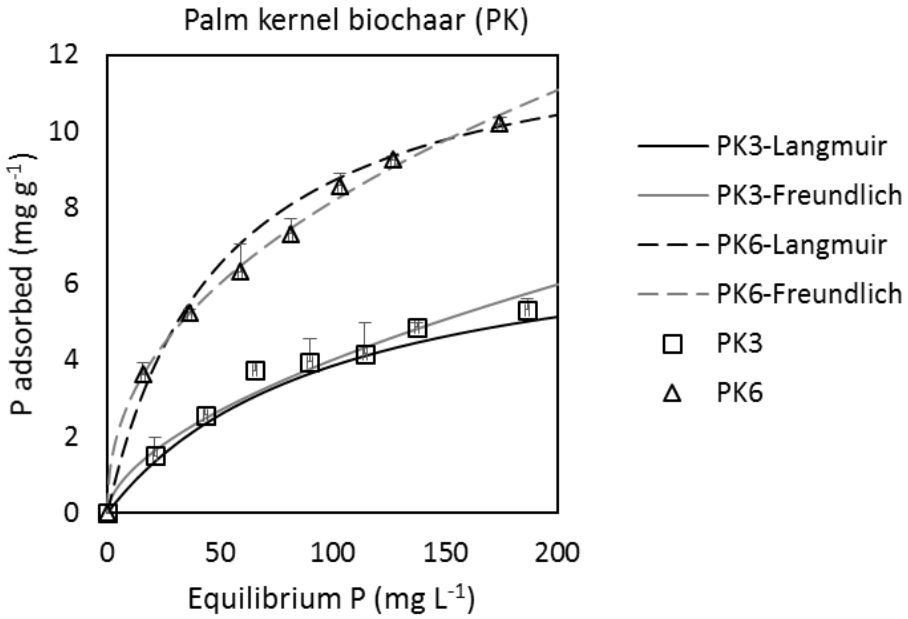

Fig. 3.5c Langmuir and Freundlich isotherms of P onto palm kernel biochar (PK300 & PK650)

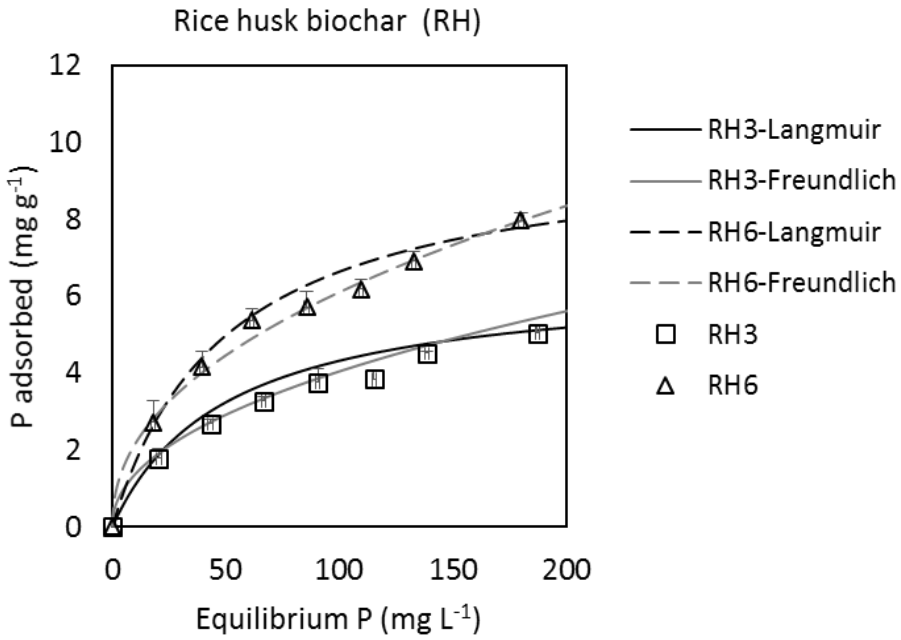

Fig. 3.5d Langmuir and Freundlich isotherms of P onto and rice husk biochar (RH300 & RH650)

,

All biochar types showed a significant *($p < 0.05$)* decrease in P adsorption with increasing equilibrium pH over the studied pH range. Feedstock type and pyrolysis temperature had influence on the optimum equilibrium pH for maximum P adsorption.

At equilibrium pH of 2.9, CC300 adsorbed 3.6 mg P g^{-1} which was statistically *($p > 0.05$)* similar to the amount of P adsorbed at equilibrium pHs of 4.5 and 4.1. However, increasing equilibrium pH from 4.1 to 9.3 statistically *($p < 0.05$)* decreased the amount of P adsorbed from 3.3 mg g^{-1} to 1.8 mg g^{-1}. Phosphorus adsorption by CC650 decreased significantly *($p < 0.05$)* from 6.3 to 5.9 from equilibrium pH of 3.2 to 4.3. Phosphorus adsorption remained statistically *($p > 0.05$)* the same when equilibrium pH increased from 4.3 to 5.1 but showed a significant *($p < 0.05$)* decrease in P adsorption from 5.5 mg g^{-1} to 2.9 mg g^{-1} at equilibrium pH's of 6.3 to 9.3. It was obvious that the equilibrium pH's for maximum P adsorption for CC300 was in a range of 2.9 to 4.1 and is 3.2 for CC650.

It is worth noting that for cocoa pod husk biochar produced at 300 ^{o}C (CP300) there was no significant variation *($p > 0.05$)* in the amount of P adsorbed as the equilibrium pH of the P solution was increased from 3.4 to 4.9. Increase in equilibrium pH from 4.9 to 6.0 significantly *($p < 0.05$)* decreased P adsorbed by 0.3 mg g^{-1}. There was no significant *($p > 0.05$)* difference in P adsorbed between equilibrium pH's 7.8 and 8.0. However, upon further increase in pH from 8.0 to 9.1, the amount of P adsorbed by CP300 decreased significantly *($p < 0.05$)* to 1.6 mg g^{-1}. Increasing the pyrolysis temperature of cocoa pod husk to 650 ^{o}C (CP650) showed a significant *($p < 0.05$)* increase in the amount of P adsorbed from 4.6 mg g^{-1} to 5.5 mg g^{-1} when the equilibrium pH was increased from 3.7 to 4.8. There was no significant *($p > 0.05$)* difference in the amount of P adsorbed between pH's 4.8 and 6.1. However, continuous increase in equilibrium pH from 6.1 to 9.6 significantly *($p < 0.05$)* decreased the P adsorbed from 3.2 mg g^{-1} to 2.2 mg g^{-1}.

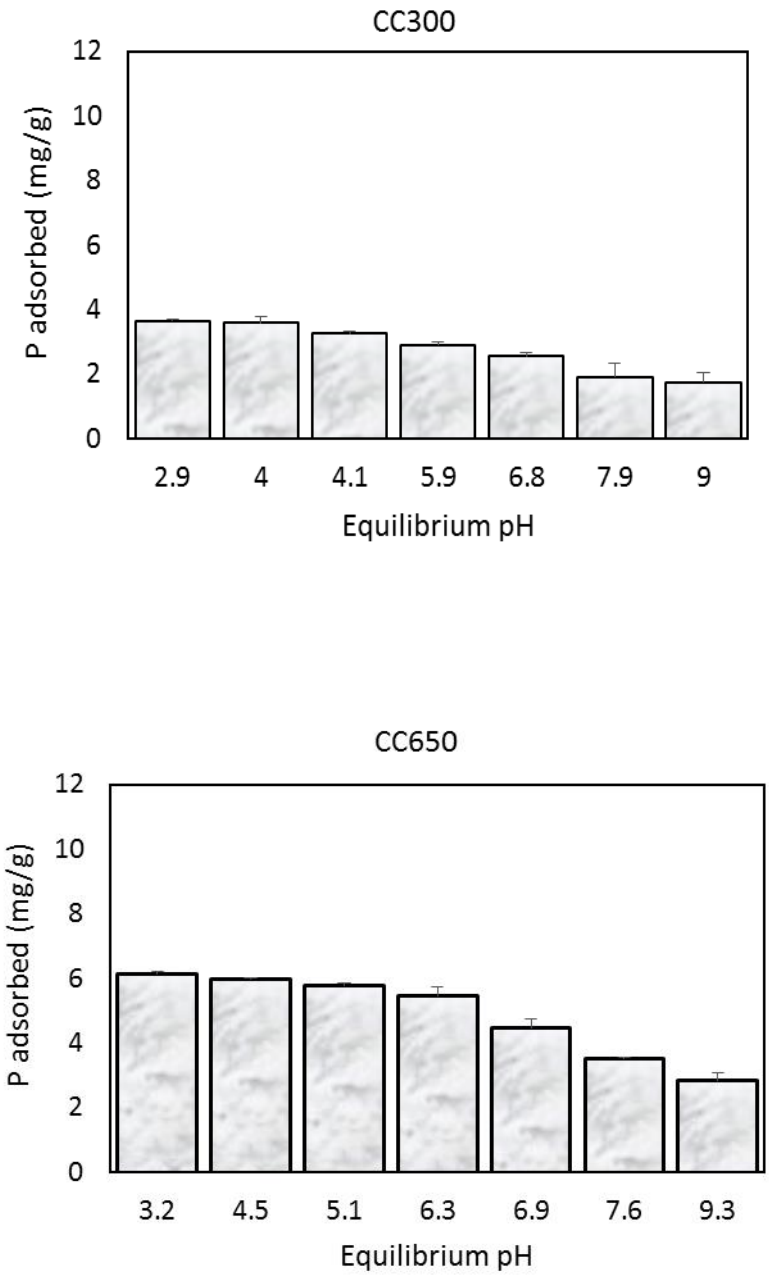

Fig. 3.6a Effect of equilibrium pH on P adsorption onto corn cob biochar (CC300 & CC650)

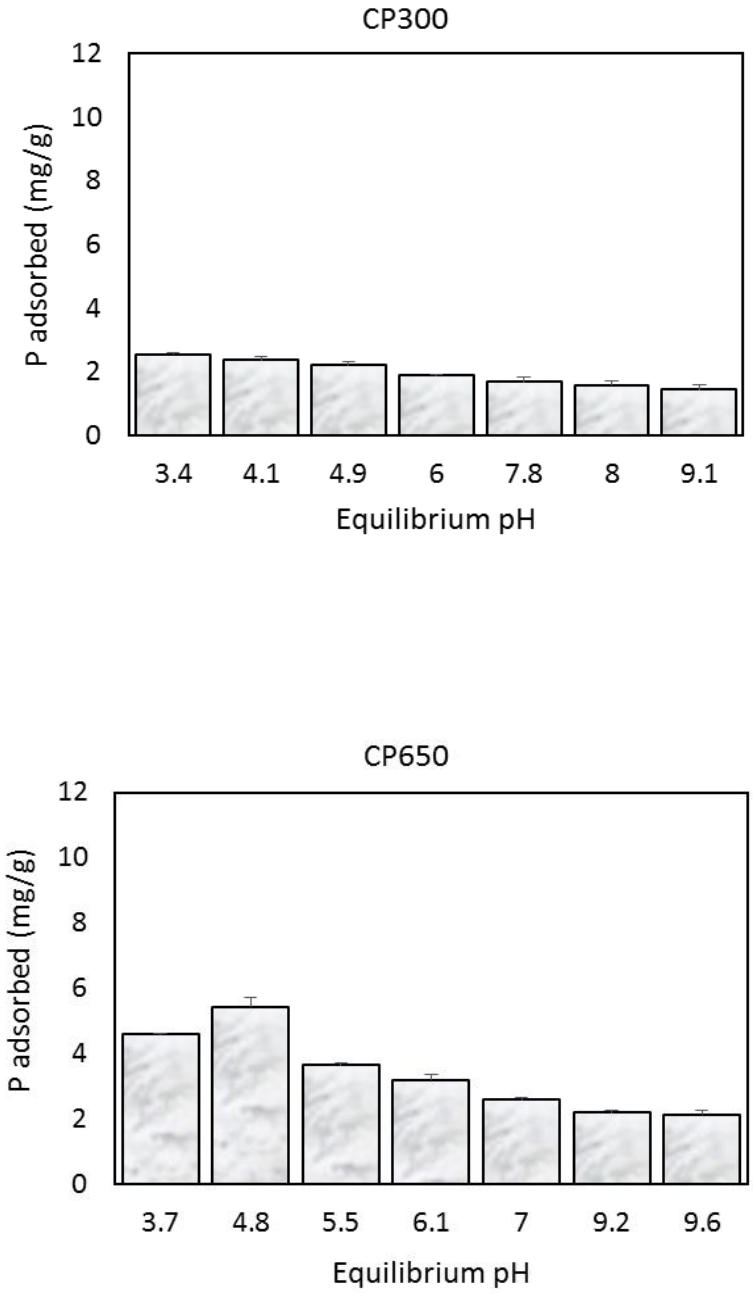

Fig. 3. 6b Effect of equilibrium pH on P adsorption onto cocoa pod husk biochar (CP300 & CP650)

Maximum P adsorption occurred at equilibrium pHs of 3.4 and 4.8 for CP300 and CP650, respectively.

Palm kernel shell biochar produced at 300 ^{o}C (PK300) showed a significant *($p < 0.05$)* variation in the amount of P adsorbed from 6.1 mg g^{-1} at equilibrium pH of 3.0 throughout to 2.3 mg g^{-1} at pH of 8.8. From the equilibrium pH of 3.6 to 7.0, the PK650 showed significant *($p < 0.05$)* reduction of P adsorbed from 11.6 mg g^{-1} to 7.8 mg g^{-1}. However, between pHs 7.0 and 8.5 the amount of P adsorbed was statistically *($p > 0.05$)* similar until it significantly *($p < 0.05$)* reduced to 5.4 mg g^{-1} at pH 9.0. The PK300 biochar type had maximum P adsorption at equilibrium pH at 4.1 with its PK650 counterpart having maximum adsorption at pH 3.6.

It is clear from the study that the amount of P adsorbed by RH300 from the equilibrium pH of 2.8 to 5.0 decreased significantly *($p < 0.05$)* from 4.0 mg P g^{-1} to 2.6 mg P g^{-1}. Further increase in the equilibrium pH showed no significant *($p > 0.05$)* variation until pH of 8.6 when the amount of P significantly *($p < 0.05$)* decreased to 1.9 mg g^{-1}. At equilibrium pH of 2.8, maximum adsorption occurred for RH300. Increasing the pyrolysis temperature of rice husk to 650^{o}C (RH650) showed significant *($p < 0.05$)* decrease in the amount of P adsorbed from 7.4 mg g^{-1} at the equilibrium pH of 3.2 throughout to 3.0 mg g^{-1} at pH of 9.0. Its maximum P adsorption occurred at equilibrium pH of 3.2.

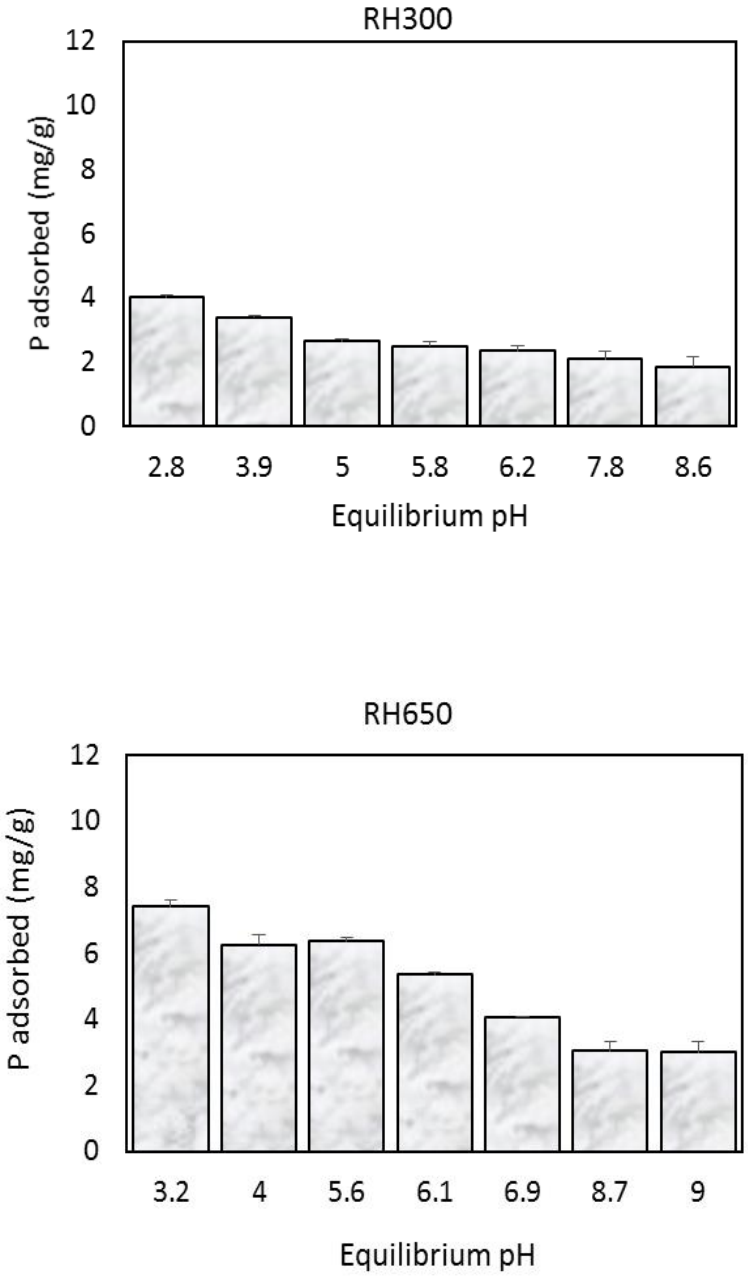

Fig. 3.6c Effect of equilibrium pH on P adsorption onto rice husk biochar (RH300 & RH650)

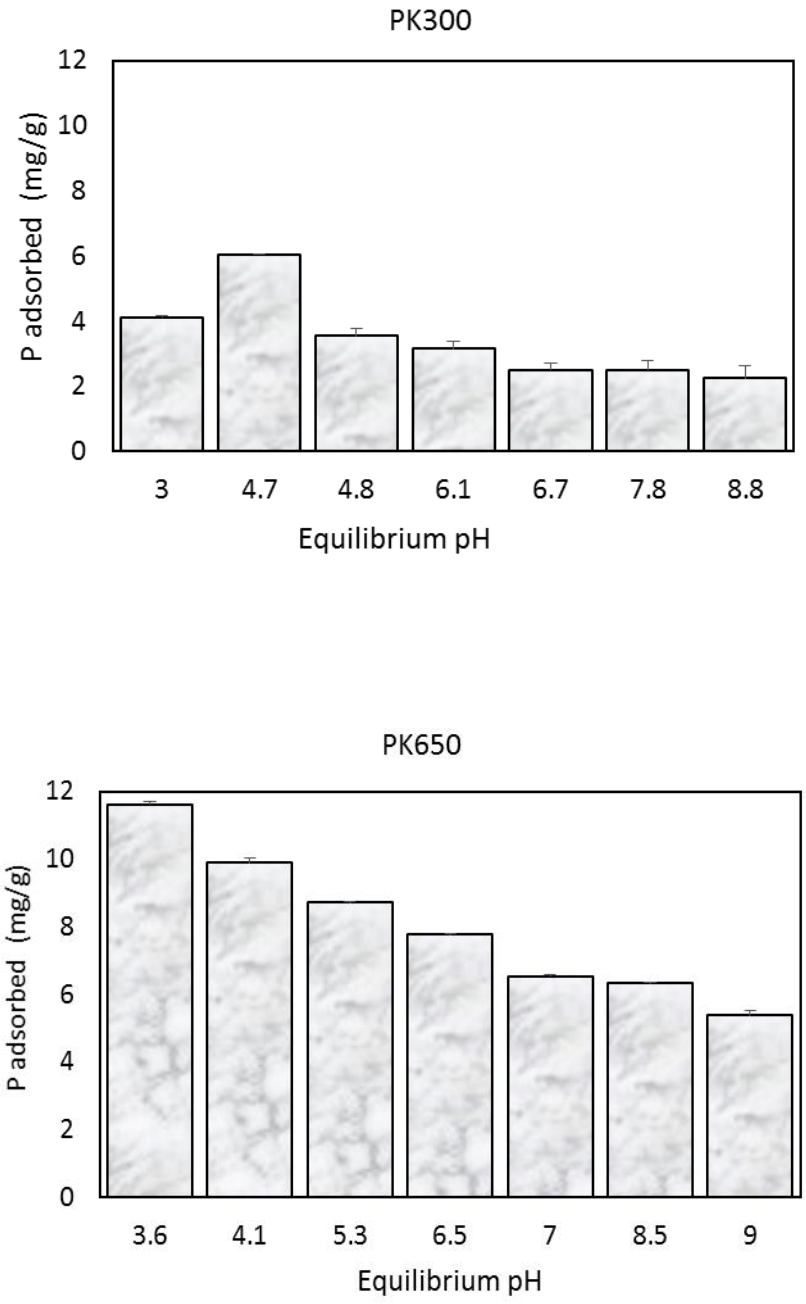

Fig. 3.6 d Effect of equilibrium pH on P adsorption onto palm kernel biochar (PK300 & PK650)

3.3.6 Change in equilibrium pH with phosphorus adsorption

The equilibrium pH of the blank (biochar samples without P solution) and the pH of the biochar samples with P solution over the initial solution pH's of 2.5 to 8.5 were measured. To further understand the mechanism of P removal by the biochar types (i.e. whether there was a release of water, proton or hydroxyl ions during the adsorption process), the amount of P adsorbed against the change in equilibrium pH were plotted (Figure 3.7 a-d). The change in pH was estimated as equilibrium pH of biochar sample with P solution minus equilibrium pH of blank.

The study showed that there was no change in pH with decreasing P adsorption for PK650, RH300, RH650, CP300, CC300 and CP650 since the changes in pH were below 0.5 pH units (Nartey et al., 2001). However, the CC650 and CP650 showed respective increases and decreases in pH which were more than pH 0.5 units. The 0.5 units increased in the change of pH of CP650 coincided with the maximum P sorption capacity, indicating the released of hydroxyl ion during the adsorption process. Similarly, the maximum P adsorption of PK300 coincided with a 0.6 unit decrease in pH, implying the release of protons during the adsorption process.

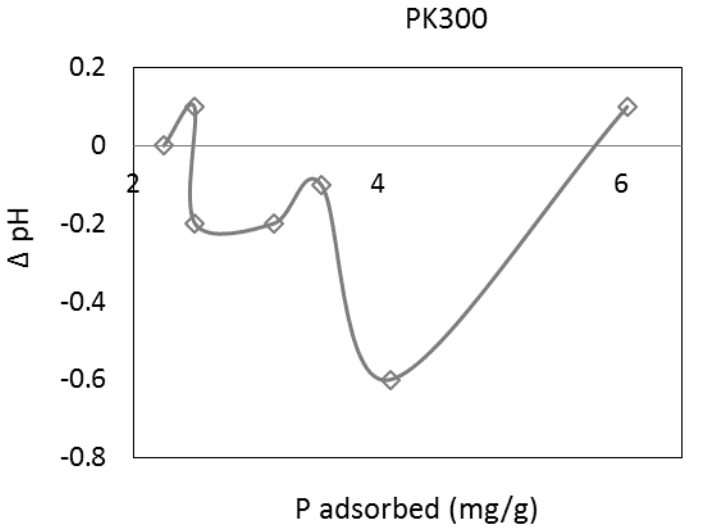

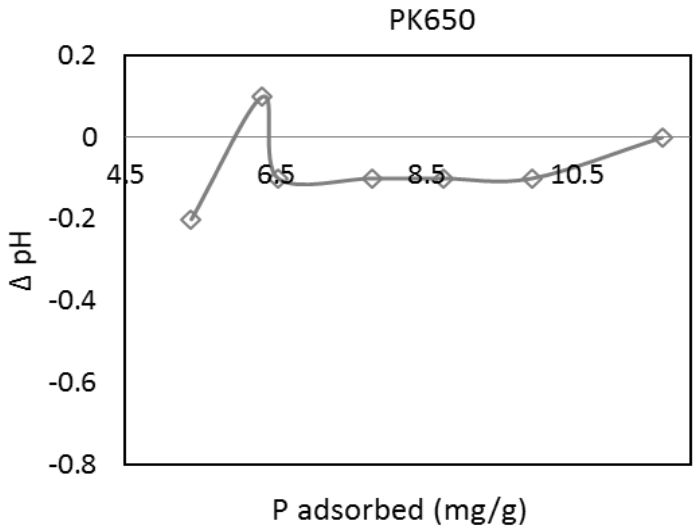

Fig.3.7a Change in equilibrium pH with P adsorption onto palm kernel biochar (PK300 & PK650)

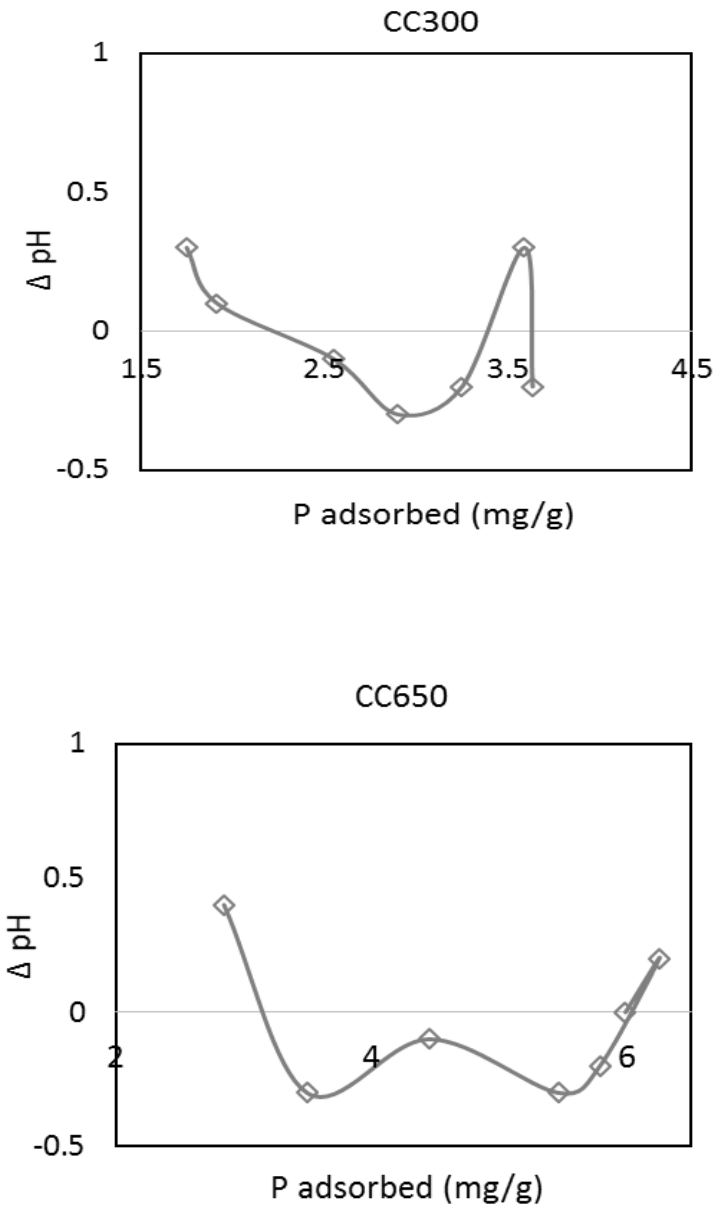

Fig. 3.7b Change in equilibrium pH with P adsorption onto corn cob biochar (CC300 & CC650)

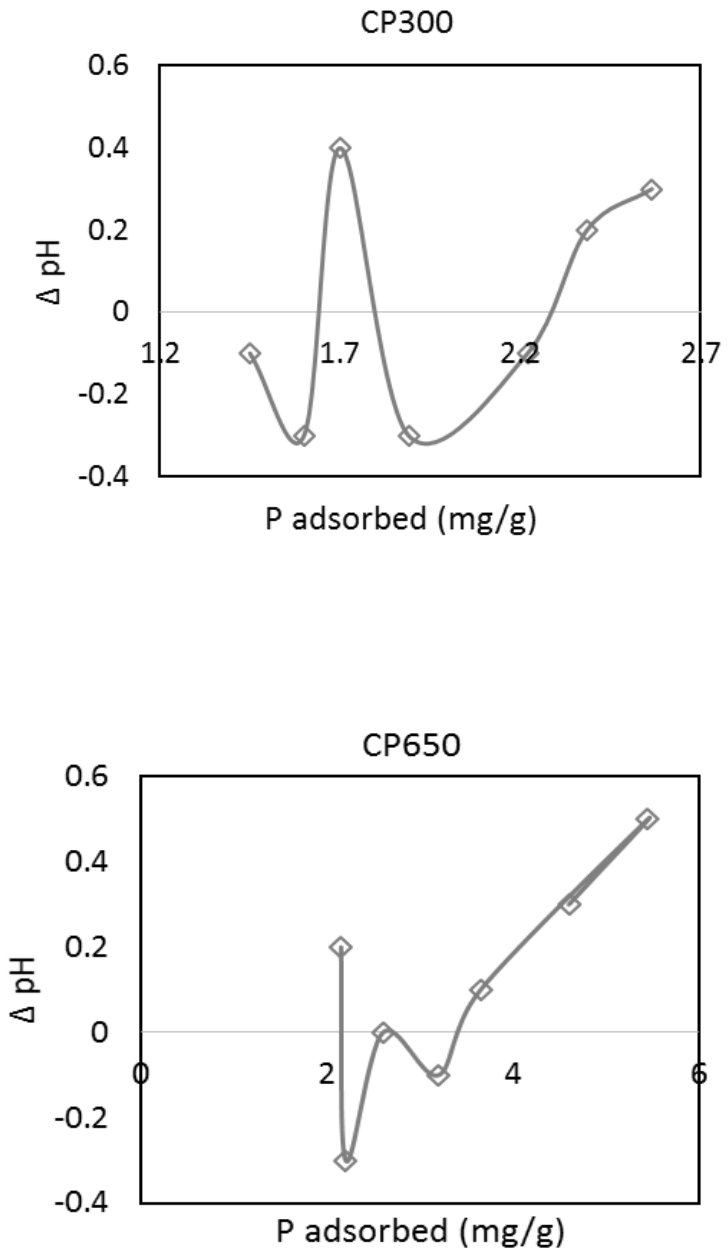

Fig. 3.7c Change in equilibrium pH with P adsorption onto cocoa pod husk biochar (CP300 & CP650)

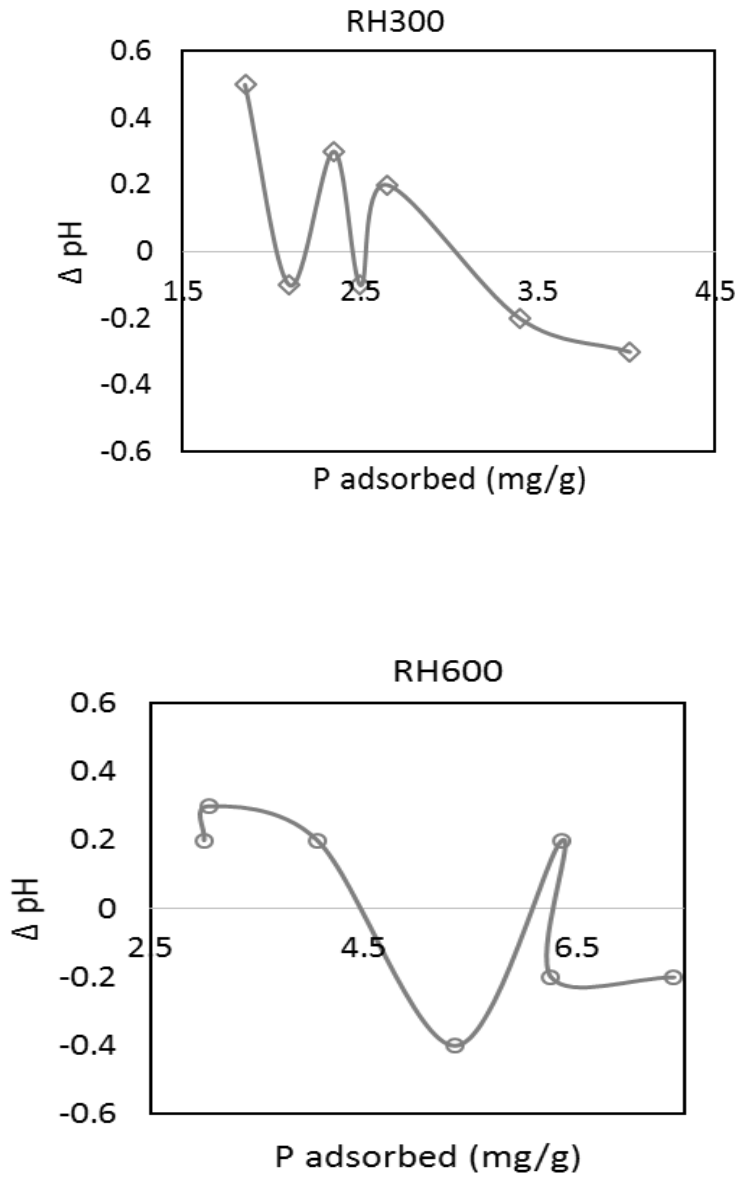

Fig. 3.7d Change in equilibrium pH with P adsorption onto rice husk biochar (RH300 & RH650)

3.4 Discussion

3.4.1 Characteristics of biochar

The pH of all the biochar types increased with increasing pyrolysis temperature. The increase in pH is likely to result from the release of alkali salts from feedstock during the pyrolysis process (Kim et al., 2011; Ahmad et al., 2014). The higher pH in the 650 ^{o}C biochar types than their 300 ^{o}C counterparts is as a result of the relatively higher levels of basic cations in the former. The pH of the CP650 and RH650 are similar to the pHs of CP and RH charred at 700^{o}C reported by Sam et al (2017). The mineralogical composition indicated that all the types had $CaCO_3$ except the PK types. This may explain in part, the alkalinity of all the CC, CP and RH biochar types. The absence of $CaCO_3$ and the low concentration of basic cations in the PK biochar types account for their slightly acid to neutral pHs. The high pH (> 10) and presence of $CaCO_3$ in the RH650 and CP650 making them the preferred choices of materials for liming acid soils. Even though biochar is mostly reported to be alkaline, slightly acidic pH biochar type (PK300) was observed in the present study. Similarly low pH of 4.84 and 4.91 has also been reported for oak wood biochar produced at 350 ^{o}C and 600 ^{o}C respectively (Nguyen et al., 2010).

The total carbon content of the biochar types increasing with increasing pyrolysis temperature irrespective of feedstock type is consistent with other studies (Chun et al, 2004; Chen et al. 2000) and have been reported to be due to carbonization (Chun et al, 2004). It is further explained that the increasing C concentration in biochar at increasing pyrolysis temperature is due to dehydration and loss of C bound H and O atoms at high temperatures through structural degradation (Antal and Gronli, 2003). This is corroborated by the loss of CH_2 functional groups at higher temepratures as evident in the FTIR spectra of all the biochar types. The high lignin, cellulose and hemicellulose

contents of palm kernel shell and corn cob biomass could have culminated in the relatively high C content of the biochar produced from these biomass as compared to the other types of biochar.

Cation exchange capacity (CEC) is used to measure biochar nutrient holding capacity, and the ability to hold cation from groundwater contamination (Jiang et al., 2012). The presence of COOH groups in all the biochar types is an attestation of their CEC. The COOH functional groups have pKas between 4.7 and 4.8 and the OH around 9 (Evangelou, 1998). Considering the biochars' pHs of between 5.5 and 10.3, these functional groups should deprotonate leading to the formation of negative charges hence CEC. Glaser et al. (2002) also ascribed the high CEC of biochar to the formation of carboxylic and OH groups by oxidation on the edges of the aromatic C of biochar. The high CEC of cocoa pod husk biochar implies less ability to adsorb anions in solution such as $H_2PO_4^-$ or HPO_4^{2-} and therefore will have low P sorption capacity. Anion adsorption should also be highest in the PK biochar types with their least CEC all things being equal. The decrease in CEC with increasing pyrolysis temperature can be attributed to the reduction in the acidic functional groups such as -COOH and -OH at 650 ^oC as also explained by Lee et al (2010).

There was an increasing enrichment of the total base cation and P content of all the biochar types as the pyrolysis temperature was raised from 300 ^oC to 650 ^oC. Zheng et al. (2013) reported that the enrichment of base cations and P with increasing pyrolysis temperature is due to their high vaporization energy. For instance, K and P vaporize at temperatures above 760 °C whiles Mg and Ca are lost only at temperatures above 1107 °C and 1240 °C, respectively (Knicker, 2007).. In consistence with the basic cations and P content values, the heavy metal concentration in the biochar was affected by the feedstock and the pyrolysis temperature. The particularly high level of Si in the RH biochar types confirms the element as a nutrient in rice. This is consistent with the high intensity peak of SiO_2 in the PAS-FTIR analysis. Silica is an important constituent of plant

photoliths as it safeguards the plant carbon from breaking down (Wilding et al., 1969; Parr, 2006) and it serves as a major component in the chemical structure of rice plant.

Nitrogen is lost during pyrolysis. Hence, the availability of the remaining nitrogen contained in biochar is considered limited. As the pyrolysis temperatures increase, nitrogen forms pyridine- like complexes that reduce availability (Bagreev et al., 2001). The decrease in nitrogen concentration with increasing pyrolysis temperature can be attributed to volatilization during heating and that some of the nitrogen containing structures in the biochar (e.g., amino acids, amines, amino sugars) are condensed into recalcitrant forms (Cao and Harris, 2010). It is, therefore palpable that the four biochar samples produced at 650 ^{o}C have low nitrogen contents (< 2.7 g kg^{-1}) as compared to 300 ^{o}C. Cocoa pod husk biochar with the high content of nitrogen coupled with its high pH and base concentrations can serve as a liming material for ameliorating tropical acid soils of Ghana including Ankasa, Bekwai and Kokofu Series. The high levels of Cu and Zn in thet CP and PK biochar types could be due to the heavy fertilization of these crops with micronutrients confirming their status as by-products of plantation crops

The functional groups on biochar surfaces are mostly determined using Photoacoustic spectroscopy-FTIR. During pyrolysis under increasing temperature there was a decrease in peaks 2925 cm^{-1}, 3400 cm^{-1}, 1396 cm^{-1} and 1720 cm^{-1} suggesting a decrease in aliphatic and polar functional groups (hydrophilic) at 650 ^{o}C. There was therefore enrichment of aromatic and hydrophobic structures at the high temperature (i.e. 650 ^{o}C) (Chun et al., 2004; Uchimiya et al., 2011; Rutherford et al., 2012). The decrease in aliphatic and polar functional groups at relatively high temperatures has been reported (Yuan et al., 2011). This assertion of aromatic condensation at relatively high pyrolysis temperatures could be due to the increasing dehydration and decarboxylation reactions as the polycondensed aromatic structures were formed and

polyaromatisation reactions became dominant (Novak et al., 2010; McBeath et al., 2013). The results of the present study were consistent with previous studies that detected broad alkyl signals on biochar pyrolysed at 300 to 400 ºC but not on biochar's above 400 ºC (McBeath et al., 2013). Biochar charred at low temperatures consists of ample amount of labile or volatile carbon which can easily be degraded, serving as a substrate and source of C and energy for soil microorganism (Khodadad et al., 2011). On the contrary, the dominant presence of aromatic carbon in the chemical structure of high pyrolysis biochar types results in the formation of recalcitrant structure.

3.4.2 Equilibrium time for P adsorption

The adsorption of P from solution increased rapidly in the first few hours and progressively decreased until approaching an apparent equilibrium varying from 6 to 12 h among the biochar types at various pyrolysis temperatures. The initial rapid phase and the proceeding slow phase of P adsorption is a commonly observed phenomenon (Saeed et al., 2005; Pellera et al., 2012). At the initial phase, the P was adsorbed by the exterior surface of the biochar and therefore the adsorption rate was rapid. Upon saturation of the exterior surface, the P ions entered into the biochar particle by the pore within the particle and were adsorbed by the interior surface of the particle (Wahab et al., 2011). As shown by the present study, the high P adsorption maximum attained by the biochar types within 6 to 12 h was due to three adsorption processes namely film diffusion, intraparticle diffusion and chemisorption working simultaneously. Previous studies have reported varying equilibrium time for P adsorption kinetics on biochar at different pyrolysis temperatures including one hour for mallee biochar at 750 ºC (Zhang et al., 2016), 15 h for *posidonia oceanica* biochar (Wahab et al., 2011) and 24 h observed for digested sugar beet tailing biochar charred at 600 ºC (Yao et al., 2011).

It's obvious that P adsorption equilibrium time varied among the eight biochar types that different adsorbents have different behavior in adsorption of P. The equilibrium time for P adsorption on the 300 ^{o}C pyrolysed biochar was faster than on the biochars produced at 650 ^{o}C as reflected in the higher CEC and lower Fe and Al contents of the 300 ^{o}C biochar types. Higher CEC would imply much higher repulsion of orthophosphate anions and higher Al and Fe contents means higher precipitation rates of the two cationic elements with orthophosphate anions especially at lower pH as evident in the isotherms. This higher precipitation at lower pH is corroborated by the highest P adsorption.

3.4.3 Phosphorus kinetic modeling

Adsorption processes are mainly controlled by the transport of adsorbate from the bulk solution to the adsorbent, film diffusion through the boundary layer, intraparticle diffusion of adsorbate, and the adsorption on the surface of the adsorbent (chemisorption or physisorption) (Alberti et al. 2012). The slowest reaction offered by one of these stages becomes the rate limiting step of the sorption process (Alberti et al., 2012).

As already stated in the results of the study, in order to predict and understand the P adsorption mechanism and the potential rate limiting steps, four mathematical models namely Pseudo First Order model, Pseudo Second-Order model, Elovich model and Weber Morris Intraparticle diffusion model were applied to the data generated from the effect of time experiment and the best-fit model was selected based on both the calculated qe values and the R^2 value. According to the kinetic modeling results, the coefficients of determination for Pseudo First Order model obtained for most of the biochar types were low (R^2 <0.95). Again, the theoretical adsorbed masses at

equilibrium, qe did not give values close to the experimental values (Qe). Therefore, the Pseudo First Order does not fit the present adsorption system for all the biochar types.

The Pseudo Second-Order proved to be the best fit to the experimental data for all the biochar samples with the highest correlation coefficients (R^2 = 0.99) as well as the calculated qe values closer to the experimental values (Qe). The adsorption rate constant, K_2 (mg g^{-1} h^{-1}) ranged from 0.06 to 0.22 mg g^{-1} h^{-1}, decreasing with increasing pyrolysis temperature across all the biochar types. The higher K_2 values for the 300 ^oC-biochar types demonstrate an increase rate of P adsorption on these adsorbents than the 650 ^oC-biochar types with time. The best fit experimental data to the second order suggests that the adsorption of orthophosphate onto the various biochar types was through chemisorption involving valency forces through covalent sharing or exchange of electrons between adsorbent and adsorbate (Ho, 2006).

The Elovich model which describes adsorption on heterogeneous adsorbents also provided a better description of the kinetics of P adsorption on all the biochar types with a high correlation coefficient. The adsorption rate, α, varied among all the adsorbents (3.25 to 39.25 mg g^{-1} h^{-1}). The desorption constant, ß (0.50 -2.70 g mg^{-1}) was relatively higher for the 300 ^oC-biochar types than the 650 ^oC-biochar types implying a higher desorption of adsorbed P. With regards to the assumption underlying Elovich model, the active surface sites on the biochar types used in the study are heterogeneous and therefore exhibit different activation energy for chemisorption.

Earlier studies on the kinetic behaviors of porous adsorbents such as biochar showed that intraparticle surface diffusion through macro- (>50 nm), meso- (2-50 nm), and micro- (<2 nm) pores could be important to the adsorption process (Mukherjee et al., 2011). However, the chemical kinetics models cannot describe the diffusion mechanism of P into the biochar types.

The possibility of intraparticle diffusion resistance affecting adsorption was determined using a Weber-Morris model (Weber and Morris, 1963). The multi-linearity of the Weber-Morris model suggests that intraparticle diffusion is not the sole rate limiting step. The earlier portion of the plot is the external surface adsorption stage i.e. film diffusion and the later stage is where the intraparticle diffusion is rate-limited (Fig. 3.4). The high intraparticle diffusion rate constant, K_i for the 650 ^oC-biochars than the 300 ^oC-biochar types could be due to the highly porous nature of biochar produced at high temperatures (Yuan et al., 2011). The lower values of the thickness of the boundary layer observed for the low pyrolysis biochar types (300 ^oC) implies that surface film diffusion plays less a role as the rate-limiting step in the overall sorption process in the 300 ^oC-biochar types.

The validity of the intrapaticle model coupled with Elovich and Pseudo Second Order model in the present study suggests that intrapaticle/film diffusion and chemisorption are the dominant mechanism in the adsorption of P on the four biochar types. These findings are in agreement with the results of P adsorption onto mallee biochar (Zhang et al., 2016).

3.4.4 Phosphorus adsorption Isotherm

Comparatively, Freundlich model fits the adsorption data better than the Langmuir model considering the relatively higher coefficient of determination for most of the biochar types. This implies that the active adsorption sites of all the biochar types were not limited to the formation of a monolayer but rather energetically heterogeneous. This was in agreement with the kinetics studies that multiple mechanism controls P adsorption onto the biochar.

It was obvious from the study that feedstock and pyrolysis temperature affects the surface chemistry of biochar and hence its affinity for P (Xu et al., 2016). Several studies have reported that the P adsorption capacity varies with different biochar types as mineral composition such as Fe, Al, PO_4^{3-}, $CaCO_3$ and MgO originated from the biomass influences P adsorption properties of biochar (Cao et al., 2009; Xu et al., 2014).

The P adsorption capacity of the eight biochar types varied from 4.12 to 13.02 mg g^{-1} in the following order: CP300 < CC300 < RH300 < CP650 < PK300 < CC650 < RH650 < PK650, which was generally consistent with the amount of negative charge (CEC) of the biochar and the Fe and Al content.

The adsorptive capacities of biochar types charred at 300 ^oC for P adsorption was relatively low. However, increasing the pyrolysis temperature to 650 ^oC raised the sorption capacity. This is in agreement with the finding of Wang et al. (2015a) who observed an increase in P adsorption at increased pyrolysis temperature in oak sawdust biochar. The 650 ^oC biochar types would be more effective in removing P anions from waste water. On the the other hand for P availability in soils, the 300 ^oC biochar types should be the preferred choice.

The n and K_f values obtained from the Freundlich equation can be used as indicators for the strength of P adsorption onto biochar. The smaller the n value, the stronger the interaction between adsorbent and adsorbate whilst the greater the value of K_f, the greater adsorption capacity (Jonker and Smedes, 2000). On the average, rice husk and palm kernel biochar types with high K_f had high adsorption ability for phosphorus.

3.4.5 Effect of equilibrium pH on P adsorption

The adsorption of ions at the solid-liquid interfaces is mostly controlled by the pH of the aqueous solution. The pH value of the P solution plays a major role in the whole adsorption process and particularly on the speciation of P anions and the surface charge of the biochar and hence its adsorption capacity (Biswas et al., 2007). All biochar types showed a decreasing P adsorption with increasing pH over the studied pH range. This trend is corroborated by the strong negative correlation between the amount of P adsorbed by the biochar types and the equilibrium pH ($r > 0.92$). This suggests that pH plays major role in P adsorption onto biochar.

The maximum P adsorption of all the biochar types occurred at equilibrium pHs between 2.8 and 4.8. In a similar study, Tetteh (2014) reported that the equilibrium pH for P sorption by cocoa pod husk and rice husk biochar ranged from 2 to 5. Feizi and Jalali (2014) also indicated that the equilibrium pH range for maximum P sorption by potato, canola and walnut shell biochar was 3 to 6.5.

Biochar mostly has low point of zero net charge (PZNC) (Mukherjee et al., 2011) and therefore at pH > 4.5 negative surface charges will be created resulting in low P sorption (Xie et al., 2014). The low affinity of P by all the biochar types at high solution pH could be as a result of the increased electrostatic anion repulsion between the negatively charged biochar surfaces and the negatively charged $H_2PO_4^-$ or HPO_4^{2-} ions, and also because of increased OH^- ion competition.

The 300 ^oC biochar types mostly CP300 showed greater inhibitory effect on P adsorption which was consistent with the observations in the experiments of adsorption isotherms. The PAS-FTIR analysis indicated ample amounts of oxygen-containing functional groups among which are -COOH and -OH contributing considerably to the negative surface charge of the biochars. As a consequence, the material had the highest CEC. With the highest CEC, it is a matter of course that

the biochar type would have the highest repulsion for the P anions which would translate into the least adsorption. This effect of CEC on P adsorption is further affirmed by the strong and significant negative correlation ($r = -0.84$; $p < 0.05$) between the CEC and the P sorption capacity of the biochar types (Appendix 3C). Similarly, Yuan et al. (2011) reported that biochar produced at 700^{o}C is less negatively charged compared with the one at 300^{o}C and 500^{o}C, indicating increase in PZNC with increasing pyrolysis temperature. The variation in the sorption capacity of the biochar types under the studied pH range suggests differences in the surface functional properties of all the biochar types as influenced by the pyrolysis temperature and the feedstock.

3.4.6 Proposed mechanism of P adsorption

Mechanism controlling orthophosphate adsorption on the biochar types varied. It is clear from the study that adsorption of P onto the biochar types was through chemisorption process, meaning it occurs at the active sites of the biochar surface involving electrostatic attraction, surface precipitation reactions and or ligand exchange.

The Al and Fe concentration of the biochar types were found to be strongly and significantly positively correlated to P sorption capacity (Appendix 3C). This was similar to the findings of Shepherd et al. (2017), mapping the mechanism of P capture in biochar and also Sibrell et al. (2009), examining P sorption in ochres with differing chemical compositions. The maximum P sorption for CP300, RH650 and CC650 occurred at equilibrium pH from 3.2 to 3.4. Within this equilibrium pH range (3.2 to 3.4), Fe and Al from the ash in the biochar will exist as free ions Fe^{3+} and Al^{3+} in solution (Marion et al., 1976). At these same equilibrium pH range, about 95% of P exists as $H_2PO_4^-$ and only 5% as H_3PO_4 since pK1 of orthophosphoric acid is 2.15 (Lindsay, 1979). Surface precipitation reaction of P with Fe and Al can occur as follows:

$$Fe^{3+} + 3H_2PO_4^- \leftrightarrow Fe(H_2PO_4)_3 \quad \text{(Surface precipitation)} \qquad \text{Eqn. 3.7}$$

$$Al^{3+} + 3H_2PO_4^- \leftrightarrow Al(H_2PO_4)_3 \quad \text{(Surface precipitation)} \qquad \text{Eqn. 3.8}$$

Phenol group was identified on CP300, RH650 and CC650 and can remove P through electrostatic attraction and or ligand exchange. Maximum adsorption for CP300, RH650 and CC650 were observed between equilibrium pH 3.2 and 3.4. These pHs are 5.6 to 5.8 pH units below the pKa of phenol (pKa = 9.0) (Evangelou, 1998). Thus the phenolic functional groups would be protonated. At these pHs, 2.1 and 2.3 above the pKa1 of orthophosphoric acid, the dominant P species in solution is $H_2PO_4^-$. Phosphorus removal by the protonated phenol can take place as:

$$R - OH_2^+ + H_2PO_4^- \leftrightarrow R - H_2PO_4 + H_2O \quad \text{(Ligand exchange)} \qquad \text{Eqn. 3.9}$$

$$R - OH_2^+ + H_2PO_4^- \leftrightarrow R - OH_2H2PO_4 \quad \text{(Electrostatic attraction)} \qquad \text{Eqn. 3.10}$$

Considering the fact that there were no changes in solution pH after adsorption, equations 3.9 and 3.10 are also plausible. In equation 3.10, the P is retained and could be exchanged by other anions back into solution. In equation 3.9, however, structural OH is replaced and the P is locked up. This mechanism may be ideal for water cleansing.

Carboxylic as a functional group with pKa value of 5.0 (Sparks, 1995) was found on RH300 and CC300. The equilibrium pHs for maximum P adsorption were 2.8 and 2.9 for RH300 and CC300 respectively. The equilibrium pHs (2.8 and 2.9) were more than 2 pH units below the pKa of carboxylic and therefore carboxylic will be protonated. The removal of P by the protonated carboxylic group can occur as:

$$\mathbf{R-COOH_2^+ \ + \ H_2PO_4^- \leftrightarrow \mathit{R}-COOH_2H_2PO_4} \quad \text{(Electrostatic attraction)} \quad \text{Eqn. 3.11}$$

Again with no change in equilibrium pH as a result of adsorption, eqn 3.11 is plausible. Orthophosphate adsorbed by RH300 and CC300 is weakly held (electrostatic attraction) and therefore can easily be exchanged by other anion into solution. The P held on the surfaces of these two biochar types can be made available for plant uptake. RH300 and CC300-laden P can serve as a slow P releasing fertilizer.

The maximum P adsorption capacity of palm kernel shell biochar produced at 650 ^{o}C (PK650) occurred at equilibrium pH of 3.6. At these pH, in addition to the existence of Fe^{3+}, Al^{3+}, there could be species of $FeOH_2^+$ and $AlOH_2^+$ (Marion et al., 1976). There was also no change in equilibrium pH after adsorption. Thus in addition to surface precipitation (Eqn. 3.7 & 3.8), PK650 can also adsorb P by ligand exchange as follows:

$$\mathbf{Fe-OH_2^+ + H_2PO_4^- \leftrightarrow Fe-O-H_2P\mathit{O}_3 + H_2O} \quad \text{(Ligand exchange)} \quad \text{Eqn. 3.12}$$

$$\mathbf{Al-OH_2^+ + H_2PO_4^- \leftrightarrow Al-O-H_2P\mathit{O}_3 + H_2O} \quad \text{(Ligand exchange)} \quad \text{Eqn. 3.13}$$

Equations 3.12 and 3.13 are mononuclear monodentate reaction involving ligand exchange. The P is strongly held on PK650. The P then becomes part of the biochar structure and is not available for plant uptake.

The equilibrium pH (4.1) at which maximum P adsorption occurred on PK300 coincided with a 0.7 unit decrease in equilibrium pH. This implies that there was a release of proton after P adsorption. At the equilibrium pH of 4.1, Fe^{3+}, Al^{3+}, $FeOH_2^+$, $AlOH_2^+$, $FeOH^{2+}$ and $AlOH^{2+}$ exist

in solution as the monomeric forms of Fe and Al (Marion et al., 1976). At this equilibrium pH (4.1), about 95% of P exist as $H_2PO_4^-$ and only 5% as H_3PO_4 since pK1 of orthophosphoric acid is 2.15 (Lindsay, 1979). Phosphorus adsorption by PK300 can therefore occur by precipitation reaction and ligand exchange with concomitant release of proton (Eqn. 3.14-3.19). Similar to P adsorption on PK650 biochar, P is strongly held and therefore cannot be made available for plant uptake. Palm kernel biochar produced at 300 ^oC and 650 ^oC can be used for wastewater treatment by removing P since the adsorbed P cannot easily be desorbed.

$$Fe^{3+} + H_2PO_4^- + 2H_2O \leftrightarrow Fe(OH)_2H_2PO_4 + 2H^+ \quad \text{(Surface precipitation)} \quad \text{Eqn. 3.14}$$

$$Al^{3+} + H_2PO_4^- + 2H_2O \leftrightarrow Al(OH)_2H_2PO_4 + 2H^+ \quad \text{(Surface precipitation)} \quad \text{Eqn. 3.15}$$

$$Fe - OH^{2+} + H_2PO_4^- \leftrightarrow FeH_2PO_4 + H^+ \quad \text{(Ligand exchange)} \quad \text{Eqn. 3.16}$$

$$Al - OH^{2+} + H_2PO_4^- \leftrightarrow Al - O - H_2PO_3 + H^+ \quad \text{(Ligand exchange)} \quad \text{Eqn. 3.17}$$

$$Fe - OH_2^+ + H_3PO_4 \leftrightarrow Fe - O - H_2PO_3 + H_3O^+ \quad \text{(Ligand exchange)} \quad \text{Eqn. 3.18}$$

$$Al - OH_2^+ + H_3PO_4 \leftrightarrow Al - O - H_2PO_3 + H_3O^+ \quad \text{(Ligand exchange)} \quad \text{Eqn. 3.19}$$

Considering the fact that, decrease in pH was only 0.7 pH units it is not likely that equations 3.14 and 3.15 occurred as these equations depict the release of 2 moles of H^+ that should have accounted for a much decrease in pH. The more plausible reactions are equations 3.16 to 3.19.

The CP650 also showed a 0.5 unit increase in pH, which coincided with its maximum P adsorption. This 0.5 increase in pH connotes the release of OH^- after P adsorption. The maximum P adsorption

occurred at equilibrium pH of 3.2. At this pH the carboxylic groups will exist mainly in the neutral form. Phosphorus adsorption by carboxylic ion can occur through ligand exchange reaction with concomitant release of OH^- ion (Eqn. 3.20). This biochar type (CP650) can also serve as a strong P adsorbent in wastewater treatment.

$$\mathbf{R-COOH} + \mathbf{H_2PO_4^-} \leftrightarrow \mathbf{R-COH_2PO_4} + \mathbf{OH^-} \qquad \text{(Ligand exchange)} \quad \text{Eqn. 3.20}$$

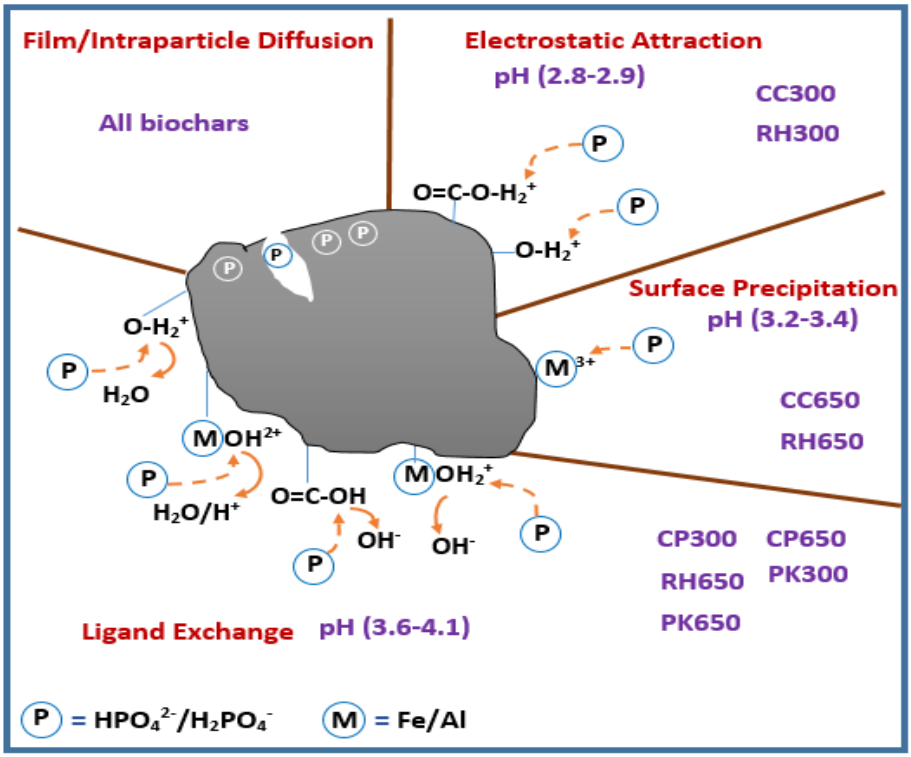

Fig. 3.8 An overview of proposed P adsorption mechanism on the biochar types

3.5 Conclusion

The study indicated that rice husk, corn cob, cocoa pod husk and palm kernel shell charred at both 300 ^{o}C and 650 ^{o}C have affinity for P adsorption. The P absorption capacity was found to be in the order of CP300 < CC300 < RH300 < CP650 < PK300 < CC650 < RH650 < PK650 and was highest at low pH and higher pyrolysis temperature. The adsorption of P increased with increasing pyrolysis temperature. Among all the four biochar types tested, palm kernel shell biochar at 650 ^{o}C had the highest P sorption capacity and should be the preferred choice for removal of the anion from wastewater. The CP300 had the least P adsorption capacity and with its high total P content, alkaline pH and the presence of carbonate could be exploited for use as a liming material on acid soils. The adsorption of P onto the heterogeneous surface of the biochar types is by chemisorption reaction involving electrostatic attraction, surface precipitation and ligand exchange which was further proceeded by surface and intraparticle diffusion.

CHAPTER FOUR

PHOSPHORUS SORPTION CHARACTERISTICS OF BIOCHAR AMENDED SOILS

4.1 Introduction

Phosphorus deficiency is one of the major constraints to food production in highly weathered Ghanaian soils due to low native P and high P fixation by iron and aluminum oxides (Guzman, 1994). Amorphous and crystalline Fe and Al oxides have been reported to be the main phosphate adsorbents in acid soils (Freese et al., 1995; Borggaard, 2002). Phosphorus is fixed by high energy sorption surfaces such as oxides and hydroxides of Fe and Al by formation of insoluble Fe and Al phosphates by ligand exchange and precipitation reactions (Galvao and Salcedo, 2009; Schoumans and Chardon, 2015). Phosphorus uptake by plant from added P input in Ghanaian soils is therefore constrained.

One possible approach of improving P availability in tropical soils has been the use of plant and animal residues through direct P release or competitive sorption reaction between organic acids and P for soil sorption sites (Kamara, 2015). Organic residues are either applied directly or recycled as compost before incorporation into soils. However, the rapid decomposition rates of organic matter and hence fast release of plant nutrients leads to a short period for soil fertility improvement (Barthes and Azontode, 2004). Large amount of organic materials would therefore be required to maintain soil fertility.

Biochar is mostly a stable solid carbon-rich product obtained from thermal decomposition of plant and animal residues under limited oxygen conditions (Lehmann and Joseph, 2009; Mohan et al., 2014). It has longer residence time for over thousand years in soil than natural organic matter due to its high aromaticity. Biochar produced from organic materials usually have high surface area,

cation exchange capacity, porosity and polar and non-polar functional groups on the surface (Laird et al., 2010). The addition of biochar to tropical soils have been reported severally to improve soil fertility and crop productivity (Lehmann and Joseph, 2009; 2011; Tang et al., 2013).

Annually, large quantities of rice husk and corn cob residues are produced (Duku et al., 2011; Shen et al., 2012; Yao et al., 2012; Qian and Chen, 2013; Xu et al., 2013). Most often these residues are regarded as waste and therefore are either burnt on the field or abandoned causing environmental nuisance. Converting organic residues into biochar will not only improve biomass management in the environment but also as soil amendment to rectify poor soil fertility constraints in the tropics (Dong et al., 2013).

The addition of biochar is known to improve P availability and hence crop productivity in Ultisols and Oxisols of the tropics (Lehmann, 2007). Biochar contains ample amount of P and therefore can directly release soluble P into soil solution to enhance P availability (Chan et al., 2007; Atkinson et al., 2010). The liming property of biochar enables it to increase soil pH, although such effect depends on the buffering capacity of the biochar and the soil, eventually reducing P adsorption by crystalline and amorphous Al and Fe oxides (Wang et al., 2012; Yuan et al., 2011). A reduction in point of zero net charge (PZNC) of soil after the addition of biochar has been observed. The decrease in PZNC culminates into an increase in soil CEC leading to an increase in electrostatic P repulsion (Easterwood and Sartain, 1990). However, the increase in plant available P after biochar application is not always the case. For instance, DeLuca et al. (2009) reported that biochar decreases P availability in most alkaline soils of the tropics due to substantial released of cations including Ca^{2+} and Mg^{2+}. Again, P adsorption significantly increased, reducing P leachates in a column studies when biochar was amended to sandy clay soil of the tropics (Novak et al., 2009).

It is obvious that biochar alters the surface chemistry of tropical soils due to its heterogeneous surface properties, and therefore can affect P retention and availability in soils (Liang et al., 2014). Even though much work has been conducted on P sorption and availability in soils using P sorption characteristics (Agbenin and Tiessen, 1995; Abekoe and Tiessen, 1998; McDowell and Condron, 2001; Villapando and Graetz, 2001), very limited work has been done on P adsorption characteristics of biochar-soil complex. Further studies using different biochar types at varying pyrolysis temperatures on soils are required to evaluate the sensitivity of biochar-soil sorption characteristics to reflect soil P availability after biochar application.

The use of sorption isotherm to evaluate P requirement is considered a better option to conventional soil test (McDowell and Condron, 2001). Sorption isotherm takes into consideration intensity and capacity factors, which are necessary for evaluating the amount of P needed for maximum plant growth. Information on the interactive effect of biochar at varying pyrolysis temperatures with Ghanaian soils on P sorption is necessary for the effective management of P for sustainable crop production in the country.

The objectives of the study were to:

1. determine the effect of corn cob and rice husk biochar at varying pyrolysis temperatures on chemical properties of the soils
2. evaluate the effect of the biochar types at varying pyrolysis temperatures on P sorption capacity of the soils
3. determine the P release pattern of the soils as influenced by the biochar types using desorption studies

4.2 Materials and methods

4.2.1 Description of Soil

Three soil types from different agro-ecological zones were used. They are Kokofu, Ankasa and Keta series from moist semi-deciduous forest, evergreen high rain forest and coastal savannah zone respectively in Ghana.

Kokofu series located in the Eastern Region of Ghana is classified according to the World Reference Base (WRB, 1998) and Soil Taxonomy System (Soil Survey Staff, 1998) as Gleyi-Plinthic Acrisol and Typic Plinthustult respectively by Dwomo and Dedzoe (2010). This area has mean temperatures of 30-35 ^{o}C during the growing season which lasts for 100-150 d. The annual rainfall average is between 800-1200 mm. due to the acidic nature of the soils, cassava and tree cash crops such as oil palm (*Elaeis guineensis*) and para-rubber (*Hevea brasiliensis*) are the widely cultivated crops.

Ankasa series formed from biotite granite schist is located in the Western Region of Ghana. According to the World Reference Base (WRB, 1998) and Soil Taxonomy System (Soil Survey Staff, 1998), Ankasa series is classified as Plinthic Ferralsol and Plinthic Acrudox respectively by Dwomo and Dedzoe (2010) due to its deeply weathered and high acidic nature. It is well drained and occurs at the middle to lower slope on the landscape. The area experiences a bi-modal rainfall distribution with a 2000 mm rainfall per annum. Cassava (*Manihot esculenta*) is the main food crop cultivated on this soil, tree cash crops such as coconut (*Cocos nucifera*), oil palm (*Elaeis guineensis*) and para-rubber (*Hevea brasiliensis*) are also grown on this soil since they are acid tolerant.

Keta series is located in the South Eastern corner of Ghana which forms part of the Volta region. According to Soil Taxonomy (Soil Survey Staff, 1998), the soil is classified as Quartzipsamment, or Arenosols according to the FAO (1998). It is developed from marine sandy deposits (Awadzi et al., 2008). The study area has a mean monthly temperature of about 30 ^{o}C in the warmest month, March, and about 26 ^{o}C in the coldest month, August. Rainfall in the area is bimodal with an annual rainfall of < 900 mm. The major season starts from April and reaches its peak in June. September to November is the minor season. The main crops grown on this soil are shallot (*Allium cepa var. aggregatum*), with pepper (*Capsicum annum*), okro (*Abelmoschus esculentus*) and tomatoes (*Solanum lycopersicum*) as the main intercrop.

4.2.2 Soil sampling

The vegetative cover was cleared from the various sampling sites and soils were sampled from a plough depth of 0-20 cm. The soil samples were brought to the laboratory, air-dried, crushed, sieved through a 2 mm sieve to remove twigs and plant roots and stored for physicochemical analyses and incubation studies.

4.2.3 Laboratory analysis of soil and soil-biochar mixture samples

4.2.3.1 Particle size analysis

The particle size distributions of the three soils were carried out by the hydrometer method of Bouyoucos modified by Day (1965). The soil samples were sieved using a 2 mm sieve to obtain the fine earth fraction. Forty grams (40 g) of the sieved soil samples were weighed into a 250 mL dispersing bottle and 100 mL of 5% Sodium Hexametaphosphate (Calgon) solution was added to form a suspension. The suspension was agitated at 180 strokes per minute on a reciprocating shaker

for 2 h. This disperses the soil into the various particles; sand, silt and clay fractions. Organic matter of the soils were destroyed using hydrogen peroxide (H_2O_2). After shaking, the soil suspensions were then transferred into 1 L graduated sedimentation cylinders and made up to the mark with distilled water.

A plunger was lowered into the cylinders and moved up and down to further agitate the suspension thoroughly to bring all materials into suspension. After the agitation, the hydrometer readings were taken for silt plus clay particles by lowering a hydrometer in the suspension 5 min after the agitation. The suspensions were made to stand for 5 h after which the second hydrometer readings were taken for clay particles only. To determine the sand content, the suspension was poured directly onto a 47 µm sieve. The residue was then washed thoroughly with tap water to get rid of any remaining silt or clay particle and then poured into a moisture can with known weight and oven dried at 105 ^{o}C for 24 h. The oven dried sand was placed in a desiccator with silica gel to cool and prevent it from absorbing moisture from the atmosphere. The weight of the sand was determined with the use of a mechanical balance. The particle size distributions for the various soil samples were then computed as follows:

$$\% \text{ clay} = \frac{\text{hydrometer reading at 5 h}}{40 \text{ g}} \times 100 \qquad (4.1)$$

$$\% \text{ silt} = \frac{\text{hydrometer reading at 5 min- hydrometer reading at 5h}}{40 \text{ g}} \times 100 \qquad (4.2)$$

$$\% \text{ sand} = \frac{\text{weight of oven dried sample}}{40 \text{ g}} \times 100 \qquad (4.3)$$

Where 40 = weight of soil sample in grams

The particle size distribution values calculated were used to determine the textural class of the soils with the aid of the USDA textural triangle (Appendix 4A).

4.2.3.2 Bulk density

The bulk density of the soils used was determined using the core sample method of Blake and Hartge (1986). The soil surface of the area where the soils were taken was cleared. A cylindrical core sampler was gently driven into the soil with the help of a mallet, far enough to fill its' volume. The surrounding of the core sampler was dug gently and the core sampler removed with care to avoid any disturbance. With the aid of a knife, the ends of the sampler were levelled and capped at both ends to prevent loss of moisture and soil. The samples were placed into polythene and labelled appropriately. The soil samples were then transferred to the laboratory and its bulk density determined.

In the laboratory, the various soil samples were emptied into clean moisture cans with known weight (W1). The cans with the soil samples were oven dried for 72 h (3 days) at 105 ^{o}C and the weight was taken after cooling in a desiccator (W2). Bulk density was calculated with the formula by Blake (1965).

$$\rho_{b\,(kg/m^3)} = \frac{\mathbf{M}}{(\pi \mathbf{d}^2/4)\mathbf{h}} \qquad (4.4)$$

Where

ρ_b= Bulk density of soil

M= mass of soil = W2-W1

W2 = Weight in gram taken after oven drying the moisture can and its contents.

W1 = Weight in gram of empty moisture can.

$\pi d^2/4$ = area of core base

d= diameter of core

h= height of core

π = 3.142

$(\pi d^2/4)$ h= volume of core (i.e. volume of soil)

4.2.3.3 pH

The soil samples were measured electrometrically using a pH-mV-Temp PL-700PV pH glass electrometer in both deionized water (1:2) and in 0.01M $CaCl_2$ solution (1:2). Ten grams (10 g) of soil and soil-biochar was weighed in triplicate into 50 mL beakers and 20 mL of deionized water was added. The suspension was shaken for 1 hr in a reciprocating shaker, left to stand for 1 hr to equilibrate. The glass electrode pH meter (pH-mV-Temp PL-700PV) was standardized using three buffer solutions of pH 4, 7 and 10. The electrode inserted in the supernatant and pH measured. The same procedure was repeated in 0.01M $CaCl_2$.

4.2.3.4 Total Carbon and Total Nitrogen

Total carbon and total nitrogen were measured using dry combustion at 1350℃ (ELTRA CS-500 analyzer). The device was initially calibrated with known standards to yield ± 2% accuracy. About 200 mg of crushed biochar (< 0.5 mm) was weighed into a crucible, inserted into the furnace, and measured.

4.2.3.5 Available phosphorus

The available phosphorus in the soil samples were determined using the method of Bray and Kurtz, (1945). Five grams (5 g) of sample (2 mm sieved) was weighed into an extraction bottle. Fifty millilitres (50 mL) of Bray 1 solution (0.03M NH_4F in 0.025M HCl) was added. The soil suspension was shaken for 3 min on a reciprocating shaker at 180 strokes per min, allowed to settle and the supernatant filtered through a 0.45 µm filter paper into a 100 mL volumetric flask and was made up to the mark with distilled water. Phosphorus in the filtrate was determined using the Watanabe and Olsen, (1965) molybdate blue-ascorbic acid colour development method as follows:

A solution of 12 g of ammonium molybdate and 0.2998 g of antimony potassium tartrate dissolved in 250 mL of distilled water was prepared and added to 1000 mL of 2.5 M H_2SO4 mixed thoroughly to a volume of 2 L in a volumetric flask and labelled Reagent A. Another solution was prepared by dissolving 1.056 g of ascorbic acid in 200 mL of Reagent A and Labelled as Reagent B.

Five millilitre (5 mL) aliquots of the filtrates were pipetted in duplicate into a 50 mL volumetric flask and the pH adjusted with *p*-nitrophenol indicator. The solution was then neutralized with a few drops of sodium hydroxide (4M NaOH) until the colour changed to yellow. Eight millilitres (8 mL) of Reagent B was then added to the sample solution and made to volume in a 50 mL volumetric flask. A blank was also prepared using 5 mL of distilled water and 8 mL of reagent B. The Spectroquant® Pharo 300 M spectrophotometer was calibrated using 0, 0.2, 0.4, 0.6, 0.8 and 1.0 mg L^{-1} standard P solutions prepared in the same manner as above. Phosphorus in the solution was determined by reading the resultant colour intensity on the Spectroquant® Pharo 300 jM spectrophotometer, at a wavelength of 712 nm. The available P concentration in the soil sample was read and calculated using the spectrophotometer reading as follows:

$$\text{P (mg/kg)} = \frac{\text{spectrophotometer reading (mgL}^{-1}) \times \text{volume of extract}}{\text{volume of aliquot} \times \text{weight of soil sample}} \quad (4.5)$$

4.2.3.6 Total phosphorus

Total P was determined by digesting 0.5 g sample with 20 ml of concentrated H_2SO_4. The mixture was digested until the digest became pale, after which 1 ml of 30% of H_2O_2 was added to clarify the digest. The flask was then cooled and the digest diluted. The digest was filtered through a 0.45 µm filter paper in a 250 ml volumetric flask and made to volume with distilled water. Phosphorus in the filtrate was determined using the molybdate ascorbic acid method of Watanabe and Olsen (1965). One millilitre (1ml) aliquots of the filtrate were taken (in duplicate) into 50 ml volumetric flasks. The phosphorus in the filtrate was determined by colour development and read on Spectroquant® Pharo 300 M spectrophotometer as described in section 4.2.3.5

4.2.3.7 Exchangeable bases

The exchangeable base cations (Ca^{2+}, Na^{+}, K^{+}, Mg^{2+}) were extracted with NH_4-acetate buffered at pH 7 and measured with Atomic Absorption Spectroscopy using a modified method (Hendershort et al., 2007; van Reeuwijk, 2002). Five (5) g soil was weighed into a 50 mL plastic bottle, 20 mL 1 M NH_4-acetate was added, and the solution was agitated for 4 h at 145 rpm on a reciprocating shaker. The solution was then filtered through a Buchner funnel with 9-13 µm filter paper into a flask, and the soil on the filter paper was washed by the addition of 10 portions of 10 mL 1 M NH_4-acetate. The solution was finally transferred to a 200 mL volumetric flask, and it was filled

to the mark with 1 M NH_4-acetate. An ionization buffer (0.2 mL/ 100 g L^{-1} CsCl to 9.80 mL solution) was added to the solution for the measurement of Na and K. For the measurement of Ca and Mg, a La-salt (0.2 mL LaCl (65 g L^{-1}) to 9.80 mL solution) was added to prevent chemical interferences. The Perkin Elmer atomic absorption spectrometer was calibrated with the appropriate standards for Ca, Mg and Na respectively and the absorbance for each element determined. Exchangeable bases were calculated as:

$$\mathbf{C}a\ (cmol_c kg^{-1}) = \frac{R \times \text{Vol. of extract} \times 10^3\ (g) \times 10^2 (cmol) \times E}{\text{Weight of soil} \times 10^6\ (\mu g) \times 40} \qquad (4.6)$$

Where 40 = Atomic mass of Ca

R = AAS (Atomic absorption spectroscopy) reading in mg L^{-1}

E = Charge of Ca

$$Mg\ (cmol_c kg^{-1}) = \frac{R \times \text{Vol. of extract} \times 10^3\ (g) \times 10^2 (cmol) \times E}{\text{Weight of soil} \times 10^6\ (\mu g) \times 24} \qquad (4.7)$$

Where 24 = Atomic mass of Mg

R = AAS (Atomic absorption spectroscopy) reading in mg L^{-1}

E = Charge of Mg

$$Na\ (cmol_c kg^{-1}) = \frac{R \times \text{Vol. of extract} \times 10^3\ (g) \times 10^2 (cmol) \times E}{\text{Weight of soil} \times 10^6\ (\mu g) \times 23} \qquad (4.8)$$

Where,

R = AAS (Atomic absorption spectroscopy) reading on mg L^{-1}

23 = Atomic weight of Na

E = Charge of Na

$$K\ (cmol_c kg^{-1}) = \frac{R \times \text{Vol. of extract} \times 10^3\ (g) \times 10^2 (cmol) \times E}{\text{Weight of soil} \times 10^6\ (\mu g) \times 39} \qquad (4.9)$$

Where,

R = AAS (Atomic absorption spectroscopy) reading on mg L^{-1}

39 = Atomic weight of K

E = Charge of Na

4.2.3.8 Cation exchange capacity

The cation exchange capacity of the biochar-soil mixture was determined using $BaCl_2$/Triethanolamine (TEA) solution buffered at pH 8.2. About 2 g of sample were weighed into 100 ml plastic bottles and 40 ml of 0.2 M $BaCl_2$ -TEA solution added. The suspension was shaken for 1 h and then filtered through a 0.45 µm filter paper. The filtrate was collected into an empty plastic bottle. The biochar residue was leached with four portions of 10 ml 0.1 M $MgSO_4$.$7H_2O$ solution. The leachate was collected into a separate clean plastic bottle. The amount of Ba^{2+} contained in the leachate was determined using Atomic absorption spectrometer. The CEC of biochar was calculated as:

$$\text{cmol}_c\text{kg}^{-1} = \frac{\text{AAS reading (mg)} \times 40\text{ ml} \times 10^3\text{ (g)} \times 10^2\text{(cmol)} \times 2^*}{\text{Weight of soil} \times 10^6\text{ (µg)} \times 137.3} \qquad (4.10)$$

4.2.3.9 Determination of iron and aluminum oxides

4.2.3.9.1 Acid ammonium oxalate extractable iron and aluminum oxides

Acid ammonium oxalate extractable iron and aluminium were determined by the method of Schwertmann (1964). A 0.5 g of ball milled sample was weighed into 40 ml centrifuge tube. Ten mls of acid ammonium oxalate solution was added. The solution was prepared by dissolving:

A. 28.3 g of Ammonium oxalate in a litre of deionised water and

B. 25.2 g of oxalic acid in a litre of deionised water. Solutions 'A' and 'B' were prepared separately.

Seven hundred ml (700 ml) of 'A' and 535 ml of 'B' were mixed and pH adjusted to 3.0 by adding 'B'. The soil suspension was shaken in the dark at room temperature for 4 h. The suspension was centrifuged at 3500 rpm for 10 mins and filtered through 0.45 µm filter paper. One ml of the filtrate was diluted using 4 ml of 2000 ppm sodium as sodium chloride solution. Iron and aluminium standards were prepared (Fe, 0 to 25 ppm; and Al, 0 to 25 ppm) and used to construct a calibration curve on the atomic absorption spectrophotometer (AAS).

The amount of Fe and Al were determined using the relationship;

$$\text{mg Fe or Al kg}^{-1}\text{ soil} = \frac{\text{AAS reading} \times \text{dilutiion factor} \times \text{extractant (10 mL)} \times 1000\text{ g}}{1000\text{ mL} \times \text{weight of sample (0.5 g)}} \qquad (4.11)$$

4.2.3.9.2 Bicarbonate-citrate-dithionite extractable iron and aluminum oxides

Bicarbonate citrate dithionite extractable iron and aluminium were determined by the method of Mehra and Jackson (1960). A 0.5 g of ball milled sample was put into a 15 ml test tube. An aliquot of 5 ml of bicarbonate-citrate buffer was added. The bicarbonate-citrate buffer solution was prepared as follows:

Two hundred and fifty ml of 1 M sodium bicarbonate solution (21 g of $NaHCO_3$ in 250 ml) was mixed with 1 L of 0.3 M sodium citrate (88.25 g of molecular formular of sodium citrate in 1 L).

An amount of 0.2 g of sodium dithionite was added using a calibrated scoop, the mixture was mixed well and the tube was put into a water bath at 80 ^{o}C. Stirring was done every 3 min. throughout a 15 minute extraction period. The tubes were removed from the water bath and 1 ml of saturated NaCl (4 M) solution was added and mixed. The stirring rod was washed off into the test tube and the soil suspension centrifuged for 5 min. at 3500 rpm. The clear supernatant was poured off into a 100 ml volumetric flask. The extraction was repeated after the soil residue was loosened using the vortex mixer. The sample suspension was then washed twice, each with 5 ml and 1 ml of bicarbonate-citrate buffer solution and saturated NaCl solution respectively. The soil suspension was centrifuged each time after washing and the clear supernatant poured into the 100 ml volumetric flask. The extract was then made to volume with distilled water. Iron and aluminium standards were prepared (Fe, 0 to 25 ppm; and Al, 0 to 25 ppm) in a matrix of the extracting solution and used to construct a calibration curve on the atomic absorption spectrophotometer (AAS). The amount of Fe and Al were determined using the relation:

$$\text{mg Fe or Al kg}^{-1}\ \text{soil} = \frac{\text{AAS reading} \times \text{dilution factor} \times \text{extractant (100 mL)} \times 1000\ \text{g}}{1000\ \text{mL} \times \text{weight of sample (0.5 g)}} \quad (4.12)$$

4.2.3 Incubation studies (soil and soil-biochar mixture)

Corn cob and rice husk biochar at three pyrolysis temperatures i.e. 300 ^{o}C, 450 ^{o}C and 650 ^{o}C were used for the incubation studies to assess their effect on P sorption and fractions in the three soil types. The biochar was mixed with soil at a rate of 1% (30.4 g/kg). Soils with and without biochar were incubated at 70% field capacity at room temperature of 28 °C and for 80 days in the dark. Each treatment was replicated four times. After the 80 days of incubation, the soil (control) and soil/biochar mixtures were air-dried and stored to use for P sorption studies and fractionation work.

4.2.4 Experimental design

The study was set up in the University of Ghana green house in a completely randomized design (CRD). Table 4.1 shows the combination of treatments consisting of soils, biochar types, biochar levels (pyrolysis temperatures) and acronyms used for the study.

4.2.5 Characterization of Soil and Soil-biochar mixture

After the incubation, chemical properties of soil-biochar mixture were determined; pH, organic carbon, cation exchange capacity, exchangeable Ca, total P, acid ammonium oxalate extractable Fe and Al, bicarbonate-citrate-dithionite extractable Fe and Al as described under laboratory analysis of soil and soil-biochar mixture samples section (4.2.3).

4.2.6 Sorption experiment

A batch sorption experiment of phosphorus on the soil with and without biochar samples were carried out to ascertain maximum adsorption of phosphorus and standard P requirement (SPR) of soils. A stock P solution of 86.0 mg/L concentration was prepared from potassium hydrogen phosphate (KH_2PO_4). Various P concentrations 0, 10.1, 21.5, 32.3, 43.0, 64.5 and 86.0 mg P L^{-1} were prepared from the stock solution. Two (2) g of each sample were weighed into each of seven 50 ml centrifuge tubes. Each of the centrifuge tube plus its content was weighed again; (the weight of the centrifuge tube plus the sample was needed in the subsequent desorption studies). Twenty (20) mL of 0.01M KCl solution containing the various P concentrations was added to each of the centrifuge tubes respectively. Two drops of toluene were added per sample per centrifuge tube to reduce microbiological activity. The sample suspension was equilibrated by shaking end-over-end on a reciprocal shaker for twenty four (24) h at room temperature (25 ^{o}C) and thereafter centrifuged at 3500 rpm for 10 mins. The supernatant was filtered through a 0.45 µm filter paper into a clean plastic bottle and phosphorus in the filtrate was determined using the colorimetric molybdenum-blue method (John, 1970).

The initial aqueous P concentration Ci (mg L^{-}) and equilibrium P concentration Ce (mg L^{-}) were measured and the P adsorbed (qt) was calculated from the mass balance equation as follows:

$$\mathbf{qt} = \frac{(\mathbf{Ci} - \mathbf{Ce})\mathbf{V}}{\mathbf{M}} \qquad (\mathbf{4.13})$$

Table 4. 1 Treatment combinations

Soil	Biochar	Pyrolysis Temp.	Acronym
Kokofu	No biochar	-	Ko
Kokofu	Rice husk	300 ^{o}C	KoR3
Kokofu	Rice husk	450 ^{o}C	KoR4
Kokofu	Rice husk	650 ^{o}C	KoR6
Kokofu	Corn cob	300 ^{o}C	KoC3
Kokofu	Corn cob	450 ^{o}C	KoC4
Kokofu	Corn cob	650 ^{o}C	KoC6
Keta	No biochar	-	K
Keta	Rice husk	300 ^{o}C	KR3
Keta	Rice husk	450 ^{o}C	KR4
Keta	Rice husk	650 ^{o}C	KR6
Keta	Corn cob	300 ^{o}C	KC3
Keta	Corn cob	450 ^{o}C	KC4
Keta	Corn cob	650 ^{o}C	KC6
Ankasa	No biochar	-	A
Ankasa	Rice husk	300 ^{o}C	AR3
Ankasa	Rice husk	450 ^{o}C	AR4
Ankasa	Rice husk	650 ^{o}C	AR6
Ankasa	Corn cob	300 ^{o}C	AC3
Ankasa	Corn cob	450 ^{o}C	AC4
Ankasa	Corn cob	650 ^{o}C	AC6

Where *V* is the volume of the aqueous solution (L) and *M* is the dry weight in grams of sample. The sorption experiments were repeated three times and the average data and standard deviations reported. The sorption data were fitted to the Langmuir and Freundlich equations.

4.2.7 Phosphorus desorption

Desorption studies were done using the residual samples which received 86.0 mg P L^{-}. After filtering the supernatant from the previous sorption experiment, the centrifuge tube plus the wet sample was weighed and a total of 20 mL of 0.01 M KCl solution was added to the sample in the centrifuge tube on a weighing balance. The suspension was then shaken for three hours and centrifuged at 3500 rpm for 10 mins at room temperature. The supernatant was filtered through a 0.45 µm filter paper into a clean plastic bottle and a suitable aliquot taken for P analysis. The P carried over between desorption steps was determined from the weight of the entrapped solution that remained after decanting the supernatant solution. The extraction was repeated for three successive times and P released into the supernatant at each extraction period was then measured. The percentage of P desorbed was calculated as P desorbability.

$$\textbf{P desorbability}\ (\%) = \frac{\textbf{P desorbed}\ (\textbf{mg kg}^{-\mathbf{1}})}{\textbf{P adsorbed}\ (\textbf{mg kg}^{-\mathbf{1}})} \times \mathbf{100} \qquad (\mathbf{4.13})$$

4.2.8 Statistical analysis

The normality of the data from the experiment was tested using Shapiro-WilK test. The data were then subjected to general analysis of variance (ANOVA) using GentStat version 12. The separation of means was tested using least significant difference (LSD) with a significance level of $p < 0.05$. Correlation analysis between the P sorption capacity and some chemical properties of the soils was done. Principal Component Analysis (PCA) was applied to the P adsorption maximum and some chemical properties of each of the soil types using the prcomp function in RStudio.

4.3 Results

4.3.1 Characteristics of Soil

Some of the physicochemical properties of the soils used for the study are shown in Table. 4.2. The bulk densities of the soils were 1.46 Mg m^{-3}, 1.13 Mg m^{-3} and 1.72 Mg m^{-3} for Kokofu, Ankasa and Keta respectively. In accordance with the USDA (2003) system of classification, the textural class of Kokofu and Ankasa was sandy clay loam and Keta was sand. Kokofu had 68.7% sand, 11.2% silt and 20.0% clay whiles Ankasa had 64.6% sand, 8.0% silt and 18.4% clay. The particle size distribution of Keta was dominated by 95.0% sand.

The pH values of Kokofu, Ankasa and Keta measured in water was 5.03 (acidic), 4.73 (strongly acidic) and 6.63 (neutral) respectively. However, pH in 0.01M $CaCl_2$ of the soils decreased to 4.40, 4.01 and 5.31 for Kokofu, Ankasa and Keta respectively.

The organic carbon in the acid soils was slightly higher than in the neutral soil (Keta). Keta had organic carbon content of 4.3 g kg^{-1} whiles Kokofu and Ankasa had 14.0 g kg^{-1} and 13.3 g kg^{-1} respectively. The respective recorded cation exchange capacity (CEC) for Kokofu, Ankasa and

Table 4.2 Physicochemical properties of soils

Property	Soil		
	Kokofu	Ankasa	Keta
Bulk density (Mg m^{-3})	1.46	1.13	1.72
Sand (%)	68.70	64.60	95.00
Silt (%)	11.20	8.00	1.00
Clay (%)	20.30	18.40	4.00
Textural class	Sandy clay loam	Sandy clay loam	Sand
pH (H_2O)	5.03	4.73	6.63
pH ($CaCl_2$)	4.40	4.01	5.31
Available P (mg kg^{-1})	1.42	1.21	0.90
Total P (mg kg^{-1})	353.58	232.75	190.80
Total N (g kg^{-1})	1.23	1.22	0.19
Organic carbon (g kg^{-1})	14.00	13.30	4.30
Exchangeable bases ($cmol_c$ kg^{-1})			
Ca^{2+}	1.27	0.32	0.40
Mg^{2+}	0.42	0.10	0.13
K^+	0.14	0.04	0.04
Na^+	0.07	0.06	0.09
CEC ($cmol_c$ kg^{-1})	15.20	12.78	3.42
Amorphous oxides (g kg^{-1})			
Fe_o	2.10	1.56	0.67
Al_o	1.21	1.39	0.17
Crystalline oxides (g kg^{-1})			
Fe_d	20.00	9.41	1.66
Al_d	3.03	2.59	0.74

Fe_o and Al_o are oxalate extractable Fe and Al; Fe_d and Al_d are dithionate-citrate-bicarbonate extractable Fe and Al

Keta was 15.20 $cmol_c\ kg^{-1}$, 12.78 $cmol_c\ kg^{-1}$ and 3.42 $cmol_c\ kg^{-1}$. Kokofu with the highest organic carbon content reflected in the high CEC level. The total nitrogen level for the three soils were 1.23 g kg^{-1}, 1.22 g kg^{-1} and 0.19 g kg^{-1} for Kokofu, Ankasa and Keta respectively.

Total phosphorus varied from 190.80 to 353.58 mg kg^{-1} of which Keta and Kokofu recorded the least (190.80 mg kg^{-1}) and the highest (353.58 mg kg^{-1}) values respectively. The available P content of the soils was in the order of Keta (0.90 mg kg^{-1}) < Ankasa (1.21 mg kg^{-1}) < Kokofu (1.42 mg kg^{-1}). The exchangeable bases of the three soil types were dominated by Ca and Mg. The exchangeable Ca ranged from 0.40 to 1.27 $cmol_c\ kg^{-1}$ with that of Mg also ranging from 0.10 to 0.42 $cmol_c\ kg^{-1}$. Kokofu had the highest concentration of exchangeable bases whiles the least was found in the Keta. Oxalate extractable Fe and Al oxides (Fe_o and Al_o) of the three soils ranged from 0.67 to 2.10 mg g^{-1} and 0.17 to 1.21 mg g^{-1} respectively. The dithionite extractable Fe and Al (Fe_d and Al_d) was also in a range of 1.66 to 20.00 and 0.74 to 3.03 mg g^{-1} respectively. The Fe_o, Al_o and Al_d concentration in Kokofu and Ankasa were almost the same but about three fold more in Keta. The Fe_d content was much higher in Kokofu i.e. 20.00 g kg^{-1} but less in Ankasa (9.41 g kg^{-1}) and Keta (1.66 g kg^{-1}).

4.3.2 Effect of biochar on soil chemical characteristics

The effect of rice husk biochar and corn cob biochar at the three pyrolysis temperatures on some chemical properties of the three soils is presented in Tables 4.3a-c. Amending the soils with the two biochar types increased the soils' pH at increasing pyrolyaia temperature. Rice husk and corn cob biochar increased the pH of Kokofu by a unit range of 0.70 to 1.20 and 1.00 to 1.47 respectively. There was 0.44 to 0.56 and 0.56 to 0.74 units increase in Ankasa upon rice husk and corn cob biochar amendment respectively. Incorporating Keta with rice husk biochar raised the pH by unit range of 0.14 to 0.57 and also corn cob biochar by unit range of 0.47 to 0.84.

Table 4.3a Effect of corn cob and rice husk biochar on some chemical properties of Kokofu

Soil/ Biochar	pH (H_2O)	OC (g kg^{-1})	CEC	Ex. Ca^{2+}	Fe_o	Fe_d	Al_o	Al_d	TP
			$cmol_c$ kg^{-1}		mg g^{-1}				mg kg^{-1}
Ko	5.03	14.0	15.20	1.27	2.10	20.00	1.21	3.03	353.
KoR3	5.73	18.3	19.30	1.41	2.65	16.81	1.08	2.55	413.6
KoR4	6.07	18.9	17.44	1.44	2.71	17.44	1.10	3.43	470.5
KoR6	6.23	17.7	16.98	1.53	2.55	17.07	0.78	3.49	460.6
KoC3	6.03	21.5	21.20	1.50	2.77	14.32	1.65	2.21	428.
KoC4	6.43	20.1	18.64	1.58	2.66	14.95	1.27	3.10	482.8
KoC6	6.43	19.2	17.20	1.65	2.54	17.70	1.12	3.47	505.8
Lsd	-	1.30	2.72	0.06	0.15	0.53	0.18	0.72	28.02

Ko = Kokofu soil; KoR3 = Kokofu soil amended with rice husk biochar at 300 ^oC, KoR4 = Kokofu soil amended with rice husk biochar at 450 ^oC; KoR6 = Kokofu soil amended with rice husk biochar at 650 ^oC; KoC3 = Kokofu soil amended with corn cob biochar at 300 ^oC; KoC4 = Kokofu soil amended with corn cob biochar at 450 ^oC; KoC6 = Kokofu soil amended with corn cob biochar at 650 ^oC.

Fe_o and Al_o are oxalate extractable Fe and Al; Fe_d and Al_d are dithionate-citrate-bicarbonate extractable Fe and Al; TP is total phosphorus; OC is organic carbon

Table 4.3b Effect of corn cob and rice husk biochar on some chemical properties of Ankasa

Soil/ Biochar	pH (H_2O)	OC (g kg^{-1})	CEC	Ex. Ca^{2+}	Fe_o	Fe_d	Al_o	Al_d	TP
			$cmol_c$ kg^{-1}			mg g^{-1}			mg kg^{-1}
A	4.73	13.3	12.78	0.32	1.56	9.41	1.39	2.59	232.70
AR3	5.17	16.5	16.45	0.35	1.66	6.45	1.21	1.54	304.11
AR4	5.30	14.9	15.65	0.36	1.72	6.99	1.24	2.39	347.01
AR6	5.23	14.3	13.89	0.45	1.68	7.08	1.19	2.34	325.40
AC3	5.30	17.3	17.88	0.46	1.68	5.79	0.93	2.71	301.01
AC4	5.47	15.5	15.21	0.47	1.68	6.09	1.31	2.31	330.92
AC6	5.47	15.1	15.01	0.48	1.51	6.45	1.18	2.98	408.22
Lsd	-	0.14	1.41	0.02	0.12	0.67	0.21	0.59	36.38

A= Ankasa soil; AR3 = Ankasa soil amended with rice husk biochar at 300 ^oC, AR4 = Ankasa soil amended with rice husk biochar at 450 ^oC; AR6 = Ankasa soil amended with rice husk biochar at 650 ^oC; AC3 = Ankasa soil amended with corn cob biochar at 300 ^oC; AC4 = Ankasa soil amended with corn cob biochar at 450 ^oC; AC6 = Ankasa soil amended with corn cob biochar at 650 ^oC.
Fe_o and Al_o are oxalate extractable Fe and Al; Fe_d and Al_d are dithionate-citrate-bicarbonate extractable Fe and Al; TP is total phosphorus; OC is organic carbon

Table 4.3c Effect of corn cob and rice husk biochar on some chemical properties of Keta

Soil/ Biochar	pH (H_2O)	OC (g kg^{-1})	CEC	Ex. Ca^{2+}	Fe_o	Fe_d	Al_o	Al_d	TP
			$cmol_c$ kg^{-1}				mg g^{-1}		mg kg^{-1}
K	6.63	4.30	3.42	0.40	0.67	1.66	0.17	0.74	190.21
KR3	6.77	6.00	6.47	0.47	0.86	1.61	0.33	0.95	209.82
KR4	6.77	5.21	5.04	0.56	0.71	1.83	0.32	0.91	222.51
KR6	7.20	4.60	6.40	0.54	0.72	1.90	0.29	1.23	247.61
KC3	7.10	4.51	6.87	0.56	0.76	1.83	0.29	0.78	249.41
KC4	7.33	5.30	6.34	0.62	0.80	1.72	0.26	0.94	230.80
KC6	7.47	5.00	5.98	0.68	0.80	1.87	0.27	0.97	270.30
Lsd	-	0.70	1.23	0.14	0.06	0.26	0.02	0.19	38.90

K= Keta soil; KR3 = Keta soil amended with rice husk biochar at 300 ^oC, KR4 = Keta soil amended with rice husk biochar at 450 ^oC; KR6 = Keta soil amended with rice husk biochar at 650 ^oC; KC3 = Keta soil amended with corn cob biochar at 300 ^oC; KC4 = Keta soil amended with corn cob biochar at 450 ^oC; KC6 = Keta soil amended with corn cob biochar at 650 ^oC.

Fe_o and Al_o are oxalate extractable Fe and Al; Fe_d and Al_d are dithionate-citrate-bicarbonate extractable Fe and Al; TP is total phosphorus; OC is organic carbon

The organic carbon content of the soils significantly ($p < 0.05$) increased upon biochar amendment. Rice husk and corn cob biochar significantly ($p < 0.05$) increased the OC content of Kokofu from 14.0 g kg^{-1} to a range of 17.7 to 18.7 g kg^{-1} and 19.2 to 21.5 g kg^{-1} respectively.

There was no significant difference ($p > 0.05$) in the OC content among the rice husk biochar treatments (KoR3, KoR4 and KoR6). Similarly, corn cob biochar treatments, KoC4 and KoC6 were statistically ($p > 0.05$) the same. Nevertheless, KoC3 treatment had a significant ($p < 0.05$) effect on the OC content of Kokofu. Adding corn cob and rice husk biochar at 450 ^oC and 650 ^oC to Ankasa (AR4, AR6, AC4 and AC6) could not significantly increase the soil's OC content. However, treatments at low pyrolysis temperatures, AR3 and AC3 significantly ($p < 0.05$) raised the OC content from 13.3 g kg^{-1} to 16.5 g kg^{-1} and 17.3 g kg^{-1} respectively. Amending Keta with the two biochar types at the three different pyrolysis temperatures did not have significant effect on the soil's OC content with the exception of rice husk biochar at 300 ^oC (KR3) which significantly ($p < 0.05$) increased the OC content from 4.3 mg kg^{-1} to 6.0 mg kg^{-1}.

The exchangeable Ca content of the three soil types increased upon the two biochar amendments. Rice husk biochar treatments (KoR3, KoR4 and KoR6) and corn cob biochar treatments (KoC3, KoC4 and KoC6) significantly raised the Ca^{2+} concentration in Kokofu from 1.27 $cmol_c$ kg^{-1} to 1.41-1.53 $cmol_c$ kg^{-1} and 1.50 -1.65 $cmol_c$ kg^{-1} respectively. The significant ($p < 0.05$) increase in Ca^{2+} content in Ankasa was from 0.32 $cmol_c$ kg^{-1} to a range of 0.35 to 0.45 $cmol_c$ kg^{-1} for the rice husk biochar treatments and 0.46 to 0.48 $cmol_c$ kg^{-1} for the corn cob biochar treatments. The Ca content of KR3 and KC3 treatments were statistically ($p > 0.05$) similar to the control soil (K). However, there was a significant ($p < 0.05$) increase with treatments of high temperature pyrolysis biochars (KC4, KC6, KR4 and KR6). Generally there was a significant ($p < 0.05$) effect of pyrolysis temperature with regards to the increase in Ca^{2+} concentration.

The CEC values of the soils upon biochar addition significantly increased proportionally with decreasing pyrolysis temperature. Averagely, the CEC of Kokofu was significantly increased from 15.20 $cmol_c\ kg^{-1}$ to a ranged of 17.20 to 21.20 $cmol_c\ kg^{-1}$, Ankasa from 12.78 $cmol_c\ kg^{-1}$ to a range of 13.89 to 17.88 $cmol_c\ kg^{-1}$ and Keta from 3.42 $cmol_c\ kg^{-1}$ to a range of 5.04 to 6.87 $cmol_c\ kg^{-1}$. Biochar types produced at 300 ^oC had much significant ($p < 0.05$) effect on the CEC of the soils.

The incorporation of the two biochar types significantly ($p < 0.05$) increased the amorphous Fe oxides (Fe_o) content of Kokofu. However, there was no significant variation ($p > 0.05$) among the biochar treatments. The amorphous Al oxides (Al_o) content of Kokofu was statistically ($p > 0.05$) the same as the biochar treatments with the exception of KoR6 and KoC3 treatments. Rice husk and corn cob biochar significantly ($p < 0.05$) decreased the crystalline Fe oxides (Fe_d) of Ko from 20.0 g kg^- to a range of 16.8 to 17.4 g kg^- and 14.3 to 17.7 g kg^{-1} respectively at deceasing pyrolysis temperature.

The study showed no significant ($p > 0.05$) effect of biochar on the Al_d and Fe_o content of Ankasa. Similarly, the Al_o content was statistically ($p > 0.05$) the same as the biochar treatments with the exception of AC3 treatment which significantly ($p < 0.05$) decreased from 1.39 g kg^- to 0.93 g kg^{-1}. The study revealed a significant ($p < 0.05$) reduction of Fe_d content of Ankasa. This was mostly significant at the low temperature biochar treatments (AR3 and AC3). The rice husk biochar treatments decreased the Fe_d content from 9.41 g kg^- to a range of 6.45 to 7.08 g kg^{-1} and corn cob biochar treatment to a range of 5.79 to 6.65 g kg^-. The study further showed no significant variation between the Al_d content of the control soil (Ankasa) and the biochar treatments except AR3 treatment which reduced it from 2.59 g kg^{-1} to 1.54 g kg^{-1}.

The results revealed a significant ($p < 0.05$) increase in the amorphous Fe and Al content of Keta soil upon biochar amendment. Adding rice husk and corn cob biochar significantly ($p < 0.05$)

increased Fe_d from 0.67 g kg^{-1} to a range of 0.86 to 0.72 g kg^{-1} and 0.76 to 0.80 g kg^{-1} respectively. The Al_d content also increased significantly ($p < 0.05$) from 0.17 g kg^{-1} to a range of 0.29 to 0.33 g kg^{-1} and 0.27 to 0.29 g kg^{-1} for rice husk and biochar treatments respectively. The two biochar types did not have any significant ($p > 0.05$) effect on the crystalline Fe oxides of Keta. Similarly, with the crystalline Al oxides the only significant ($p < 0.05$) effect was when Keta was amended with rice husk biochar pyrolysed at 650 ^oC (AR6), thus increasing Al_d content of Keta from 0.74 g kg^- to 1.23 g kg.

The corn cob biochar and rice husk biochar amendments significantly ($p < 0.05$) increased the total P content of Kokofu from 353.6 mg kg^{-1} to a range of 428.8 to 505.8 mg kg^- and 413.6 to 460.6 mg kg^{-1} respectively. The increase in total P content of Kokofu upon biochar amendment was significant ($p < 0.05$) at increasing pyrolysis temperature. There was also a significant ($p < 0.05$) increase in total P content of Ankasa from 232.7 mg kg^{-1} to a range of 301.0 to 408.2 mg kg^{-1} for corn cob biochar treatments and 304.1 to 347.0 mg kg^{-1} rice husk biochar treatments. However, there was no significant ($p > 0.05$) differences among all the biochar-Ankasa treatments with the exception of AC6 which had a significantly ($p < 0.05$) higher total P content of 408.2 mg kg^{-1}. Apart from rice husk biochar produced at 300 ^oC (KR3) and 450^oC (KR4), the other biochar treatments significantly ($p < 0.05$) increased the total P content of Keta. The significant ($p < 0.05$) increase was from 190.2 mg kg^{-1} to 230.8 mg kg^{-1}, 247.6 mg kg^{-1}, 249.4 mg kg^{-1} and 270.3 mg kg^{-1} for KC4, KR6, KC3 and KC6 treatments respectively. There was not much significant variation of total P content among the biochar treatments.

4.3.4 Phosphorus sorption of soils and biochar amended soils

The Langmuir isotherms of the soils and biochar amended soils expressing the amount of P adsorbed against the equilibrium P concentration are shown in Fig.4.1a-c. The P sorption maximum (P_{max}), binding energy, standard P requirements (SPR) (P adsorbed at 0.2 mg P L^{-1}) together with the coefficient of determination (R^2) value for the Langmuir equation are shown in Table 4.4a-c. The P sorption maximum of Kokofu significantly ($p < 0.05$) decreased from 384.6 mg kg^{-1} to 256.1 mg kg^{-} and 303.0 mg kg^{-1} upon the application of corn cob biochar produced at 300 ^oC and 450 ^oC respectively. However, the P_{max} of corn cob biochar at 650 ^oC amendment was statistically ($p > 0.05$) similar to the control (Kokofu). Similar to the corn cob biochar, there was a significant ($p < 0.05$) decrease in the P_{max} of the Kokofu to 270.3 mg kg^{-1} and 322.6 mg kg^{-1} when rice husk biochar pyrolysed at 300 ^oC (KoR3) and 450 ^oC (KoR4) was incorporated respectively. Again rice husk biochar at 650 ^oC (KoR6) did not significantly ($p > 0.05$) reduce the P_{max} of Kokofu.

Amendment of corn cob biochar at 300 ^oC (AC3), at 450 ^oC (AC4) and rice husk biochar at 300 ^oC (AR3) significantly ($p < 0.05$) decrease the P_{max} of Ankasa from 333.3 mg kg^{-1} to 200.0 mg kg^{-1}, 256.4 mg kg^{-1} and 217 mg kg^{-1} respectively. Treatments AC6, AR4 and AR6 show no significant ($p > 0.05$) effect on the reduction of P_{max} of Ankasa. Contrary to the P_{max} of the two acid soils, Kokofu and Ankasa, the study showed an increase in P_{max} of Keta upon the incorporation of the two biochar types at the various pyrolysis temperatures. The P_{max} of Keta was statistically ($p > 0.05$) the same as the P_{max} of KC3.

Upon the amendment of corn cob biochar produced at 450 ^oC (KC4) and 650 ^oC (KC6) the Langmuir sorption maximum of Keta significantly ($p < 0.05$) increased from 104.2 mg kg^{-} to 178.6 mg kg^{-1} and 188.7 mg kg^{-1} respectively.

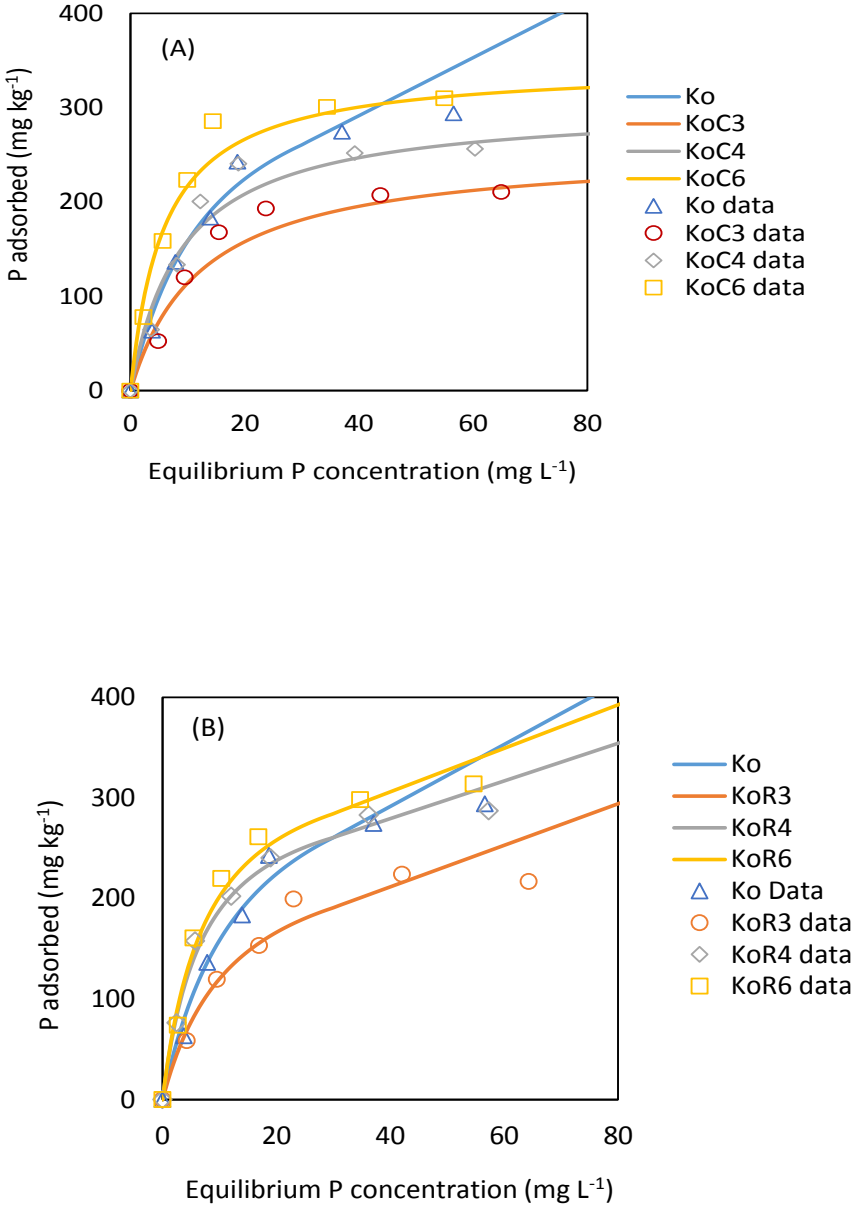

Figure 4.1a. Phosphorus adsorption isotherm for (A) Kokofu soil amended with corn cob biochar at three pyrolysis temperatures, (B) Kokofu soil amended with rice husk biochar at three pyrolysis temperatures

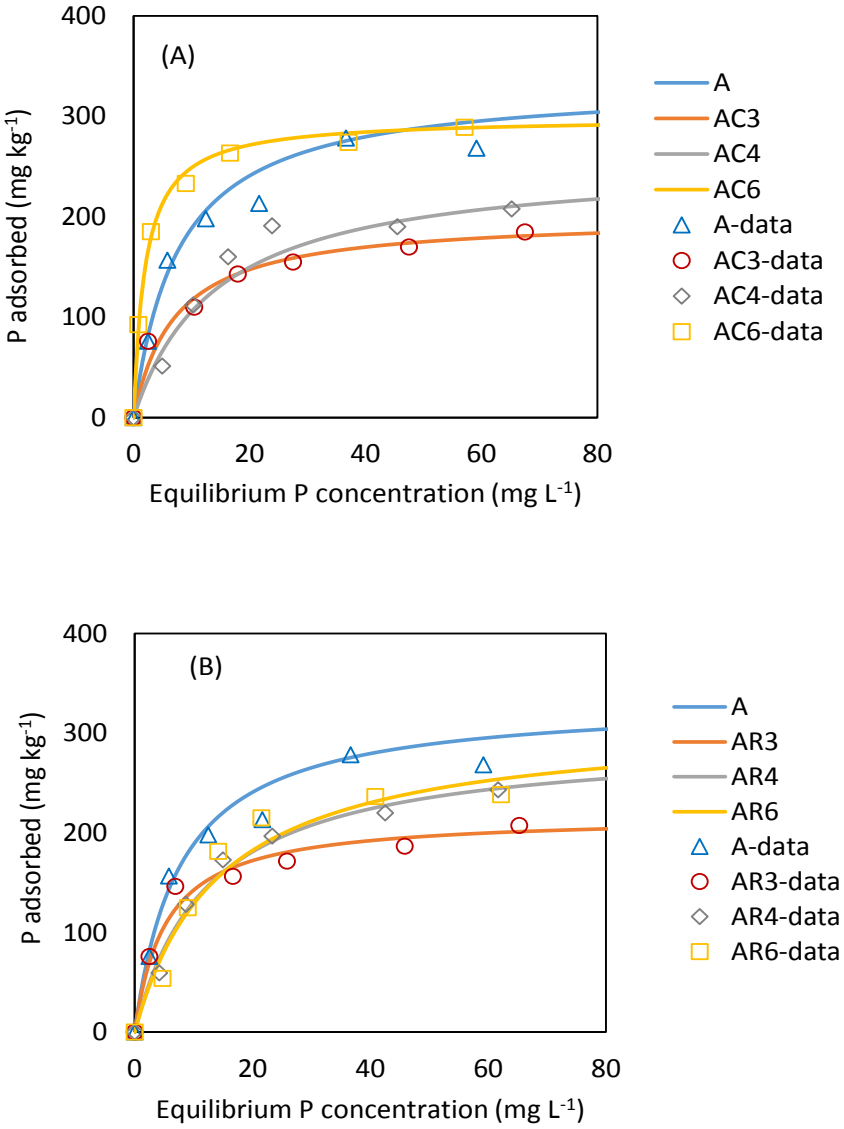

Figure 4.1b. Phosphorus adsorption isotherm for (A) Ankasa soil amended with corn cob biochar at three pyrolysis temperatures, (B) Ankasa soil amended with rice husk biochar at three pyrolysis temperatures

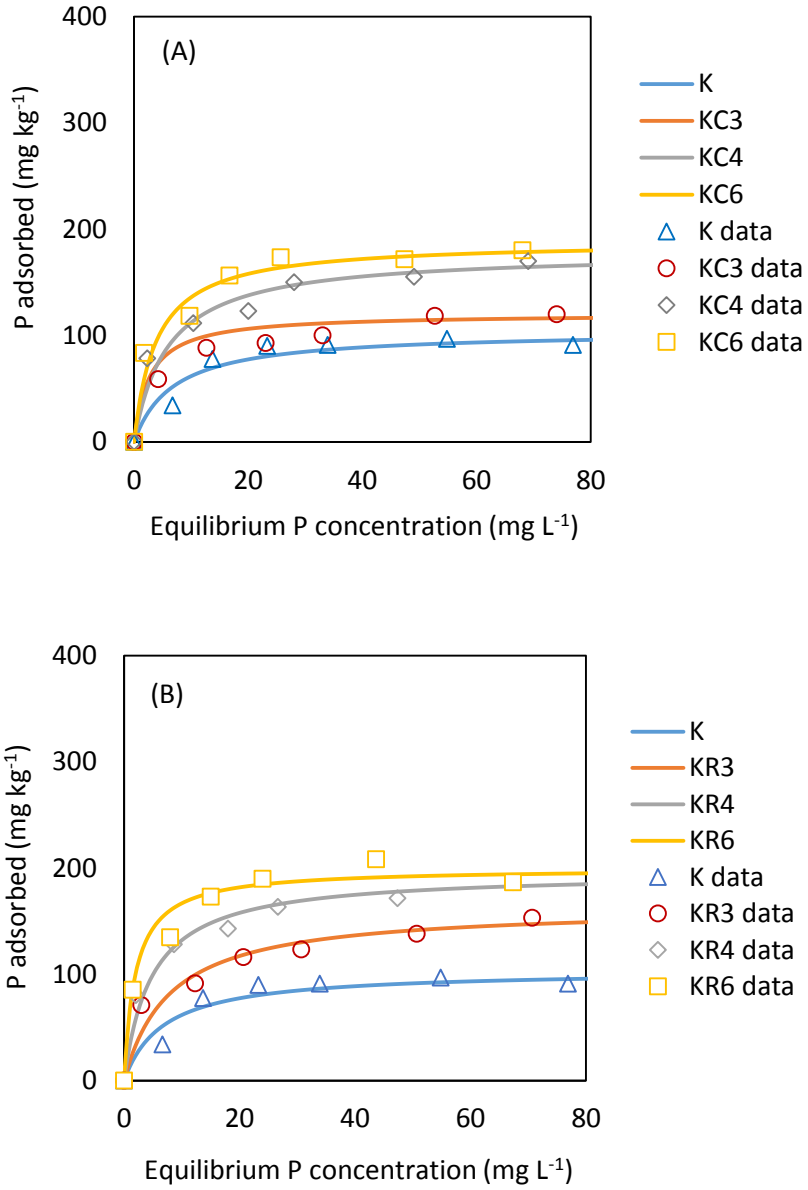

Figure 4.1c. Phosphorus adsorption isotherm for (A) Keta soil amended with corn cob biochar at three pyrolysis temperatures, (B) Keta soil amended with rice husk biochar at three pyrolysis temperature

Table 4.4a Sorption parameters for Kokofu with and without corn cob and rice husk biochar at temperatures 300 ºC, 450 ºC and 650 ºC

Soil/Biochar	Langmuir			P desorbability	SPR
	P_{max} *(mg kg^{-1})*	*K (L mg^{-1})*	R^2	*(%)*	*(mg kg^{-1})*
Ko	384.6e	0.07	0.90	38.0	120.32
KOR3	270.3ab	0.08	0.98	43.5	79.04
KoR4	322.6cd	0.14	0.99	31.2	104.69
KoR6	356.1e	0.13	0.99	24.7	111.70
KoC3	256.1a	0.08	0.97	52.7	77.80
KoC4	303.0bc	0.11	0.98	37.7	95.36
KoC6	344.8de	0.17	0.99	34.2	115.44

Table 4.4b Sorption parameters for Ankasa with and without corn cob and rice husk biochar at temperatures 300 ºC, 450 ºC and 650 ºC

Soil/Biochar	Langmuir			P desorbability	SPR
	P_{max} *(mg kg^{-1})*	*K (L mg^{-1})*	R^2	*(%)*	*(mg kg^{-1})*
A	333.3d	0.13	0.98	33.6	100.08
AR3	217.4ab	0.19	0.99	35.6	80.65
AR4	294.1cd	0.08	0.99	45.7	83.33
AR6	312.5d	0.07	0.96	42.2	85.79
AC3	200.0a	0.14	0.99	43.2	70.56
AC4	256.4bc	0.07	0.97	46.8	74.25
AC6	298.5d	0.50	0.99	13.7	88.27

P_{max} is P sorption maximum; *K* is binding affinity, SPR is standard P requirement; R^2 is coefficient of determination

Table 4.4c Sorption parameters for Keta with and without corn cob and rice husk biochar at temperatures 300 ºC, 450 ºC and 650 ºC

Soil/Biochar	Langmuir			P desorbability	SPR
	P_{max} (mg kg^{-1})	K (L mg^{-1})	R^2	(%)	(mg kg^{-1})
K	104.2a	0.15	0.98	49.0	39.68
KR3	164.0b	0.13	0.99	38.6	58.31
KR4	196.1cd	0.20	0.99	23.2	74.87
KR6	200.0d	0.51	0.99	16.4	85.18
KC3	120.5a	0.38	0.99	24.9	48.54
KC4	178.6bc	0.17	0.99	31.2	67.16
KC6	188.7cd	0.26	0.99	26.0	76.37

P_{max} is P sorption maximum; K is binding affinity, SPR is standard P requirement; R^2 is coefficient of determination

There was a significant ($p < 0.05$) increase in P_{max} of Keta upon rice husk biochar incorporation at increasing pyrolysis temperature (KR3, KR4 and AR6) ranging from 164.0 mg kg^{-1} to 200.0 mg kg^{-}.

The standard P requirement was computed by using the equation derived from the amount of P adsorbed against equilibrium P concentration graphs. Although the requirement for P concentration of the solution of different crops range from 0.005 to 0.3 mg P L^{-1} (Fox, 1981), a concentration of 0.02 mg P L^{-1} is often used in calculating the SPR which is the amount of sorbed P at this concentration in solution (Osodeke et al., 1993). The SPR of the two acid soils, Kokofu (120.3 mg kg^{-1}) and Ankasa (100.8 mg kg^{-1}) are medium but that of Keta (39.7 mg kg^{-1}), neutral soil is low according to Juo and Fox (1977). Adding corn cob and rice husk biochar to Kokofu had a SPR in a range of 77.8 to 115.4 mg kg^{-1} and 79.0 to 111.7 mg kg^{-1} respectively. Among the biochar-Kokofu treatments only KoR3, KoC3 and KoC4 had a low SPR of 79.0 mg kg^{-}, 77.8 mg kg^{-1} and 95.4 mg kg^{-1} respectively.

All the biochar amended treatments of Ankasa had low SPR values ranging from 80.65 to 85.79 mg kg^{-1} for rice husk biochar treatments and 70.56 to 88.27 mg kg^{-1} corn cob treatments. Similarly, the SPR values for the Keta-biochar treatments were all low even though relatively higher than the control soil (Keta). These values ranged from 58.31 to 85.18 mg kg^{-1} and 48.54 to 76.34 mg kg^{-1} for rice husk biochar and corn cob biochar treatments respectively. The lower SPR values with biochar amended soils indicate that the addition of biochar at 300 ^{o}C enhanced P availability.

4.3.5 Phosphorus sorption maximum in relation to soil properties

The relationships of some of the soil chemical properties such as Fe and Al oxides, pH, organic carbon, CEC and exchangeable Ca on P sorption maximum (P_{max}) of each of the soil types were studied (Table 4.5). The P_{max} of Kokofu was significantly and positively correlated with the extractable pedogenic crystalline Al and Fe oxides i.e. Fe_d and Al_d having correlation coefficient (r) of 0.56 and 0.75 respectively. However, the amorphous oxides (Fe_o and Al_o) together with OC and CEC were significantly and negatively related to the P_{max}.

Similar to Kokofu, the amorphous and crystalline Fe and Al oxides positively predicted the P_{max} of Ankasa significantly with the exception of Fe_o. The coefficient of correlation for Fe_d, Al_o, and Al_d was 0.75, 0.67 and 0.61 respectively. The OC and CEC of Ankasa-biochar was negatively correlated with the P_{max} having coefficient of correlation of -0.93 and -0.92 respectively. The P_{max} of Keta-Biochar was also significantly and positively correlated with extractable pedogenic crystalline Al and Fe oxides i.e. Fed, Al_o and Al_d except Fe_o. The increase in P_{max} of Keta-Biochar was significantly and positively proportional to the increase in pH, OC and exchangeable Ca.

Multiple regression showed that Fe and Al oxides significantly explained about 71%, 75% and 60% variation in the P_{max} of Ankasa, Kokofu and Keta amended soils respectively (Table 4.6). Combining Ca with pH did not predict the P sorption maximum of the acid soils. However, in the neutral soil (Keta) more of 70% variation in Pmax was accounted for by Ca and pH. The addition of OC to Ca and pH significantly predicted the P sorption maximum of Kokofu, Ankasa and Keta i.e. 75.0%, 76.2% and 79.7% respectively.

Table 4.5 Pearson correlation coefficient values between some chemical properties of soil-biochar mixture and P sorption capacity each for Kokofu, Ankasa and Keta

Soil properties	Kokofu	Ankasa	Keta
pH	-0.27	-0.37	0.46*
Ca	-0.21	-0.24	0.61*
Fe_o	-0.85**	0.24	0.27
Fe_d	0.82**	0.75**	0.49*
Al_o	-0.56*	0.67*	0.59*
Al_d	0.75**	0.61*	0.80**
CEC	-0.96**	-0.92**	0.39
OC	-0.81**	-0.93**	0.48*

** = $p < 0.01$; * = $p < 0.05$

Table 4.6 Multiple regression equations for predicting P sorption maximum of biochar amended soils

Soil-biochar property	Regression model ($Y = b_1X_1 + ... + b_nX_n + b_o$)	R^2
Ankasa		
Fe and Al oxides	P_{max} = 36.05 Fe_o + 144.29 Al_o + 17.69 Fe_d + 42.41 Al_d – 183.96	0.71*
Ca and pH	P_{max} = 54.51 Ca – 77.09 pH + 654.54	0.12^{ns}
Ca, pH and OC	P_{max} = 117.83* Ca – 35.30 pH – 282.70 OC + 841.73	0.76*
Kokofu		
Fe and Al oxides	P_{max} = 3.05 Fe_d – 48.74 Al_o + 26.91 Al_d – 106.72 Fe_o + 519.28	0.75**
Ca and pH	P_{max} = 79.30 Ca – 34.21 pH + 408.87	0.03^{ns}
Ca, pH and OC	P_{max} = 7.39 Ca + 70.22 pH – 256.21 OC + 364.67	0.74*
Keta		
Fe and Al oxides	P_{max} = 25.77 Fe_d + 264.33 Al_o + 105.49 Al_d – 18 Fe_o – 38.57	0.60*
Ca and pH	P_{max} = 189.48 Ca + 5.36 pH + 13.02	0.70**
Ca, pH and OC	P_{max} = 172.64 Ca + 11.77 pH + 165.36 OC – 104.60	0.79**

P < 0.05*; p < 0.01** : ns = not significant

The two dimensional Principal Component Analysis (PCA) plot was done to provide an overview of the relationships among the different soil properties of the three soils and the P_{max} (Fig. 4.2). In the PCA, the direction and length of the arrows show the extent of correlation between soil properties and the principal components i.e. X and Y axes. In the PCA analysis, the soil properties are indicated by the arrows (vectors) and therefore arrows with low angles are highly correlated, whiles the arrows that are perpendicular imply lack of correlation (r = 0). Three significant components were obtained.

However, only the two first components were used in order to facilitate interpretation of the bi-dimensional graph because component 3 constituted less than 10.2% of the total data variance. Three distinct soil types i.e. Kokofu, Ankasa and Keta were therefore established. The first PCA axis explains the bulk of the variance in the data set i.e. the soil properties (74.3%), separates the acid soils (i.e. Kokofu and Ankasa) from the neutral soil (Keta). The second PCA describes 15.5% of the variance, separating Kokofo and Keta from Ankasa.

4.3.6 Phosphorus desorption

A linear regression model was used to assess the effect of P binding energy (K) on the amount of P desorbed as shown in Fig. 4.3. The relationship between binding energy and P desorbed followed a negative linear pattern with a high significant correlation coefficient (r = -0.82). This implies that a decrease in P binding affinity resulted in an increased P desorption. Having a coefficient of determination of 68.1%, it is therefore obvious that more than 50% of P desorbed was caused by the binding energy between P and the adsorbent (soil-biochar). The relatively high binding energy in biochar amended Keta (0.13-0.51 L mg^{-1}) and Ankasa soils

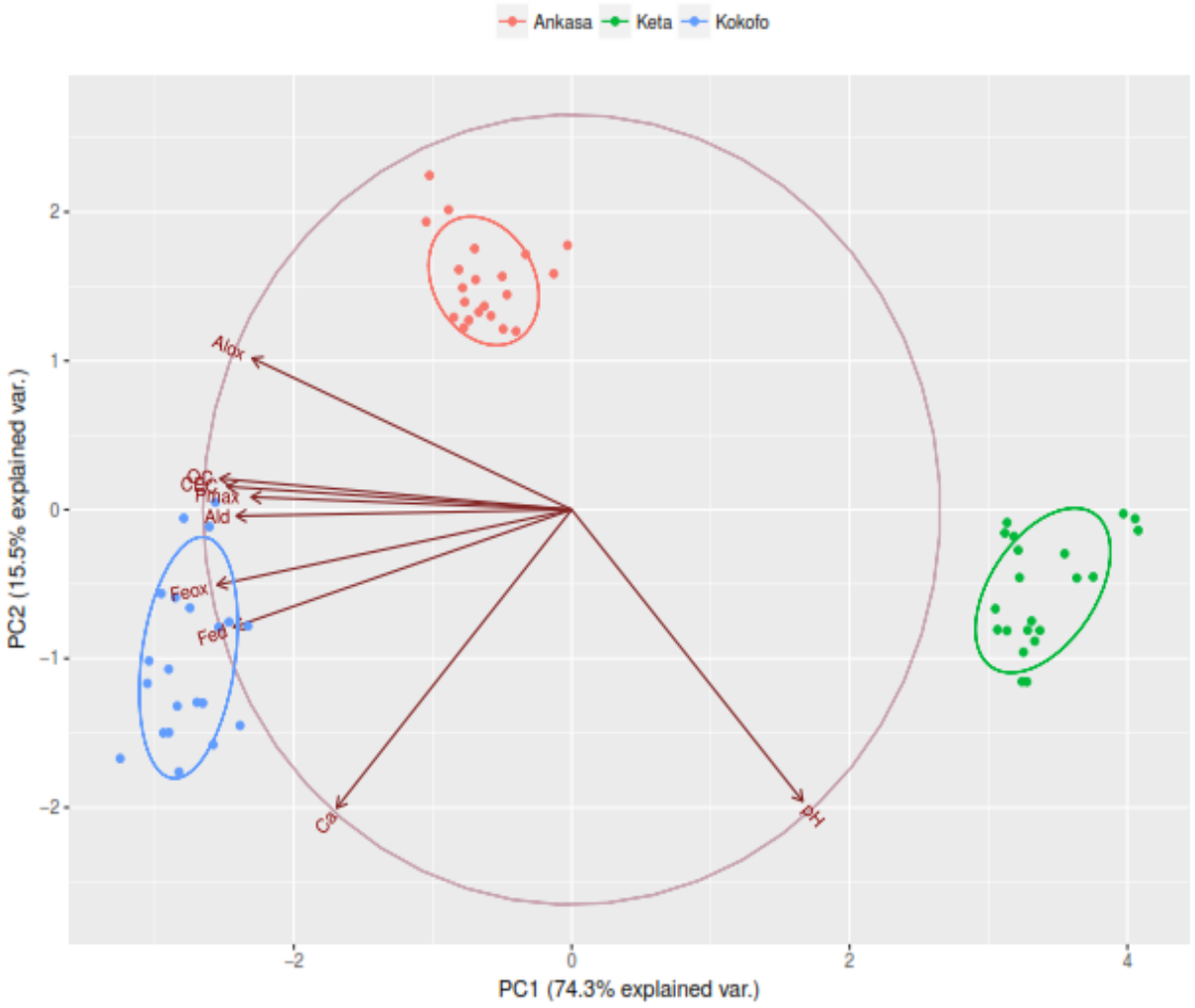

Fig. 4.2 Principal component analysis of some chemical properties of biochar amended soils

.

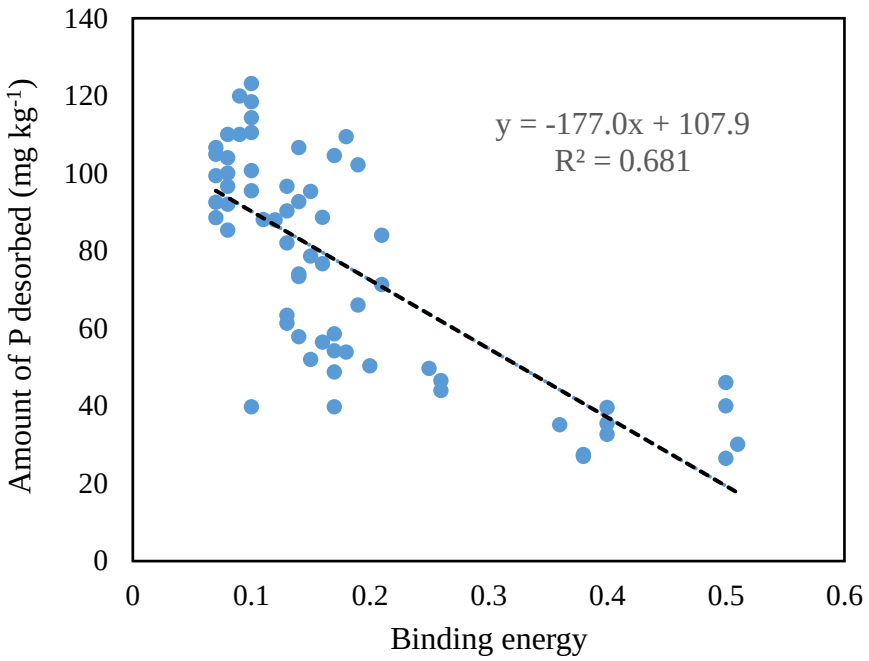

Fig. 4.3 Relationship between the Langmuir binding energy and P desorbed of the samples

(0.08-0.50 L mg^{-1}) than Kokofu soil (0.07-0.17 L mg^{-1}) reflected in the low percentage P desorbability in those soils. The amount of phosphorus desorbed from the soils and biochar amended soils by three successive extractions with 0.01M KCl are shown in Figures 4.4a-c. Phosphorus desorbability was calculated by the percent ratio of the amount of P desorbed to the amount of P adsorbed. Desorbability of P is used to indicate the degree of P desorption from the soils and soil-biochar treatments. There was significantly *($p < 0.05$)* more P released at the first extraction followed by low amount of P desorbed for the subsequent second and third extractions. Generally the amount of P desorbed from all the treatments decreased significantly *($p < 0.05$)* with successive extractions.

The total amount of P desorbed from Kokofu (Ko) for the three successive extractions was 111.6 mg kg^{-1} indicating 38% of P desorbability. The amount of desorbed P in Ko decreased to 86.0 mg kg^{-1}, 77.4 mg kg^{-1}, 96.7 mg kg^{-1} and 105 mg kg^{-1} with concomitant P desorbability of 31.2%, 24.7%, 37.7% and 34.2% for treatments KoR4, KoR6, KoC4 and KoC6 respectively. However, the application of biochar at 300 ^{o}C and 450 ^{o}C to Kokofu i.e. KoR3 and KoC3 increased P desorbability from 38.0% to 43.5% and 52.7% respectively.Out of 238.2 mg P kg^{-1} adsorbed by Ankasa, 90 mg P kg^{-1} was desorbed using the 0.01M KCl extractant giving a percentage P desorbability of 33.6. Upon the amendment of Ankasa with both biochar types the percent P desorbability increased with the exception of AC6 treatment which was 19.9% less of the control (Ankasa). The P desorbability range for Ankasa-corn cob biochar treatments was from 35.6 to 45.7% and 13.7 to 43.2% for Ankasa-rice husk biochar treatment.

The amount of P desorbed out of the 91.2 mg P kg^{-1} adsorbed by Keta (K) was 48.6 mg kg^{-1} representing 49% P desorbability.

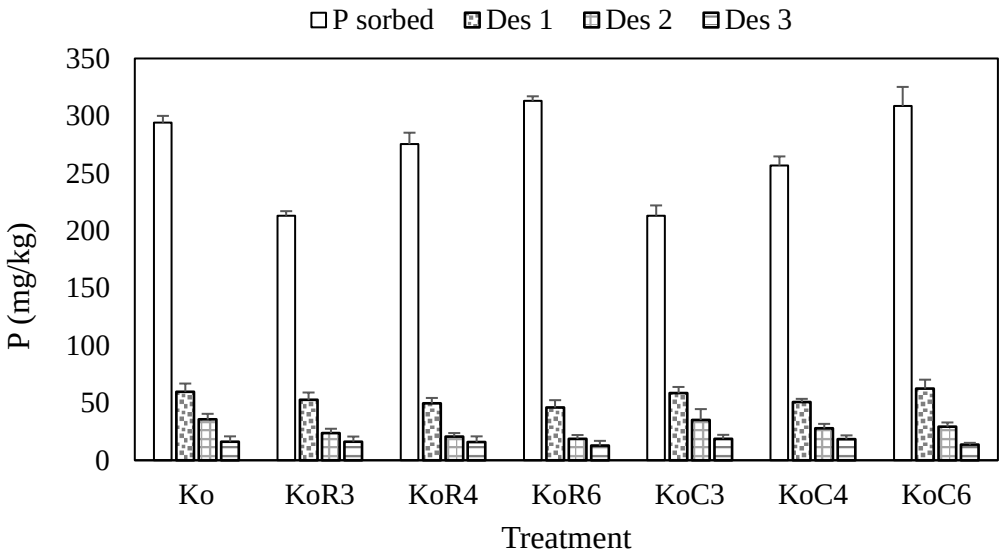

Fig. 4.4a Amount of phosphorus desorbed from the Kokofu and biochar-Kokofu mixture for three successive extraction

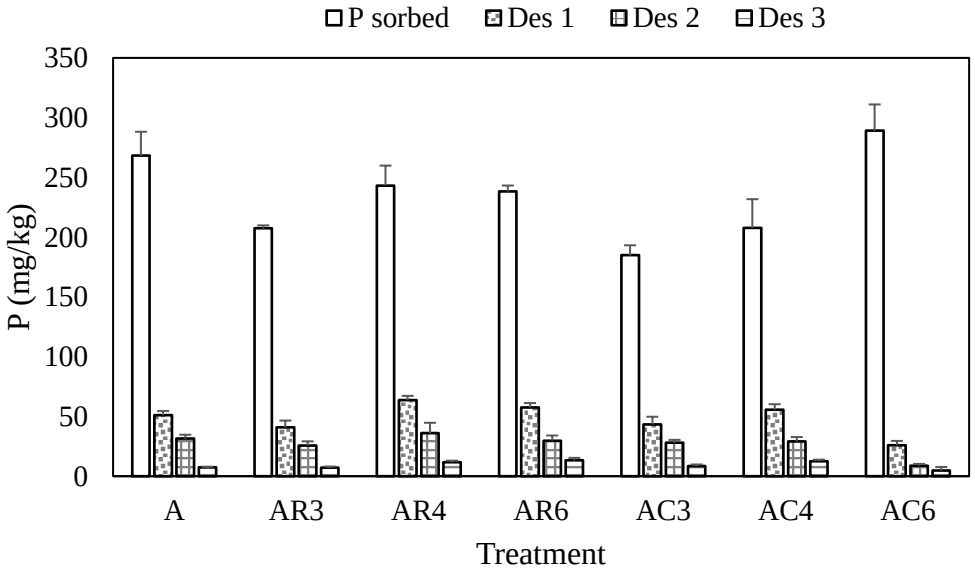

Fig. 4 4b Amount of phosphorus desorbed from the Ankasa and biochar-Ankasa mixture for three successive extraction

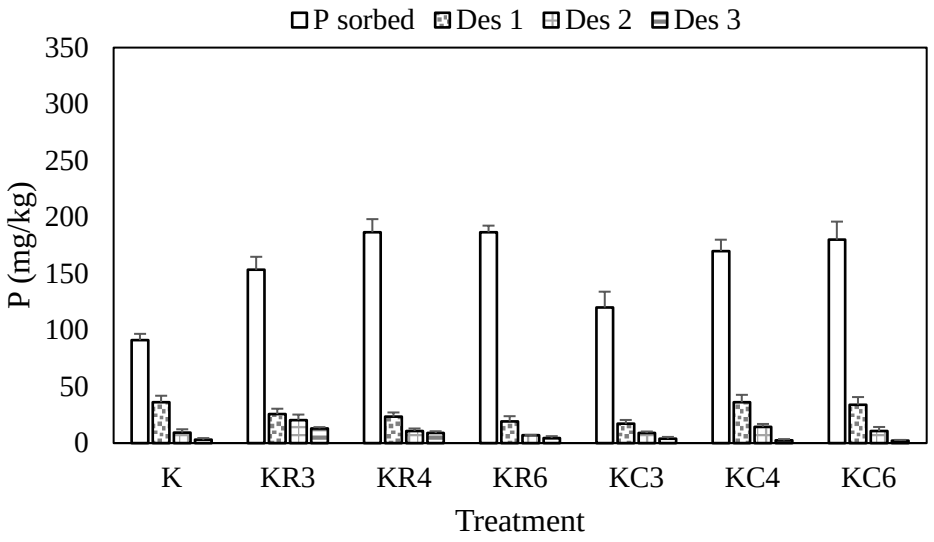

Fig. 4.4c Amount of phosphorus desorbed from the Keta and biochar-Keta mixture for three successive extraction

Phosphorus desorbability decreased when the two biochar types were added to Keta. The percentage P desorbability decrease was by 10.4, 25.8, 32.6, 24.1, 17.8 and 23 for KR3, KR4, KR6, KC3, KC4 and KC6 treatments respectively from the control soil (Keta).

4.4 Discussion

4.4.1 Characteristics of soil

The pH exhibited by the soils in water was higher than that in $CaCl_2$ solution giving a negative change in pH value (i.e. $\Delta pH = pH\ CaCl_2 - pH\ H_2O$) of 0.63, 0.72 and 1.32 for Kokofu, Ankasa and Keta respectively. This suggests that the surfaces of the soil colloids were negatively charged and therefore may tend to adsorb plant nutrients such as Ca^{+2}, Mg^{+2} and NH_4^+ that will be subsequently made available for plant uptake. The negative charge in pH value could be attributed to the highly weathered nature of the soils (Abekoe and Sahrawat, 2001).

The bulk density of the Kokofu and Ankasa are medium and that of Keta is high. Bulk density values of the soils are similar to what have been reported by Owusu-Bennoah et al. (2000) for the former soils and Asomaning (2011) for the latter soil. Coder (1996) reported that bulk density values of 1.3 Mg m^{3-} and above have the potential of limiting plant root growth especially soils from semi-deciduous forest. This will impede plant roots from exploring nutrients within the soil. There is therefore the need for physical manipulation to provide good tilth for crop production.

Most soils in Ghana are characterized by low organic carbon due to fast decomposition rates of organic matter as a result of high temperature (Bationo et al., 2003). However, the continuous deposition of litter from the vegetation and slow rate of organic matter turnover as a result of

low temperature and high rainfall in semi-deciduous forest and evergreen high rain forest may have accounted for the relatively high organic carbon content of the two acid soils than Keta. Keta, which is mainly sand deposits have low organic matter. The organic carbon value of Keta was similar to the findings of Awadzi et al. (2008) and Asomaning (2011).

The available P content of the soils were low (<15 mg kg^{-1}).The low amount of P in semi-deciduous forest and evergreen high rain forest (Kokofu and Ankasa) could be attributed to low levels of mineral apatite of the parent materials and also Al and Fe phosphate precipitation at low soil pH (Warren, 1992; Abekoe and Sahrawat, 2001). The low P content in Keta could be due to the low level of organic matter. Increase in available P can be enhanced by the competition of organic ligands for Al and Fe oxides surface and also direct release of mineralized P (Jones et al., 1996).

The total N content of Kokofu and Ankasa were low (1-2 g kg^{-1}) and Keta was very low (< 1 g kg^{-1}) according to the classification scheme defined by Landon (1984). Highly weathered tropical soils are generally low in nitrogen probably due to the low organic carbon content (Abekoe and Sahrawat, 2001).

Cation exchange capacity (CEC) measures the negative surface potential of soils at pH of 7. It also measures the sum of the total exchangeable cations that a soil can hold or adsorb (Jiang et al., 2012). Therefore, high CEC values indicate high plant nutrient storage capacity. The CEC of the soils were low most especially Keta. This can be attributed to the low activity clay content as well as the highly weathered nature of tropical soils. The relatively higher CEC of Kokofu than Ankasa and Keta could be due to the high exchangeable bases.

The low amount of exchangeable cations i.e. Ca^{2+}, Mg^{2+}, Na^{+} and K^{+} in Ankasa soil may be due to the excessive leaching of basic cations as a result of the high rainfall in that location.

Kokofu soil with relatively high exchangeable cations content compared to Ankasa soil can be ascribed to less leaching of the basic cations down the soil profile.

The Fe_o and Al_o represent the amorphous Fe and Al content of the soils and that of the Fe_d and Al_d the amount of crystalline Fe and Al oxides. The extractable Fe and Al oxides were more predominant in the acid soils (Kokofu and Ankasa) than in Keta due to the low pH and the high clay texture. The low Fe and Al oxide content of Keta could be attributed to the sandy texture.

4.4.2 Effect of biochar on soil characteristics

The pH of the soils increased upon the addition of the two biochar types with increasing pyrolysis temperatures. This is due to the initial pH and the inherent base cation concentration including Ca, Mg, K and Na of the biochar types. It was obvious from the study that the high carbonate content of biochar produced at 650 ^oC induced greater increases in soil pH. In an Oxisol, the pH value of 4.2 increased to 6.1 when biochar with initial pH of 9.8 was added (Van Zwieten, 2010a). Yuan & Xu (2011) also observed an increase in soil pH after the addition of maize straw biochar and reported that it was due to the highly basic nature of the biochar as a result of the abundance of its organic and inorganic carbonate content.

The addition of the two biochar types increased the organic carbon pool of the three soil types. Similar to the present study, Aon et al. (2015) reported that biochar amendments in tropical soils add substantial amount of organic carbon to the soil which eventually improves the soil organic carbon content. Corn cob and rice husk biochar produced at low temperatures (i.e. 300 ^oC and 450 ^oC) with high organic carbon content due to less decarboxylation explains the much significant effect on the soil organic carbon than at high temperature (i.e. 650 ^oC) (Van Zwieten

et al., 2010a). The increase in organic C content of the soils was greater in the corn cob biochar treatments. This is obviously due to the relatively high total C content of corn cob biochar.

In the present study the CEC of the soils increased when biochar was incorporated. The increase in soil CEC was more significant at the low pyrolysis temperatures i.e. 300 ^{o}C and 450 ^{o}C. These observations are in agreement with earlier studies that application of biochar increased CEC of highly weathered tropical soils at decreasing pyrolysis temperatures and therefore serves as a good buffering capacity of soil (Cheng et al. 2008; Yuan & Xu, 2011). After the incubation of Ultisol with rice straw biochar applied at a rate of 2.4 t ha^{-1} for 2 weeks the CEC of soil increased from 4 to 17% (Yuan et al., 2012). Similarly, the addition of *Leucaena leucocephala* biochar raised the CEC of the highly weathered soil from 7.41 to 10.8 $cmol_c$ kg^{-1} after the biochar addition (Jien and Wang, 2013). The CEC of fresh biochar is mostly low, but it increases with time as the biochar is aged through abiotic oxidation (Cheng et al. 2008). The large surface area and the abiotic oxidation of biochar leads to the increase in soil CEC (Cheng et al., 2006; Liang et al., 2006). Large CEC values up to 490 $cmol_c$ kg^{-1} have been reported for biochar (Cheng et al., 2008). Mostly, reported CEC values for soil components include < 5 $cmol_c$ kg^{-1} for sand, < 10 $cmol_c$ kg^{-1} for sesquioxides, < 15 $cmol_c$ kg^{-1} for kaolinite, < 150 $cmol_c$ kg^{-1} for smectite, and < 250 $cmol_c$ kg^{-1} for organic matter in soil (Brady and Weil, 2008). The increased CEC of the studied soil types by the two biochar types is logical because several studies have reported that the inherent CEC of biochar is higher than soil and organic matter (Sohi et al., 2009). The CEC of the two biochar types is three fold and ten fold more than the acid soils and the neutral soil respectively. The increase in soil CEC upon the biochar addition gives an indication of high negative surface charge potential which helps to retain exchangeable cations that are essential plant macronutrients and therefore improve soil fertility.

The exchangeable Ca content of the soils increased after the application of corn cob and rice husk biochar. The observed increase in exchangeable Ca in the biochar treated soils may be attributed to the ash content of the biochar. The ash content of biochar helps for the immediate release of the occluded mineral nutrients like K, Ca, Mg and Na for crop use (Sohi et al., 2009). In line with the results of the present studies, Wang et al. (2014) observed 60 to 67% increase in exchangeable Ca, K, Mg and Na after biochar addition in some tropical soils. It was clear from the study that the high total base cation of the 650 ^{o}C-produced biochar types led to the significant increase in the exchangeable Ca content of the soil types.

Generally, the amount of pedogenic extractable oxides of Fe and Al decreased in the acidic soils with the exception of the amorphous Fe oxides (Fe_o). This observation was consistent with those of Chintala et al. (2014) who reported a decrease in crystalline and amorphous Fe and Al oxides concentration of acid soils after the application of corn stoves biochar and ponderosa pine wood biochar. The decrease in Fe and Al oxides can be attributed to increase in soil pH after biochar application, thereby leading to the precipitation of extractable Al and Fe oxides as hydroxides. Again, organic ligands discharged from biochar can promote the formation of organo-metallic complexes with extractable Al and Fe oxides (Chintala et al., 2014).

In the neutral soils these oxides increased probably due to the direct release of the substantial amount of Fe and Al oxides in the biochar types. The increasing amount of Fe_o in the three soil types could indicate the effect of labile carbon from biochar especially at the low pyrolysis temperatures (i.e. 300 ^{o}C and 450 ^{o}C) hindering the crystallization of the iron oxides (Huang and Wang, 199). Bigham et al. (2002) affirmed that crystallization of ferrihydrite was normally inhibited or delayed by organic acids adsorbed on the ferrihydrite surface impeding aggregation prior to hematite formation.

Total P content of the soils increased upon the addition of corn cob and rice husk biochar. This is consistent with other studies who reported a significant increase in total P in an Alfisol after the addition of biochar (Sinclair et al., 2010; Brewer et al., 2011). The increase in total P was more significant at biochar types produced at 650 ^{o}C. Increasing total soil P with increasing pyrolysis temperature could be due to the increase in P enrichment at high temperatures.

4.4.3 Phosphorus sorption in soils and biochar amended soils

The Langmuir equation effectively explained P sorption by the three soil types, showing increase in P sorption with increasing P concentration but at decreasing rate. This observation is consistent with other studies (Abekoe and Sahrawat, 2001; Asomaning, 2011) and could be attributed to the fact that the competitive adsorption of P on the soil surface sites was not obvious at low P concentration while their competition enhanced with increase in P concentration (Lair et al., 2009).

The sorption maxima of the two acid soils, Kokofu (384.5 mg kg^{-1}) and Ankasa (333.3 mg kg^{-1}) was relatively higher than the neutral soil, Keta (104.2 mg kg^{-1}). The relatively high P sorption capacity of the former is due to the high content of amorphous and crystalline Fe and Al oxides (Jiang et al., 2015). It is obvious from the study that these oxides are the main P adsorbent in the acid soils, contributing to more than 70% variation in the amount of P adsorbed. Kokofu with relatively high content of Fe and Al oxides showed much decrease in P availability.

Incorporating biochar types into the acid soils increased P bioavailability with decreasing pyrolysis temperature. The result of the present study is consistent with those of Morales et al (2013) who found that biochar reduces P fixing capacity of degraded tropical soils. Similarly,

Cu et al. (2011) also found a decrease in P adsorption onto ferrihydrite when amended with straw biochar. Phosphorus availability in solution due to reduced P sorption capacity of the two acids soil was more sensitive to corn cob biochar than rice husk biochar. This could probably be as a result of the high pH, high CEC and low Fe and Al content of corn cob biochar. The inhibitory effect of both biochar types produced at 300 ^{o}C on P adsorption onto the acid soils was relatively greater than at 450 ^{o}C and 650 ^{o}C. Therefore, biochar produced at 300 ^{o}C can be considered as an appropriate amendment in acid soils making P more bioavailable for plant uptake.

The negative surface potential of soil at pH 7 is explained by its cation exchange capacity (CEC) (Jiang et al., 2012). Adding biochar to the soils raised the organic carbon content with a concomitant increase in CEC, however the CEC decreased at increasing pyrolysis temperature. Easterwood and Sartain (1990) reported a reduction in point of zero net charge (PZNC) of soil after the addition of white clover biochar. A decrease in PZNC would culminates into an increase CEC. This may have led to an increase in electrostatic anion repulsion between the negatively charged soil-biochar surface and the negatively charged P ions (HPO_4^{2} / $H_2PO_4^{-}$).

In the present study, an increase in organic content reduces the P adsorption capacity of the acid soils. Koopmans et al. (2003) in study on ^{31}P Nuclear Magnetic Resonance Analysis of P speciation some of organic amended soils of the tropics found that organic P was mainly found as orthophosphate monoester such as inositol phosphate. Due to the high surface charge density of inositol phosphate these P compounds are strongly sorbed by hydroxides of Fe and Al in soils (Turrion et al., 2001), thus competing with inorganic P for adsorption sites. Experiment by Schneider and Haderlein (2016) suggested that dissolved organic matter from biochar inhibits P sorption in highly weathered, iron oxides rich soils. Such a competition reaction has

been reported between P and several low molecular weight organic acids and anions (Gerte et al., 2000).

Substantial sorption of Fe and Al oxides onto biochar as reported by Xu et al. (2014) especially at the low pyrolysis temperature (300-450 ^{o}C) with high CEC might have enhanced P bioavailability. Murphy and Stevens (2010) reported that biochar plays a role in controlling P availability by changing soil pH and P sorption capacity. It is, therefore, possible that the increase in the acid soil pH upon biochar addition leads to the precipitation of polymeric Fe and Al oxides (Yuan et al., 2011).

Unlike the decrease in P sorption in Kokofu and Ankasa amended with biochar, Keta showed increase in P sorption with increasing pyrolysis temperature. This was in line with that of Zhai et al. (2014) who reported an increase in P sorption at increasing pyrolysis temperature in a slightly alkaline soil when maize residue biochar produced at different pyrolysis temperature was added. The results of the present study revealed that the Langmuir sorption maximum of Keta amended soil was predicted by Ca, Fe_d, Al_d, Al_o and OC. Borggaard et al. (1990) reported that Al oxides (Al_d and Al_o) are more effective P adsorbent than Fe oxides. Other studies have also indicated that Al and Fe oxides from biochar control P adsorption in neutral and alkaline soils (Xu et al., 2013). Earlier studies suggested that deceased in P availability is due to the chemical retention of Ca rather than the hydrolytic reactions of Al and Fe (Agbenin, 1995; Soil Survey Staff, 2010; Zhang et al., 2010; Cui et al., 2011). This will be seen in the P fractionation studies where the Ca bound P (HCl-Pi) pool was higher than the Al and Fe bound P (NaOH-Pi) pool. Reduced P availability in neutral and alkaline soils has also been reported to be due to P fixation by added alkaline and alkaline earth metals in char (DeLuca et al., 2009; Qian et al., 2013; Xu et al., 2014).

Amending Keta soil with the biochar increased Ca^{2+} concentration and hence the ionic strength of soil solution leading to P adsorption (Murphy and Stevens, 2010). Mukherjee et al. (2011) further elucidated that the residual charge of the electrostatically attracted divalent cations such as Ca^{2+} and Mg^{2+} forms metal bridge bonds with P. The formation of Ca-P and Mg-P precipitate could therefore be the mechanism underlying the increase in P sorption in the neutral soil (Keta). Interaction occurs between organic matter and mineral oxides, inhibiting their crystallization and hence increasing P sorption capacity (Borggaard et al., 1990). This may have explained the direct relationship between organic C and P sorption maximum of the biochar amended neutral soil. It is clear from the study that it is not advisable to add biochar to alkaline or neutral soils since it could reduce P availability for plant uptake.

4.4.4 Phosphorus desorption in soils and biochar amended soils

Generally for all the soil and soil-biochar mixtures, large amount of P was desorbed from each of the sample at the initial extraction with 0.01 M $CaCl_2$ but further decreased with successive extractions. This observation is similar to previous studies (Akekoe and Sahrawat, 2001; Asomaning, 2011). Asomaning (2011) reported that there was a high initial amount of P desorbed in the first 2 h followed by slow desorption to 6 h.

Substantial amount of P was released ranging from 33.6 to 49.0% into the solution at P loadings of 86.6 mg L for the soils. The increased amount of P desorbed from the three soils implies high P bioavailability and leaching potential of the sorbed P (Singh and Gilkes, 1991).

The biochar type and pyrolysis temperature influenced the amount and percentage of P desorbed by altering the binding energy of P to the soils (Xu et al., 2014). Generally the increase P desorbability was more sensitive to biochar type charred at 300 ^{o}C in the two acid soils.

Similar results for higher P desorption from an Oxisol amended with wheat straw biochar produced at 350 ^{o}C than 700 ^{o}C was observed by Xu et al. (2014). Reduction of P binding energy in acid soils by different biochar types pyrolysed at low temperatures with concomitant increase in P released have been reported in literature (Qian et al., 2013).

Pyrolysis biochar at high temperatures most especially at 650 ^{o}C seems to decrease the amount of P desorbed in acid soils. Frost et al. (2012) reported that the disappearance of hydroxyl groups on biochar carbon lattice around 600 ^{o}C would cause Al-phosphate or Fe-phosphate complex to change from1 an outer sphere mode to an inner sphere mode, hence affecting the amount of P desorbed using neutral salt such as KCl and $CaCl_2$. Biochar additions decreased P desorbability in Keta. The less amount of P released in neutral or alkaline soils have been ascribed to increasing binding energy as a result of increasing soil pH upon char incorporation (pH > 7) (Qian et al., 2013).

4.5 Conclusion

The study indicated that biochar influences P cycling and distribution in tropical soils. Phosphorus availability increased in the acid soils but decreased in the alkaline soil. The effect of biochar P availability was sensitive to the pyrolysis temperature of the biochar types. Biochar produced at low temperatures (300 ^{o}C and 450 ^{o}C) can be considered as appropriate amendments in acid soils to make P more available for plant uptake. However, biochar application to neutral or alkaline soils can be considered as inappropriate P management practices since it increases P adsorption and lowers P desorbability

.

CHAPTER FIVE

SHORT-TERM EFFECT OF CORN COB AND RICE HUSK BIOCHAR ON PHOSPHORUS FRACTIONS IN THREE CONTRASTING SOILS

5.1 Introduction

Soils from Ghana are highly weathered, acidic and dominated by large quantities of sesquioxides (Abekoe and Tieseen, 1998; Brady and Weils, 2001). These sesquioxides geochemically fix phosphorus (P) resulting in P deficiency and often limit crop production (Cross and Schlesinger, 1995). In neutral to alkaline soils, P is adsorbed to soil surfaces at low solution orthophosphate concentration whereas at high concentration it's mainly precipitated as calcium-P i.e. dicalcium or octacalcium phosphates, hydroxyl apatite and eventually least soluble apatites (Borrero et al., 1988; Castro and Torrent, 1998; Tunesi et al., 1999; Hinsinger, 2000). Applied P to acidic soils from organic and inorganic sources gradually reacts with Fe and Al compounds and is transformed into relatively insoluble P compounds (Lindsay, 1979; Nartey et al, 1997; Verma *et al*., 2005). Phosphorus therefore exists in several forms based on the reactivity in the soil environment (Lan et al., 2012).

The various forms of P in soils have been examined using chemical sequential extraction techniques (Chang and Jackson, 1957; Williams et al., 1980; Hedley et al., 1982b) among which Hedley fractionation method is widely used (Cross and Schlesinger, 1995; Asomaning et al., 2015). Hedley chemical fractionations gives a very simple and rapid analysis of P fractions in soils and sediments (Hedley et al., 1982b). This sequential procedure involves the use of various chemical reagents to selectively solubilize the Al, Fe, or Ca phosphate phases in soil (Chang *et* al., 1957; Hedley et al., 1982a,b). This chemical reagents are of varying extraction strength, culminating into different soil P with varying levels of lability namely most

labile P, moderately labile P and recalcitrant P fractions (Hedley et al. 1982a). Identification of soil P compounds is helpful in revealing the controlling phases of soil P dynamics (Sui et al., 1999; Delgado and Torrent, 2000).

Biochar is mostly a stable solid carbon-rich product obtained from thermal decomposition of plant and animal residues under limited oxygen conditions (Lehmann and Joseph, 2009; Yu and Teruo, 2013; Mohan et al., 2014). Biochar usually has high surface area, high surface charge density as well as hydrophilic and hydrophobic surface properties (Laird et al., 2010). Hence, its application changes soil P forms by altering the chemical properties of tropical soils (Liang et al., 2014). Wang et al. (2014) reported an increase in most labile P (resin-P, $NaHCO_3$ extractable Pi) and moderately labile P (NaOH extractable Pi) fractions in sandy soils upon the addition of cattle manure and sewage sludge biochar. A high increment in NaOH-Pi and $NaHCO_3$-Pi was observed in soils amended with organic matter (Li et al., 2015). In contrast, a number of studies have reported no effect of biochar on soil P fractions. For instance, Simard et al. (2001) observed a decrease in most labile P in woody biochar amended tropical soils. Similarly, the incorporation of mallee biochar in clay soils led to a significant decrease in P availability i.e. $NaHCO_3$-extractable inorganic P form (Zhang et al., 2016). Such conflicting results call for detailed studies on biochar effect on P forms in Ghanaian soils. Information on the short term effect of biochar on P forms and distribution is important for assessing P availability in soils (Tiessen et al., 1984), and consequently the potential risks for polluting aquatic ecosystems.

Phosphorus forms in biochar and hence its P bioavailability in soil is largely controlled by biomass type and the pyrolysis temperature (Cantrell et al., 2012). Biomass contains variable amounts of inorganic P as well as organic P. With increasing pyrolysis temperature, the total P increases (Hossain et al., 2011; Uchimiya and Hiradate, 2014; Wu et al., 2011). However, most

of the P are fixed in the ash compounds such as Ca-P, Mg-P, Fe-P at high temperatures and therefore bioavailable P decreases (Cantrell et al., 2012; Iqbal et al., 2015). Studies by Christel et al. (2014) confirmed no P availability at pyrolysis temperatures above 700 ^{o}C when determining P availability in pig slurry biochar using diffusive gradients in thin film techniques. This is obviously due to the formation of unstable P compounds during thermal breakdown (Cantrell et al., 2012; Thygesen et al., 2011). The need for assessing P forms in biochar at varying carbonization conditions prior to its application merits research since it can affect P availability in soil solution for plant uptake. The objectives of the study were to:

1. evaluate the P fractions in biochar at three pyrolysis temperatures
2. find out the effect of biochar at different temperatures on the P fractions of soils

5.2 Materials and methods

5.2.1 Phosphorus Fractionation

The less than 2 mm soil and soil-biochar mixture after the incubation experiment (chapter four) was subjected to chemical sequential P extraction using a modified Hedley fractionation procedure (Table 5.1) (Hedley et al. 1982a; Tiessen and Moir, 2008; Asomaning et al., 2015) to determine the most labile phosphorus pool (Resin Pi, $NaHCO_3^-$ extractable Inorganic (Pi) and organic P (Po)), moderately labile phosphorus pool (NaOH extractable Pi and Po) and stable P (HCl extractable Pi, residual P).

Table 5.1 Modified Hedley fractionation procedure

Phosphorus pool	Extraction Procedure
Resin-Pi	Sample + resin + deionized water – Shake for 16 h and Centrifuge
	Resin + 0.5 M $NaHCO_3$ - shake for 1 h
	↓
	Sample + 0.5 M $NaHCO_3^-$ - Shake for 16 h and centrifuge
$NaHCO_3$ -Pi	Aliquot
$NaHCO_3$ -Pt	Aliquot- H_2SO_4 + $K_2S_2O_8$ digestion
$NaHCO_3$ -Po	Total P minus inorganic P
	↓
	Sample + 0.1 M NaOH - Shake for 16 h and centrifuge
NaOH-Pi	Aliquot
NaOH-Pt	Aliquot- H_2SO_4 + $K_2S_2O_8$ digestion
NaOH-Po	Total P minus inorganic P
	↓
HCl-Pi	Sample + 1 M HCl - Shake for 16 h and centrifuge
	↓
Residual P	Sample + conc. H_2SO_4 – Digestion (360 ^oC)

Pi, Po and Pt means inorganic, organic and total phosphorus respectively.

5.2.1.1 Resin-Pi

Anion exchange resin membrane (AEM) (ANION 204UZRA, 1 cm x 6 cm) was used to extract resin- Pi. The AEM strips were charged using 0.5 M $NaHCO_3$ and finally rinsed with deionized water. Two (2) g samples were weighed into 50 ml centrifuge tube containing 30 mL deionized water in quadruple and shaken end-to-end for 16 hours on an electrical shaker overnight. Soil particles adhered to the resin strips after shaking were washed off with deionized water. The strips were then placed in centrifuge tubes containing 30 ml of 0.5 M $NaHCO_3$ and was shaken for 1 h. An aliquot of 15 mL of the extract was taken and phosphate was determined colourimetrically by the method of Bray and Kurtz (1945).

5.2.1.2 $NaHCO_3$ extractable P fraction- Pi

The sample suspension obtained after the removal of the resin strips was centrifuged for 10 min at 3500 rpm and the clear supernatant decanted. Thirty ml of 0.5 M $NaHCO_3$ was added to the treatment and then shaken end to end for 16 h on an electrical shaker at room temperature. The soil/biochar suspension was centrifuged for 10 min at 3500 rpm and filtered using a 0.45 µm filter paper. An aliquot of 15 mL was pipetted into a centrifuged tube and 6 ml of 0.9 M H_2SO_4 was added and kept in a fridge for 30 min to precipitate the organic matter. This was then centrifuged at 3500 rpm for another 10 min. The clear supernatant was then decanted into 50 ml volumetric flask and then analysed for $NaHCO_3$ extractable inorganic-P as under 5.2.1.1.

5.2.1.3 $NaHCO_3$ extractable-total P (Pt) and organic P

Eight (8) ml aliquot of the filtrate obtained under 5.2.1.2 was pipetted into an autoclave tube. One ml of 18 M H_2SO_4 was added, followed by 0.2 g potassium persulphate ($K_2S_2O_8$) and autoclaved

for 1 h at 121 ^{o}C. Eight (8) mL of the digested sample was taken for P determination, as $NaHCO_3$ extractable total-P ($NaHCO_3$ extractable-Pt). Organic $NaHCO_3$ extractable-P was calculated as difference between the total amount and the inorganic P as under 5.2.1.1.

5.2.1.4 NaOH extractable P fractions -Pi

Residual samples obtained under section 5.2.1.2 was weighed to calculate the amount of $NaHCO_3$-Pi transferred to the subsequent P extraction. Thirty ml of 0.1 M NaOH was added to the sample residue and then shaken end to end for 16 h on a mechanical shaker at room temperature. The sample suspension was then centrifuged for 10 min at 3500 rpm and filtered through 0.45 µm filter paper. An aliquot of 10 mL of the filtrate was pipetted into a centrifuge tube and 1.6 ml of 0.9 M H_2SO_4 was added and kept in a fridge for 30 min to precipitate the organic matter. This was then centrifuged at 3500 rpm for another 10 min. The clear supernatant was then decanted into 50 ml volumetric flask and then analysed as under 5.2.1.1, as NaOH extractable inorganic-P (NaOH extractable-Pi).

5.2.1.5 NaOH extractable-total P (Pt) and organic P

Ten (10) mL aliquot of the filtrate obtained under 5.2.1.5 was pipetted into clean screw cap glass test tube. One mL of 18 M H_2SO_4 was added, followed by 0.2 g potassium persulphate ($K_2S_2O_8$) and autoclave digestion during 1 h at 121 ^{o}C. The digested sample was decanted into 50 mL volumetric flask for P determination, as NaOH extractable total-P (NaOH extractable-Pt). NaOH extractable organic-P (NaOH-Po) was calculated as difference between the total amount and the inorganic P as under 5.2.1.1.

5.2.1.6 HCl extractable-P

Residual samples obtained under section 5.2.1.4 was weighed to calculate the amount of $NaHCO_3$-Pi transferred to the subsequent P extraction. Thirty (30) mL of 1 M HCl was added to the sample residue obtained and then shaken end to end for 16 h on a mechanical shaker at room temperature. The soil suspension was then centrifuged for 10 min at 3500 rpm and filtered. An aliquot of 5-15 mL was pipetted into a 50 ml volumetric flask and then analysed as under 5.2.1.1.

5.2.1.7 Residual P

Thirty (30) mL of deionized water was added to the sample residue in the tubes and then shaken for 1hr, centrifuged and the supernatant decanted prior to the extraction of the subsequent the residual P. The sample residue was then transferred into a 250 ml Kjeldahl flask and 20 mls of concentrated H_2SO_4 was added. The mixture was digested until the digest became clear after which 1 ml of 30% of H_2O_2 was added to clarify the digest. The flask was then cooled and the digest filtered through 0.45 µm filter paper in a 100 ml volumetric flask and made to volume with distilled water. The residual P analysed as under 5.2.1.1.

5.2.2 Statistical analysis

The normality of the data from the experiment was tested using Shapiro-WilK test. The data were then subjected to analysis of variance (ANOVA) using GentStat version 12. The separation of means was tested using least significant difference (LSD) with a significance level of $p < 0.01$ and $p < 0.05$. Correlation analysis among the P fractions and some chemical properties of the soils was done.

5.3 Results

5.3.1 Phosphorus fractions

In order to ascertain the reliability of the modified Hedley fractionation procedure in assessing P fractions in the two biochar types (corn cob and rice husk biochar) and also biochar amended soils (Kokofu, Ankasa and Keta), a linear regression model was applied as shown in Fig. 5.1. It is clear that the sum of P fractions underestimated total P of the soil and soil-biochar mixture by 1%. The high coefficient of determination, R^2 (91.5%) shows that the modified Hedley fractionation procedure was appropriate.

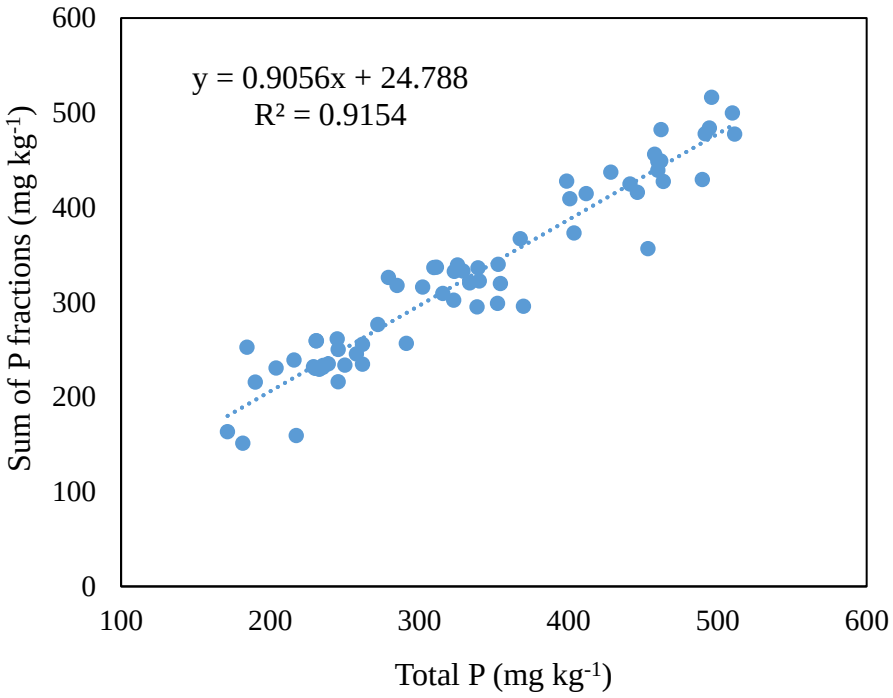

Fig. 5. 1 Relationship between the sum of P fractions and total P of the samples

5.3.2 Phosphorus fractions in Biochar

Phosphorus fractions including the total P content of the rice husk and corn biochar at the three pyrolysis temperatures are shown in Table 5.2. The percentage proportion of each of the P pools are also shown in Fig. 5.2. The total P content increased significantly at increasing pyrolysis temperatures, 300 ^{o}C to 650 ^{o}C for the two biochar types. The total P increase varied from 1186.6 to 1523.9 mg kg^{-1} and 1540.8 to 1936.9 mg kg^{-1} for rice husk biochar and corn cob biochar respectively.

Resin extractable inorganic P (Resin-Pi) and $NaHCO_3$ extractable inorganic P ($NaHCO_3$-Pi) express the readily or most labile inorganic P and therefore are considered to be readily available for plant uptake. The $NaHCO_3$-Pi describes the P fraction adsorbed weakly on the biochar colloidal surfaces. The amount of most labile inorganic P (resin-Pi and $NaHCO_3$-Pi) in the two biochar types gradually decreased with increasing pyrolysis temperature. For instance, the amount of resin-Pi significantly ($p < 0.05$) decreased from 142.7 mg kg^{-1} (11.1%) to 121.2 mg kg^{-1} (8.3%) and 261.4 mg kg^{-1} (17.1%) to 156.8 mg kg^{-1} (9.6%) in rice husk and corn cob biochar respectively. Even though there was no significant variation ($p > 0.05$) of the $NaHCO_3$-Pi pool among the rice husk biochar treatments (RH300, RH450, RH650), the percentage proportion decreased from 6.2% to 4.4% at increasing pyrolysis temperature. However, among the corn cob biochar treatments, $NaHCO_3$-Pi pool of CC450 (81.7 mg kg^{-1}) was significantly ($P < 0.05$) higher than CC650 (61.9 mg kg^{-1}) but statistically similar ($p > 0.05$) to CC300 (72.8 mg kg^{-1}).

Table 5.2 Phosphorus fractions in corn cob and rice husk biochar charred at 300 °C, 450 °C and 650 °C

Biochar	Resin-Pi	$NaHCO_3$-Pi	NaOH-Pi	ΣPo	HCl-Pi	Residual P	Total P
				mg kg^{-1}			
RH300	142.7	80.2	48.5	179.4	141.2	697.1	1186.6
RH450	154.6	71.5	35.8	172.1	119.0	783.1	1270.7
RH650	121.1	64.9	37.3	145.4	212.5	884.0	1522.9
CC300	261.4	72.8	23.9	169.2	110.0	894.0	1540.8
CC450	231.1	81.7	30.7	125.6	166.6	956.3	1704.7
CC650	156.8	61.9	21.3	150.4	182.6	1068.0	1936.9
Lsd	39.5	12.8	12.5	59.7	36.7	154.5	81.9

ΣPo = (NaOH-Po + $NaHCO_3$-Po); RH300 = rice husk biochar at 300 °C; RH450 = rice husk biochar at 450 °C; RH650 = rice husk biochar at 650 °C; CC300 = corn cob biochar at 300 °C; CC450 = corn cob biochar at 450 °C; CC650 = corn cob biochar at 650 °C

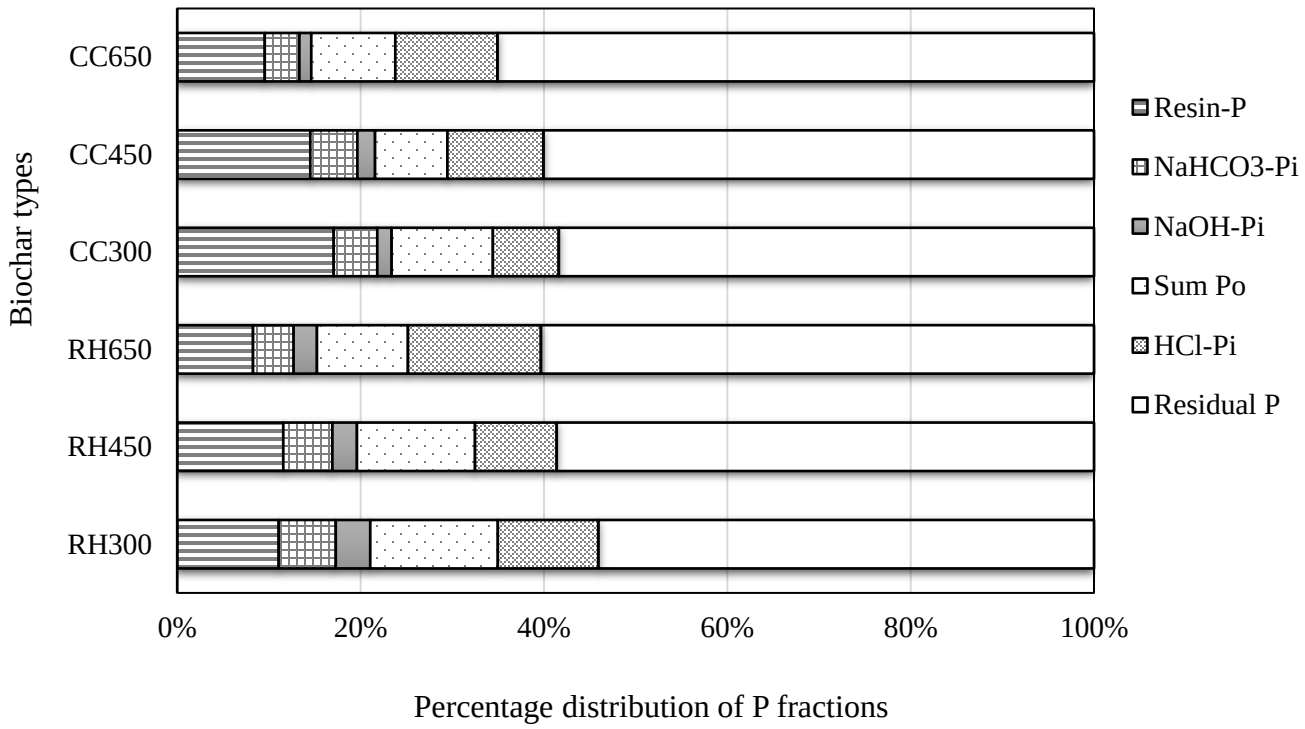

Fig. 5.2 Percentage phosphorus fractions distribution of corn cob and rice husk biochar charred at 300 ^{o}C, 450 ^{o}C and 650 ^{o}C.

The chemically amorphous and crystalline Fe and Al bound inorganic P pool (NaOH-Pi) values of the two biochar types were statistically ($p > 0.05$) the same. These values ranged from 21.9 to 30.7 mg kg^{-1} and 35.8 to 48.5 mg kg^{-1} for rice husk biochar and corn cob biochar respectively. The study showed an increasing trend in the Ca-bound inorganic P pool (HCl-Pi) with increasing pyrolysis temperature of the two biochar types. The HCl-Pi pool of corn cob biochar produced at 650 ºC (CC650) was 212.5 mg kg^{-1} (14.5%) and this was statistically higher ($p < 0.05$) than when produced at 300 ºC and 450 ºC accounting for 141.2 mg kg^{-1} (11.0%) and 119.0 mg kg^{-1} (8.9%) respectively.

Organic P pools comprised $NaHCO_3$-Po and NaOH-Po. The extractable $NaHCO_3$-Po is the organic P adsorbed on the biochar surfaces and is easily mineralizable and therefore is considered to be labile organic P pool. The extractable NaOH-Pi is also considered to be moderately labile P pool because the P is strongly bound by chemical sorption to Fe and Al oxides organic complexes. The organic P pool of the rice husk biochar treatments varied from 125.6 to 169.2 mg kg^{-1} and 145.4 and 179.4 mg kg^{-1} for corn cob biochar. There was no significant ($p > 0.05$) effect of pyrolysis temperature on the organic P pool, although there was a marginal decreasing trend with increasing pyrolysis temperature.

The most resistant and insoluble fraction of phosphorus is considered the residual P. The residual P pool was the dominant P fraction accounting for 54.1 to 60.3% for rice husk biochar and 58.4 to 65.1% for corn cob biochar samples. The residual P pool of rice husk biochar was statistically similar ($p > 0.05$) among the varying pyrolysis temperatures ranging from 697.0 to 884.0 mg kg^{-1}. However, there was a significant ($p < 0.05$) increase in the residual P pool of corn cob biochar as the pyrolysis temperature was increased from 300 ºC through to 650 ºC varying from 894.0 to 1068.0 mg kg^{-1}.

5.3.3 Phosphorus fractions of soil and soil-biochar mixture

The effect of biochar on the P pools in the three soils are presented in Table 5.3a-c. Figure 5.3 shows the percentage distribution of the P pools in the soils as affected by the addition of the two biochar types. The P pools in the three soil types were significantly ($p < 0.05$) affected by the two biochar types at the various pyrolysis temperatures. Corn cob biochar addition significantly ($P < 0.05$) increased resin-Pi content in Kokofu (Ko) which follows the order: KoC3 > KoC4 ≈ KoC6. The resin-Pi concentration in Ko increased by 28.2 mg kg^{-1}, 22.3 mg kg^{-1}, 21.7 mg kg^{-1} for KoC3, KoC4 and KoC6 respectively. Even though the incorporation of rice husk biochar to Kokofu significantly ($p < 0.05$) increased the resin-Pi content from 12.92 mg kg^{-1} to a range of 22.42 to 28.22 mg kg^{-1}, the rice husk treatments (KoR3, KoR4, KoR6) were statistically the same ($p > 0.05$). Amending Ankasa with corn cob and rice husk biochar increased resin-Pi proportionally with increasing pyrolysis temperature. The resin-Pi increase was from 8.19 mg kg^{-1} to a range of 33.31 to 41.14 mg kg^{-1} and 14.99 to 22.28 mg kg^{-1} for corn cob biochar treatments and rice husk treatments respectively.

Similar to Ankasa, there was a significant ($p < 0.05$) proportional increase in resin-Pi pool of Keta (K) by 20.92 mg kg^{-1}, 7.68 mg kg^{-1} and 17.03 mg kg^{-1} in KC3, KC4 and KC6 treatments respectively. This increase was much significant ($p < 0.05$) in the KC3 and KC6. Rice husk amendments in Keta also increased the resin-Pi pool from 11.85 mg kg^{-1} to a range of 19.71 to 23.19 mg kg^{-1}. However, there was no significant ($p > 0.05$) changes in the resin-Pi content among the rice husk biochar treatments (KR3, KR4 and KR6).

Table 5. 3a Phosphorus fractions of Kokofu and biochar amended Kokofu soil at three pyrolysis temperatures (300 ^{o}C, 450 ^{o}C and 650 ^{o}C)

Soil	Resin-P	$NaHCO_3$-Pi	NaOH-Pi	ΣPo	HCl-Pi	Residual P
			mg kg^{-1}			
Ko	12.9	16.6	43.4	59.9	23.1	140.6
KoR3	28.2	25.6	52.8	117.6	29.0	167.4
KoR4	22.4	28.0	57.2	79.3	33.0	218.5
KoR6	22.5	24.5	57.6	76.7	34.5	230.0
KoC3	41.2	29.6	46.1	107.2	36.8	161.7
KoC4	35.2	26.7	54.5	106.1	37.6	221.2
KoC6	34.6	26.6	51.1	95.1	52.8	237.7
Lsd	3.8	5.4	4.4	18.8	4.0	17.6

ΣPo = (NaOH-Po + $NaHCO_3$-Po); Ko= Kokofu soil; KoR3 = Kokofu soil amended with rice husk biochar at 300 ^{o}C, KoR4 = Kokofu soil amended with rice husk biochar at 450 ^{o}C; KoR6 = Kokofu soil amended with rice husk biochar at 650 ^{o}C; KoC3 = Kokofu soil amended with corn cob biochar at 300 ^{o}C; KoC4 = Kokofu soil amended with corn cob biochar at 450 ^{o}C; KoC6 = Kokofu soil amended with corn cob biochar at 650 ^{o}C.

Table 5.3b Phosphorus fractions of Ankasa and biochar amended Ankasa soil at three pyrolysis temperatures (300 ºC, 450 ºC and 650 ºC)

Soil	Resin-P	$NaHCO_3$-Pi	NaOH-Pi	ΣPo	HCl-Pi	Residual P
			mg kg^{-1}			
A	8.2	10.8	33.5	50.6	9.6	119.7
AR3	22.3	17.5	42.5	89.8	16.0	133.5
AR4	15.8	18.0	41.5	86.3	23.0	142.6
AR6	15.0	16.0	50.4	86.8	23.5	145.9
AC3	41.1	24.5	35.5	59.6	23.8	129.7
AC4	35.2	19.5	36.2	63.9	27.0	147.6
AC6	33.3	17.5	43.8	83.1	36.3	151.5
Lsd	5.3	4.3	4.6	13.7	3.2	8.2

ΣPo = (NaOH-Po + $NaHCO_3$-Po); A= Ankasa soil; AR3 = Ankasa soil amended with rice husk biochar at 300 ºC, AR4 = Ankasa soil amended with rice husk biochar at 450 ºC; AR6 = Ankasa soil amended with rice husk biochar at 650 ºC; AC3 = Ankasa soil amended with corn cob biochar at 300 ºC; AC4 = Ankasa soil amended with corn cob biochar at 450 ºC; AC6 = Ankasa soil amended with corn cob biochar at 650 ºC.

Table 5.3c Phosphorus fractions of Keta and biochar amended Keta soil at three pyrolysis temperatures (300 ^{o}C, 450 ^{o}C and 650 ^{o}C)

Soil	Resin-P	$NaHCO_3$-Pi	NaOH-Pi	ΣPo	HCl-Pi	Residual P
			mg kg^{-1}			
K	11.9	17.0	12.4	31.1	12.5	73.0
KR3	23.2	27.5	20.5	47.0	20.3	88.0
KR4	20.8	25.5	23.5	39.0	29.8	100.3
KR6	19.7	20.0	25.5	27.8	32.0	102.3
KC3	32.8	23.5	18.4	64.6	26.8	265.6
KC4	19.5	22.5	24.0	48.9	30.5	249.5
KC6	28.9	19.0	23.8	47.5	32.5	252.5
Lsd	3.2	4.1	5.1	12.6	7.5	12.5

ΣPo = (NaOH-Po + $NaHCO_3$-Po); K= Keta soil; KR3 = Keta soil amended with rice husk biochar at 300 ^{o}C, KR4 = Keta soil amended with rice husk biochar at 450 ^{o}C; KR6 = Keta soil amended with rice husk biochar at 650 ^{o}C; KC3 = Keta soil amended with corn cob biochar at 300 ^{o}C; KC4 = Keta soil amended with corn cob biochar at 450 ^{o}C; KC6 = Keta soil amended with corn cob biochar at 650 ^{o}C.

\

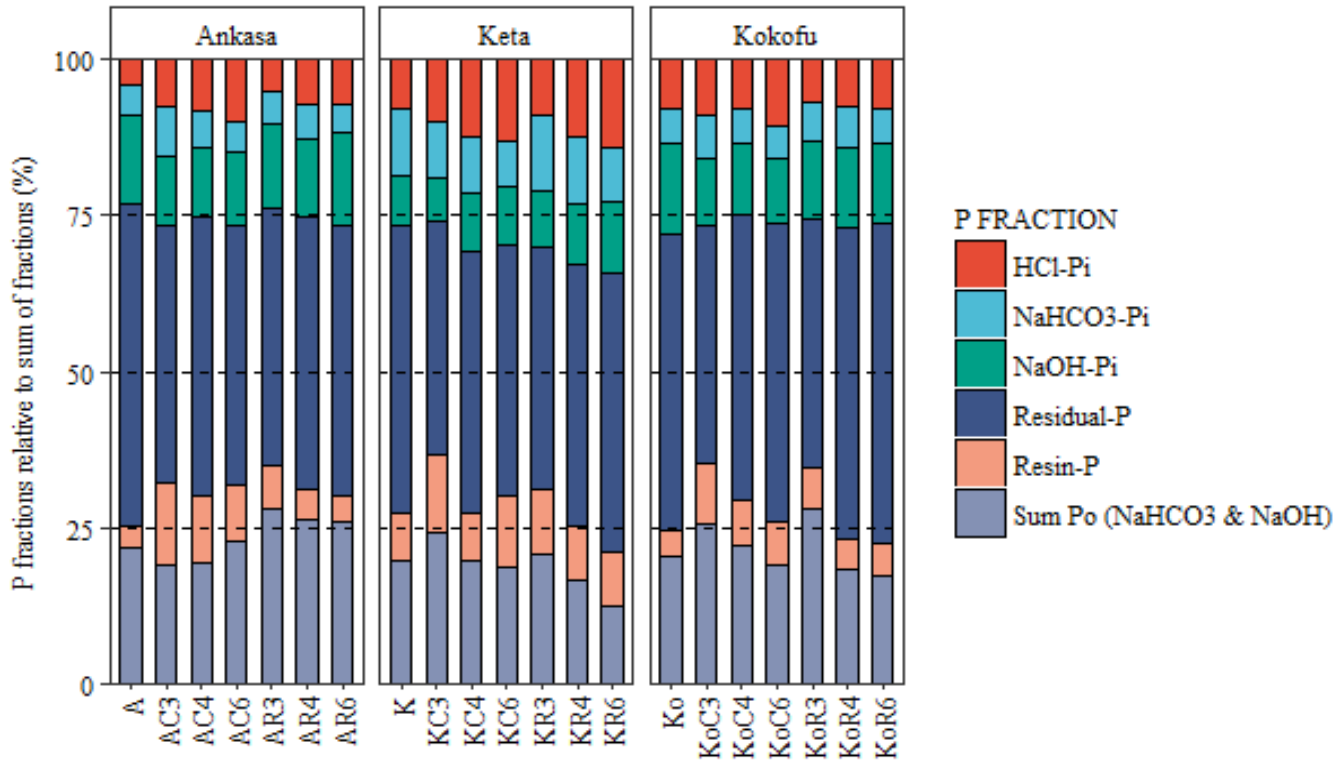

Figure 5.3 Percentage phosphorus fractions distribution of corn cob and rice husk biochar amended soils (Kokofu, Ankasa and Keta) produced at 300 ^{o}C, 450 ^{o}C and 650 ^{o}C

The $NaHCO_3$-Pi pool of Kokofu was adversely affected by both biochar types. However, the $NaHCO_3$-Pi pool of the various pyrolysis temperature treatments for both corn cob and rice husk biochar were statistically similar ($p > 0.05$). The $NaHCO_3$-Pi pool of Ko increased from 16.62 mg kg^- to a range of 24.49 to 25.55 mg $kg^-$and 26.60 to 29.55 mg kg^- for rice husk and corn cob biochar treatments respectively. Ankasa with $NaHCO_3$-Pi pool of 10.80 mg kg^{-1} significantly ($p < 0.05$) increased to 17.50 mg kg^{-1} when rice husk biochar charred at 300^oC was added (i.e. AR3 treatment). The increase in AR3 was statistically the same ($p > 0.05$) when the pyrolysis temperature of the added rice husk biochar was increased to 450 ^oC and 650 ^oC. For the corn cob biochar treatments, the AC3 had much significant ($p < 0.05$) effect on the $NaHCO_3$-Pi of Ankasa than the AC4 and AC6 treatments. The increase in $NaHCO_3$-Pi of Ankasa upon corn cob biochar amendment varied from 17.50 to 24.50 mg kg^{-1}. It was obvious that the $NaHCO_3$-Pi fraction of Keta significantly ($p < 0.05$) increase only when both biochar types produced at 300 ^oC and 450 ^oC were incorporated. Averagely, the significant ($p < 0.05$) increase of the $NaHCO_3$-Pi of Keta was from 17.00 mg kg^{-1} to 25.2 and 23.75 mg kg^{-1} for 300 ^oC and 450 ^oC-produced biochar amendment respectively.

The NaOH-Pi which represents P chemisorbed to Al and Fe oxides was the largest inorganic P pool in the biochar amended acid soils (i.e. Kokofu and Ankasa) varying from 10.3 to 14.9%. Adding the two biochar types to Kokofu significantly ($p < 0.05$) increased the NaOH-Pi pool with the exception of corn cob biochar produced at 300 ^oC i.e. KoC3 treatment. The study did not show significant variation ($p > 0.05$) among the biochar treatments with regards to the NaOH- Pi pool. With the exception of AC3 and AC4, biochar addition seems to have significant ($p < 0.05$) effect on the NaOH-Pi concentration of Ankasa. Treatment AR6 showed much significant effect ($p < 0.05$) on the NaOH-Pi concentration of Ankasa by 16.85 mg kg^{-1} increment. The content of NaOH-

Pi in Keta also showed a significant ($p < 0.05$) increase from 12.40 mg kg^{-1} to a range of 20.50 to 25.50 mg kg^{-1} and 18.43 to 24.00 mg kg^{-1} by the addition of rice husk and corn cob biochar respectively. However, comparing the biochar treatments there was no significant ($p > 0.05$) variations among them.

The Ca-bound inorganic P fraction (HCl-Pi) of Kokofu was 23.06 mg kg^{-1} representing 7.8% of the total P fraction. This HCl-P pool of Ko significantly ($p < 0.05$) increased proportionally with increasing pyrolysis. The significant ($p < 0.05$) increase ranged from 29.00 to 34.50 mg kg^{-1} and 36.80 to 52.80 mg kg^{-1} for rice husk and corn cob amendments respectively. Similar trend was also observed in Ankasa, which had its HCl-Pi content of 9.57 mg kg^{-1} (4.1%) significantly ($p < 0.05$) raised to a range of 16.00 to 23.50 mg kg^{-1} for rice husk treatments and 23.80 to 36.25 mg kg^{-1} for corn cob treatments increasing proportionally with increasing pyrolysis temperature. The HCl-Pi pool recorded the highest inorganic P fraction in the biochar treated neutral soil (Keta) ranging from 7.9 to 14.1%. Biochar addition significantly ($p < 0.05$) raised the HCl-Pi concentration of Keta more than two folds. This increase in HCl-Pi of Keta was from 12.50 mg kg^{-1} to a range of 20.25 to 32.00 mg kg^{-1} for rice husk amended treatments and 26.75 to 32.50 mg kg^{-1} for the corn cob amended treatments.

The organic P pool comprised the sum of $NaHCO_3$-Po and NaOH-Po. The sum of the organic P pool (Po) of the three soil types were adversely affected by the two biochar types. The Po fraction of Kokofu representing 20.2% of the total sum of fraction significantly ($p < 0.05$) increased in the order of KoR6 < KoR4 < KoC4 < KoC6 <KoC3 < KoR3. Ankasa had its sum of Po (50.59 mg kg^{-1}) statistically similar ($p > 0.05$) to AC3 (59.60 mg kg^{-1}) and AC4 (63.85 mg kg^{-1}) but significantly lower ($p < 0.05$) than AC6 (83.12 mg kg^{-1}), AR3 (89.79 mg kg^{-1}), AR4 (86.25 mg kg^{-1}) and AR6 (86.82 mg kg^{-1}). The Po of Keta has also increased significantly ($p < 0.05$) with biochar

amendments except when rice husk pyrolysed at 650 ^{o}C was applied. The changes in the organic Po of biochar amended Keta soil was in the order of KR6 < K < KR4 < KR3 < KC6 < KC4 < KC3.

The residual P pool was the predominant P fractions in all the treatments, accounting for 39.8 to 51.6%, 41.3 to 51.5% and 37.5 to 46.2% in Kokofu, Ankasa and Keta biochar amendments respectively. Apart from the application of biochar produced at 300 ^{o}C, there was a significant ($p < 0.05$) increase in the residual P pool of Kokofu by biochar produced at 450 ^{o}C and 650 ^{o}C. However, the effect of the biochar types at 450^{o}C and 650^{o}C was statistically similar ($p > 0.05$). The two biochar types at the three pyrolysis temperatures significantly ($p < 0.05$) increased the residual P fraction of Ankasa from 119.9 mg kg^{-1} to a range of 129.7 to 151.1 mg kg^{-1} and 133.5 to 145.9 mg kg^{-1} for corn cob and rice husk treatments correspondingly. Again the addition of the two biochar types significantly ($p < 0.05$) raised the residual P pool of Keta. However, the increase was statistically similar ($p > 0.05$) among all the biochar treatments.

5.3.4 Relationship between phosphorus fractions and some chemical properties of biochar amended soils

Table 5.4 shows the correlation coefficient describing the relationship among phosphorus fractions in the biochar amended three soil types. Principal component analysis showing the correlation among the P fractions and soil chemical properties is depicted in Fig. 5.4. In the PCA, the direction and length of the arrows show the extent of correlation between soil properties and the principal components i.e. X and Y axes. In the PCA analysis, the soil parameters (P fractions and soil chemical properties) are indicated by the arrows (vectors) and therefore arrows with low

Table 5.4 Correlation coefficient showing the relationship among phosphorus fractions in the biochar amended three soil types (Kokofu, Ankasa and Keta)

Phosphorus fractions	Resin-Pi	$NaHCO_3$-Pi	NaOH-Pi	Sum Po	HCl-Pi	Residual P
Resin-Pi	1.00	0.56**	-0.48*	0.40	0.56**	0.33
$NaHCO_3$-Pi		1.00	-0.19	0.41	0.54*	0.36
NaOH-Pi			1.00	0.75**	0.72**	0.89**
Sum Po				1.00	0.37	0.68**
HCl-Pi					1.00	0.61**
Residual P						1.00

**p < 0.01; *p < 0.05

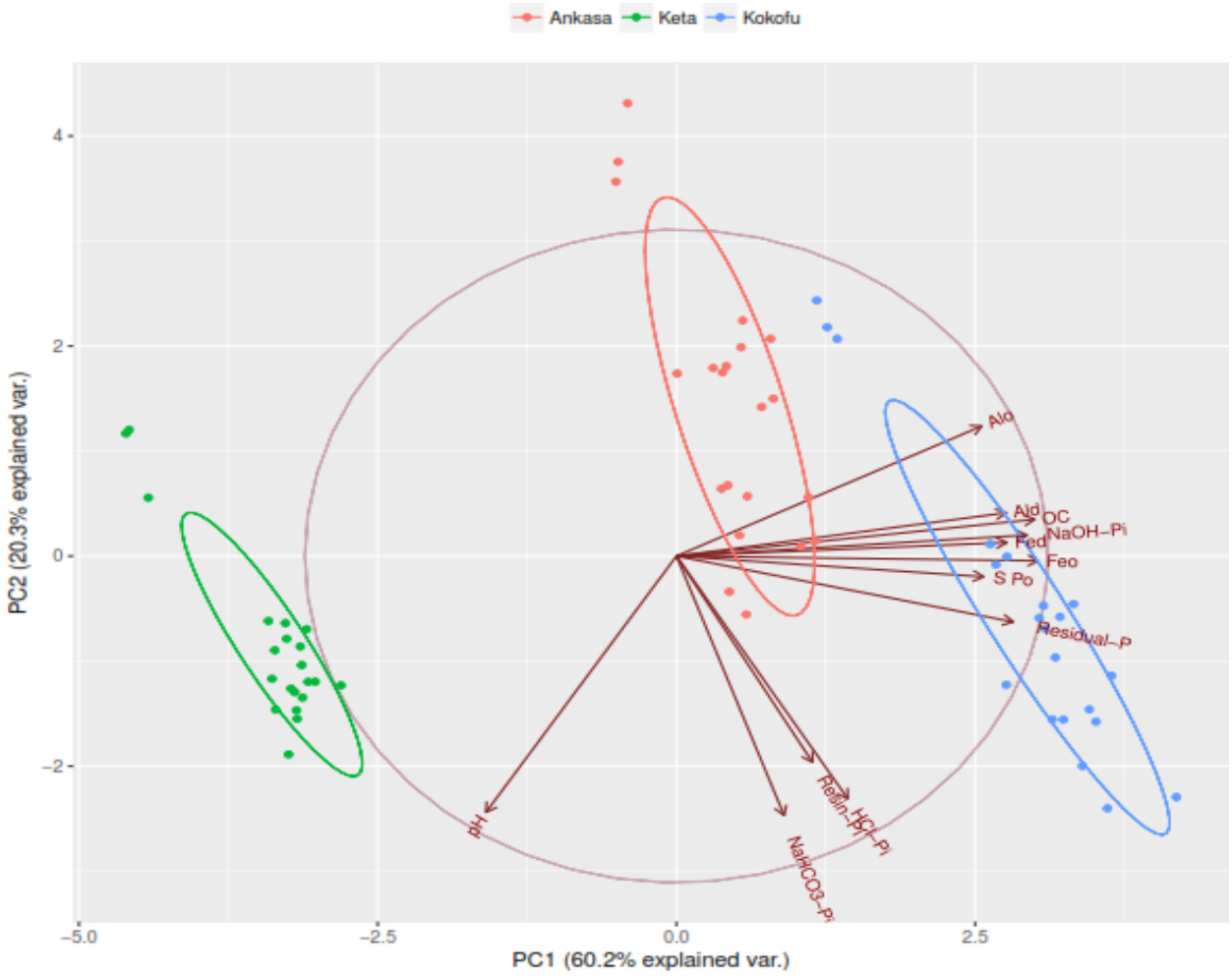

Fig. 5.4 Principal Component Analysis of phosphorus fractions and some chemical properties of the three biochar amended soils

angles are highly correlated, whiles the arrows that are perpendicular implies lack of correlation (r = 0). The study showed a high significant ($p < 0.01$; $p < 0.05$) correlation coefficient (r) among the soil P fractions with the exception of few P fractions, ranging from 0.19 to 0.89. This implies that each P fraction is a continuum of the other. The resin-Pi and $NaHCO_3$-Pi which are considered the most labile inorganic P were positively correlated (r = 0.56) but was negatively related to the NaOH-Pi pool of the biochar amended soils. The residual P pool was positively correlated with the sum of Po (r = 0.68), HCl-Pi (r = 0.61) and NaOH-Pi (r = 0.89) pools of the biochar-soil mixture.

The correlation coefficient showing the relationship between P fractions and soil chemical properties are shown in Table 5.5a-c. The organic C content was directly proportional to the most labile P (resin-Pi and $NaHCO_3$-Pi) and also with the sum of Po for all the biochar amended soil types. A significant and positive relationship was found between Ca and HCl-Pi pool (r = 0.73-0.88) as well as with the residual P pool (r = 0.61-0.78). Increasing pH led to an increase in most labile Pi in the two acid soils (i.e. Kokofu and Ankasa). The Ca-bound P (HCl-Pi) and residual P pools of the biochar amended three soils were also found to be positively correlated with pH. Generally, the crystalline (Fe_d and Al_d) and amorphous (Fe_o and Al_o) mineral oxides were positively related with the residual P pool of the soils.

Table 5.5a Correlation coefficient showing the relationship between some chemical properties and phosphorus fractions in biochar amended Kokofu soil

	Resin-Pi	$NaHCO_3^-$	NaOH-Pi	Sum Po	HCl-Pi	Residual P
OC	0.88**	0.75**	0.28	0.68**	0.51*	0.34
Ca	0.68**	0.55*	0.38	0.10	0.88**	0.78**
pH	0.66**	0.67**	0.58**	0.42	0.80**	-0.82**
Fe_o	0.69**	0.79**	0.44*	0.63*	0.38	0.40
Fe_d	-0.84*	-0.66*	-0.21	-0.69*	-0.31	-0.16
Al_o	0.53*	0.22	-0.54*	0.27	0.08	-0.48*
Al_d	-0.37	0.04	0.31	-0.27	0.21	0.56*

Fe_o and Al_o are oxalate extractable Fe and Al; Fe_d and Al_d are dithionate-citrate-bicarbonate extractable Fe and Al; OC = organic carbon; **$p < 0.01$; *$p < 0.05$

Table 5.5b Correlation coefficient showing the relationship between some chemical properties and phosphorus fractions in biochar amended Keta soil

	Resin-Pi	$NaHCO_3^-$	NaOH-Pi	Sum Po	HCl-Pi	Residual P
OC	0.43*	0.41	0.51*	0.45*	0.12	0.16
Ca	0.15	-0.08	0.70**	-0.13	0.73**	0.61**
pH	0.48*	0.41	0.51*	0.23	0.68**	0.65**
Fe_o	0.51*	0.41	0.25	0.47*	0.12	0.30
Fe_d	0.31	-0.02	0.15	-0.10	0.45*	0.49*
Al_o	0.53*	0.73**	0.56**	0.31	0.44*	0.43*
Al_d	0.03	-0.06	0.55*	-0.27	0.43*	0.30

Fe_o and Al_o are oxalate extractable Fe and Al; Fe_d and Al_d are dithionate-citrate-bicarbonate extractable Fe and Al; OC = organic carbon; **$p < 0.01$; *$p < 0.05$

Table 5.5c Correlation coefficient showing the relationship between some chemical properties and phosphorus fractions in biochar amended Ankasa soil

	Resin-Pi	$NaHCO_3^-$	NaOH-Pi	Sum Po	HCl-Pi	Residual P
OC	0.65**	0.63**	-0.08	0.48*	0.20	-0.26
Ca	0.74**	0.54*	0.25	0.07	0.83**	0.64**
pH	0.66**	0.65**	0.28	0.42*	0.86**	0.77**
Fe_o	0.08	0.31	0.09	0.14	-0.15	0.22
Fe_d	-0.78**	-0.78**	0.47*	-0.31	-0.62**	0.73**
Al_o	-0.51*	-0.51*	0.45*	-0.01	-0.33	0.39
Al_d	0.21	0.11	-0.13	-0.29	0.44*	0.40

Fe_o and Al_o are oxalate extractable Fe and Al; Fe_d and Al_d are dithionate-citrate-bicarbonate extractable Fe and Al; OC = organic carbon; **$p < 0.01$; *$p < 0.05$

5.4 Discussion

5.4.1 Phosphorus fractions in biochar

Corn cob and rice husk biochar showed an increasing trend in total P content with increasing pyrolysis temperature. This observation is similar to what have been reported for other biochar types under varying carbonization levels (Cantrell et al., 2012; Ippolito et al., 2015). The increasing amount of total P with increasing temperature could be due to the loss of highly volatile compounds including carbon, oxygen, hydrogen as well as nitrogen, thereby concentrating the remaining P in the biochar (Cantrell et al., 2012; Wang et al., 2012). The amount of total P concentration in corn cob biochar was relatively more than rice husk biochar because of the variation of P in the feedstock (Lehman, 2007; Ippolito et al., 2015).

The resin-Pi and $NaHCO_3$-Pi show the amount of phosphorus in biochar that are easily released into soil solution. The NaOH-Pi expresses the amount of P chemisorbed onto Al and Fe oxides on biochar surfaces and therefore are considered moderately available in solution. It is obvious from the study that the inorganic P (most labile P: resin-Pi and $NaHCO_3$-Pi; moderately labile P: NaOH-Pi) recovery in the two biochar type decreased with increasing temperature, thereby indicating less available P at high temperatures. However, a decrease in Fe and Al bound P (NaOH-Pi) has been reported for hydrochar at different temperatures of 200 to 700 ^oC (Schneider and Haderlein, 2016). The findings in the present study are in agreement with solid-state ^{31}P NMR analysis which showed that soluble P in low temperature biochar were converted to more stable P forms such as crandallite ($CaAl_3(OH)_5(PO_4)_2$) and wavellite ($Al_3(OH)_3(PO4)_2 \cdot 5H_2O$) at high temperatures (Xu et al., 2016). Cao and Harris (2010) also reported that the stable P minerals species, such as whitlockite and brushite, were found to explain the decrease in Pi recovery at high pyrolysis biochar. This implies

that biochar produced at lower temperatures can be used to improve P bioavailability in tropical soils.

The calcium bound P phase of the two biochar types which is associated with apatite increased with increasing pyrolysis temperature. This pool expresses stable inorganic P, however in tropical soils it can act as a buffer for P bioavailability in soil solution (Guo et al., 2000). Uchimiya and Hiradate (2014) using ^{31}P NMR analysis on manure biochar also observed decreasing NaOH-Pi but increasing HCl-Pi with increasing pyrolysis temperature from 300 ^{o}C to 800 ^{o}C. The powder XRD and PAS-FTIR analyses on the biochar types indicated the presence of calcite and carbonate in the biochar, which increased when pyrolysis temperature was raised from 300 ^{o}C to 650 ^{o}C. Loss of labile C compounds with increasing pyrolysis is likely to thermally promote the formation of crystalline hydroxyapatite and other recalcitrant calcium phosphate minerals (Uchimiya and Hiradate, 2014). This explains the high recovery of Ca bound P at the high temperature in the present study.

In general, the organic P ($NaHCO_3$-Po and NaOH-Po) decreased with increasing temperature in the two biochar types. This was consistent with other studies on different biochar types at varying pyrolysis temperatures (Cantrell et al., 2012; Wang et al., 2012; Xu et al., 2016). Jin et al. (2016), using ^{31}P NMR analysis reported that organic P (phytase) was transformed to inorganic P (orthophosphate and pyrophosphate) when animal manure was charred at 400 ^{o}C. Xu et al. (2016) also indicated that organic P ($NaHCO_3$-Po and NaOH-Po) is converted into stable organic P at high pyrolysis temperatures. This may in part explain the low recovery of organic P fractions at high pyrolysis temperature (e.g. 650 ^{o}C) in the present study.

The residual pool explains the recalcitrant P pool due to the complexity of its component involving a mixture of organic and inorganic P in very stable forms (Hedley et al., 1982a). Similar to Ca-

bound P trend in the biochar types, the residual P content was directly proportion to the increase in pyrolysis temperature. In consonance with what have been reported in literature, the residual pool accounted for the largest P fraction in the biochar types (Wang et al., 2012; Schneider and Haderlein, 2016). This indicates a high stability of P at high temperatures and therefore biochar of such high temperature (650 ^{o}C) can not easily discharge P into soil solution for plant uptake. The organic and inorganic P fractions of the biochar types were inversely related to the residual P pool. It is, therefore, worth noting that inorganic P as well as organic P moves to recalcitrant P pool at high temperature (650 ^{o}C). This implies that inorganic P has the tendency to migrate to the long term plant available P pool when biochar is pyrolysed at high temperatures.

5.4.2 Phosphorus fraction in soil and biochar amended soils

Resin extractable inorganic P (resin-Pi) and $NaHCO_3$ extractable P ($NaHCO_3$-Pi) which express the readily or most labile inorganic P was in a range of 4% to 7% of the sum of total P. This proportion was similar to those found in several studies in both tropical (Araujo and Salcedo, 1997; Araujo et al., 1993b; Agbenin and Tiessen, 1994; Cross and Schlesinger, 2001; Asomaning et al., 2015) and temperate regions (Roberts et al., 1985; Henriksen, 2017). Estimated P from resin-Pi and $NaHCO_3$-Pi has been found to be highly correlated with plant P uptake in previous studies (Bowman et al., 1978; van der Zee et al., 1987; Menon et al., 1989; Sharpley, 1991) and are therefore considered to be plant available (Mattingly, 1975; Hedley et al., 1982b; Tiessen et al., 1984; Cross and Schlesinger, 1995). The most labile P level of the soils increased upon the addition of biochar with decreasing pyrolysis temperature. This observation is consistent with Guo et al. (2000) and Wang et al. (2014) who found a drastic build-up of resin-Pi and $NaHCO_3$-Pi in highly weathered tropical soils after biochar incorporation. This implies that corn cob and rice husk

biochar can be used to improve P availability in soil solution for plant uptake. In contrast, Dormaar and Chang (1995) reported no increase in most labile P pool in manured soils, indicating that P added from the manure has been transformed into moderately labile or stable P forms. The high buildup of most labile P pool may increase the risks of particulate and dissolved P losses in surface runoff or downward movement into ground water inducing P eutrophication especially in Keta soil which is found to be sandy.

Biochar effect on most labile P pool of the soils corresponded with P fractions dynamics in the biochar types. The increase in the most labile P in the three soil types was more sensitive to the addition of biochar type produced at 300 ^{o}C. This could be due to the more available P in low pyrolysis biochar than at high pyrolysis temperature which might have been directly released into the soil solution (Wang et al., 2014) and also the presence of ample amount of carboxylic and phenolic groups on the biochar.

Soil organic matter has also been reported to play an important role in maintaining P availability in soils. The increase in organic carbon led to an increase in resin-Pi and $NaHCO_3$-Pi indicating that the addition of labile organic carbon from the biochar seems to maintain high levels of most labile P pool of the three soil type. The effect of organic carbon on most labile P was further explained by the positive correlation between sum of Po and resin-Pi as well as $NaHCO_3$-Pi of the soils. Schneider and Haderlein (2016) indicated that organic carbon from biochar improves the labile P content of most tropical soils. Asomaning et al. (2015) also observed elevated levels of inorganic P in Keta soils after continues application of manure. Mineralization and competitive sorption reaction of the labile carbon with P at the soil exchange sites could have resulted in the increased in the most labile P. This assertion confirms the increasing organic carbon with increasing resin-Pi but at a decreasing Al and Fe bound P (NaOH-Pi) of the soils.

The $NaHCO_3$-Pi pool is considered to be associated with Fe and Al (Hedley et al., 1982a; Tiessen et al., 1984; Wager et al., 1986) through chemisorption to the surfaces of amorphous and crystalline Fe and Al oxides (McLaughlin et al., 1977). The use of NaOH as an extractant can also recover some of the P bound to Ca (Williams et al., 1971) and this was further demonstrated by the direct relationship between Fe/Al-bound P and Ca bound P pool in the soils. In terms of P availability in soil solution for plant uptake, the NaOH-Pi pool is referred to as moderately labile P. The NaOH-Pi pool as the largest inorganic P fractions was relatively higher in the two acid soils (i.e. Kokofu and Ankasa) than the neutral soil (Keta) due to the high level of Al and Fe oxides in the former soils. The large proportion of the NaOH-Pi suggests that it was a major sink for added P from the biochar. Phosphorus is geochemically adsorbed by amorphous and crystalline Fe and Al oxides in highly weathered soils and therefore leads to the increase in the moderately labile P as well as the residual (stable) P fractions. Buehler et al. (2002) reported that labeled P was converted from the resin-Pi to NaOH-Pi in a cattle manure biochar amended soils of the tropics. The addition of the corn cob and rice husk biochar raised the moderately labile P pool of the three soil types. Similarly, Kashem et al. (2004) reported an increase in NaOH-Pi concentration in soils amended with biosolids and biochar. The increase in Al and Fe bound P in these soils implies P bioavailability in soil solution in the long term. Even though Al and Fe P fractions have low bioavailability, it can be taken up by plants when available soil P is severely depleted (Shen et al., 2004).

The high recovery of NaOH-Pi in the three soil types could be due to high amount of P existing as Fe and Al complexes in corn cob and rice husk biochar (Wang et al., 2012). This assertion confirms the increasing amount of moderately labile P pool with increasing pyrolysis temperature since Fe and Al oxides are dominant at high temperatures. From environmental perspectives, high Al and Fe bound P should reduce the risk of P release into water bodies, however, eroded soil particles

may still reach drinking water bodies. Phosphorus associated with Fe and Al oxide minerals may be solubilized under more reducing condition such as in water bodies (Pierzynski et al., 1994). Given the large proportion of NaOH-Pi, the acid soils may be more vulnerable to reductive dissolution of Fe and Al bound P than the neutral soil.

The HCl-Pi fraction is mostly considered to be associated with the primary minerals such as apatite (Tiessen et al., 1994). The proportion of Ca bound P was relatively lower as compared with the Al and Fe bound P in the acid soils. However, HCl-Pi fraction was higher than NaOH-Pi fraction in the neutral soil. The generally low amount of Ca-bound P in the soils is due to the intense weathering of these soils of which Ca-P is transformed to Fe-P and Al-P (Cross and Schlesinger, 1995). Using X-ray adsorption near edge structure (XANES) spectroscopy and chemical P fractionation, amorphous and crystalline Fe and Al and Ca were found to be important sink of P in both acid and neutral soils (Beauchemin et al., 2003; Simard et al., 1995). Addition of the two biochar types raised the HCl-P pool of the soils with increasing pyrolysis temperature. Biochar types produced at 650 ^{o}C with relatively high Ca content had much effect of the HCl-P pool of the soils. This observation is similar to that of Ch'ng et al. (2014) who also reported a significant increase in Ca-P fractions in mollisols upon the application of biochar. This obviously explains the increasing soil Ca content with increasing Ca bound P pool of the soils. The increased pH in biochar amended soils has led to an increase in Ca bound P (HCl-Pi). This observation was also reported by Mukherjee et al. (2011) indicating that Ca-P formation increased with increasing soil pH after biochar addition.

The extractable sum of Po is usually reported to be associated with humic and fulvic acids (Frossard, 1995). The organic pool is considered biologically active and therefore can mineralize to supply P to crops in the long run (Schmidt et al., 1996). This pool can therefore serve as a sink

or a source of mostly labile and moderately labile P through biotic processes (Zheng et al., 2013; Kashem et al., 2004; Negassa and Leinweber, 2009). The sum of Po was much higher in the acid soils than the neutral soil probably due to the high level of organic carbon in the former soils. The organic P pool of the soils increased upon corn cob and rice husk biochar amendment biochar amendment. The amount of organic P pool was positively correlated with the organic carbon content of the soil-biochar mixture. This explains the accumulation of soil organic matter as a requirement for the increase in organic P pool (Qian et al., 2004). The relatively low level of organic P pool in rice husk biochar amended soils than the corn cob biochar amended soils could be due to the relatively low proportion of organic P ($NaHCO_3$-Po and NaOH-Po) in rice husk biochar (Hedley and McLaughlin, 2005; Wang et al., 2012). There was a positive correlation between organic P pool and Fe_o as also reported by Asomaning (2015) on tropical sandy soils which has received continuous application of manure. This goes to indicate the relevance of Fe in stabilizing P in soils.

Most often in weathered and well drained soils, the residual P pool is considered the most resistant and insoluble fraction. The residual pool has been reported to express the recalcitrant P pool due to the complexity of its component involving a mixture of organic and inorganic P in very stable forms (Hedley et al., 1982a). This pool consists of occluded P that has been incorporated into the soil matrices by diffusion or entrapment in the coatings or concretions of amorphous and crystalline Fe and Al oxides. Organic P compounds have also been found to form part of residual P pools since some stable organic matter cannot be extracted using 0.1M NaOH and 0.5M $NaHCO_3$ extractants (Hedley et al., 1982a), accounting for more than 60% of the residual P pool (Tiessen et al., 1983). It is also known that Ca bound P that are not easily extracted by the weak acid (i.e. 1M HCl) is further recovered in the residual P pool (Syers et al., 1968). In the present study, the

residual P pool increased with increasing NaOH-Pi, sum of organic P and HCl-Pi pools in the neutral and acid soils amended with the two biochar types. Averagely the residual P pool was in a range of 37.5% to 57.6% representing the largest P pool in the three biochar amended soils. This was in agreement with previous results in soils from the same agro-ecological zone in Ghana (Abekoe and Sahrawat, 2001**;** Asomaning et al., 2015) and from Nigeria (Udo, 1977; Udo and Ogunwale, 1977). The residual P pool values also indicate the extent of weathering in the three soil types. Weathering leads to a progressive change of Ca bound P to residual P (Walker and Syers, 1976). The two acid soils i.e. Kokofu and Ankasa with low levels Ca bound P but rather high levels of residual P indicates high degree of weathering in these soils than Keta. The increase in residual P pool in the soils was much significant in biochar treatments produced at 450 ^{o}C and 650 ^{o}C. This is obviously due to the high amount of stable P forms in biochar charred at high pyrolysis temperatures.

5.5 Conclusion

The study showed that pyrolysis temperature affects the P fractions in biochar that subsequently influence P bioavailability in soils. Increasing pyrolysis temperature leads to the transformation of most labile P (resin-P, $NaHCO_3$-Pi & Po) and moderately labile P (NaOH-Pi & Po) to a recalcitrant P pool (HCl-Pi & residual-P) in corn cob and rice husk biochar. The application of biochar to soils improves upon the most labile P pool especially with biochar types produced at low temperature (i.e. 300-450 ^{o}C) thereby making P immediately available for plant uptake. The marginal increase in the moderately labile P and recalcitrant P is also of much interest since it will be made available for plant uptake in the long term.

CHAPTER SIX

SUMMARY, CONCLUSION AND RECOMMENDATION

6.1 Summary

The main goal of the study focused on phosphorus reactions in biochar and biochar amended soils. In chapter three, the study showed that pyrolysis temperature and feedstock type affect the physiochemical properties of biochar. The pH, total P, total C, total cation bases as well as heavy metal concentrations of the four biochar types namely cocoa pod husk, palm kernel shell, rice husk and corn cob increased with increasing pyrolysis temperature. However, total nitrogen and cation exchange capacity decreased otherwise. The powder X-ray diffraction analysis indicated that calcite and quartz were the dominant crystalline minerals in the biochar types. Increasing pyrolysis temperature from 300 ^{o}C to 650 ^{o}C decreased the polar functional groups such as phenolic and carboxylic groups.

Investigating the effect of shaking time on P adsorption onto the biochar types showed that maximum adsorption was reached within 6 to 12 h (equilibrium time). Biochar produced at 300 ^{o}C reached equilibrium of maximum P adsorption faster than at 650 ^{o}C. Applying kinetics models to predict the mechanism of P adsorption showed that pseudo second order and Elovich models best explained the P adsorption implying chemisorption reaction. The rate limiting step controlling P adsorption into the pores of the biochar types was not only limited to intraparticle diffusion but also film diffusion. Comparatively, Freundlich model best fit the data considering the relatively high R^2 for most of the biochar types as compared with the Langmuir model. This implies that the active adsorption sites of all the biochar types were not limited to the formation of a monolayer but rather energetically heterogeneous. This was in agreement with the kinetics studies that multiple mechanism controls P adsorption onto the biochar types regardless of the pyrolysis

temperature and also the feedstock. The P sorption capacity of all biochar types was in a range of 4.12 to 13.02 mg g^{-1} increasing in the order of CP300 < CC300 < RH300 < CP650 < PK300 < CC650 < RH650 < PK650. Increasing equilibrium solution pH decreased P adsorption onto the four biochar types at the two pyrolysis temperatures. Maximum P adsorption for the biochar types occurred at equilibrium pH of 2.8 to 4.8.

In chapters four and five, phosphorus sorption and fractionation experiments were conducted on three soils after the application of corn cob and rice husk biochar produced at three pyrolysis temperatures i.e. 300 ^{o}C, 450 ^{o}C and 650 ^{o}C. The textural class of the two acid soils (Kokofu and Ankasa) were sandy clay loam and that of the neutral soil (Keta) was sandy. Kokofu and Ankasa were dominated with high level of Fe and Al oxides whiles Keta was of low amount of Fe and Al oxides content. The study showed a variation in the effect of the two biochar types on chemical properties of the soils types. The CEC, OC, pH, Ca content and amorphous Fe oxides (Fe_o) increased upon the addition of biochar. However, the amorphous Al oxides (Al_o) and crystalline Fe and Al oxides (Fe_d and Al_d) content decreased. In Keta, all the above-mentioned chemical properties increased.

The P sorption capacity of Kokofu (384.5 mg kg^{-1}) and Ankasa (333.3 mg kg^{-1}) were three times more than Keta (104.2 mg kg^{-1}). The addition of corn cob and rice husk biochar to the acid soils decreased the P sorption capacity at increasing pyrolysis temperature. However, the P sorption capacity of Keta increased at increasing pyrolysis temperature. The amount of P adsorbed in the biochar amended acid soils was predicted by Al and Fe oxides. The P sorption maximum of biochar amended Keta soil was predicted by Ca, Fe_d, Al_d and Al_o. The results of the P sorption capacity showed that the amount of P adsorbed at equilibrium P concentration of 0.2 mg L^{-1} (standard P requirement) for Kokofu, and Ankasa was medium and Keta was low in accordance with Juo and

Fox (1977). Application of biochar lowered the standard P requirement (SPR) of the acid soils especially biochar types produced at 300-450 ^{o}C. Generally for all the soil and soil-biochar mixtures, large amount of P was desorbed from each of the samples at the initial extraction with 0.01 M $CaCl_2$ which further decreased with successive extractions. The relatively high binding energy in Keta amended soils (0.13-0.51 L mg^{-1}) and Ankasa (0.08-0.50 L mg^{-1}) than Kokofu (0.07-0.17 L mg^{-1}) reflected in the low percentage P desorbability in those soils. At the end of the three extractions, 24.7 to 52.7%, 16.4 to 49.0 and 13.7 to 45.7% of the P adsorbed by biochar amended Kokofu, Keta and Ankasa soils were released respectively.

The use of the modified Hedley P fractionation procedure in assessing the various P fractions in the biochar types and the biochar amended soils was suitable of the study. The study revealed that increasing pyrolysis temperature generally reduces the amount of most labile P (resin-Pi & $NaHCO_3$-Pi), moderately labile P (NaOH-Pi) and sum of organic P ($NaHCO_3$-Po & NaOH-Po) in the two biochar types. The amount of Ca-bound P and residual P increased with increasing pyrolysis temperature. Application of the biochar types to the soils significantly raised the amount of most labile P and Ca-bound P. The increase in the most labile P pool (resin-Pi & $NaHCO_3$-Pi) was much significant at low temperature i.e. 300 ^{o}C and 450 ^{o}C.

6.2 Conclusion

Feedstock and pyrolysis temperature affect P adsorption capacity of biochar by altering the surface properties of biochar. Biochar produced at low temperatures has low P sorption capacity compared to high pyrolysis temperatures. Phosphorus adsorption onto biochar is controlled by chemisorption through electrostatic attraction and surface precipitation and ligand exchange reactions. The high P sorption capacity of biochar types produced at high temperatures (650 ^{o}C) especially palm kernel

shell biochar can be considered as adsorbent for P removal from wastewater prior to discharge into drinking water bodies in order to reduce P eutrophication. Rice husk biochar and corn cob biochar produced at 300 ^{o}C can be used to improve plant available P in soils.

Biochar influences P cycling and distribution in tropical soils. The effect of biochar on P availability in tropical soils is more sensitive to pyrolysis temperature than feedstock. Biochar produced at low temperatures (300 ^{o}C and 450 ^{o}C) reduce P sorption in acid soils and also increase the most labile P pool thereby increasing P availability in soil solution for plant uptake. Addition of biochar types reduce SPR of acid soils and hence reduction in fertilizer requirement. Application of biochar to near neutral soils is not an appropriate practice since it decreases P availability.

6.3 Recommendation

Based on the results obtained from the study, the following recommendations were made:

1. Post-sorption characterization such as X-ray diffraction, FTIR and scanning electon microscopy need to be done on these biochar types to further elucidate the mechanism of P adsorption.
2. Future studies should include Ritie Nth order model and Langmiur-Freundlich Isotherm models to fully understand P adsorption by the biochar types.
3. Apart from deploying Hedley Fractionation method for assessing P fractions, X-ray adsorption near edge structure (XANES) as well as solid and or liquid state ^{31}P nuclear magnetic resonance analysis (^{31}P NMR) should be included to futher understand P fractions in biochar and biochar amended soils.
4. Future studies should focus on the long term effect of biochar at various pyrolysis temperatures on P sorption characteristics and fractions in tropical soils.

5. The study recommends the use of biochar produced at low temperature (300-450 ^{o}C) for improving P availability in tropical acid soils.
6. Greenhouse/field experiment should be conducted using a test crop (e.g. maize) in a highly acid soil of the tropics amended with biochar types at varying pyrolysis temperatures.

REFERENCES

Abekoe, M.K. & Sahrawat, K.L. (2003). Long-term cropping effect on phosphorus fractions in an Ultisol of the humid forest zone in West Africa. *Communications in Soil Science and Plant Analysis. 34* (3): 427-437.

Abekoe, M.K. & Sahrawat, K.L. (2001). Phosphorus retention and extractability in soils of the humid zones in West Africa. *Geoderma.* 102: 175-187.

Abekoe, M.K. & Tiessen, H. (1998). Phosphorus forms, lateritic nodules and soil properties along a hillslope in northern Ghana. *Catena*. 33:1-15.

Abrams, M.M. & Jarrel, W.M., (1992). Bioavailability index of phosphorus using ion-exchange resin impregnated membranes. *Soil Science Society of America* Journal. 56: 1532-1537

Acquaye, D.K. & Oteng, J.W. (1972). Factors influencing the status of phosphorus in surface soils in Ghana. *Ghana Journal of Agricultural Science*. 5: 221-228.

Agbenin, J.O. & Tiessen, H. (1994). Phosphorus transformations in a toposequence of Lithosols and Cambisols from semi-arid northeastern Brazil. *Geoderma.* 62, 345-362.

Agbenin, J.O. (1995). Phosphorus sorption by three cultivated savanna Alfisols as influenced by pH. *Nutrient Cycling In Agroecosystems.* 44, 107–112.

Agodzo, S. K., Huibers, F. P., Chenini, F., Van Lier, J. B. & Duran, A., (2008). Use of wastewater in irrigated agriculture. Country studies from Bolivia, Ghana and Tunisia. *Energy Fuels.* 18(2): 590-598

Ahenkorah, Y., Amatekpor, J. K., Dowuona, G. N. N. & Yentumi, D. S. (1993). Soil Resources of Ghana. In: Soil and Water Resources of Ghana; their conservation management and

constraints to their utilization for sustainable development. Page 41

Ahmad, M., Rajapaksha, A.U., Lim, J.E., Zhang, M., Bolan, N., Mohan, D., Vithanage, M., Lee, S.S., & Ok, Y.S., (2014). Biochar as a sorbent for contaminant management in soil and water: a review. *Chemosphere*. 99, 19-33

Alberti, G., Amendola, V., Pesavento, M, & Biesuz, R. (2012). Beyond the synthesis of novel solid phases: Review on modeling of sorption phenomena. *Coordination Chemistry Reviews.* 256:28–45

Almeelbi, T., Bezbaruah, A., (2012). Aqueous phosphate removal using nanoscale zero-valent iron. *Journal of Nanoparticle Research*.14, 1-14.

Alvarez, R., Evans, L. A., Milham, P. J., & Wilson, M. A. (2004). Effects of humic material on the precipitation of calcium phosphate. *Geoderma, 118* (3–4), 245-260.

Al-Wabel, M.I., Al-Omran, A., El-Naggar, A.H., Nadeem, M., & Usman, A.R. (2013). Pyrolysis temperature induced changes in characteristics and chemical composition of biochar produced from conocarpus wastes. *Bioresource Technology.* 131:374-379.

Amer, F. A., Mahmoud A. A., & Sabet, V. (1995). Potential and Surface-Area of Calcium Carbonate as Related to Phosphate Sorption, *Soil Science Society America Journal*. 49, 1137–1142.

Amonette, J.E. & Joseph, S. (2009). Physical properties of biochar. In 'Biochar for environmental management. Science and Technology'. (Eds J Lehmann, S Joseph). 33–53.

Anbia, M. & Hariri, S.A. (2010). Removal of methylene blue from aqueous solution using nanoporous SBA-3. *Desalination*. 26(1-2): 61–66.

Andrew, N.S., Richard, W.M. & Kleimann, P.J.A. (2004). Amounts, forms and solubility of

phosphorus in soils receiving manure. *Soil Science Society America Journal*. 68: 2048-2057.

Antal, M.J., &. Gronli. M. (2003). The art, science, and technology of charcoal production, *Industrial and Engineering Chemistry Reserach*. 42: 1619-1640.

Aon, M., Khalid, M., Zahir, Z.A. & Ahmad, R. (2015). Low temperature produced citrus peel and greenwaste biochar improved maize growth and nutrient uptake, and chemical properties of calcareous soil. *Pakistan Journal of Agricultural Science*. 52:627-636.

Arai, Y., Sparks, D.L., (2007). ATR-FTIR spectroscopic investigation on phosphate adsorption mechanisms at the ferrihydrite-water interface. *Journal of Colloid Interface Science*. 241, 317-326.

Arau´jo, M.S.B., Salcedo, I.H., & Sampaio, E.V.S.B. (1993b). Efeito de fertilizac_o˜es fosfatadas anuais em solos cultivados com cana-de-ac_ucar: II. Formas dispone veis e efeito residual do P acumulado. Revista Brasileira de Ciencia do Solo, Campinas, SP, Brasil 17, 397– 403.

Araujo, M.S.B., & Salcedo, I.H. (1997). Formas preferenciais de acumulacodefosforo em solos cultivados com cana-de-acucar na Regiao Nordeste. Revista Brasileira de Ciencia do Solo, Vic¸osa, MG, Brasil 21, 643– 650.

Armando, S.N.L. (1998). Phosphorus dynamics is soils under slah and burn cultivation in the semi-arid northeast of Brazil. Ectropics 11(2): 93-106.

Arshad, M., Rahmatullah, M. A. & Yousaf, M. (2000). Soil properties related to phosphorus sorption as described by modified Freundlich equation in some soils. *International Journal of Agriculture and Biology*. 2: 290-292.

Aslam, M., Sharif, M., Rahmatullah, M., Salim, A. & Yasin, M. (2000). Application of

Freundlich isotherm to determine phosphorus requirement of several rice soils. *International Journal of Agriculture and Biology*. 2: 286-288.

Asomaning, S.K. (2011). Phosphorus fractions and sorption characteristics of some cultivated soils at Anloga, Ghana. PhD. Thesis presented to University Ghana, Department of soil science.

Asomaning, S.K., Abekoe, M.K., Dowuona, G.N.N., Borggard, O.K., Kristensen, J.A, & Breuning-Madsen, H. (2015). Sustainable long-term intensive application of manure to sandy soils without phosphorus leaching: a case study from Ghana. *Acta Agriculturae Scandinavica, Section B-Soil & Plant Science*, 65:8, 747-754.

Atkinson, C.J., Fitzgerald, J.D. & Hipps, N.A., (2010). Potential mechanisms for achieving agricultural benefits from biochar application to temperate soils: a review. *Plant Soil* 337, 1-18.

Awudzi, T.W., Ahiahor, E. & Breuning-Madsen, H. (2008). The soil-land use system in a sand spit area in the semi-arid coastal savannah region of Ghana-development, sustainability and threat. *West African Journal of Applied Ecology*. 13. 181-194.

Barron, V., Herruzo, M. & Torrent. J. (1988) Phosphate adsorption by aluminous hematites of different shapes. *Soil Science Society of America Journal*. 52:647-651.

Barrow, N. J. (1978). Surface reactions of phosphate in soil. *Agricultural Science*. 2:33-37.

Barrow, N. J. (1979). The description of phosphate adsorption curves. *Journal of Soil Science*. 29: 447- 462.

Barrow, N.J., (1974). The slow reactions between soil and anions. 1. Effect of time, temperature, and water content of a soil on the decrease in effectiveness of phosphate for plant growth. *Soil Science Society of America Journal*. 118:380-386.

Barthes, B. & Azontonde, A. (2004). Effect of a legume cover crop (mucuma pruriens var utilis) on soil carbon in an ultisol under maize in southern Benin. *Soil Use and Management*. 20: 231-239.

Bationo, A., Mokwunye, A.U., Vlek, P.L.G et al. (2003). Soil fertility management for sustainable landus in West Africa Sudano-Sahelian Zone. In: Soil fertility management in Africa: A regional perspective, Gichuru et al. (eds.) *Academy of Science Pubublication (ASP) and TSBF-CIAT*, Nairobi, Kanya

Beauchemin, S., Hesterberg, D., Chou, J., Beauchemin, M., Simard, R. R., & Sayers, D. E. (2003). Speciation of phosphorus in phosphorus-enriched agricultural soils using X-ray absorption near-edge structure spectroscopy and chemical fractionation. *Journal of Environmental Quality*. *32*, 1809-1819.

Bigham, J.M., Fitzpatrick, R.W. & Schulze, D.G. (2002) Iron Oxides. In: Soil Mineralogy with Environmental Applications (J.B. Dixon & D.G. Schulze, editors). SSSA Book Series, Madison, Wisconsin, USA, pp. 323–366.

Biswas, B.K., Inoue, K., Ghimire, K.N., Harada, H., Ohto, K. & Kawakita, H. (2008). Removal and recovery of phosphorus from water by means of adsorption onto orange waste gel loaded with zirconium, *Bioresource Technology*. 99, 8685–8690.

Blanchard, G., Maunaye, M. & Martin, G. (1984). Removal of heavy metals from waters by means of natural zeolites. *Water Research.* 18, 1501–1507.

Boanini, E., Gazzano, M., & Bigi, A. (2010). Ionic substitutions in calcium phosphates synthesized at low temperature. *Acta Biomaterialia, 6*, 1882-1894.

Bohme, L., Langer, U., & Bohme, F. (2005). Microbial biomass, enzyme activities and microbial community structure in two European long-term field experiments.

Agriculture, Ecosystem and Environment. 109, 141-152.

Bolan, N.S., Barrow, N.J. & Posner, A.M. (1985). Describing the effect of time on sorption of phosphate by iron and aluminium hydroxides. *Journal of Soil Science* 36, 181-197.

Borggaard, O.K. (2002). Soil chemistry in a pedological context. 6th ed. DSR Forlag, Frederisksberg.

Borggaard, O.K., Jdrgensen, S.S., Moberg, J.P. & Raben-Lange, B., (1990). Influence of organic matter on phosphate adsorption by aluminium and iron oxides in sandy soils. *Journal of Soil Science.* 41, 443–449.

Borrero, C., Pena, F., Torrent J. (1988). Phosphate sorption by calcium carbonate in some soils of the Mediterranean part of Spain. *Geoderma*. 42, 261–269

Bourke, J., Manley-Harris, M., Fushimi, C., Dowaki, K., Nunoura, T. & Antal, M.J. (2007). Do all carbonized charcoals have the same chemical structure? A model of the chemical structure of carbonized charcoal. *Industrial and Engneering Chemistry Research*. 46, 5954–5967.

Bowman, R.A. (1989) A sequential extraction procedure with concentrated sulphuric acid and dilute base for soil organic phosphorus. *Soil Science Society of America Journal.* 53:362–366

Bowman, R.A., & Cole, C.V. (1978) Transformations of organic phosphorus substrates in soils as evaluated by NaHCO3 extraction. *Soil Science Society of America Journal.* 125:49-54

Bowman, R.A., Olsen, S.R., & Watanabe, F.S. (1978). Greenhouse evaluation of residual phosphate by four phosphorus methods in neutral and calcareous soils. *Soil Science Society of America Journal.* 42:451-454.

Brady, N.C., & Weil, R.R. (2002). The nature and properties of soils. Prentice Hall, Upper Saddle River, NJ.

Bray, R.H., & Kurtz, L.T. (1945). Determination of total, organic and available forms of phosphorus in soils. *Soil Science.* 64:101–109.

Breeuwsma, A., Wostett, J. H. M., Vleeshouwer, J. J., van slobbe, A. M. & Bouma, J. (1986). Derivation of land qualities to assess environmental problems from soil surveys. *Soil Science Society of America Journal*. 50:186190.

Brewer, C.E., Schmidt-Rohr, K., Satrio, J.A. & Brown, R.C., (2009). Characterization of biochar from fast pyrolysis and gasification systems. *Environmental Progressive Sustainable Energy*. 28, 386–396.

Brewer, C.E., Y-Y. Hu, K. Schmidt-Rohr, T.E. Loynachan, D.A. Laird, & Brown, R.C. (2012). Extent of pyrolysis impacts on fast pyrolysis biochar properties. *Journal of Environmental Quality*. 41: 1115-1122

Bridgewater, A.V. (1994). Catalysis in thermal biomass conversion. *Appl. Catal. A*. 116: 5-47.

Bridgewater, A.V. (1999). Principles and practice of biomass fast pyrolysis processes for liquids. *Journal of Analytical Applied Pyrolysis*. 51(1-2): 3-22.

Bridgewater, A.V. (2006). Review: biomass for energy. *Journal of Science Food Agriculture*. 86: 1755-1768.

Bridgewater, A.V. (2007). IEA bioenergy update 27: biomass pyrolysis. *Biomass Bioenergy*. 31: I-V.

Bridgewater, A.V. & Peacocke, G.V.C. (2000). Fast pyrolysis processes for biomass. Renew. Sustain. Energy Rev. 4: 1-73. Bridgwater, A.V., D. Meier, and D. Redline. 1999. An overview of fast pyrolysis of biomass. *Organic Geochemistry*. 30: 1479-1493.

Bridle, T.R. & Pritchard. D. (2004). Energy and nutrient recovery from sewage sludge via pyrolysis. *Water Science Technology*. 50:169–175.

Brodowski, S., John, B., Flessa, H., & Amelung, W. (2006). Aggregate occluded black carbon in soil. *European Journal of Soil Science.* 57: 539-548

Brown, R.A., Kercher, A.K., Nguyen, T.H., Nagle, D.C. & Ball, W.P. (2006). Production and characterization of synthetic wood chars for use as surrogates for natural sorbents. *Organic Geochemistry*. 37: 321 – 333.

Brown, W. E. (1962). Octacalcium phosphate and hydroxyapatite. *Nature, 196*, 1050-1055.

Buehler, S., Oberson, A., Rao, I. M, Friesen, D. K. & Frossard, E. (2002). Sequential phosphorus extraction of a P labeled Oxisol under contrasting agricultural systems. *Soil Science Society of America Journal*. 66: 868–877.

Cantrell, K.B., Hunt, P.G., Uchimiya, M., Novak, J.M. & Ro, K.S., (2012). Impact of pyrolysis temperature and manure source on physicochemical characteristics of biochar. *Bioresource Technology.* 107, 419–428.

Cao, X., Harris, W. G., Josan, M. S., & Nair, V. D. (2007). Inhibition of calcium phosphate precipitation under environmentally-relevant conditions. *Science of Total Environment. 383*, 205-215.

Cao, X.D., Ma, L.N., Gao, B., & Harris, W., (2009). Dairy-manure derived biochar effectively sorbs lead and atrazine. *Environmental Science and Technology*. 43, 3285e3291.

Castro, B. & Torrent, J. (1998). Phosphate sorption by calcareous Vertisols and Inceptisols as evaluated from extended P-sorption curves. *European Journal of Soil Science*. 49, 661-667.

Cayuela, M.L., Sánchez-Monedero, M.A., Roig, A., Hanley, K., Enders, A, & Lehmann, J.

(2013). Biochar and denitrification in soils: when, how much and why does biochar reduce NO emissions? Sci Report 3:17–32.

Ch'ng, H.Y., Ahmed, O.H. & Muhamad A.N. & Majid, N.M.A. (2014). Improving Phosphorus Availability in an Acid Soil Using Organic Amendments Produced from Agroindustrial Wastes. *Scientific World Journal*. 23:453-478.

Chan, K.Y., Van Zwieten, L., Meszaros, I., Downie, A, & Joseph, S. (2007). Agronomic values of greenwaste biochar as a soil amendment. *Soil Research*. 45: 629-634.

Chang, S.C. & Jackson, M.L. (1957) Fractionation of soil phosphorus. *Soil Science* 84:133–144

Chang, T.W. & Wang, M.K., (2002). Assessment of sorbent/water ratio effect on sorption using dimensional analysis and batch experiments. *Chemosphere.* 48, 419-426.

Chaudhry, E. H., Ranjha, A. M., Gill, M. A. & Mehdi, S. M. (2003). Phosphorus requirement of maize in relation to soil characteristics. *International Journal of Agriculture and. Biology*. 5(4): 625-629.

Chen, B.L., Zhou, D.D. & Zhu, L.Z., (2013). Transitional adsorption and partition of nonpolar and polar aromatic contaminants by biochars of pine needles with different pyrolysis temperatures, *Environmental Science and Technology.* 42, 5137–5143.

Chen, C.R., Condron, L.M, Davis, M.R. & Sherlock, R.R (2000). Effects of afforestation on phosphorus dynamics and biological properties in a New Zealand grassland soil. *Plant Soil.* 220:151–163

Chen, H.X., Du, Z.L., Guo, W. & Zhang, Q.Z. (2011). Effects of biochar amendment on cropland soil bulk density, cation exchange capacity, and particulate organic matter content in the North China plain, Chinese. *Journal of Applied Ecology*. 22: 2930-

2934.

Chen, T., Zhang, Y.X., Wang, H.T., Lu, W.J., Zhou, Z.Y., Zhang, Y.C. & Ren, L.L., (2014). Influence of pyrolysis temperature on characteristics and heavy metal adsorptive performance of biochar derived from municipal sewage sludge. *Bioresource Technology*. 164, 47-54

Cheng, C.H. & Lehmann, J. (2009). Ageing of black carbon along a temperature gradient. *Chemosphere* 75, 1021–1027.

Cheng, C.H., Lehmann, J., Thies, J.E., Burton, S.D. & Engelhard, M.H. (2006). Oxidation of black carbon by biotic and abiotic processes. *Organic Geochemistry*, 37, 1477–1488.

Cheng, W., Wang, S.G., Lu, L., Gong, W.X., Liu, X.W., Gao, B.Y. & Zhang, H.Y. (2008). Removal of malachite green (MG) from aqueous solutions by native and heat-treated anaerobic granular sludge. *Biochemical Engineering Journal*. 45: 231-267.

Cheung, C.W., Porter, J.F. & McKay, G. (2001). Sorption kinetic analysis for the removal of cadmium ions from effluents using bone char. *Water Research*. 25:211-231.

Chien, S.H. & Clayton, W.R. (1980). Application of Elovich equation to the kinetics of phosphate release and sorption in soils. *Soil Science Society of America Journal.* 44, 265–268.

Chien, S.H., Edmeades, D., McBride, R. & Sahrawat, K.L. (2014). Review of maleic–itaconic acid copolymer purported as urease inhibitor and phosphorus enhancer in soils. *Agronomy Journal.* 106:423–430.

Chintala, R., Mollinedo, J., Schumacher, T.E., Malo, D.D., Papiernik, S.K., Clay, D.E., Kumar, S., & Gulbrandson, D.W., (2013). Nitrate sorption and desorption in biochars from fast pyrolysis. *Microporous Mesoporous Material*. 179, 250-257.

Chintala, R., Schumacher, T.E., Mcdonald, L.M., Clay, D.E., Malo, D.D., Papiernik, S.K., Clay, S.A., Julson, J.L., (2014). Phosphorus Sorption and Availability from Biochars and Soil/Biochar Mixtures. *Clean-Soil, Air, Water.* 42 (5), 626-634

Christel, W., Bruun, S., Magid, J., & Jensen, L.S., (2014). Phosphorus availability from the solid fraction of pig slurry is altered by composting or thermal treatment. *Bioresource Technology.* 169, 543–551.

Chun, Y., Sheng, G.Y., Chiou, C.T., Xing, B.S., (2004). Compositions and sorptive properties of crop residue-derived chars, *Environmental Science and Technology.* 38, 4649–4655.

Clark, T., Stephenson, T., Pearce, P.A., (1997). Phosphorus removal by chemical precipitation in a biological aerated filter. *Water Research.* 31, 2557–256.

Clough, T.J, Bertram, J.E., Ray, J.L., Condron, L.M., O'Callaghan, M., Sherlock, R.R, & Wells, N.S. (2010). Unweathered wood biochar impact on nitrous oxide emissions from a bovine-urine-amended pasture soil. *Soil Science Society of America Journal.* 74:852-860.

Coder, K.D. (1996). Construction damage assessments: Trees and sites. University of Georgia Cooperative Extension Service Publication. 96-39.

Cornell, R.M. & Giovanoli, R. (1986). Factors that govern the formation of multi-domainic geothites. Clay Minerals. 34: 557-564.

Cross, A.F., & Schlesinger, W.H. (1995). A literature review and evaluation of the Hedley fractionation: applications to the biogeochemical cycle of phosphorus in natural ecosystems. Geoderma 64:197–214.

Cui, H.J., Wang, M.K., Fu, M.L. & Ci, E., (2011). Enhancing phosphorus availability in

phosphorus-fertilized zones by reducing phosphate adsorbed on ferrihydrite using rice straw-derived biochar. *Journal of Soils and Sediments*. 11, 1135–1141

Delgado, A., & Torrent, J. (2000). Phosphorus forms and desorption patterns in heavily fertilized calcareous and limed acid soils. *Soil Science Society of America Journal* 64: 2031-2037.

DeLuca, T.H., MacKenzie, M.D. & Gundale, M.J. (2009). 'Biochar effects on soil nutrient transformations', in Lehmann, J. and Joseph, S. Biochar for environmental management: science and technology, Earthscan, United Kingdom: 251–70.

Demirbas, A. (2004). Effects of temperature and particle size on bio-char yield from pyrolysis of agricultural residues. *Journal of Analytical and Applied Pyrolysis.* 72, 243–248

Demirbas, A. (2006). Production and Characterization of Bio-Chars from Biomass via Pyrolysis. *Energy Sources*, Part A. 28: 413-422.

Detenbeck, N.E., Brezonik, P.L., (1991). Phosphorus sorption by sediments from a soft-water seepage lake. 1. An evaluation of kinetic and equilibrium models. *Environmental Science and Technology*. 25, 395-403.

Dick, W.A, & Tabatabai, M.A (1977) Determination of orthophosphate in aqueous solutions containing labile organic and inorganic phosphorus compounds. *Journal of Environmental Quality*. 6:82–85

Dimirkou, A. & Ioannou, A. (1998). Kinetics of phosphate sorption by goethite-and bentonite-goethite (b-g) system. *Commication in Soil Science and Plant Analysis.* 29: 2119-2134.

Dimirkou, A., Mitsios.I, Ioannu, A., Pashalidis, C. & Doula, M. (1993). Kinetic study of phosphorus desorption by alfisols and entisols. *Communication in Soil Science and*

*Plant Anal*ysis 24: 989-1001.

Dodds, W. K., Bouska, W. W., Eitzmann, J. L., Pilger, T. J., Pitts, K. L., Riley, A. J., Schloesser, J. T., Thornbrugh, D. J., (2008). Eutrophication of US freshwaters: Analysis of potential economic damages. *Environmental Science and Technology*. 43, 12-19.

Dong, X., Ma, L. Q., Zhu, Y., Li, Y., & Gu, B. (2013). Mechanistic investigation of mercury sorption by Brazilian pepper biochars of different pyrolysis temperatures based on X-ray photoelectron spectroscopy and flow calorimetry, *Environmental Science and Technology*. 47, 12156–12164.

Dormaar, J. F., & Chang, C. (1995). Effects of 20 annual applications of excess feedlot manure on labile soil phosphorus. *Canadian Journal of Soil Science*. 75:507–512

Downie, A., Crosky, A. & Munroe, P. (2009). Chapter 2 – Physical properties of biochar. In: *Biochar for Environmental Management* (eds J. Lehmann & S. Joseph), pp. 13-32. Earthscan, London.

Du, Z., Wang, Y., Huang, J., Lu, N., Liu, X., Lou, Y., & Zhang, Q. (2014). Consecutive biochar application alters soil enzyme activities in the winter wheat-growing season. *Soil Science*. 179, 75-83

Duku, M.H., Gu, S., Hagan, E.B., (2011). Biochar production potential in Ghana-a review. *Renewable and Sustainable Energy Reviews*. 15: 3539-3551.

Dwomo, O. & Dedzoe C.D. (2010). Oxisol (ferralsol) development in two agro-ecological zones of Ghana: a preliminary evaluation of some profiles. *Journal of Science and Technology***.** 30 (2):11-28.

Earl, K.D., Syers, J.K., & McLaughlin, J.R. (1979). Origin of the effect of citrate, tartrate and

acetate on phosphate sorption by soils and synthetic gels. *Soil Science Society of America Journal*. 43:674–678.

Easterwood, G.W, & Sartain, J.B. (1990) Clover residue effectiveness in reducing orthophosphate sorption on ferric hydroxide coated soil. *Soil Science Society of America Journal.* 54, 1345–1350.

Eduah, J.O. (2012). Removal of nitrate, phosphorus and escherichia coli from simulated wastewater using modified biosand filter system. M.Phil Thesis presented to University Ghana, Department of soil science.

Eriksson, A.K., Gustafsson, J.P., & Hesterberg, D. (2015). Phosphorus speciation of clay fractions from long-term fertility experiments in Sweden. *Geoderma.* 241-242:68–74.

Evangelou, V.P (1998). Environmental soil and water chemistry: principles and applications. John Wiley and Sons. Inc. Canada

FAO (2008). FAOSTAT Accessed on http://faostat.fao.org/default.aspx (accessed on April 2011)

Feizi, M. & Jalali, M. (2014) Sorption of aquatic phosphorus onto native and chemically-modified plant residues: modeling the isotherm and kinetics of sorption process. *Desalination and Water Treatment*. 45:121-133

Feng, J.W., Zheng, S. & Maciel, G.E. (2004). EPR investigations of the effects of inorganic additives on the pyrolysis and char/air interactions of cellulose. *Energy & Fuels* 18(4), 1049-1065.

Fitter, A. H., & Sutton, C. D. (1975). The use of the Freundlich isotherm for soil phosphate sorption data. *Journal of Soil Science*. 26:241 -246.

Fox, R. L., & Kamprath, E. J. (1970). Phosphate Sorption Isotherms for Evaluating the

Phosphate Requirements of Soils. *Soil Science Society of America Proceedings.* 34: 902-907.

Freeman, J. S., & Rowell, D. L. (1981). The adsorption and precipitation of phosphate onto calcite. *Journal of Soil Science. 32*, 75-84.

Freese, D., Lookman, R., Merckx, R. & Riemsdijk, W.H., (1995). New method for long-term phosphate desorption from soils. *Soil Science.Society of.America Journal*. 59: 1295-1300.

Frossard, E.M., Brossard, M.J., Hedley, M.J., & Metherell, A. (1995). Reactions controlling the cycling of P in soils, in: H. Tiessen (Ed.), Phosphorus in the Global Environment, John Wiley & Sons, Chichester, England, pp. 107-137.

Frost, R., Palmer, S, & Pogson, R. (2012) Thermal stability of crandallite $CaAl_3(PO_4)_2(OH)\cdot(H_2O)$. Journal of Thermal Analysis and Calorimetry 107:905–909

Funke, A., & Ziegler, F. (2010). Hydrothermal carbonization of biomass: A summary and discussion of chemical mechanisms for process engineering. *Biofuels, Bioproduction and. Biorefining.* 4:567-675.

Galvao, S.R.S, & Salcedo, I.H. (2009). Soil phosphorus fractions in sandy soils amended with cattle manure for long periods. R. Bras. Ci. Solo. 33: 613-622

Garcia-Perez, M. (2008). The formation of polyaromatic hydrocarbons and dioxins during pyrolysis. Washington State University.

Gaskin, J., Steiner, C., Harris, K., Das, K., Bibens, B., (2008). Effect of low-temperature pyrolysis conditions on biochar for agricultural use. Trans. ASABE 51 (6), 2061–2069.

Gaunt, J. & J. Lehmann. (2008). Energy balance and emissions associated with biochar

sequestration and pyrolysis bioenergy production. *Environmental Science and Technology*. 42: 4152-4158.

Geelhoed, J.S., Van Riemsdijk, W.H. and Findenegg, G.R. (1999). Simulation of the effect of citrate exudation from roots on the plant availability of phosphate adsorbed on goethite. European Journal of Soil Science 50:379–390.

Gérard, F. (2016). Clay minerals, iron/aluminum oxides, and their contribution to phosphate sorption in soils. A myth revisited. *Geoderma* 262:213–226.

Gerke, J., Beibner, L. & Romer, W. (2000). The quantitative effect of chemical phosphate mobilization by carboxylate anions on P uptake by single root. The basic concept and determination of soil parameters. *Journal of Plant Nutrition and Soil Science.* 163:207-212

Glaser, B., Haumaier, L., Guggenberger, G. & Zech, W. (2001). The 'Terra Preta' phenomenon: a model for sustainable agriculture in the humid tropics. *Naturwissenschaften*, 88, 37–41.

Glaser, B., Lehmann, J. & Zech, W. (2002). Ameliorating physical and chemical properties of highly weathered soils in the tropics with charcoal – a review. *Biology & Fertility of Soils*, 35, 12. 160-177.

Goldberg, S. & Sposito, G. (1984). A chemical model of phosphate adsorption by soils: I. Reference oxide minerals. Soil Science Society of America Journal 48:772–778.

Grossl, P. R., & Inskeep, W. P. (1991). Precipitation of dicalcium phosphate dihydrate in the presence of organic acids. Soil Science Society of America Journal *55*, 670-675.

Gruhn, P., Goletti, F. and Yudelman, M. (2000). Integrated Nutrient Management, Soil fertility and sustainable Agriculture: Current Issue and Future Challenges, Food, Agriculture

and the Environment Discussion Paper 32

Guo, F., Yost, R.S., Hue, N.V., Evensen, C.I., & Silva, J.A. (2000). Changes in phosphorus fractions in soils under intensive plant growth. *Soil Science Society of America Journal*. 64(5):1681-1689.

Guzman, G., Alcantara, E., Barron, V. & Torrent, J. (1994). Phytoavailability of phosphate adsorbed on ferrihydrite, hematite and goethite. *Plant Soil*.159, 219–225.

Hamer, U., Marschner, B., Brodowski, S. & Amelung, W. (2004). Interactive priming of black carbon and glucose mineralisation. *Organic Geochemistry*, 35, 823–830

Hammond, et al. (2009). The best use of biomass? Greenhouse gas life cycle analysis of predicted pyrolysis systems. MSc thesis, University of Edinburgh.

Hartley, M., House, W.A., Callow, M.E., Leadbeater, B.S.C., (1997). Coprecipitation of phosphate with calcite in the presence of photosynthesizing green algae, *Water Research.* 31, 2261–2268.

Harvey, O.R., Herbert, B.E., Rhue, R.D., Kuo, L.J., (2011). Metal interactions at the biochar-water interface: energetics and structure-sorption relationships elucidated by flow adsorption microcalorimetry. *Environmental Science and Technology*. 45, 5550-5556

Hassan, M.H., T.M.I. Mahlia, and H. Nur. (2012). A review on energy scenario and sustainable energy in Indonesia. *Renewable and Sustainable Energy Reviews*. 16: 2316-28.

Haynes, R.J., and Mokolobate, M.S. (2001). Amelioration of Al toxicity and P deficiency in acid soils by addition of organic residues: A critical review of the phenomenon and the mechanisms involved. *Nutrient Cycling in Agroecosystem*. 59:47–63.

He, Z.L., Yang, X. Yuan, K.N. & Zhu, Z.X. (1998). Desorption and plant-availability of

phosphate sorbed by some important minerals. *Plant Soil.* 162:89–97.

Hedley, M. J., & McLaughlin, M. (2005). Reactions of phosphate fertilizers and by-products in soils. In J. T. Sims, & A. N. Sharpley (Eds.), *Phosphorus: Agricultre and the Environment*, pp. 181-252. Madison, Wisconsin, USA: American Society of Agronomy,Inc.; Crop Science Society of America, Inc.; Soil Science Society of America, Inc.

Hedley, M. J., White, R. E., & Nye, P. H. (1982b). Plant-induced changes in the rhizosphere of rape seedlings. Ill. Changes in L-value, soil phosphate fractions and phosphatase activity, *New Phytologist.* 9*1:45-56.*

Hedley, M.J., Stewart, J.W.B. & Chauhan, B.S. (1982a) Changes in inorganic and organic soil phosphorus fractions induced by cultivation practices and by laboratory incubations. *Soil Science Society of America Journal.* 46:970–976.

Heimberg, J.A., Wahl, K.J., Singer, I.L. & Erdemir, A., (2001). Superlow friction behavior of diamond-like carbon coatings: time and speed effects. *Applied Physics Letters*. 78(17):2449-2451.

Henriksen, S.W. (2017). Phosphorus fractions in some virgin and cultivated Danish soils. Master thesis presented to University of Copenhagen, Department of Earth Science and Natural Resource Management.

Hesketh, N. & Brookes, P.C. (2000). Development of an indicator for risk of phosphorus leaching. *Journal of Environmental Quality.* 29:105-110.

Hieltjes, A.H.M, & Lijklema, L. (1980) Fractionation of inorganic phosphates in calcareous sediments. *Journal of Environmental Quality.* 9:405–407

Hilscher, A., & Heister, K., Siewert, C., & Knicker, K. (2009) Mineralization and structural

changes during the initial phases of microbial degradation of pyrogenic plant residues in soil. *Organic Geochemistry.* 40, 332–342.

Hinsinger, P. (2001). Bioavailability of soil inorganic P in the rhizosphere as affected by root-induced chemical changes: a review. *Plant and Soil.* 237, 173–195.

Ho, Y.S., (2006). Review of second-order models for adsorption systems. *Journal of Hazardous Material.* 136, 681–68

Ho, Y.S. (2004). Citation review of Lagergren kinetic rate equation on sorption reactions. *Scientometrics.* 59, 171–177.

Ho, Y.S. & McKay, G. (1998). Kinetic models for the sorption of dye from aqueous solution by wood. *Process Safety and Environmental Protection*.76, 183–191.

Hossain, M., Strezov, V., Chan, K.Y., Ziolkowski, A., & Nelson, P.F., (2011). Influence of pyrolysis temperature on production and nutrient properties of wastewater sludge biochar. *Journal of Environmental Management.* 92, 223-228

Houba, V.J.G., Novozamsky, I., Huibregts, A.W.N., & Van Der Lee, J.J., (1986). Comparison of soil extractants by 0.01M $CaCl_2$, EUF, and some conventional extraction procedures. *Plant and Soil*. 96: 433- 437.

Huang, P.M & Wang, M.K. (1997). Formation chemistry and selected surface properties of iron oxides. In: Soil and environment- soil processes from mineral to landscape scale. K. Auerswald, H. Stanjek, and J.M. Bigham (eds.). Advances in GeoEcology 30. Caten Verlag, Reiskircheri, Germany. Pg. 241-270.

Huang, P.M, & Violante, A. (1986). Influence of organic acids on crystallization and surface properties of precipitation products of aluminium. In *Interactions of Soil Minerals with Natural Organics and Microbes* (eds P.M Huang & M. Schnitzer), pp.159-221.

Soil Science Society of America. Madison, WI.

Huang, W.W., Wang, S.B., Zhu, Z.H., Li, L., Yao, X.D., Rudolph, V., Haghseresht, F., (2008). Phosphate removal from wastewater using red mud. *Journal of Hazardous Materials*, 158(1):35-42.

Hue, N.V. (1991). Effects of organic acids/anions on P sorption and phytoavailability in soils with different mineralogies. *Soil Science*. 156: 463–471.

Hunt, J.F., Ohno, T., He, Z.Q., Honeycutt, C.W, & Dail, D.B. (2007). Inhibition of phosphorus sorption to goethite, gibbsite, and kaolin by fresh and decomposed organic matter. *Biology and Fertility of Soils*. 44: 277–288.

IBI. (2014). Standardized Product Definition and Product Testing Guidelines for Biochar that is used in Soil. 2 ed. International Biochar Initiative (http://www.biochar-international.

Ibrikci, H., Hanlon, E.A. & Rechcigl, J.E., (1992). Initial calibration and correlation of inorganic phosphorus soil test methods with a Bahia grass field trial. *Communication of Soil Science and Plant Analysis*. 23: 2569- 2579.

Inskeep, W. P., & Silvertooth, J. C. (1988). Inhibition of hydroxyapatite precipitation in the presence of fulvic, humic, and tannic acids. *Soil Science Society of America Journal, 52*, 941-946.

Ioannou, A., Dimirkou, A., & Papadopoulos, P. (1998). Phosphate sorption by goethite and kaolinite-goethite (k-g) system as described by isotherms. *Communication of Soil Science and Plant Analysis.* 29: 2175-2190.

Ippolito, J. A., Barbarick, K. A., Heil, D. M., Chandler, J. P., & Redente, E. F. (2003). Phosphorus retention mechanisms of a water treatment residual. *Journal of*

Environmental Quality. *32*, 1857-1864

Ippolito, J.A., Spokas, K.A., Novak, J.M., Lentz, R.D. & Cantrell, K.B. (2015). Biochar elemental composition and factors influencing nutrient retention. In: Lehmann, J., Joseph, S. (Eds.), Biochar for Environmental Management: Science, Technology and Implementation. Taylor and Francis, London, pp. 139–163.

Iqbal, H., Garcia-Perez, M., Flury, M., (2015). Effect of biochar on leaching of organic carbon, nitrogen, and phosphorus from compost in bioretention systems. *Science of Total Environment*. 521, 37–45.

Ivanoff, D.B., Reddy, K.R, & Robinson, S. (1998) Chemical fractionation of organic phosphorus in selected histosols. *Soil Science.* 163:36–45.

Iyamuremye, F., R.P. Dick, and Baham. J. (1996). Organic amendments and phosphorus dynamics: II. Distribution of soil phosphorus fractions. Soil Sci. 161:436–443.

Jaszbereni, I. & Loch, J., (1996). Soil phosphate adsorption and desorption in 0.01M calcium chloride electrolyte. *Communition of Soil Science and Plant Anal*ysis. 27: 1211-1225.

Javid, S. & Rowell, D. L. (2003). Effect of soil properties on phosphate adsorption in calcareous soils of Pakistan. *Pakistan Journal of Soil Sci*ence. 21(4):47-55.

Jiang, C., Yu, G., Li, Y., Cao, G., Yang, Z.P., Sheng, W, & Yu, W. (2012). Nutrient resorption of coexistence species in alpine meadow of the Qinghai Tibetan Plateau explains plant adaptation to nutrient-poor environment. Ecological Engneering. 44:1–9.

Jiang, J., Yuan, M., Renkou, X., And Bish, D.L., (2015). Mobilization of phosphate in variable-charge soils amended with biochars derived from crop straws. *Soil & Tillage Research*. 146: 139-147

Jiao, Y., Hendershot, W. H., & Whalen, J. K. (2008). Modeling phosphate adsorption by agricultural and natural soils. *Soil Science Society of America Journal* 72:1078

Jien, S.H, & Wang, C.S. (2013). Effects of biochar on soil properties and erosion potential in a highly weathered soil. *Catena.* 110:225–233.

Jin, Y., Liang, X., He, M., Liu, Y., Tian, G., & Shi, J., (2016). Manure biochar influence upon soil properties, phosphorus distribution and phosphatase activities: a microcosm incubation study. *Chemosphere.* 142, 128-135.

John, M.K., (1970). Colorimetric determination of phosphorus in soil and plant materials with ascorbic acid. *Soil Science.* 109 (4), 214–220.

Jonasson, R.G., Martin, R.R., Guiliacci, M.E. & Tazaki, K. (1988). Surface recations of goethite with phosphate. *Journal of Chemical Society*. Faraday Transactions I. 84: 2311-2315.

Jones, B.E.H., Haynes, R.J., & Phillips, I.R. (2010). Effect of amendment of bauxite processing sand with organic materials on its chemical, physical and microbial properties. *Journal of Environmental Management*. 91: 2281–2288.

Jones, D.L., Darrah, P.R., & Kochian. L.V. (1996). Critical evaluation of organic acid mediated iron dissolution in the rhizosphere and its potential role in root iron uptake. *Plant Soil.* 180:57–66.

Jonker, M. T. O.; Smedes, F. (2000). Preferential sorption of planar contaminants in sediments from lake Ketelmeer, the Netherlands. *Environmental Science & Technology*, *34* (9), 1620-1626.

Joseph, S., Graber, E. R., Chia, C., Munroe, P., Donne, S., Thomas, T., Nielsen, S., Marjo, C., Rutlidge, H., Pan, G. X., Li, L., Taylor, P., Rawal, A., & Hook, J.(2010): Shifting

paradigms: development of high-efficiency biochar fertilizers based on nano-structures and soluble components, Carbon Manage., 4, 323–343.

Joseph, S., Peacocke, C., Lehmann, J. & Munroe, P. (2009). Developing a biochar classification and test methods. In: Biochar for environmental management: science and technology (eds J. Lehmann & S. Joseph), pp. 107–126. Earthscan, London; Sterling, VA.

Juo, A.S.R., Fox, R.L (1977). Phosphate sorption characteristics of some benchmark soils of West Africa. *Soil Science*. 114:370-376.

Kaczala, F., Marques, M., & Hogland, W. (2009). Lead and vanadium removal from a real industrial wastewater by gravitational settling/sedimentation and sorption onto Pinus sylvestris sawdust. *Bioresource Technology*. 100(1): 235–243.

Kamara A., Hawanatu, S.K. & Mohamed, S.K. (2015). Effect of rice straw biochar on soil quality and the early growth and biomass yield of two rice varieties. *Journal of Agriculture Science*. 6:798-806.

Kammann, C.I., Schmidt, H.P., Messerschmidt, N., Linsel, S., Steffens, D., Müller, C., Koyro, H.W., Conte, P., Joseph, S. (2015) Plant growth improvement mediated by nitrate capture in co-composted biochar. *Environmental Science and Technology* 47: 456-876

Kämpf, N., Curi, N., & Marques, J.J., (2009). Intemperismo e ocorrência de minerais no ambiente do solo. In: Melo, V.F., Alleoni, L.R.F. (Eds.), Química e mineralogia do solo — Parte I: Conceitos básicos. Sociedade Brasileira de Ciência do Solo, Viçosa, pp. 333–380

Kappler, A., Wuestner, M. L., Ruecker, A., Harter, J., Halama, M., & Behrens, S.

(2014).Biochar as an electron shuttle between bacteria and Fe(III) minerals. *Environmental Science and Technology Letters.* 1:339-344.

Karaca, S., Gurses, A., Ejder M., Acikyildiz, M., (2014). Kinetic modeling of liquid-phase adsorption of phosphate on dolomite. *Journal of Colloids and Interface Science*. 277, 257–263.

Karageorgiou, K., Paschalis, M., Anastassakis, G.N.J., (2007). Removal of phosphate species from solution by adsorption onto calcite used as natural adsorbent, *Journal of Hazardous Materials*. 139, 447–452.

Kashem, M.A., Akinremi, O.O., & Racz, G.J. (2004). Phosphorus fractions in soil amended with organic and inorganic phosphorus sources. *Canadian Journal of Soil Science.* 84:83–90.

Kasozi, G.N., Zimmerman, A.R., Nkedi-Kizza, P., Gao, B., (2010). Catechol and humic acid sorption onto a range of laboratory-produced black carbons (Biochars). *Environmental Science and Technology*. 44, 6189–6195.

Keiluweit, M., Nico, P.S., Johnson, M.G., & Kleber, M. (2010). Dynamic Molecular Structure of Plant Biomass-Derived Black Carbon (Biochar), *Environmental Science and Technology*. 44(4): 1247–53.

Khodadad, C. L. M., Zimmerman, A. R., Uthandi, S., Green. S. J. J., and Foster, J. S.(2011): Taxa-specific changes in soil microbial composition induced by pyrogenic carbon amendments. *Soil Biology and Biochemistry.* 43, 385–392.

Kim, J., W. Li, B. L. Phillips, and C. P. Grey. (2011). Phosphate adsorption on the iron oxyhydroxides goethite (α-FeOOH), akaganeite (ß-FeOOH), and lepidocrocite (ϒ-FeOOH): A31P NMR study. *Energy and Environmental Science*. 4:4298-4305

Kirk, G.J.D., Santos, E.E., & Santos, M.B. (1999). Phosphate solubilization by organic anion excretion from rice growing in aerobic soils: Rates of excretion and decomposition, effects of rhizosphere pH and effects on phosphate solubility and uptake. *New Phytologist Journal.* 142:185–200.

Knicker, H. (2007). How does fire affect the nature and stability of soil organic nitrogen and carbon? A review on *Biogeochemistry. 85*, 91–118.

Kolb, S.E., Fermanich, K.J, & Dornbush, M.E. (2007). Effect of charcoal quantity on microbial biomass and activity in temperate soils. Soil Sci Soc Am J. 73: 1173–1181.

Koopmans, G.F., Chardon, W.J., Dolfing, J. & Oenema, O. (2003). Wet chemical and phosphorus -31 NMR of phosphorus speciation in a sandy soil receiving long term fertilizer or animal manure applications. *Journal of Environmental Quality*. 32: 287-295.

Krishnan, K.A. & Haridas, A. (2008). Removal of phosphate from aqueous solutions and sewage using natural and surface modified coir pith, *Journal of Hazardous Material*. 152: 527–535.

Krull, E., Lehmann, J., Skjemstad, J., Baldock, J, & Spouncer L. (2009). The global extent of black C in soils: is it everywhere? In Schr¨oder H G (ed.) Grasslands: *Ecology, Management and Restoration. Nova Science*, Hauppauge. pp. 13–17

Kumar, P., Sudha, S., Chand, S., Srivastava, V.C., (2010). Phosphate removal from aqueous solution using coir-pith activated carbon. *Separation Science and Technology*. 45, 1463–1470.

Kumari, K., Moldrup, P., Paradelo, M., Elsgaard, L., Hauggaard-Nielsen, H., de Jonge, L.W., (2014). Effects of biochar on air and water permeability and colloid and phosphorus leaching in soils from a natural calcium carbonate gradient. *Journal of Environmental*

Quality. 43 (2), 647–657.

Kuo, S. & Lotse, E. G. (1974). Kinetics of phosphate adsorption and desorption by hematite and gibbsite. *Soil Science*. 116:400-406.

Laird, D. A., Brown, R. C., Amonette, J. E., & Lehmann, J. (2009). Review of the pyrolysis platform for coproducing bio-oil and biochar. *Biofuels, Bioproduct and Biorefining*. 3, 547-562

Laird, D.A., Fleming, P., Davis, D.D., Horton, R., Wang, B. & Karlen, D. (2010). Impact of biochar amendments on the quality of typical Midwestern agricultural soil. *Geoderma*, 158: 44– 449.

Lan, Z.M., Lin, X.J., Wang, F., Zhang, H. & Chen, C.R. (2012). Phosphorus availability and rice grain yield in a paddy soil in response to long-term fertilization. *Biology and Fertility of Soils.* 48, 579–588

Landon, J.R. (1984). Tropical Soil Manual. Booker Agriculture International Limited, Londres. 450 pp.

Langmuir, I. (1918). The Adsorption of Gases on Plane Surfaces of Glass, Mica and Platinum. Journal of America Chemical Society 40: 1361.

Lazaridis, N.K., Asouhidou, D.D., (2003). Kinetics of sorptive removal of chromium (VI) from aqueous solutions by calcined Mg-Al-CO_3- hydrotalcite. *Water Research*, 37(12):2875-2882.

Lee, J.W., Kidder, M., Evans, B.R., Paik, S., Buchanan, A.C., Garten, C.T., Brwon, R.C., (2010). Characterization of biochars produced from corn stovers for soil amendments. *Environmental Science and Technology*. 44, 7970-7974.

Lehmann, J. & Joseph, S. (2009) Biochar for environmental management: An introduction. In

Biochar for Environmental Management, Science and Technology; Lehmann, J., Joseph, S., Eds.; Earthscan: London, UK; pp. 1–12.

Lehmann, J. (2007). Bio-energy in the Black. Front. Ecol. Environ. 5: 381-387.

Lehmann, J., Gaunt, J. & Rondon, M. (2006). Biochar Sequestration in terrestrial ecosystem- a review. Mitigation and Adoptation Strategies for Global Change. 11:403-427.

Li, Q., Xu, X.T. Cui, H., Pang, J., Wei, Z.B., Sun, Z., and J. Zhai, J. (2012). Comparison of two adsorbents for the removal of pentavalent arsenic from aqueous solutions. Journal of Environmental Management 98: 98-106.

Li, W., Feng, J., Kwon K. D., Kubicki, J. D. & Phillips, B.L. (2010). Surface speciation of phosphate on boehmite (ϒ -AlOOH) determined from NMR spectroscopy. Langmuir 26:4753-4761

Li, X.M., Shen, Q.R., Zhang, D.Q., Mei, X.L., Ran, W., Xu, Y.C., & Yu, G.H., (2013). Functional groups determine biochar properties (pH and EC) as studied by twodimensional ^{13}C NMR correlation spectroscopy. PLoS One. 8:65949-65969.

Liang, B., J., Lehmann, D., Solomon, J., Kinyangi, J., Grossman, B., O'Neill, J. O., Skjemstad, J., Thies, F. J., Luizao, J., Petersen, H., & Neves, E. G. (2006). Black carbon increases cation exchange capacity in soils. *Soil Science Society of America Journal*. 70: 1719-1730

Liang, Y., Cao, X., Zhao, L., Xu, X., And Harris, W., (2014). Phosphorus Release from Dairy Manure, the Manure-Derived Biochar, and Their Amended Soil: Effects of Phosphorus Nature and Soil Property. *Journal of Environmental Quality*. 43:1504-1509

Lima, H.N., Schaefer, C.E.R., Mello, J.W.V., Gilkes, R.J. & Ker, J.C. (2010). Pedogenesis and pre-Colombian land use of "Terra Preta Anthrosols" ("Indian Black earth") of Western

Amazonia. Geoderma. 110: 1-17.

Lima, I.M., & Marshall, W.E. (2010). Granular activated carbons from broiler manure: physical, chemical and adsorptive properties. *Bioresource Technology.* 96: 699-706.

Lindsay, W. L. (1979). Chemical Equilibria in Soils, John Wiley & Sons, New York.

Liu, Y., Sheng, X., Dong, Y., Ma, Y., (2012). Removal of high-concentration phosphate by calcite: Effect of sulfate and pH, *Desalination.* 289, 66-71.

Loganathan, V.A., Feng, Y.C., Sheng, G.D. & Clement, T.P. (2009). Cropresidue-derived char influences sorption, desorption and bioavailability of atrazine in soils. *Soil Science Society of America Journal*. 73, 967–974.

Lu, X., Leng, Y., (2005). Theoretical analysis of calcium phosphate precipitation in simulated body fluid, *Biomaterials*. 26, 1097-1108.

Lua, A. C., Yang, T., & Guo, J. (2004) Effects of pyrolysis conditions on the properties of activated carbons prepared from pistachio-nut shells. *Journal of Analytical and. Appllied Pyrolysis.* 72, 279-287.

Luengo, C., Brigante, M., Antelo, J. & Avena, M. (2006). Kinetics of phosphate adsorption on goethite: comparing batch adsorption and ATR-IR measurements. *Journal Colloid Interface Science.* 300: 511-518.

Magid J, Tiessen H, Condron LM (1996) Dynamics of organic phosphorus in soils under natural and agricultural ecosystems. In: Piccolo A (ed) Humic substances in terrestrial ecosystems. Elsevier, Amsterdam, pp 429–466

Major, J., Lehmann, J., Rondon, M. & Goodale, C. (2010a). Fate of soil-applied black carbon: downward migration, leaching and soil respiration. *Global Change Biology*, 16, 1366–1379.

Major, J., Rondon, D., Molina, B., Riha, S. & Lehmann, J. (2009). Maize yield and nutrition during 4 years after biochar application to a Colombian savanna oxisol. *Plant Soil*. 333: 117-128.

Malik, P. K., (2004). Dye removal from wastewater using activated carbon developed from sawdust: Adsorption equilibrium and kinetics. *Journal of Hazardous Materials*, 113: 81-88

Manning, B.A., Goldberg, S., (1996). Modeling competitive adsorption of arsenate with phosphate and molybdate on oxide minerals. *Soil Science Society of America Journal*. 60, 121-131.

Manu, A., Bationo, A. & Geiger, S.C. (1991). Fertility status of selected millet producing soils of West Africa with emphasis on phosphorus. *Soil Science.* 152: 315-320.

Maria, S.B.A., Schaefer, E.R.C., & Sampaio, E.V.S.B. (2004). Soil phosphorus fractions from toposequences of semi-arid latosols and luvisols in northern Brazil. *Geoderma*. 119: 309-321.

Marion, G.M., Hendricks, D.M., Dutt, G.R., & Filler, W.H. (1976). Aluminum and silica solution in soils. Soil Science. 127: 76-85.

Masek O. (2011). Biochar production technologies, http://www.geos.ed.ac.uk/sccs/ biochar/documents/BiocharLaunch-OMasek.pdf.

Mattingly, G.E.G. (1975). Labile phosphate in soils, Soil Sci. 119: 369-375.

McBeath, A. V., Smernik, R. J., Krull, E. S., and Lehmann, J.(2013): The influence of feedstock and production temperature on biochar carbon chemistry: A solid-state 13C NMR study, *Biomass and Bionenergy*. 60, 121–129.

McDowell, R.W., and Condron. L. (2001). Influence of soil constituents on soil phosphorus

sorption and desorption. *Communication of Soil Science and Plant Analysis*. 32:2531–2547.

McDowell, R.W., Sharpley, A.N., (2003). Phosphorus solubility and release kinetics as a function of soil test P concentration. *Geoderma*. 112: 143– 154.

McHenry, M.P. (2009). Agriculture biochar production, renewable energy generation and farm sequestration in Western Australia: certainty, uncertainty and risk. *Agriculture, Ecosystem and Environment.* 129:1-7.

McKean S.J. And Warren, G.P., (1996). Determination of soil phosphate desorption characteristics in soils using successive resin extraction. *Communication of Soil Science and Plant Analysis.* 27: 2397-2417.

McLaughlin, J.R., Ryden, J.C. & Syers, J.K. (1977). Development and evaluation of a kinetic model to describe phosphorus sorption by hydrous ferric oxide gels. *Geoderma* 18:295-307.

Meng, F.W., (2005). Study on a Mathematical Model in Predicting Breakthrough Curves of Fixed-bed Adsorption onto Resin Adsorbent. MS Thesis, Nanjing University China, p.28-36

Menon, R.G., Chien, S.H. & Hammond, L.L., (1990). Development and evaluation of the Pi soil test for plant available phosphorus. *Communication of Soil Science and Plant Analysis.* 114: 211- 216.

Menon, R.G., Hammond, L.L. & Sissingh, H.A. (1989). Determination of plant available phosphorus by the iron hydroxide-impregnated filter paper (Pi) soil test. *Soil Science Society of America Journal.* 53:110-115.

Millero, R.M., Miller, S.P., Jastrow, J.D., Rivetta, C.B., (2001). Mycorrhizal mediated

feedbacks influence net carbon gain and nutrient uptake in Andropogon gerardii. *New Phytologist.* 155, 149-162

Mohan, D., Pittman, C.U., & Steele, P.H. (2006). Pyrolysis of Wood/Biomass for Bio-oil: A Critical Review. *Energy Fuels*. 20: 848-889.

Mohan, D., Sarswat, A., Ok, Y. S. & Pittman, J. (2014). Organic and inorganic contaminants removal from water with biochar, a renewable, low cost, and sustainable adsorbent -a critical review. *Bioresource Technology*. 2014, *160*, 191-202.

Mok, W.S., &. Antal, M.J. (1983). Effects of pressure on biomass pyrolysis. II: Heats of reaction of cellulose pyrolysis. *Thermochimica Acta.* 68: 165-186.

Mokwunye, U. (1975). The influence of pH on the adsorption of phosphate by soils from Guinea and Sudan savannah zones of Nigeria. *Soil Science Society of America Proceedings.* 39. 1100-1102.

Morales, M. M., Comerford, N., Guerrini, I.A., Falcao, N.P.S. & Reeves, J.B. (2013). Sorption and desorption of phosphate on biochar and Biochar-soil mixtures. Soil Use and Management. 29, 306-314

Mostafapour, F.K., Bazrafshan, J., Farzadkia, M., & Amini, S. (2013). Arsenic removal from aqueous solutions by salvadora persica stem ash. Journal of Chemistry 740847: 8.

Mukherjee, A., Zimmerman, A. R. & Harris, W. (2011). Surface chemistry variations among a series of laboratory-produced biochars. *Geoderma.*163, 247-255.

Muljadi, D., Posner, A.M. & Quirk., J.P. (1966). The mechanism of phosphate adsorption by kaolinite, gibbsite, and pseudoboehmite I. The isotherms and the effect of pH on adsorption. *Journal of Soil Science*. 17:212-229.

Murphy, J. & Riley, J.P. (1962) A modified single solution method for the determination of

phosphate in natural waters. *Analytica Chimica Acta*. 27:31–36

Murphy, P.N.C. & Stevens, R.J., (2010). Lime and gypsum as source measures to decrease phosphorus loss from soils to water. *Water, Air and Soil Pollution*. 212, 101–111.

Nagarajah, S., Posner, A., & Quirk. J. (1968). Desorption of phosphate from kaolinite by citrate and bicarbonate. *Soil Science Society of America. Proceedings.* 32:507–510.

Nartey, E., Dowuona, G.N., Ahenkorah, Y. & Mermut, A.R. (1997). Variability in the properties of soil on two topsequences in northern Ghana. *Ghana Journal of Agriculture Science. 3*0:115-126.

Nartey, E., Matsue, N. & Henmi, T. (2001). Adsorptive mechanism of orthosilic acid on nano ball allophane. *Clay Science.* 11(2): 152-135.

Negassa, W., & Leinweber, P., (2009). How does the Hedley sequential phosphorus fractionation reflect impacts of land use and management on soil phosphorus: a review. *Journal of Plant Nutrition and Soil Science.* 172, 305–325.

Nelson, N.O., Agudelo, S. C., Yuan, W.Q, & Gan, J. (2011). Nitrogen and phosphorus availability in biochar-amended soils. *Soil Science.* 176: 218–226.

Neves, D., Thunman, H., Matos, A. Tarelho, L. & Gómez-Barea, A. (2011). Characterization and prediction of biomass pyrolysis products. *Progress in Energy and Combustion Science.* 37: 611-630.

Nguyen, B.T., Lehmann, J., Hockaday, W.C., Joseph, S. & Masiello, C.A. (2010). Temperature sensitivity of black carbon decomposition and oxidation. *Environmental Science and Technology*. 44, 3324-3331.

Novak, J.M., Busscher, W.J., Watts, D.W., Laird, D.A., Ahmedna, M.A. & Niandou, M.A.S. (2010). Short-term CO_2 mineralization after additions of biochar and switchgrass to a

Typic Kandiudult. *Geoderma*, 154, 281–288.

Oliveira, C., Georgieva, P., Rocha, F., Ferreira, A., & Feyo de Azevedo, S. (2007). Dynamical model of brushite precipitation. *Journal of Crystal Growth., 305*, 201-210.

Olsen, S. R. & Watanabe, F. S. (1957). A method to determine a phosphorus adsorption maximum of soils as measured by the Langmuir isotherm. *Soil Science Society of America Proceedings*. 21:144-149.

Olsen, S. R., Cole, C. V., & Watanabe, F. S. (1954). Estimation of available phosphorus in soils by extraction with sodium bicarbonate. *Circular 939, U.S. Dept. of Agriculture*, 939.

Osodeke, V.E., Asawalam, O.K., Kamalu, O.J. & Ugwa, I.K. (1993). Phosphorus sorption characteristics of some soils of the rubber belt of Nigeria. *Communition of Soil Science and Plant Analysis.* 24: 1733:114-123.

Owusu-Bennoah, E. & Acquaye, D. K. (1989). Phosphate sorption characteristics of selected major Ghanaian soils. *Soil Science.* 148:114-123.

Owusu-Bennoah, E., Fardeau, I.C. and Zapata, F. (2000). Evaluation of bioavailable phosphorus in some acid soils of Ghana using 32P isotopic exchange method. *Ghana Journal Agriculture Science.* 33: 139-146.

Pandey, P.K., Choubey, S., Verma, Y., Pandey, M., and Chandrashekhar, K. (2009). Biosorptive removal of arsenic from drinking water. *Bioresource Technology.* 100(2): 634–637.

Parfitt, R. L. (1989). Phosphate reactions with natural allophane, ferrihydrite and goethite. Journal of Soil Science. 40:359Y369.

Parfitt, R.L. (1979). The availability of P from phosphate-goethite bridging complexes–

desorption and uptake by ryegrass. *Plant Soil.* 53:55–65

Parr, J. F. (2006): Effect of fire on phytolith coloration, Geoarcheology, 21,171–185.

Pellera, F.M., Giannis, A., Kalderis, D., Anastasiadou, K., Stegmann, R., Wang, J.Y., Gidarakos, E., (2012). Adsorption of Cu (II) ions from aqueous solutions on biochars prepared from agricultural byproducts. *Journal of Environmental Management*. 96, 35-42.

Peng, X., Ye, L.L., Wang, C.H., Zhou, H. & Sun, B. (2011). Temperature- and duration-dependent rice straw-derived biochar: Characteristics and its effects on soil properties of an Ultisol in southern China. *Soil and Tillage Research.* 112:159-166.

Plazinski, W., Rudzinski, W., Palzinska, A., (2009). Theoretical models of sorption kinetics including a reaction mechanism: a review. *Advance Colloid and Interface Science*. 152:2-13.

Pratt, C., Parsons, S.A., Soares, A., Martin, B.D., (2012). Biologically and chemically mediated adsorption and precipitation of phosphorus from wastewater. *Current Opinion in Biotechnology*. 23 (6), 890-896.

Psenner, R., Boström. B., Dinka, M. (1988) Fractionation of phosphorus in suspended matter and sediment. Arch Hydrolbiol Beih Ergebn Limnol 30:83–112

Qian, L. & Chen, B., (2013). Dual role of biochars as adsorbents for aluminum: the effects of oxygen-containing organic components and the scattering of silicate particles. *Environmental Science and Technology*. 47, 8759-8768.

Qian, P. & Schoenau, J. J. (2000). Fractionation of P in soil as influenced by a single addition of liquid swine manure. *Canadian. Journal of Soil Science.* 80: 561–566

Qiu, Y., Zheng, Z., Zhou, Z., Sheng, G.D., 2009. Effectiveness and mechanisms of dye adsorption

on a straw-based biochar. *Bioresource Technology*. 100, 5348–5351

Robbins, C.W., Westerman. H. & Freeborn, L.L (1999). Phosphorus forms and extractability from three sources in a recently exposed calcareous subsoil. *Soil Science Society of America Journal*. 63, 1717-1724.

Roberts, T.L., Stewart, J.W.B., & Bettany, J.R., (1985). The influence of topography on the distribution of organic and inorganic soil phosphorus across a narrow environmental gradient. *Canadian Journal of Soil Science*. 65, 651–665.

Rosa, S., Laranjeira, M.C.M., Riela, H.G., Fάvere, V.T., (2008). Cross-linked quaternary chitosan as an adsorbent for the removal of the reactive dye from aqueous solutions. *Journal of Hazardous Materials*. 34:231-267.

Rudzinski, W., & Panczyk, T. (2000). Kinetics of isothermal adsorption on energetically heterogeneous solid surfaces: a new theoretical description based on the statistical rate theory of interfacial transport, *J. Phys. Chem*. B 104: 9149–9162.

Rumhayati, B., Bisri, C., Kusumawati, H., and Yasmin, F. (2012). Phosphate and nitrate removal from drinking water sources using acrylamide-ferrihydrite gel. *Indonesian Journal of Chemistry*. 12 (3): 287-290.

Russel, E. J. & Prescott, J. A. (1916). The reaction between dilute acid and the phosphorus compound of the soil. *Journal of Agricultural Science Cambridge*.8:65-110.

Rutherford, D.W., Wershaw, A.L. & Cox, L.G. (2012). Changes in composition and porosity occurring during the thermal degradation of wood and wood components. US Geological Survey Scientific Investigation Report, Reston, VA.

Ruttenberg, K.C. (1992) Development of a sequential extraction method for different forms of phosphorus in marine sediments. Limnol Oceanogr 37:1460–1482

Saavedra, C., & Delgado, A. (2005). Phosphorus fractions and release patterns in typical Mediterranean soils. *Soil Science Society of America Journal. 69*, 607-615.

Saeed, A., Akhter, M.W., Iqbal, M., (2005). Removal and recovery of heavy metals from aqueous solution using papaya wood as a new biosorbent. *Separation and Purification Technology*. 45, 25-31.

Sahrawat, K. L., Jones, M. P. and Diatta, S. (1998). Plant phosphorus and rice yield in an Ultisol of the humid forest zone in West Africa. *Communications in Soil Science and Plant Analysis*.29: 997-1005.

Sam, A.S., Asuming-Brempong, S. Nartey, E.K. (2017). Microbial activity naad metabolic quotient of microbes in soils amended with biochar and contaminated with atrazine and paraquat. *Acta Agriculturae Scandinavica, Section B-Soil & Plant Science,* 67:6, 492-509.

Sanchez, P.A., and Uehara, G. (1980). Management considerations for acid soils with high phosphorus fixation capacity. p. 471–514. *In* F.E. Khasawneh et al. (ed.). The role of phosphorus in agriculture. ASA, Madison, WI.

Sanyal, S.K., De Datta, S.K. & Chan, P.Y (1993). Phosphate sorption-desorption behavior of some acidic soils of South and Southeast Asia. *Soil Science Society of American Journal*. 57: 937-945

Sato, S., Solomon, D., Hyl, C., Ketterings, Q. M., & Lehmann, J. (2005). Phosphorus speciation in manure and manure-amended soils using XANES spectroscopy. *Environmental Science and Technology*. *39* (19), 7485-7491.

Scheidegger, A.M. & Sparks, D.L. (1996). A critical assessment of sorption-desorption mechanisms at the soil mineral/water interface. *Soil Science.* 161:813-831.

Schmidt, H.P., Pandit, B.H., Martinsen, V., Cornelissen, G., Conte, P. & Kammann, C.I. (2015). Fourfold increase in pumpkin yield in response to low-dosage root zone application of urine-enhanced biochar to a fertile tropical soil. *Agriculture.* 5:723–741.

Schmidt, J.P., S.W. Buol, & Kamprath, E.J. (1996). Soil phosphorus dynamics during seventeen years of continuous cultivation: Fractionation analysis. *Soil Science Society of America Journal.* 60:1168-1172.

Schneider, F., & Haderlein, S.B. (2016).Potential effects of biochar on the availability of phosphorus mechanistic insights. *Geoderma.* 277, 83–90

Schoenau, J. J., Stewart, J. W. B. & Bettany, J. R. (1989). Forms and cycling of phosphorus in prairie and boreal forest soils. *Biogeochemistry.* 8: 223–237.

Schoumans, O.F, & Chardon, W.J. (2015). Phosphate saturation degree and accumulation of phosphate in various soil types in Netherlands. *Geoderma.* 237-238:325-335.

Schwertmann, U. (1991). Solubility and dissolution of iron oxides. *Plant and Soil.* 130, 1–25.

Shafie, S.T., Salleh, M.A.M., Hang, L.L., Rahman, M.M., & Ghani, W.A.W.A.K. (2012). Effect of pyrolysis temperature on the biochar nutrient and water retention capacity. *Journal of Purity, Utility Reaction and Environment.* 1 323-337.

Sharpley, A.N., (1991). Soil phosphorus extracted by iron- aluminum oxide -impregnated filter paper. *Soil Science Society of America Journal.* 55: 1038-1041

Shen, J., Li, R., Zhanga, F., Fan, J., Tang, C., Rengel, Z. (2004). Crop yields, soil fertility and phosphorus fractions in response to long-term fertilization under the rice monoculture system on a calcareous soil. *Field Crops Research.* 86, 225–238.

Shepherd, J.G., Joseph, S., Sohi, S.P., Heal, K.V., (2017). Biochar and enhanced phosphate

capture: Mapping mechanisms to functional properties. *Chemosphere*. 179, 57-74.

Shinogi, Y., Yoshida, H., Koizumi, T., Yamaoka, M., & Saito, T. (2003) Basic characteristics of low-temperature carbon products from waste sludge. *Advances in Environmental Research.* 7: 661–665.

Sibanda, H.M. & Young, S.D. (1986). Competitive adsorption of humus acids and phosphate on goethite, gibbsite and two tropical soils. *Journal of Soil Science. 37:* 197-204.

Sibbesen, E., (1978). An investigation of the anion- exchange resin method for soil phosphate extraction. *Plant and Soil*. 50: 305-321.

Sibrell, P.L., Montgomery, G. A., Ritenour, K.L. & Tucker, T.W., (2009). Removal of phosphorus from agricultural wastewaters using adsorption media prepared from acid mine drainage sludge. *Water Research.* 43, 2240-2250.

Siddique, M.T. & Robinson, J.S. (2004). Differences in phosphorus retention and release in soils amended with animal manures and sewage sludge. *Soil Science Society of America Journal*. 68(4), 1421-1428.

Simard, R. R., Cluis, D., Gangbazo, G. & Beauchemin, S. (1995). Phosphorus status of forest and agricultural soils from a watershed of high animal density. *Journal Environmental Quality*. 24:1010–1017.

Sinclair, K., P. Slavich, S. Morris, S. Kimber, A. Downie. & L. Van Zwieten. (2010). Influence of biochar on soil fertility, carbon storage and biomass in subtropical pasture: Results from a 3-year field study. In: Proceedings of the 3rd International Biochar Conference, Rio de Janeiro, Brazil, 12-15 September 2010. p. 169-170.

Singh, B. & Gilkes, R.L. (1991). Phosphorus sorption in relation to soil properties for major soil types of south-western Australia. *Australian Journal of Soil Research*. 63:1350-

1358.

Smeck, N.F. (1985). Phosphorus dynamics in soils and landscape. Geoderma. 36:185-189

Sø, H.U., Postma, D., Jakobsen, R. & Larsen, F., (2011). Sorption of phosphate onto calcite; results from batch experiments and surface complexation modeling. *CeochimCosmochimActa*. 75, 2911-2923.

Sohi, S., Loez-Capel, S.E., Krull, E. & Bol, R. (2009). Biochar's roles in soil and climate change: a review of research needs. CSIRO, land and water science report 05/09, February; 64 pp., www.ias.ac.in/currsci/10nov2010/1218.pdf

Sohi, S.P., Krull, E., Lopez-Capel, E. & Bol, R. (2010). 'Chapter 2–A review of biochar and its use and function in soil', Advances in Agronomy 105: 47–82.

Soil Survey Staff, (1998, 2010). Keys to Soil Taxonomy, 11th ed. USDA Natural Resources Conservation Service, Washington, DC.

Sommers, L.E., Williams, J.D., & Syers J.K, Armstrong, D.E. & Harris, R.F (1972) Fractionation of organic phosphorus in lake sediments. *Soil Science Society of America Proceedings*. 36:51–54

Sparks, D.L. (2003). Environmental soil chemistry. 2nd ed. London: Academic Press.

Spielvogel, S., Prietzel, J. & Kogel-Knabner, I. (2008). Soil organic matter stabilization in acidic forest soils is preferential and soil type-specific. Eur. J. Soil Sci. 59, 674-692.

Spokas, K.A. (2010). Review of the stability of biochar in soils: predictability of O:C molar ratios. *Carbon Management*, 1, 289–303.

Spokas, K.A., K.B. Cantrell, J.M. Novak, D.W. Archer, J.A. Ippolito, H.P. Collins, A.A. Boateng, I.M. Lima, M.C. Lamb, A.J. McAloon, R.D. Lentz, and K.A. Nichols. (2012). Biochar: A Synthesis of Its Agronomic Impact beyond Carbon Sequestration.

Journal of Environmental Quality. 41: 973-989.

Spokas, K.A., Novak, J.M., Stewart, C.E., Cantrell, K.B., Uchimiya, M., DuSaire, M.G. *et al.* (2011). Qualitative analysis of volatile organic compounds on biochar. *Chemosphere*, 85, 869–882.

Sposito, G. (2008).The Chemistry of Soils, 2nd ed. New York, NY: Oxford University Press.

Steiner, C., Glaser, B., Teixeira, W.G., Lehmann, J., Blum, W.E.H, & Zech, W. (2008). Nitrogen retention and plant uptake on a highly weathered central Amazonian Ferralsol amended with compost and charcoal. *Journal of Plant Nutrition and Soil Science*. 171:893–899.

Steiner, C., Teixeira, W.G., Lehmann, J., Nehls, T,, de Macˆedo, J.L.V., Blum, W.E.H., & Zech, W. (2007). Long term effects of manure, charcoal, and mineral fertilization on crop production and fertility on a highly weathered Central Amazonian upland soil. *Plant Soil.* 291: 275–290.

Stevenson, F.J, & Cole, M.A. (1999). Cycles of the Soil: Carbon, Nitrogen, Phosphorus, Sulfur, Micronutrients. 2nd Ed. John Wiley and Sons, Inc., New York.

Stewart, C.E., Zheng, J., Botte, J, & Cotrufo, M.F. (2012) Co-generated fast pyrolysis biochar mitigates greenhouse gas emissions and increase carbon sequestration in temperate soils. *GCB Bioenergy* 5:153–164.

Strauss, R., Brummer, G. W. & Barrow, N.J. (1997). Effects of crystallinity of goethite: II. Rates of sorption and desorption of phosphate. *European Journal of Soil Science* 48:101-114

Stumm, W. & Leckie, J.O. (1970). Proceedings of the 5th International Pollution Research Conference. San Francisco, CA: Pergamon; Phosphate exchange with sediments; its

role in the productivity of surface water.

Subedi, R., Taupe, N., Pelissetti, S., Petruzzelli, L., Bertora, C., Leahy, J., Grignani, C., (2016). Greenhouse gas emissions and soil properties following amendment with manure-derived biochars: influence of pyrolysis temperature and feedstock type. *Journal of Environmental Management.* 166, 73-83.

Sui, Y., Thompson M. L., and Mize, C. W. (1999). Redistribution of biosolids-derived total P applied to a Mollisol. *Journal of Environmental Quality.* 28:1068-1074.

Tang, J., Zhu, W., Kookana, R, and Katayama A. (2013). Characteristics of biochar and its application in remediation of contaminated soil. *Journal of Bioscience and Bioengineering.* 116 (6), 653-659.

Tetteh, J.L. (2014). Adsorptive characteristics of phosphorus onto four biochar types. M.Phil Thesis presented to University Ghana, Department of soil science.

Thygesen, A., Wernberg, O., Skou, E. & Sommer, S.G., (2011). Effect of incineration temperature on phosphorus availability in bio-ash from manure. *Environmental Technology.* 32, 633-638.

Tiessen, H. & Moir, J.O. (2008) Characterisation of available P by sequential extraction. In: Carter MR, Gregorich EG (eds) Soil sampling and methods of analysis, 2nd edn. CRC, Boca Raton, pp 293-306

Tiessen, H., & Moir, J.O. (1993) Characterization of available P by sequential extraction, in: M.R. Carter (Ed.), Soil Sampling and Methods of Analysis, Lewis, Boca Raton, FL, 1 , pp. 293-306.

Tiessen, H., Stewart, J.W.B., Cole, C.V., (1984). Pathways of phosphorus transformation in soils of differing pedogenesis. Soil Science Society of America Journal 48, 853– 858

Tisdale, S.L., Nelson, W.L & Beaton, J.D. (1985). *Soil Fertility and Fertilizers*. 4 edition. Macmillan Publishing Company, New York, USA. pp. 189-248

Tisdale, S.L., Havlin, J.L., Beaton, J.D. & Nelson. W.L. (1999). Soil fertility and fertilizers: An introduction to nutrient management. 6499 pp.

Torrent, J., U. Schwertmann, and V. Barron. (1992). Fast and slow phosphate sorption by goethite-rich natural materials. Clays and Clay Minerals. 40:14-21.

Trasar-Cepeda, M.C., Gil-Stores, F. & Giutain-Ojea, F. (1986). Charaterization del en suelos gailegos: Estudio comparative del los procedimientos de Chang y jackson. 1957, y de hedley et al., 1982. An Edafol. Agrobiol. 45: 37-52.

Triana, S.J., Sposito, G., Hesterberg, D. & Kafkafi, U. (1986). Effects of pH and organic acids on orthophosphate solubility in an acidic, montimorillonitic soil. *Soil Science Society of America Journal*. 50: 45- 52.

Trolove, S. N., Hedley, M. J., Kirk, G. J., Bolan, N. S. & Loganathan, P. (2003). Progress in selected areas of rhizosphere research on P acquisition. *Australian Journal of Soil Research*. 41: 471-499

Tsai, W.T., Liu, S.C., Chen, H.R., Chang, Y.M., Tsai, Y.L., (2012). Textural and chemical properties of swine-manure-derived biochar pertinent to its potential use as a soil amendment. *Chemosphere.* 89:198-203.

Tunesi, S., Poggi, V., Gessa, C. (1999). Phosphate adsorption and precipitation in calcareous soils: the role of calcium ions in solution and carbonate minerals. *Nutrient Cycling in Agroecosystems.* 53, 219–227.

Turner, B.L., Newman, S., & Reddy, K.R. (2006) Overestimation of organic phosphorus in wetland soils by alkaline extraction and molybdate colorimetry. *Environmental*

Science and Technology. 40:3349–3354

Turrion, M.B., Gallardo, J.F., Haumair, L., Gonzalez, M.L. & Zech, W. (2001). 31P NMR characterization of phosphorus fractions in natural and fertilized soils. *Animals and Forest Science.* 58: 89-98.

Uchimiya, M. & Hiradate, S., (2014). Pyrolysis temperature-dependent changes in dissolved phosphorus speciation of plant and manure biochars. *Journal of Agriculture and Food Chemistry*. 62, 1802–1809.

Udo, E.J. & Ogunwale, J.A., (1977). Phosphorus fractions in selected Nigerian soils. *Soil Science Society of America Journal*. 41, 1141– 1146.

Udo, E.J. (1977). Forms and distribution of phosphorus in three Nigerian soil profiles along a toposequence. *Tropical Agriculture*. *54*, 149–156.

Uras, U., Carrier, M., Hardie, A.G. & Knoetze, J.H. (2011). Physicochemical characterization of biochars from vacuum pyrolysis of South African agricultural wastes for application as soil amendments. *Journal of Analytical and Applied Pyrolysis.* 98:207-213.

USEPA Ecological restoration: A tool to manage stream quality, Report EPA 841-F-95-007; US EPA: Washington, DC, USA, 1995.

Uzoma, K.C,, Inoue, M., Andry, H., Fujimaki, H., Zahoor, A., & Nishihara, E. (2011). Effect of cow manure biochar on maize productivity under sandy soil condition. *Soil Use Management*. 27:205-212.

Van der Zee, S.E.A.T.M., Fokkink, L.G.J. & van Riemsdijk, W.H. (1987). A new technique for assessment of reversibly adsorbed phosphate. *Soil Science Society of America Journal*. 51:599-604.

Van Eck, G.T.M. (1982) Forms of phosphorus in particulate matter from the Holland Diep/Haringuliet, The Netherlands. *Hydrobiologia.* 92:665–681.

Van Zwieten, L., Kimber, S., Morris, S., Chan, K., Downie, A., Rust, J., Joseph, S. & Cowie, A. (2010a). Effects of biochar from slow pyrolysis of papermill waste on agronomic performance and soil fertility. *Plant Soil.* 327: 235-246.

Verheijen, F., Jeffery, S., Bastos, A.C, van der Velde, M. & Diafas, I. (2010). Biochar application to soils: a critical scientific review of effects on soil properties, processes and functions. European Commission; http://eusoils. jrc.ec.europa.eu/esdb archive/eusoils docs/other/EUR24099.pdf.

Verma, S., Subehia, S.K. & Sharma, S.P. (2005). Phosphorous fractions in an acid soil continuously fertilized with mineral and organic fertilizers. *Biology and Fertility Soils*. 41, 295-300.

Villapando, R.R., & Graetz, D.A. (2001). Phosphorus sorption and desorption properties of the spodic horizon from selected Florida Spodosols. *Soil Science Society of America Journal.* 65:331–339.

Wager, B.I., Stewart, J.W.B. & Moir, J.O. (1986). Changes with time in the form and availability of residual fertilizer phosphorus on Chernozemic soils. *Canadian Journal Soil Science*. 66:105±119.

Wahab, M.A., Hassine, R.B. & Jellali, S., (2011). Removal of phosphorus from aqueous solution by *Posidonia oceanica* fibers using continuous stirring tank reactor, *Journal of Hazardous Materials.* 191, 333–341.

Walker, T.W. & Syers, J.K., (1976). The fate of phosphorus during pedogenesis. *Geoderma* 15, 1 –19.

Wang, L., & Nancollas, G. H. (2008). Calcium orthophosphates: Crystallization and dissolution. *Chemical Research.* 108, 4628-4669.

Wang, T., Camps-Arbestain, M., Hedley, M. & Bishop, P. (2012). Predicting phosphorus bioavailability from high-ash biochars. *Environmental Pollution.* 357, 173–187.

Wang, T., Camps-Arbestain, M., Hedley, M., (2014). The fate of phosphorus of ash-rich biochars in a soil-plant system. *Plant Soil.* 375, 61–74.

Wang, X., Liu, F., Tan, W., Li, W., Feng, X. & Sparks, D.L. (2013). Characteristics of phosphate adsorption–desorption onto ferrihydrite: comparison with well-crystalline Fe (hydr)oxides. *Soil Science*. 178, 1–11

Wang, Z., Guo, H., Shen, F., Yang, G., Zhang, Y., Zeng, Y., Wang, L., Xiao, H. & Deng, S., (2015a). Biochar produced from oak sawdust by lanthanum (La)-involved pyrolysis for adsorption of ammonium (NH_4^+), nitrate (NO_3^-), and phosphate (PO_4^{3-}). *Chemosphere* .119, 646-653.

Weber, W.J., Morris, J.C., (1963). Kinetics of adsorption on carbon from solution. *Journal of Sanitation Engneering: Division of American Society of Civic Engneering*. 89, 31-60.

Wei, S., Tan, W., Liu, F., Zhao, W., & Weng, L. (2014). Surface properties and phosphate adsorption of binary systems containing goethite and kaolinite. Geoderma 213: 478–484.

Weng, L.P., Vega, F.A., & Van Riemsdijk, W.H. (2011). Competitive and synergistic effects in pH dependent phosphate adsorption in soils: LCD modeling. *Environmental Science and Technology* 45 (19): 8420–8428.

Weng, L., Van Riemsdijk, W.H., & Hiemstra, T. (2012). Factors controlling phosphate interaction with iron oxides. *Journal of Environmental Qualility*. 45:231-267.

White, R.E. (1981). Retention and release of phosphate by soils and soil constituents. In soils and agriculture. P. B. Tinker (ed.). A halsted Press Book. John Wiley and Sons. NY pp. 71-114.

Wilding, L. P., Brown, R. E., & Holowaychuk, N. (1969): Asccesibility and properties of occluded carbon in biogenetic opal. *Soil Science*, 103, 56–61.

Williams, J.D.H., Mayer, T. & Nriagu, J.O. (1980). Extractability of phosphorus from phosphate minerals common in soils and sediments. *Soil Science Society of America Journal*. 44:4 62-465.

WRB, 1998. World Reference Base for Soil Resources. World Resources Report. No. 84. FAO, Rome.

Wu, F.C.; Tseng, R.L.; Huang, S.C.; & Juang, R.S. (2009). Characteristics of pseudo-second-order kinetic model for liquid-phase adsorption: A mini-review. *Chemical Engineering. Journal 151*, 1–9.

Wu, H., Yip, K., Kong, Z., Li, C.-Z., Liu, D., Yu, Y. & Gao, X.,(2011). Removal and recycling of inherent inorganic nutrient species in mallee biomass and derived biochars by water leaching. *Industrial and Engneering Chemistry Research*. 50, 12143–12151.

Xie, M., Chen, W., Xu, Z., Zheng, S. & Zhu, D., (2014). Adsorption of sulfonamides to demineralized pine wood biochars prepared under different thermochemical conditions. *Environmental Pollution*. 186, 187-194.

Xu, G., Shao, H.B. & Sun, J.N., (2013). What is more important for enhancing nutrient bioavailability with biochar application into a sandy soil: direct or indirect mechanism? *Ecological Engneering*. 52, 119–124.

Xu, G., Sun, J., Shao, H., & Chang, S.X. (2014). Biochar had effects on phosphorus sorption and desorption in three soils with differing acidity. *Ecological Engineering*. 62: 54– 60

Xu, G., Zhang, Y., Shao, H., & Sun, J. (2016). Pyrolysis temperature affects phosphorus transformation in biochar: Chemical fractionation and 31P NMR analysis. *Science of the Total Environment*. 569–570: 65–72

Yao, F.X., Camps Arbestain, M., Virgel, S., Blanco, F., Arostegui, J., Maciá-Agulló, J.A, & Macías, F. (2010) Simulated geochemical weathering of a mineral ashrich biochar in a modified Soxhlet reactor. *Chemosphere*. 80, 724–732.

Yao, Y., Gao, B., Chen, J., Yang, L., (2012). Engineered biochar reclaiming phosphate from aqueous solutions: mechanisms and potential application as a slow-release fertilizer. *Environmental Science and Technology*. 47 (15), 8700–8708

Yao, Y., Gao, B., Inyang, M., Zimmerman, A.R., Cao, X.D., Pullammanappallil, P. & Yang, L.Y., (2011). Removal of phosphate from aqueous solution by biochar derived from anaerobically digested sugar beet tailings. *Journal of Hazardous Materials*. 190 (1–3), 501-507.

Yin, C. (2012). Microwave-assisted pyrolysis of biomass for liquid biofuels production. *Bioresource Technology*. 120: 273-284.

Yip, K.; Xu, M.; Li, C.-Z.; Jiang, S. P.; Wu, H. (2011). Biochar as a fuel: Mechanistic understanding on biochar thermal annealing at mild temperatures and its effect on biochar reactivity. *Energy Fuels.* 25, 406-414.

Yoshimura, M., Sujaridworakun, P., Koh, F., Fujiwara, T., Pongkao, D., Ahniyaz, A., (2004). Hydrothermal conversion of calcite crystals to hydroxyapatite. *Materials Science and*

Engneering. 24, 521–525.

Yu, L. M. & Teruo, M. (2013). Biochar derived from dairy cattle carcasses as an alternative source of phosphorus and amendment for soil acidity. *Soil Science and Plant Nutrition*. *59*: 628-641.

Yuan, J., Xu, R. & Zhang, H., (2011). The forms of alkalis in the biochar produced from crop residues at different temperatures. *Bioresource Technology.* 102: 3488-3497.

Yuan, J.H & Xu, R.K. (2012). Effects of biochars generated from crop residues on chemical properties of acid soils from tropical and subtropical China. *Soil Research.* 50:570-578.

Zeldowitsch, J. (1934). Über den Mechanismus der katalytischen Oxidation von CO und MnO_2, *Acta Physicochimica URSS*. 1, 364–449.

Zhai, L., CaiJi, Z., Liu, J., Wang, H., Ren, T., Gai, X., Xi, B., Liu, H., (2014). Short-term effects of maize residue biochar on phosphorus availability in two soils with different phosphorus sorption capacities. *Biology and Fertility Soils*. 51, 113–122.

Zhang, A., Cui, L., Pan, G., Li, L., Hussain, Q., Zhang, X., Zheng, J. & Crowley, D., (2010). Effect of biochar amendment on yield and methane and nitrous oxide emissions from a rice paddy from Tai Lake plain of China. Agriculture. *Ecosystem and Environment.* 139, 469–475.

Zhang, H., Chen, C., Gray, E.M., Boyd, S.E., Yang, H., Zhang, D., (2016). Roles of biochar in improving phosphorus availability in soils: a phosphate adsorbent and a source of available phosphorus. *Geoderma.* 276, 1-6.

Zhang, H., Voroney, R.P., Price, G.W., (2015a). Effects of temperature and processing conditions on biochar chemical properties and their influence on soil C and N

transformations. *Soil Biology and Biochemstry*. 83, 19-28

Zhang, J., Liu, J., Liu, R.L., (2015b). Effects of pyrolysis temperature and heating time on biochar obtained from the pyrolysis of straw and lignosulfonate. *Bioresource Technology*. 176, 288-291.

Zhao, L., Cao, X., Masek, O. & Zimmerman, A. (2013). Heterogeneity of biochar properties as a function of feedstock sources and production temperatures. *Journal of Hazardous Materials.* 256-257:19.

Zheng, H.Z., Deng, X., Zhao, J., Luo, Y., Novak, J., Herbert, S. & Xing, B. (2013). Characteristics and nutrient values of biochars produced from giant reed at different temperatures. *Bioresource Technology*. 130, 463–471.

APPENDICES

Appendix 3A

X- ray powder diffraction of cocoa pod husk biochar

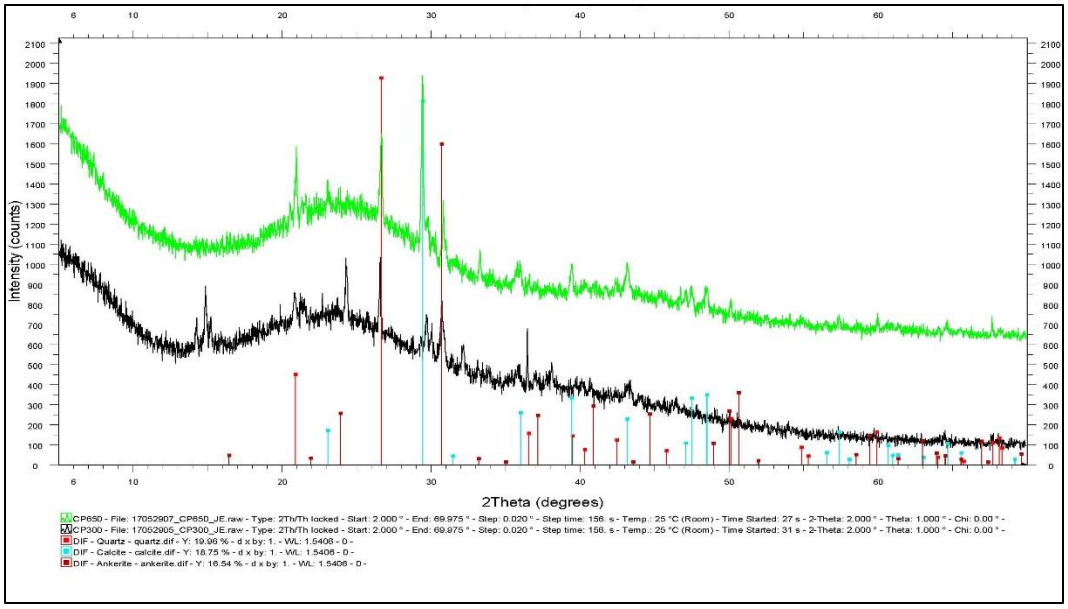

X-ray powder diffraction of palm kernel biochar

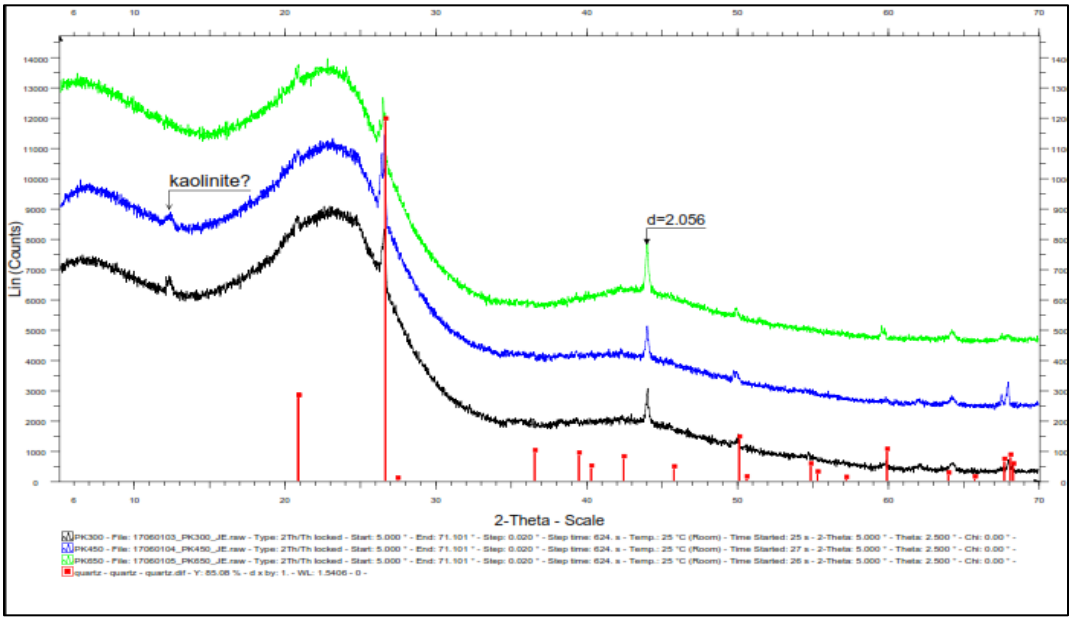

X- ray powder diffraction of rice husk biochar

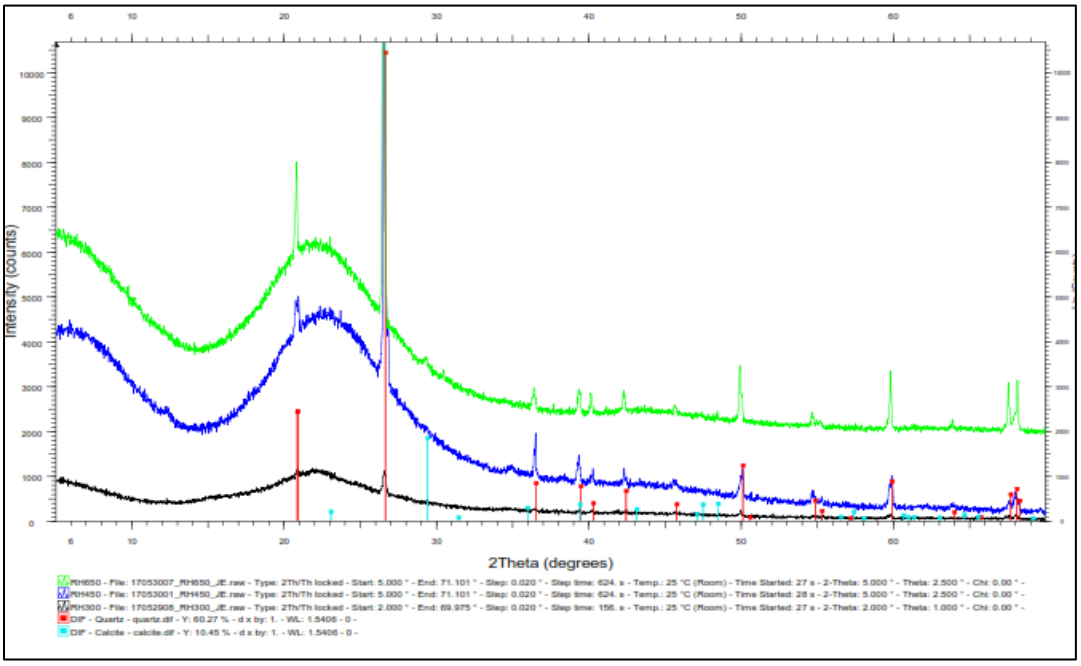

X- ray powder diffraction of corn cob biochar

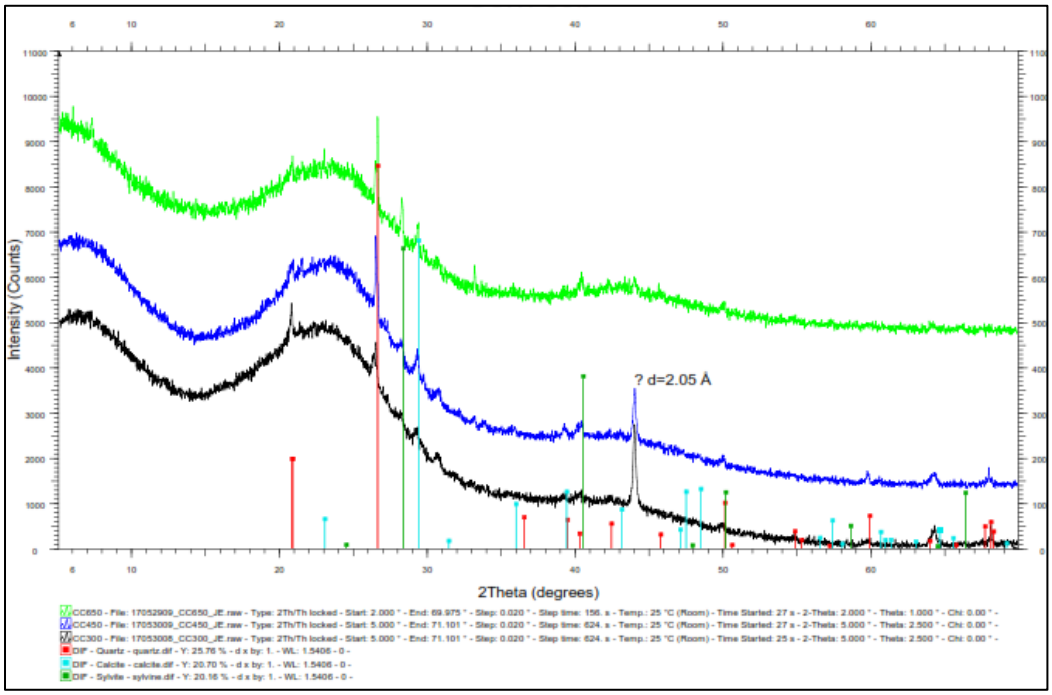

Appnedix 3B

Demensionless factor (R_L) for the biochar types

CP300	CP650	CC300	CC650	PK300	PK650	RH300	RH650
0.7	0.8	0.8	0.8	0.8	0.7	0.7	0.7
0.5	0.7	0.7	0.7	0.7	0.5	0.5	0.5
0.4	0.6	0.6	0.6	0.6	0.4	0.4	0.4
0.3	0.5	0.5	0.5	0.5	0.3	0.3	0.3
0.3	0.4	0.4	0.4	0.4	0.3	0.3	0.3
0.3	0.4	0.4	0.4	0.4	0.3	0.3	0.3
0.2	0.3	0.3	0.3	0.3	0.2	0.2	0.2

Appendix 3C

Pearson correlation coefficient values between elements concentration and P sorption capacity for all biochar types at the different pyrolysis temperatures. * = $p < 0.05$

Elements	P sorption capacity
Fe	0.74*
Mn	-0.22
Mg	-0.50
Al	0.94*
Cu	0.05
Zn	-0.31
Ca	-0.35
Na	-0.25
K	-0.51
CEC	-0.84*

Appendix 4A: Textural triangle used for textural class

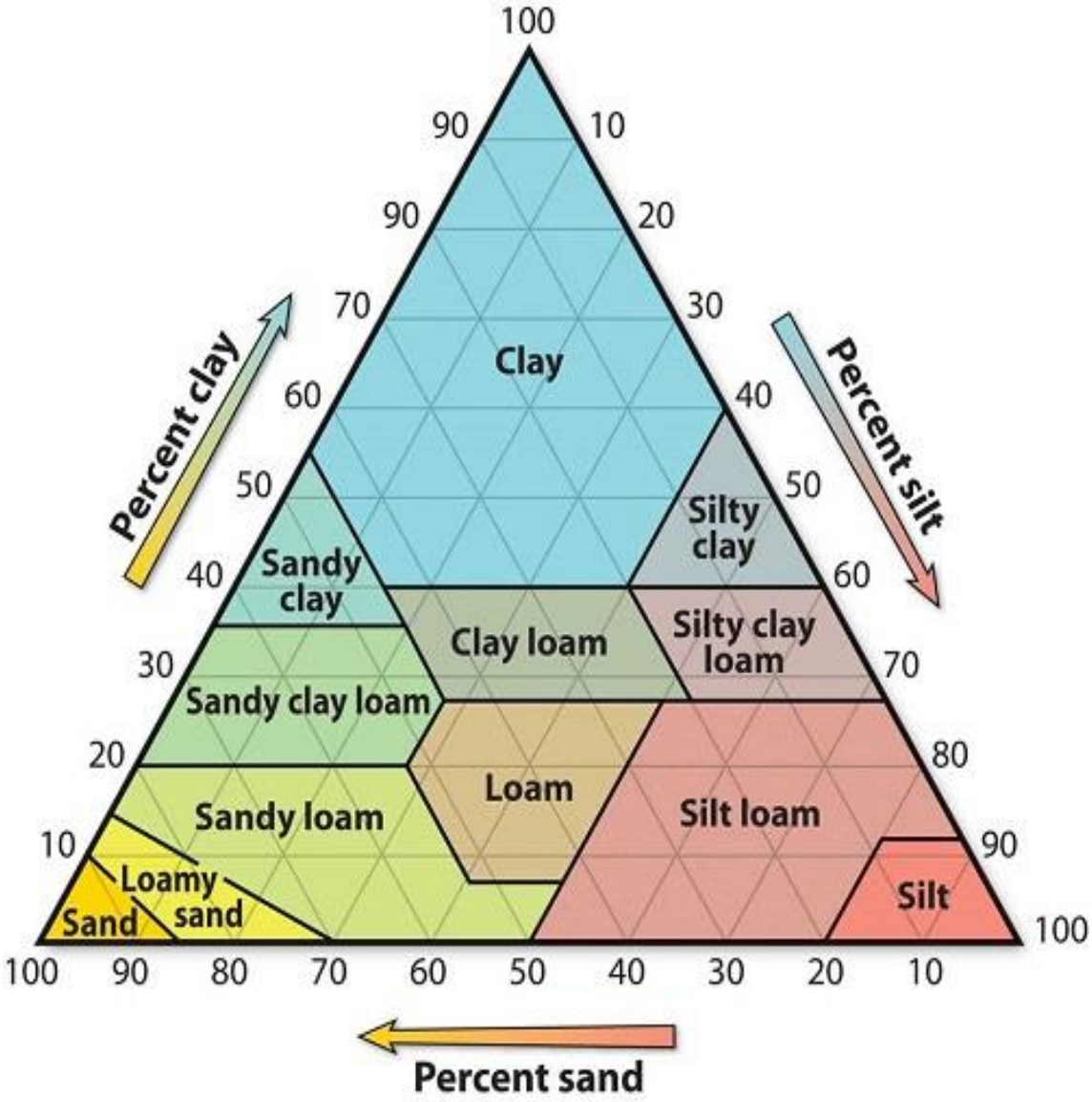

Appendix 4B. Analysis of variance on chemical properties of biochar amended soils

Al_d (Ankasa)

Source of variation	d.f.	s.s.	m.s.	v.r.	F pr.
Treatment	6	3.6591	0.6098	5.22	0.005
Residual	14	1.6363	0.1169		
Total	20	5.2954			

Analysis of variance

Al_d (Keta)

Source of variation	d.f.	s.s.	m.s.	v.r.	F pr.
Treatment	6	0.46007	0.07668	6.26	0.002
Residual	14	0.17159	0.01226		
Total	20	0.63166			

Al_d (Kokofu)

Source of variation	d.f.	s.s.	m.s.	v.r.	F pr.
Treatment	6	4.4436	0.7406	4.35	0.011
Residual	14	2.3821	0.1702		
Total	20	6.8257			

Al_o (Ankasa)

Source of variation	d.f.	s.s.	m.s.	v.r.	F pr.
Treatment	6	0.36623	0.06104	4.45	0.010
Residual	14	0.19197	0.01371		
Total	20	0.55820			

Al_o (Keta)

Source of variation	d.f.	s.s.	m.s.	v.r.	F pr.
Treatment	6	0.0494141	0.0082357	62.37	<.001
Residual	14	0.0018485	0.0001320		
Total	20	0.0512626			

Al_o (Kokofu)

Source of variation	d.f.	s.s.	m.s.	v.r.	F pr.
Treatment	6	1.22802	0.20467	19.08	<.001
Residual	14	0.15020	0.01073		
Total	20	1.37821			

Ca (Ankasa)

Source of variation	d.f.	s.s.	m.s.	v.r.	F pr.
Treatment	6	0.0806706	0.0134451	134.18	<.001
Residual	14	0.0014028	0.0001002		
Total	20	0.0820735			

Ca (Keta)

Source of variation	d.f.	s.s.	m.s.	v.r.	F pr.
Treatment	6	0.391126	0.065188	10.86	<.001
Residual	14	0.084034	0.006002		
Total	20	0.475160			

Ca (Kokofu)

Source of variation	d.f.	s.s.	m.s.	v.r.	F pr.
Treatment	6	0.268663	0.044777	33.14	<.001
Residual	14	0.018914	0.001351		
Total	20	0.287578			

Fe_d (Ankasa)

Source of variation	d.f.	s.s.	m.s.	v.r.	F pr.
Treatment	6	25.9145	4.3191	29.89	<.001
Residual	14	2.0231	0.1445		
Total	20	27.9376			

Fe_d (Keta)

Source of variation	d.f.	s.s.	m.s.	v.r.	F pr.
Treatment	6	0.23014	0.03836	1.71	0.192
Residual	14	0.31450	0.02246		
Total	20	0.54464			

Fe_d (Kokofu)

Source of variation	d.f.	s.s.	m.s.	v.r.	F pr.
Treatment	6	63.02742	10.50457	116.56	<.001
Residual	14	1.26168	0.09012		
Total	20	64.28910			

Fe_o (Ankasa)

Source of variation	d.f.	s.s.	m.s.	v.r.	F pr.
Treatment	6	0.103781	0.017297	3.84	0.018
Residual	14	0.062983	0.004499		
Total	20	0.166764			

Fe_o (Keta)

Source of variation	d.f.	s.s.	m.s.	v.r.	F pr.
Treatment	6	0.071507	0.011918	8.88	<.001
Residual	14	0.018800	0.001343		
Total	20	0.090307			

Fe_o (Kokofu)

Source of variation	d.f.	s.s.	m.s.	v.r.	F pr.
Treatment	6	0.875624	0.145937	19.50	<.001
Residual	14	0.104750	0.007482		
Total	20	0.980374			

OC (Ankasa)

Source of variation	d.f.	s.s.	m.s.	v.r.	F pr.
Treatment	6	0.320581	0.053430	8.56	<.001
Residual	14	0.087400	0.006243		
Total	20	0.407981			

OC (Keta)

Source of variation	d.f.	s.s.	m.s.	v.r.	F pr.
Treatment	6	0.063429	0.010571	6.20	0.002
Residual	14	0.023867	0.001705		
Total	20	0.087295			

OC (Kokofu)

Source of variation	d.f.	s.s.	m.s.	v.r.	F pr.
Treatment	6	0.979257	0.163210	29.37	<.001
Residual	14	0.077800	0.005557		
Total	20	1.057057			

Appendix 4C. Analysis of variance on P sorption maximum (Pmax)

Pmax (Ankasa)

Source of variation	d.f.	s.s.	m.s.	v.r.	F pr.
Treatment	6	47087.3	7847.9	19.30	<.001
Residual	14	5692.6	406.6		
Total	20	52779.9			

Pmax (Keta)

Source of variation	d.f.	s.s.	m.s.	v.r.	F pr.
Treatment	6	25367.1	4227.8	22.44	<.001
Residual	14	2637.2	188.4		
Total	20	28004.3			

Pmax (Kokofu)

Source of variation	d.f.	s.s.	m.s.	v.r.	F pr.
Treatment	6	58602.5	9767.1	14.22	<.001
Residual	14	9612.9	686.6		
Total	20	68215.4			

Appendix 5A. Analysis of variance on P fractions of biochar

HCl-Pi

Source of variation	d.f.	s.s.	m.s.	v.r.	F pr.
Treatment	5	23132.6	4626.5	10.85	<.001
Residual	12	5119.1	426.6		
Total	17	28251.8			

NaOH-Pi

Source of variation	d.f.	s.s.	m.s.	v.r.	F pr.
Treatment	5	1471.49	294.30	5.95	0.005
Residual	12	593.95	49.50		
Total	17	2065.44			

$NaHCO_3$-Pi

Source of variation	d.f.	s.s.	m.s.	v.r.	F pr.
Treatment	5	943.83	188.77	3.63	0.031
Residual	12	623.19	51.93		
Total	17	1567.02			

Residual-P

Source of variation	d.f.	s.s.	m.s.	v.r.	F pr.
Tretament	5	252688.	50538.	6.70	0.003
Residual	12	90468.	7539.		
Total	17	343156.			

Resin-Pi

Source of variation	d.f.	s.s.	m.s.	v.r.	F pr.
Treatment	5	45737.2	9147.4	18.58	<.001
Residual	12	5908.5	492.4		
Total	17	51645.8			

Sum of organic P

Source of variation	d.f.	s.s.	m.s.	v.r.	F pr.
Treatment	5	6118.	1224.	1.09	0.416
Residual	12	13513.	1126.		
Total	17	19631.			

Total P

Source of variation	d.f.	s.s.	m.s.	v.r.	F pr.
Treatment	5	1143961.	228792.	107.89	<.001
Residual	12	25448.	2121.		
Total	17	1169409.			

Appendix 5B. Analysis of variance on biochar amended Ankasa P fractions

HCl-Pi

Source of variation	d.f.	s.s.	m.s.	v.r.	F pr.
Treatment	6	1263.543	210.590	62.38	<.001
Residual	14	47.261	3.376		
Total	20	1310.804			

NaOH-Pi

Source of variation	d.f.	s.s.	m.s.	v.r.	F pr.
Treatment	6	614.031	102.339	14.88	<.001
Residual	14	96.255	6.875		
Total	20	710.286			

$NaHCO_3$-Pi

Source of variation	d.f.	s.s.	m.s.	v.r.	F pr.
Treatment	6	300.446	50.074	8.44	<.001
Residual	14	83.040	5.931		
Total	20	383.486			

Residual P

Source of variation	d.f.	s.s.	m.s.	v.r.	F pr.
Treatment	6	2336.79	389.47	17.82	<.001
Residual	14	305.91	21.85		
Total	20	2642.70			

Resin-Pi

Source of variation	d.f.	s.s.	m.s.	v.r.	F pr.
Treatment	6	2716.858	452.810	50.35	<.001
Residual	14	125.894	8.992		
Total	20	2842.752			

Sum of organic P

Source of variation	d.f.	s.s.	m.s.	v.r.	F pr.
Treatment	6	4514.22	752.37	12.31	<.001
Residual	14	855.45	61.10		
Total	20	5369.67			

Total P

Source of variation	d.f.	s.s.	m.s.	v.r.	F pr.
Treatment	6	50628.3	8438.1	19.55	<.001
Residual	14	6042.5	431.6		
Total	20	56670.9			

Appendix 5C. Analysis of variance on biochar amended Keta P fractions

HCl-Pi

Source of variation	d.f.	s.s.	m.s.	v.r.	F pr.
Treatment	6	983.14	163.86	8.94	<.001
Residual	14	256.50	18.32		
Total	20	1239.64			

NaOH-Pi

Source of variation	d.f.	s.s.	m.s.	v.r.	F pr.
Treatment	6	370.517	61.753	7.24	0.001
Residual	14	119.336	8.524		
Total	20	489.853			

$NaHCO_3$-Pi

Source of variation	d.f.	s.s.	m.s.	v.r.	F pr.
Treatment	6	239.143	39.857	7.29	0.001
Residual	14	76.500	5.464		
Total	20	315.643			

Residual-P

Source of variation	d.f.	s.s.	m.s.	v.r.	F pr.
Treatment	6	2256.58	376.10	7.40	0.001
Residual	14	711.42	50.82		
Total	20	2968.00			

Resin-Pi

Source of variation	d.f.	s.s.	m.s.	v.r.	F pr.
Treatment	6	837.531	139.588	40.83	<.001
Residual	14	47.860	3.419		
Total	20	885.390			

Sum of organic P

Source of variation	d.f.	s.s.	m.s.	v.r.	F pr.
Treatment	6	2758.09	459.68	8.89	<.001
Residual	14	723.85	51.70		
Total	20	3481.94			

Total P

Source of variation	d.f.	s.s.	m.s.	v.r.	F pr.
Treatment	6	13036.5	2172.8	4.40	0.010
Residual	14	6906.4	493.3		
Total	20	19942.9			

Appendix 5D. Analysis of variance on biochar amended Kokofu P fractions

HCl-Pi

Source of variation	d.f.	s.s.	m.s.	v.r.	F pr.
Treatment	6	1527.633	254.606	50.00	<.001
Residual	14	71.290	5.092		
Total	20	1598.923			

NaOH-Pi

Source of variation	d.f.	s.s.	m.s.	v.r.	F pr.
Treatment	6	524.794	87.466	14.06	<.001
Residual	14	87.065	6.219		
Total	20	611.859			

$NaHCO_3$-Pi

Source of variation	d.f.	s.s.	m.s.	v.r.	F pr.
Treatment	6	314.196	52.366	5.55	0.004
Residual	14	132.143	9.439		
Total	20	446.339			

Residual P

Source of variation	d.f.	s.s.	m.s.	v.r.	F pr.
Treatment	6	27232.7	4538.8	45.00	<.001
Residual	14	1412.1	100.9		
Total	20	28644.8			

Resin Pi

Source of variation	d.f.	s.s.	m.s.	v.r.	F pr.
Treatment	6	1682.857	280.476	59.45	<.001
Residual	14	66.050	4.718		
Total	20	1748.907			

Sum of organic P

Source of variation	d.f.	s.s.	m.s.	v.r.	F pr.
Treatment	6	7552.9	1258.8	10.94	<.001
Residual	14	1610.6	115.0		
Total	20	9163.5			

Total P

Source of variation	d.f.	s.s.	m.s.	v.r.	F pr.
Treatment	6	46850.7	7808.4	30.50	<.001
Residual	14	3583.9	256.0		
Total	20	50434.6			

PCA showing P Fractions and some chemical proeprties of the biochar (corn cob and rice husk) amended soils (Kokofu, Ankasa and Keta)

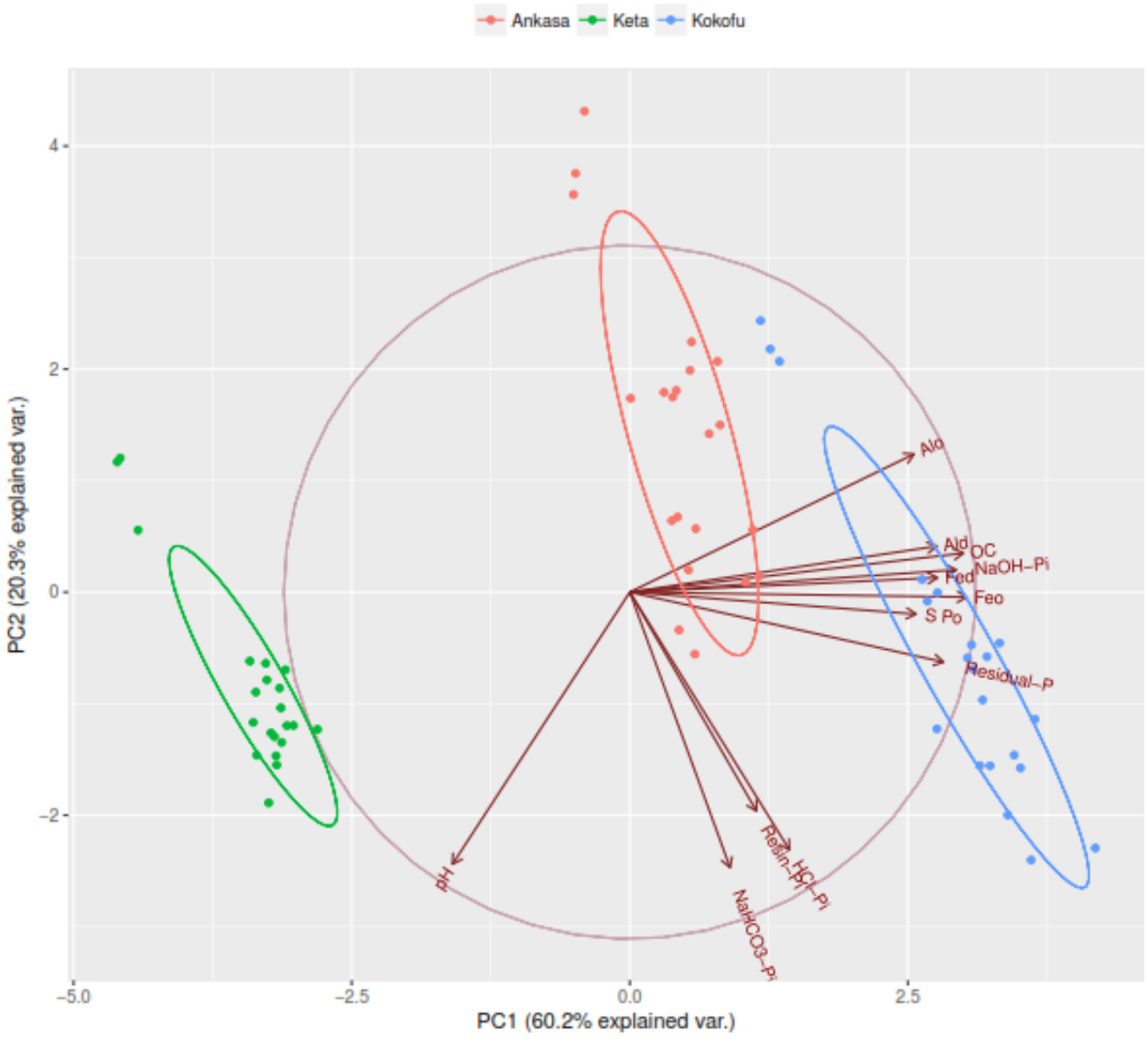

PCA showing P Fractions and soil chemical properties of biochar (corn corn and rice husk) amended Kokofu soil

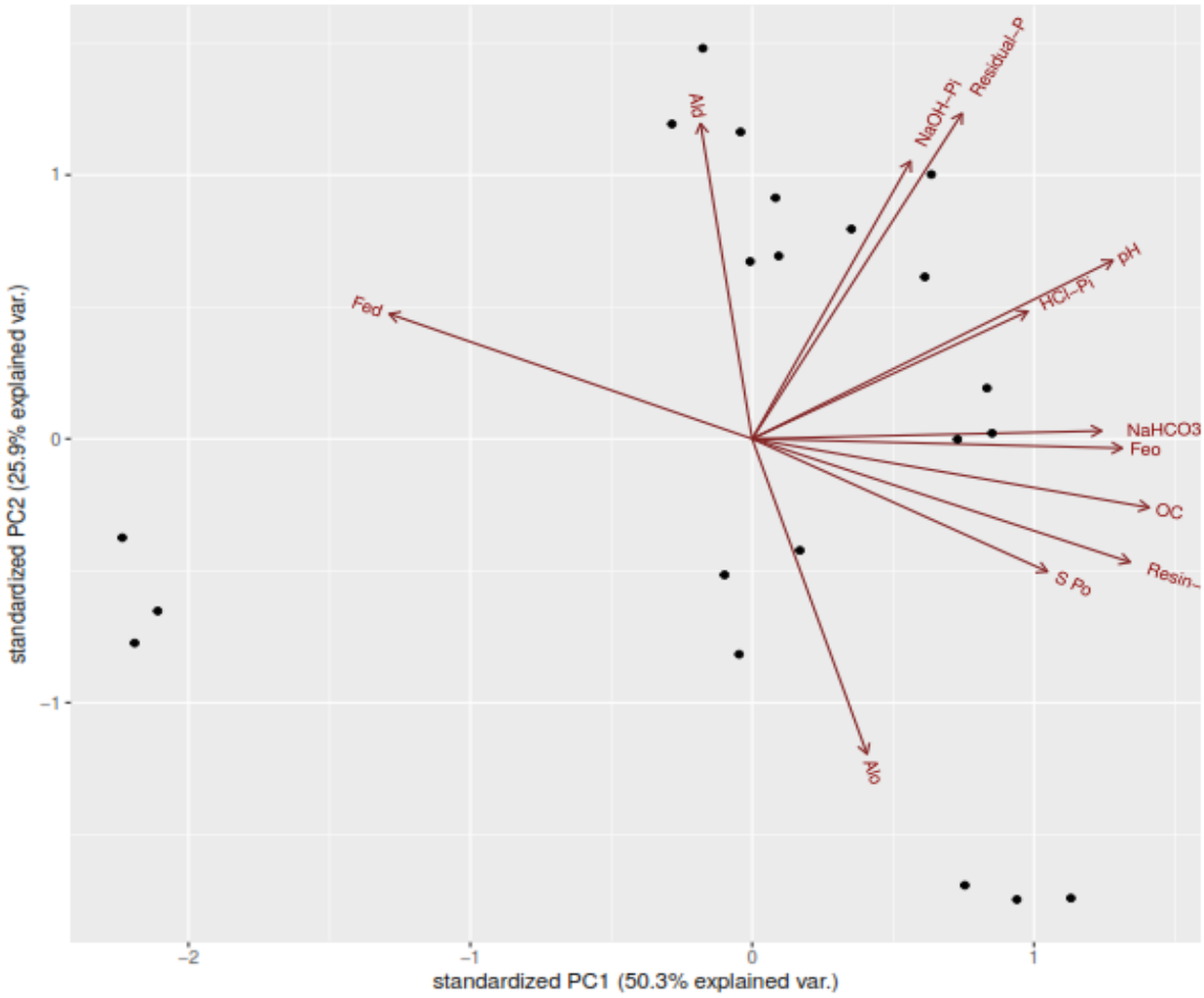

PCA showing P Fractions and soil chemical properties of biochar (corn corn and rice husk) amended Ankasa soil

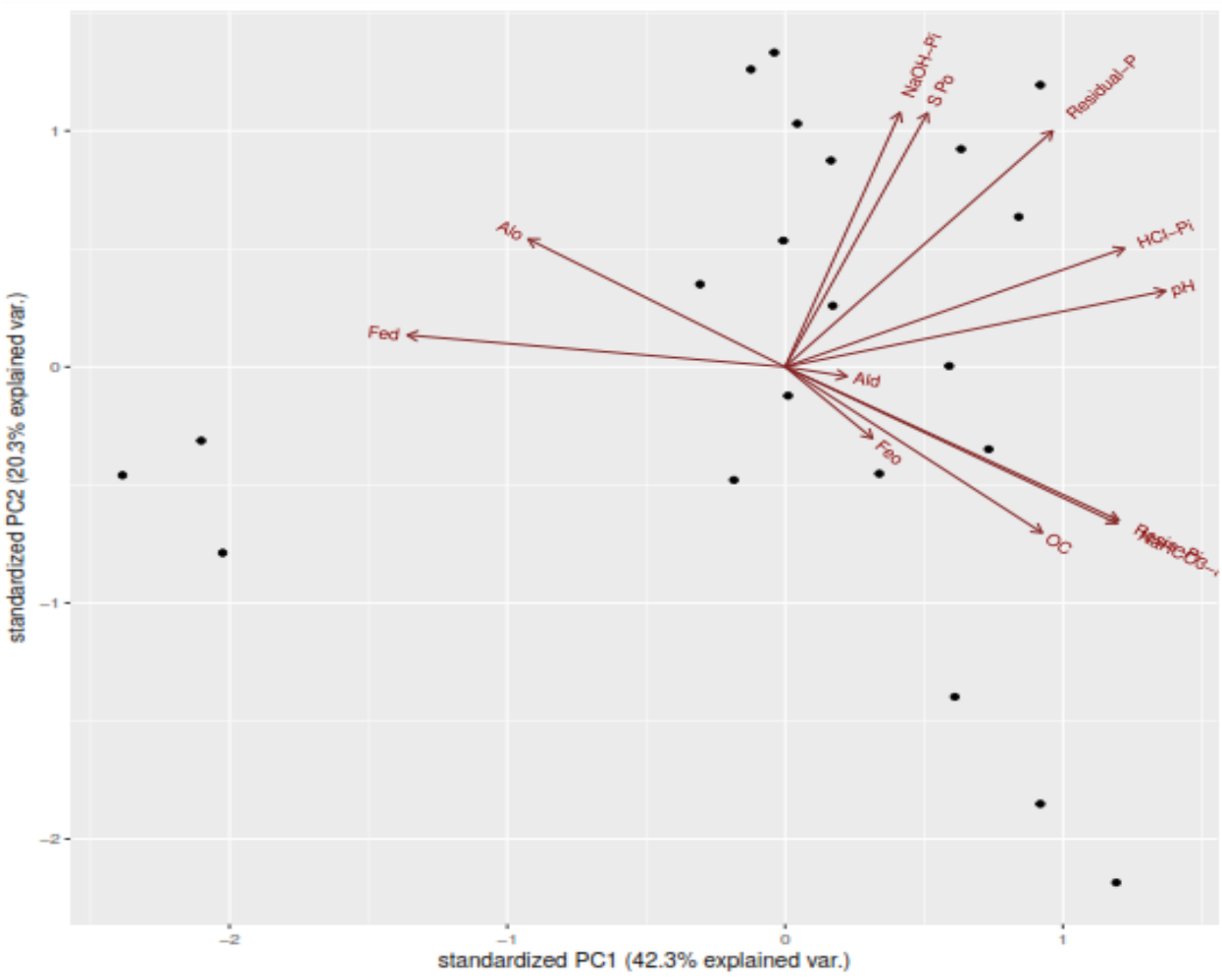

PCA showing P Fractions and soil chemical properties of biochar (corn corn and rice husk) amende Keta soil